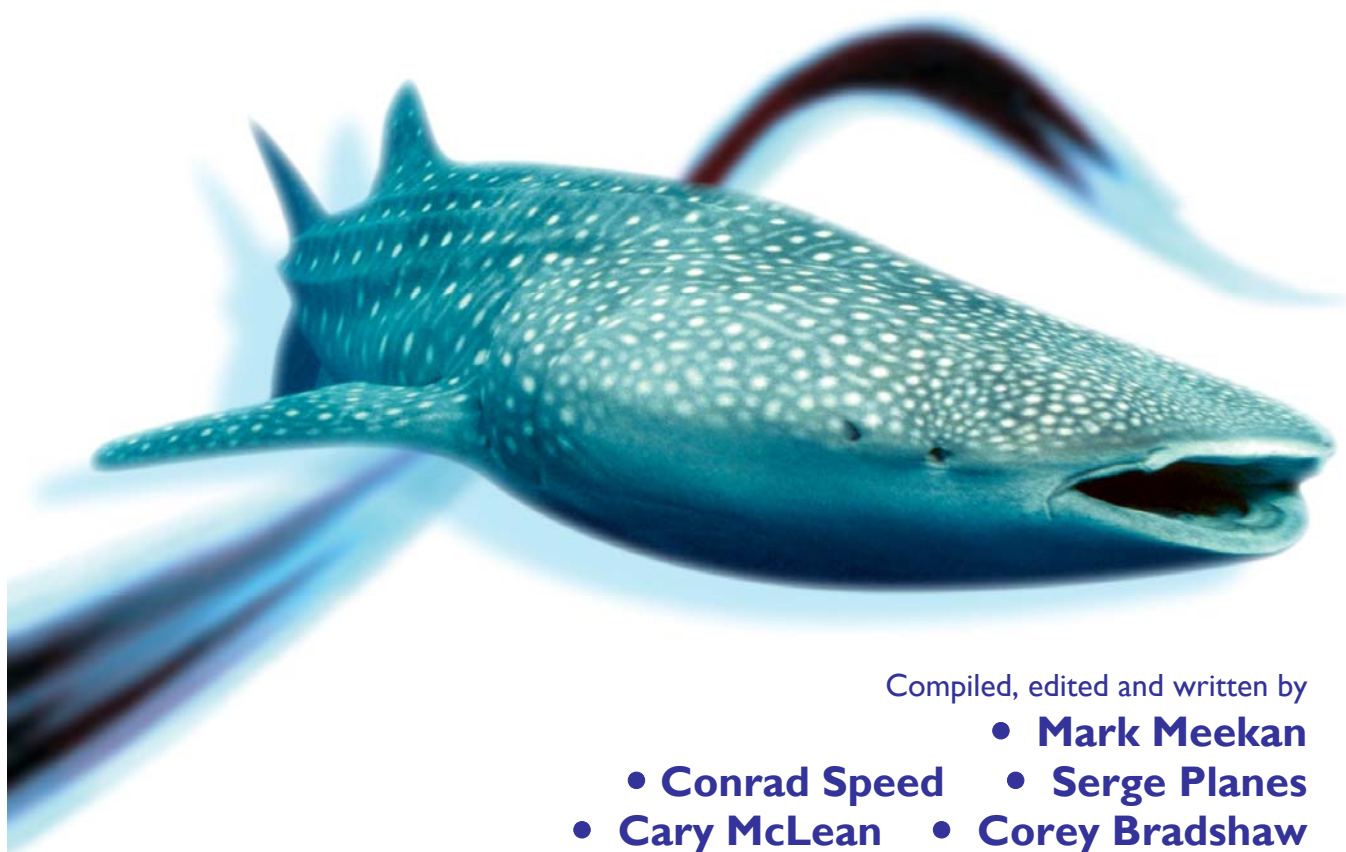


**FINAL REPORT to the
Western Australian Marine Science Institution**

*Population monitoring protocols for whale sharks
(*Rhincodon typus*)*



Compiled, edited and written by

- **Mark Meekan**
- **Conrad Speed**
- **Serge Planes**
- **Cary McLean**
- **Corey Bradshaw**

MARCH 2008



Australian Government
**Department of the Environment,
Water, Heritage and the Arts**



*western australian
marine science institution*



Australian Government



**AUSTRALIAN INSTITUTE
OF MARINE SCIENCE**



**Charles Darwin
UNIVERSITY**



UPVD
Université de Perpignan *Via Domitia*

National Library of Australia Cataloguing-in-Publication entry:

Population monitoring protocols for whale sharks (*Rhincodon typus*) /
Mark Meekan ... [et al..].

ISBN : 9780642322470 (pbk)

1. whale shark -- monitoring -- standards.
2. whale shark -- counting
3. zoological surveys -- standards

Meekan, Mark Gregory

597.31

This report should be cited as:

Meekan MG, Speed CW, Planes S, McLean C, Bradshaw CJA (2008) Population monitoring for whale sharks (*Rhincodon typus*). Report prepared for the Australian Government Department of the Environment, Water, Heritage and the Arts. Australian Institute of Marine Science, Townsville. 195 pp.

Published: March 2008 by Australian Institute of Marine Science.

DISCLAIMER

The views and opinions expressed in this publication are those of the authors and do not necessarily reflect those of the Australian Government or the Minister for the Environment, Heritage and the Arts. While reasonable effort has been made to ensure that the contents of this publication are factually correct, the Commonwealth does not accept responsibility for the accuracy or completeness of the contents, and shall not be liable for any loss or damage that may be occasioned directly or indirectly through the use of, or reliance on, the contents of this publication.

Population monitoring protocols for whale sharks (*Rhincodon typus*)

compiled, edited and written by

**Mark G Meekan^{1§}, Conrad W Speed^{1,2}, Serge Planes³
Cary McLean⁴ and Corey JA Bradshaw^{2,5,6}**

¹ Australian Institute of Marine Science
PO Box 40197, CASUARINA MC NT 0811

² School for Environmental Research, Institute of Advanced Studies
Charles Darwin University, DARWIN NT 0909

³ EPHE - UMR CNRS 8046, Universite de Perpignan
52 Avenue Paul Alduy, PERPIGNAN Cedex 66860, France

⁴ Australian Institute of Marine Science
PMB 3, TOWNSVILLE MC QLD 4810

⁵ Research Institute for Climate Change and Sustainability,
School of Earth and Environmental Sciences
University of Adelaide, ADELAIDE SA 5005

⁶ South Australian Research and Development Institute
PO Box 120, HENLEY BEACH SA 5022

§ Corresponding author

CONTENTS

List of Figures	vii
List of Tables	xi
Acknowledgements	xiv
Publications and Author Lists	xv
Executive Summary	xvii
1. Introduction	1
1.1 BACKGROUND.....	1
1.2 AIMS.....	3
1.3 FORMAT OF THE REPORT.....	3
2. Sampling Methods for Monitoring Whale Sharks in Australian Waters	5
2.1 STUDY SITE AND SAMPLING.....	5
2.2 CONVENTIONAL TAGS.....	8
2.3 PHOTO-IDENTIFICATION.....	8
2.4 TISSUE SAMPLING – COLLECTION TECHNIQUES.....	11
2.4.1 Faecal material.....	11
2.4.2 Biopsy Spear.....	12
2.4.3 Microplanes.....	12
2.5 SATELLITE TRACKING OF WHALE SHARKS.....	15
2.5.1 Satellite tags.....	15
2.5.2 Fin tags.....	17
2.5.3 Pop-up Archival Satellite Tags (PSAT).....	17
3. Genetic Sampling of Whale Sharks	21
3.1 OVERVIEW.....	21
3.2 MICROSATELLITE MARKERS.....	22
3.2.1 Introduction.....	22
3.2.2 Methods.....	22
3.2.2.1 Construction of enriched microsatellite library.....	22
3.2.3 Results.....	23
3.2.4 Conclusion.....	25
3.3 POPULATION GENETIC STRUCTURE OF THE WHALE SHARK (<i>RHINCODON TYPUS</i>).....	26
3.3.1 Introduction.....	26
3.3.2 Materials and methods.....	26
3.3.2.1 Sample collection and laboratory procedures.....	26
3.3.2.2 Data analysis.....	27
3.3.3 Results.....	28

3.3.4 Discussion.....	34
3.3.4.1 Control region morphology.....	35
3.3.4.2 Genetic diversity and effective population size.....	35
3.3.4.3 Population structure.....	36
3.3.4.4 Marine phylogeography.....	37
3.3.4.5 Conservation implications.....	38
4. Photograph Matching Techniques and Demographic Models	39
4.1 OVERVIEW.....	39
4.2 VALIDATION OF COMPUTER-AIDED MATCHING	41
4.2.1 Introduction	41
4.2.2 Methods	41
4.2.2.1 Matching software, fingerprint creation and image matching.....	41
4.2.2.2 I ³ S matching validation.....	45
4.2.2.3 Assessing ‘by-eye’ matches using I ³ S.....	46
4.2.2.4 Horizontal angle (yaw).....	46
4.2.2.5 Number of spot pairs.....	46
4.2.2.6 Population Size Analysis.....	47
4.2.3 Results	48
4.2.3.1 I ³ S (Interactive Individual Identification Software) matching validation	48
4.2.3.2 Assessing ‘by-eye’ matching using I ³ S.....	51
4.2.3.3 Horizontal angle	53
4.2.3.4 Number of spot pairs.....	55
4.2.3.5 Whale shark population size using I ³ S matches.....	57
4.2.3.6 Whale shark population size using validated I ³ S matches.....	58
4.2.4 Discussion.....	60
4.2.4.1 I ³ S Analysis & Information Criterion Algorithm.....	60
4.2.4.2 Estimating population size	61
4.3 MODELLING OF DEMOGRAPHY: INFERRING POPULATION TRENDS FOR THE WORLD’S LARGEST FISH FROM MARK-RECAPTURE ESTIMATES OF SURVIVAL	62
4.3.1 Introduction	62
4.3.2 Materials and Methods	63
4.3.2.1 Study area and population.....	63
4.3.2.2 Data collection.....	64
4.3.2.3 Mark-recapture analysis.....	64
4.3.2.4 Population models.....	65
4.3.2.5 Model structure.....	65
4.3.2.6 Parameter estimates and assumptions	66
4.3.2.7 Elasticities of λ to changes in matrix parameters.....	68
4.3.3 Results	68
4.3.3.1 Survival and capture probabilities.....	68
4.3.3.2 Sex differences in survival	69
4.3.3.3 Size differences in survival	70
4.3.3.4 Population models.....	70
4.3.4 Discussion.....	73

4.4 SCARRING PATTERNS AND RELATIVE MORTALITY RATES OF INDIAN OCEAN WHALE SHARKS.....	76
4.4.1 Introduction	76
4.4.2 Materials and methods.....	77
4.4.2.1 Scarring databases and image matching.....	77
4.4.2.2 Scarring categories	78
4.4.2.3 Database comparisons.....	79
4.4.2.4 Effects of scarring on apparent survival.....	79
4.4.2.5 Shipping activity around aggregations	80
4.4.3 Results	80
4.4.4 Discussion.....	85
5. Satellite Tagging.....	89
5.1 OVERVIEW.....	89
5.2 PSAT TAG VALIDATION.....	90
5.2.1 Introduction	90
5.2.2 Methods	91
5.2.2.1 Tagging.....	91
5.2.2.2 Data processing.....	92
5.2.2.3 Accuracy and precision.....	92
5.2.3 Results	93
5.2.3.1 Locations from light levels	94
5.2.3.2 Depth and temperature.....	97
5.2.4 Discussion.....	98
5.2.4.1 Locations from light levels	98
5.2.4.2 Depth and temperature.....	99
5.3 SAT TAG TRACKS AND GEOSTROPHIC CURRENTS.....	100
5.3.1 Introduction	100
5.3.2 Methods	101
5.3.2.1 Tagging.....	101
5.3.2.2 Environmental data.....	102
5.3.2.3 Passive diffusion model.....	107
5.3.2.4 Analysis.....	107
5.3.3 Results	108
5.3.4 Discussion.....	112
5.4 WHALE SHARK DIVE PATTERNS AND OCEANOGRAPHY.....	114
5.4.1 Introduction	114
5.4.2 Methods	114
5.4.2.1 Tag Data	114
5.4.2.2 Oceanographic Data.....	117
5.4.3 Results	117
5.4.4 Discussion.....	122

6. Analysis of Historical Data Sets	125
6.1 OVERVIEW.....	125
6.2 OCEANOGRAPHIC AND ATMOSPHERIC PHENOMENA INFLUENCE THE ABUNDANCE OF WHALE SHARKS AT NINGALOO REEF, WESTERN AUSTRALIA	126
6.2.1 Introduction	126
6.2.2 Methods	127
6.2.2.1 <i>Whale shark abundance data</i>	127
6.2.2.2 <i>Oceanographic and atmospheric parameters</i>	127
6.2.2.3 <i>Analysis</i>	128
6.2.3 Results	129
6.2.3.1 <i>Relative abundance of whale sharks 1995-2004</i>	129
6.2.3.2 <i>Weekly SOI and SST from 1995-2004</i>	131
6.2.3.3 <i>Weekly SOI, SST SL and WS from 1998-2004</i>	132
6.2.4 Discussion.....	134
6.3 DECLINE IN WHALE SHARK SIZE AND ABUNDANCE AT NINGALOO REEF OVER THE PAST DECADE: THE WORLD’S LARGEST FISH IS GETTING SMALLER	141
6.3.1 Introduction	141
6.3.2 Materials and methods.....	143
6.3.2.1 <i>Tourist operator-collected data</i>	143
6.3.2.2 <i>Reduction in total length over time</i>	144
6.3.2.3 <i>Relative shark abundance and climate variation</i>	145
6.3.2.4 <i>Evidence of intrinsic and extrinsic control in SPUE rate of change</i>	146
6.3.3 Results	147
6.3.4 Discussion.....	156
6.3.5 Conclusions and conservation remarks	158
7. Conclusions and Recommendations.....	159
8. References.....	163
Appendix 1	183
Appendix 2	193
Appendix 3	195

LIST OF FIGURES

Figure 2.1.	Map of study site, Ningaloo Reef, WA.	6
Figure 2.2.	Research vessel used for whale shark work during 2005-7.	7
Figure 2.3.	A) Researchers exiting vessel in pursuit of whale shark. B) Researcher positioning in relation to whale shark for photo-id (far) and satellite tag attachment (close)	7
Figure 2.4.	The left flank of a whale shark tagged using a conventional fish tag (yellow dart below dorsal fin).	8
Figure 2.5.	Standard reference area use for photo-identification of whale sharks	10
Figure 2.6.	Whale shark faecal sample collected at Ningaloo Reef	11
Figure 2.7.	A) Hawaiian-Sling pole spear with biopsy tip attached, B) .Biopsy tip for tissue sampling of whale sharks, C) Biopsy tip and whale shark tissue sample being placed in vial of DMSO	13
Figure 2.8.	Microplanes trialled for taking skin samples from whale sharks. A) Coarse grade , B) medium ribbon grade.	14
Figure 2.9.	A) Applicator & bolt, B) Applicator, fin clasp and satellite tag and C) Satellite tag ready for deployment	15
Figure 2.10.	A double-tagged whale shark showing fin clasp on leading edge of 1 st dorsal fin and satellite tag (above left pectoral fin) and 2 PSATs below dorsal fin on left and right flanks	16
Figure 2.11.	Fin tag without neoprene cover	17
Figure 2.12.	PTT-100, Microwave Telemetry Pop-up archival tag showing titanium dart and tether.	18
Figure 2.13.	Application of Pop-up Archival Tag (PSAT).	19
Figure 2.14.	PSAT tag embedded in sub-dermal layer of whale shark flank/dorsal fin.	19
Figure 3.1.	Steps followed to isolate microsatellite-containing fragments.	23
Figure 3.2.	Last PCR results before cloning P1, P2, P3: probe 1, 2 or 3 - : control without probe.	24
Figure 3.3.	Second trial to analyse whale shark DNA.	24
Figure 3.4.	Geographic distribution and number of whale shark skin biopsy samples obtained for each geographic location.	27
Figure 3.5.	Schematic diagram showing the consensus of all 28 haplotypes for the complete CR sequences of the whale shark. Blocks with different patterns represent repeated fragments along the CR sequence. Arrows represent primers used in PCR amplification.	29
Figure 3.6.	Neighbour-joining tree of the phylogenetic relationships of 28 haplotypes. Maximum likelihood distances were estimated using the HYK85+I model of	

	molecular evolution. Bootstrap values greater than 50 are indicated above nodes.	32
Figure 3.7.	Haplotype mismatch distribution. Note that all comparisons with 10 or greater differences between the sequences involve haplotype H9. Dotted line is the expected frequency given a demographically stable population.	33
Figure 4.1.	Fingerprint file creation (reference points and spot highlighting shown).	42
Figure 4.2.	Results of searching an unknown image in I ³ S, showing unknown image and the top 50 ranking of the most likely matches (right side of the screen).	43
Figure 4.3.	Visual comparison of unknown individual and matched individuals (left side of the screen). The top image is unknown, and the bottom image is the matched image from the database.....	44
Figure 4.4.	Spot cloud of matching spot pairs (left side of the screen). The red spots are the fingerprint from the unknown shark, and the blue spots are the fingerprint from a shark found in the database. The green lines denote the distance between match spot pairs.....	44
Figure 4.5.	An individual whale shark at differing angles of yaw (A: 0°, B: 10°, C: 20°, D: 30°, E 40°). This type of sequence was used to determine the effect of horizontal angle on the I ³ S matching process.	46
Figure 4.6.	I ³ S matching validation IC weights (w_i). Distribution of IC weights for known matched (a) and non-matched pairs (b), and I ³ S matching validation evidence ratios (ER_i) for known matched (c) and non-matched pairs (d) are shown.....	49
Figure 4.7.	Median (a) IC weights (w_i) for known matched pairs showing images matched and not matched with I ³ S; (b) Median evidence ratios (ER_i) for known matched pairs showing images matched and not matched using I ³ S.....	50
Figure 4.8.	By-eye versus I ³ S matching Results. (a) Median IC weights (w_i) for by-eye matched images that were matched and not matched using I ³ S; (b) Median evidence ratios (ER_i) for by-eye matched images that were matched and not matched using I ³ S.....	52
Figure 4.9.	Effect of angles of yaw. (a) Mean IC weights (w_i) for horizontal angle categories, where images at 0° were matched against images skewed by 10°, 20°, 30° and 40°. Dotted lines show results for non-matching pairs; (b) Mean evidence ratios (ER_i) for horizontal angle categories, where images at 0° were matched against images skewed by 10°, 20°, 30° and 40°.	54
Figure 4.10.	Effects of spot-pair number. (a) Relationship between complementary log-log-transformed (clog-log) I ³ S scores and log ₁₀ -transformed number of spot pairs. The fitted line illustrates the correlation observed using a linear regression; (b) Comparison of clog-log-transformed w_i with log ₁₀ -transformed number of spot pairs.	56
Figure 4.11.	Mean validated and unvalidated (< 0.2) w_i for inter-annual resights used for population modelling.	58
Figure 4.12.	Indian Ocean whale shark aggregation sites – Ningaloo Reef (Western Australia), Seychelles and Mozambique.....	78

Figure 4.13.	Classification of scar severity.	79
Figure 4.14.	Percentage occurrence of individuals within scar categories by location.....	81
Figure 4.15.	Observed and expected numbers of sharks in each scarring category among aggregation sites. *b = bites, bt = blunt trauma and la = lacerations and amputations.	82
Figure 4.16.	A) Position of scars on body by aggregation site B) Position of scars on body by aggregation site (nicks and abrasions omitted).	83
Figure 5.1.	Sat tag track vs location estimates from PSATs 1 and 2 derived from 3 levels of data processing (a) raw light level (b) Kalman filtered (c) Kalman filtered with SST integration.	95
Figure 5.2.	Scatterplots of replicate measurements of: (a) depth (n=1634 pairs); and (b) temperature (n=1320 pairs) from PSATs 1 and 2. Line is provided for reference only.....	97
Figure 5.3.	Distribution of whale shark tracks throughout the Indian Ocean and bathymetry.....	101
Figure 5.4.	Example of geostrophic current map for the mid Austral winter period (June 2005).....	103
Figures 5.5	a-f. Actual cumulative tracks of individual whale sharks (left) compared with probability distribution maps based on modelled passive diffusion by geostrophic currents (right). The modelled maps are parameterised with weekly starting points of whale sharks.....	104
Figures 5.5	a-f.....	105
Figures 5.5	a-f.	106
Figure 5.6.	Example of chlorophyll-a concentration map for the mid-winter period (June 2005).....	109
Figure 5.7.	Partial residual plots of the relationship between the complementary log-log (clog-log) of the observed cell occupancy probability and the (A) log of chlorophyll-a concentration and (B) the clog-log of the passive-movement predicted cell occupancy probability.	111
Figure 5.8.	a) Track locations of tagged whale sharks (b) 3-dimensional dive tracks of whale sharks in relation to bathymetry.....	116
Figure 5.9.	a) distribution of temperature and (b) distribution of dissolved oxygen levels throughout the Indian Ocean in which the whale sharks were observed.....	119
Figure 5.10.	a) frequency distribution of temperatures and (b) dissolved oxygen levels corresponding to dives by whale sharks.....	120
Figure 5.11.	Frequency distribution of depths occupied by whale sharks during dives.....	121
Figure 6.1.	The weekly abundance of whale sharks observed off Ningaloo Reef from March to July between years (a) 1995 – 1999, and (b) 2000 – 2004.....	130
Figure 6.2.	Partial residual plot generated from the most-parsimonious generalized linear model relating weekly whale shark abundance between 1995 and 2004 to the	

	Southern Oscillation index (SOI). The solid line is the fitted linear model. The dashed lines are the approximate 95 % point-wise confidence intervals.....	132
Figure 6.3.	Partial residual plots generated from the most-parsimonious generalized linear model relating weekly whale shark abundance between 1998 and 2004 to the Southern Oscillation index (SOI) and sea surface temperature (SST). The solid lines represent the fitted linear models. The dashed lines are the approximate 95 % point-wise confidence intervals.....	133
Figure 6.4.	Weekly AVHRR satellite image composite of sea-surface temperature variability in the East Indian Ocean during the annual period when average whale shark abundances tend to be high (1 st week of May).	135
Figure 6.5.	Oceanographic models indicating the relative differences in the circulation patterns and strength of major currents (as denoted by thickness of arrows) in the North East Indian Ocean during (a) La Niña and (b) El Niño climatic periods.....	137
Figure 6.6.	Weekly Topex/ Poseidon altimetry composite of Sea Surface height and associated geostrophic flow (direction and velocity) in the East Indian Ocean during the annual period when whale shark abundances tend to peak (1 st week of May).....	138
Figure 6.7.	Weekly SeaWiFs satellite image composite of chlorophyll- <i>a</i> concentration in the East Indian Ocean during the annual period when whale shark abundances tend to peak (1 st week of May).	139
Figure 6.8.	Estimated total length distribution for whale sharks seen at Ningaloo from A. 1995-2004, B. only 1995-1996 and C. only 2003-2004. There is a noticeable loss of larger individuals in the more recent distribution.	148
Figure 6.9.	Mean length of all whale sharks observed at Ningaloo Reef from 1995 – 2004.	150
Figure 6.10.	A. Total number of sharks seen at Ningaloo Reef in April and May from 1995 – 2004 after removing individuals seen more than once per day, and total vessel search time (hours) as an index of effort; B. Relative abundance corrected for effort ; C. Monthly and two-monthly running mean of the Southern Oscillation Index (SOI) from 1995 – 2004.	153
Figure 6.11.	Southern Oscillation Index (SOI)-detrended whale shark sightings per unit effort (SPUE) for A. small (< 6 m total length) males, B. large (≥ 6 m TL) males, C. small females and D. large females.....	154
Figure 6.12.	A. SOI-detrended SPUE versus year for all individuals combined, large (≥ 6 m total length) males only, and large females only; B. SOI-detrended SPUE rate of change and standardised SPUE according to the Gompertz-logistic (GL) and exponential (EX) dynamical models; C. The same relationship for large males only; D. The same relationship for large females only. Model results are presented in Table 6.6.	156

LIST OF TABLES

Table 3.1.	Location, numbers of individuals (N), number of haplotypes (n), haplotype (h) and nucleotide (π) diversity estimates and standard deviations observed on the CR of the whale shark within five major geographic locations.....	30
Table 3.2.	Geographic distribution of haplotypes found in 50 whale sharks. Sample locations were grouped by geographic proximity (SA – South Africa, NW Pac – Northwestern Pacific, NE Pac – Northeastern Pacific).....	31
Table 3.3.	Estimate of pairwise Φ_{ST} values using both HKY85+I (bellow diagonal) and Tamura & Nei’s (above diagonal) genetic distances. Bolded values were significant ($P = 0.05$) after Bonferroni correction.....	32
Table 3.4.	Population size and age estimates for whale sharks globally.....	34
Table 4.1.	Open-population models for whale shark population re-assessment using MARK.....	47
Table 4.2.	Summary of population size estimates from closed and open populations for ^{13}S resights.....	57
Table 4.3.	Results for model analysis using non-validated (unvalidated) ^{13}S dataset - Small sample size corrected Akaike Information Criterion (AICc), change in AICc ($\Delta AICc$), AIC weights (w AICc), number of parameters (k) and deviance.....	58
Table 4.4.	Summary of population size estimates from closed and open populations for validated ^{13}S resights.....	59
Table 4.5.	Results for model analysis using validated ^{13}S dataset - Small sample size corrected Akaike’s Information Criterion (AICc), change in AICc ($\Delta AICc$), AIC weights (w AICc), number of parameters (k) and deviance.....	59
Table 4.6.	Model ranking of Cormack-Jolly-Seber mark-recapture models estimating apparent survival (ϕ) and recapture probability (p) for whale sharks participating in the Ningaloo Reef (Western Australia) aggregation from 1992 to 2004. .	69
Table 4.7.	Time-variant model-averaged estimates of apparent survival ($\hat{\phi}$) derived using Cormack-Jolly-Seber (CJS) mark-recapture models for whale sharks participating in the Ningaloo Reef (Western Australia) aggregation from 1992 to 2004.....	69
Table 4.8.	Matrix parameters calculated for each Model Scenario considered when age at first reproduction (α) = 13, for both annual and biennial reproduction frequencies.....	71
Table 4.9.	Matrix parameters calculated for each Model Scenario considered when age at first reproduction (α) = 25, for both annual and biennial reproduction frequencies.....	72
Table 4.10.	Percentage of individuals within scar type and body location category among three Indian Ocean aggregations observed.....	81

Table 4.1.1.	Five most highly ranked Cormack-Jolly-Seber models testing the effects of scarring (s) and time (t) on apparent survival (ϕ) and resight probability (p) of whale sharks participating in the Ningaloo Reef aggregation between 1992 and 2006, and at Seychelles between 2001 and 2006.....	84
Table 4.1.2.	Apparent survival estimates for whale sharks with and without scarring at Ningaloo Reef and Seychelles based on Cormack-Jolly-Seber mark-recapture models.	84
Table 5.1.	Accuracy of location estimates resulting from 3 levels of data processing	93
Table 5.2.	Accuracy of location estimates resulting from 3 levels of data processing	96
Table 5.3.	Precision of location estimates resulting from 3 levels of PSAT data processing and depth and temperature data from PSATs 1 and 2	96
Table 5.4.	Comparison of tagged whale sharks, sex (F = female, M = male, ? = unknown), total track length (km) and the average movement speeds of whale sharks (km/hr^{-1}) with average, mode, minimum and maximum of geostrophic current velocities (km/hr^{-1}) within their observed migration routes.....	110
Table 5.5.	Model comparison using Akaike's Information Criterion corrected for small sample size (AIC_c) and Bayesian Information Criterion (BIC).....	110
Table 6.1:	Correlation matrix between Southern Oscillation index (SOI), sea surface temperature (SST), sea level (SL) and along shelf wind shear (WS) from 1998-2004.	131
Table 6.2:	Generalised linear mixed-effects models and information-theoretic statistics based on the change in Akaike's Information Criterion corrected for small samples (ΔAIC_c) for model scenario 1 using Southern Oscillation index (SOI) and sea surface temperature (SST) to estimate trends in weekly whale shark abundance from 1995-2004. Notations; D = % deviance explained ΔAIC_c = change in AIC_c between models, w_i = AIC_c weight.	131
Table 6.3:	Generalised linear mixed-effects models and their information-theoretic statistics based on the change in Akaike's Information Criterion corrected for small samples (ΔAIC_c) for model scenario 2 using Southern Oscillation index (SOI), sea surface temperature (SST), sea level (SL) and wind shear (WS) to estimate trends in weekly whale shark abundance from 1998-2004. Notations; D = % deviance explained, ΔAIC_c = change in AIC_c between models, w_i = AIC_c weight.	133
Table 6.4.	Four models applied to the relationship between mean total length (TL) and year for whale sharks from Ningaloo Reef between 1995 and 2004. Models are ranked according to Akaike's Information Criterion corrected for small sample size (AIC_c). Shown for each model are the number of parameters (k), the maximum log-likelihood (LL), the difference in AIC_c for each model from the top-ranked model (ΔAIC_c), AIC_c weight ($w\text{AIC}_c$), and the percent deviance explained (%DE) in the response variable (TL).	149
Table 6.5.	Comparison of general linear models (GLM) examining the relationship between total length (TL) and temporal variables for whale sharks at Ningaloo Reef from 1995 – 2004. A. TL versus <i>year</i> and <i>month</i> , and B. Five top-ranked GLMs examining the relationship between <i>year</i> , <i>month</i> and sex and TL. Models	

are ranked according to the Bayesian Information Criterion (BIC). Shown for each model are the number of parameters (k), the maximum log-likelihood (LL), the difference in BIC for each model from the top-ranked model (ΔBIC), BIC weight ($wBIC$), and the percent deviance explained (%DE) in the response variable (TL). 151

Table 6.6. Comparison of general linear models (GLM) examining the relationship between total length (TL) and temporal variables for whale sharks at Ningaloo Reef from 1995 – 2004. **A.** TL versus *year* and *day of year (doy)*, and **B.** Five top-ranked GLMs examining the relationship between *year*, *doy* and sex and TL..... 152

Table 6.7. Comparison of two population dynamical models (Gompertz-logistic and exponential) describing the relationship between rate of change in Southern Oscillation Index (SOI)-detrended whale shark sightings per unit effort (SPUE) for **A.** All individuals combined, **B.** large (≥ 6 m total length) males only and **C.** large females only..... 155

ACKNOWLEDGEMENTS

The work described in this report was supported by funding from the following organisations:

Australian Government Department of Environment, Water, Heritage and the Arts (DEWHA)

National Heritage Trust (NHT)

West Australian Department of Environment and Conservation (DEC)

National Oceanic and Atmospheric Administration (NOAA)

SeaWorld Research and Rescue Foundation Inc

Woodside Energy Ltd (WEL)

BHP Billiton (BHPB)

Chevron

Australian Institute of Marine Science (AIMS)

CSIRO Marine and Atmospheric Research (CSIRO MAR)

West Australian Marine Sciences Institute (WAMSI)

We acknowledge the help and support of staff at the West Australian Department of Environment and Conservation office in Exmouth, particularly, Jenny Cary, Roland Mau and Emily Wilson. We thank T. Maxwell, R. Davis, and F. McGregor. Engineering and fabrication of the Ramset HD200 powder actuated tag applicator was conducted by M. Horsham. The Telonics tags were built by M. Horsham, J. Cordell and M. Sherlock. All research in this report was approved by the ethics committee of Charles Darwin University.

PUBLICATIONS AND AUTHOR LISTS

Sampling methods for monitoring of whale sharks in Australian waters

Speed CW, Meekan MG, McLean C, Bradshaw CJA

Genetic sampling of whale sharks

Microsatellite markers

Planes S, Meekan MG, Speed CW, Bradshaw CJA

Population genetic structure

Published as: Castro ALF, Stewart BS, Wilson SG, Hueter RE, Meekan MG, Motta PJ, Bowen BW, Karl SA (2007) Population genetic structure of Earth's largest fish, the whale shark (*Rhincodon typus*). *Molecular Ecology* 16:5183-5192

Photographic matching techniques and demographic models

Validation of computer-aided matching

Published as: Speed CW, Meekan M, Bradshaw CJA (2007) Spot the match - wildlife photo-identification using information theory. *Frontiers in Zoology* 4:2

Modelling of demography

Published as: Bradshaw CJA, Mollet HF, Meekan MG (2007) Inferring population trends for the world's largest fish from mark-recapture estimates of survival. *Journal of Animal Ecology* 76:480-489

Scarring patterns and relative mortality rates

Published as: Speed CW, Meekan MG, Rowat D, Pierce S, Marshall AD, Bradshaw CJA (2008) Scarring patterns and relative mortality rates of Indian Ocean whale sharks. *Journal of Fish Biology* DOI: 10.1111/j.1095-8649.2008.01810.x

Satellite Tagging

PSAT validation

Published as: Wilson SG, Stewart BS, Polovina JJ, Meekan MG, Stevens JD, Galuardi B (2007) Accuracy and precision of archival tag data: a multiple-tagging study conducted on a whale shark (*Rhincodon typus*) in the Indian Ocean. *Fisheries Oceanography* 16:547-554

SAT tag tracks and geostrophic currents

Published as: Sleeman JC, Meekan MG, Stewart BS, Wilson SG, Polovina JJ, Stevens JD, Boggs GS, Bradshaw CJA. (In review). To go or not to go with the flow: environmental influences on whale shark migration patterns *Marine Ecology Progress Series*.

Whale shark dive patterns and oceanography

Published as: Sleeman JC, Meekan MG, Stewart BS, Wilson SG, Polovina JJ, Stevens JD, Boggs GS, Bradshaw CJA. (in prep). How whale shark dive patterns relate with ocean temperature and dissolved oxygen: is habitat use linked to physiological limitations? To be submitted to Marine Ecology Progress Series

Analysis of historical datasets

Oceanographic and atmospheric phenomena

Published as: Sleeman JC, Meekan MG, Fitzpatrick BS, Steinberg CR, Ancel R, Bradshaw CJA. (In review) Oceanographic and atmospheric phenomena influence the abundance of whale sharks at Ningaloo Reef, Western Australia. Submitted to Journal of Experimental Marine Biology and Ecology.

Decline in whale shark size and abundance at Ningaloo Reef over the past decade

Published as: Bradshaw CJA, Fitzpatrick BW, Steinberg CC, Brook BW, Meekan MG (In press) Decline in whale shark size and abundance at Ningaloo Reef over the past decade: the world's largest fish is getting smaller. Biological Conservation

Conclusions and Recommendations

Meekan MG

EXECUTIVE SUMMARY

- This project aims to: (1) Review current monitoring methods and highlight viable data collection and analysis techniques (2) Develop new protocols for genetic analysis to assist in understanding the population structure of whale sharks at Ningaloo Reef. (3) Use photo-identification techniques as a basis for mark-recapture and demographic analyses of population and stock structure (4) Use satellite tagging techniques to document migration and diving patterns and to compare these to environmental variables such as water temperature and ocean productivity (5) Analyse historical databases of whale shark sightings provided by ecotourism operators to determine how abundances of sharks are influenced by oceanographic phenomena and trends in population composition and abundance through time.
- The project is an international collaboration among staff from AIMS, Charles Darwin University, University of Adelaide, South Australian Research and Development Institute, CSIRO, NOAA, Hubbs Seaworld, the University of Texas and the University of Perpignan (France).
- The results described in this report have been obtained from field work undertaken at Ningaloo Reef, Western Australia during April-May in 2004-2007. This project is ongoing with the next scheduled field work in April-May 2008.
- Development of microsatellite markers for genetic tagging proved to be a far greater technical challenge than was originally anticipated and took 24 months to complete. A full library of markers is now available and work has commenced on collating and processing genetic samples from the Ningaloo Reef and other Indian Ocean populations.
- We contributed to a worldwide study of the genetics of whale sharks. There was an absence of population structure across the Indian and Pacific oceans indicating that oceanic expanses and land barriers in Southeast Asia are not impediments to whale shark dispersal. We did, however, find population structure (AMOVA, $F_{ST}=0.153$, $P<0.001$) between the Atlantic and Indo-Pacific ocean basins.
- The global pattern of shared haplotypes in whale sharks is a compelling argument for development of broad international approaches for management and conservation of whale sharks.
- We assessed the use of open-access software for automated matching of photo-identification images of whale sharks. We developed an information criterion (IC) algorithm that resulted in a parsimonious ranking of potential matches of individuals in an image library.
- The software provided accurate and reliable image matches.
- We used the 12-year photographic identification library of whale sharks from Ningaloo Reef to construct Cormack-Jolly-Seber estimates of survival within a capture-mark-

recapture framework. Of the 16 model combinations considered, 10 (63 %) indicated a decreasing population.

- Assuming relatively slow vital rates, size-biased survival probabilities suggest the Ningaloo Reef population of whale sharks is declining, although more reproductive data are needed to confirm this conclusion.
- We interrogated the photo-identification data bases focusing on potential threats to this species. We recorded scars on whale sharks in three Indian Ocean aggregations (Australia, Seychelles and Mozambique), and examined whether scarring (mostly attributed to boat strikes and predator attacks) influences apparent survival rates using these photo-identification libraries.
- Scarring was most prevalent in the Seychelles aggregation (67 % of individuals). Predator bites were the most frequent source of scarring (aside from minor nicks and abrasions) and 27 % of individuals had scars consistent with predator attacks. A similar proportion of sharks had blunt trauma, laceration and amputation scars, the majority of which appeared to be caused by ship strike. Predator bites were more common (44 % of individuals) and scars from ship collisions were less common at Ningaloo Reef than at the other two locations.
- We found no evidence for an effect of scarring on apparent survival for the Ningaloo or Seychelles populations
- We conclude that while scarring from natural predators and smaller vessels appears to be unrelated to whale shark survival, the effects of deaths related to ship strike need to be quantified to assist in future management of this species.
- Ongoing work aims to quantify the extent of interchange among three major whale shark aggregations, representing the approximate eastern- (Ningaloo) and western-most (Seychelles, Mozambique) extent of the distribution of whale sharks within the Indian Ocean
- Satellite tagging of whale sharks has aimed to determine not only the migratory pathways of whale sharks, but to also understand the mechanisms by which these long distance voyages take place.
- We validated location estimates from Pop-up archival Satellite Tags (PSAT), by attaching two PSATs and one Argos satellite-linked transmitter (SAT tag) to one whale shark at Ningaloo Reef. Our findings support the use of archival light data from PSATs to reconstruct the large-scale movements of these animals.
- Long distance (100-1000 km) migrations of sharks from Ningaloo were recorded by SAT tags in 2005, 2006 and 2007. Tracks from these tags show that the Ningaloo population of sharks is part of a wider Indian Ocean stock that is likely to encompass much of the south eastern Indian Ocean and the waters of South East Asia.

- We used these tracks to investigate how migratory patterns of whale sharks were influenced by geostrophic surface currents. This was done by utilizing a passive diffusion model parameterised with observed whale shark starting positions and weekly maps of surface current velocity and direction (derived from altimetry). Our results indicate that whale sharks departing from Ningaloo are likely to use active locomotion in their migration, rather than surface currents to passively drift.
- SAT tags also record and transmit information about diving behaviour by whale sharks. This allowed us to investigate how whale shark dive patterns during long distance migrations were linked with ocean temperatures and dissolved oxygen levels by overlaying 3-dimensional satellite tracks of tagged sharks with oceanographic data.
- Whale sharks appear to selectively dive within water bodies of warm temperatures ($24.01 < 30\text{ }^{\circ}\text{C}$) and high levels of dissolved oxygen ($4 < 5\text{ ml l}^{-1}$) for the majority of dives (usually $>60\%$). This pattern of habitat selection may relate to physiological limitations of large aquatic poikilotherms and energetic conservation mechanisms.
- Ongoing work includes analysis of SAT tag tracks from tags deployed in 2006 and 2007. In two instances, SAT tags were recovered from beaches at Ningaloo after they had detached from the animal. This allowed the detailed (every 2 sec) records held in the archive of the tag to be downloaded (while attached the tags only transmit summary information to satellites). These are now being compared with oceanographic data collected by Acoustic Doppler Current Profilers and water temperature loggers deployed by AIMS at Ningaloo.
- A summary of migration tracks and diving behaviour obtained from the 43 PSAT deployments on sharks from 2002-2007 is also currently in preparation. A PhD student will commence a detailed analysis of the dive records from these tags in April 2008.
- Seasonal observations of whale shark abundance recorded by ecotourism operators at Ningaloo Reef from 1995-2004 provide a historical data set that can be used to investigate temporal patterns in abundance of whale sharks in relation to oceanographic phenomenon and decadal trends in population composition and size.
- The SOI positively influenced whale shark abundance such that during La Niña years, more sharks were sighted, and fewer were recorded during El Niño years. This may reflect changes in the strength of oceanographic processes such as the Leeuwin Current in response to the Southern Oscillation, which may act to transport sharks to the region and/or affect their prey by driving productivity events.
- Analysis of ecotourism records shows that mean shark length declined linearly by nearly 2.0 m and relative abundance measured from ecotourism sightings (corrected for variation in search effort and environmental stochasticity) has fallen by approximately 40 % over the last decade.

- This population-level result confirms previous predictions of population decline based on mark-recapture estimates of survival. The majority of these changes are driven by reductions in the number of large individuals in the population.
- These reductions have occurred despite the total protection of whale sharks in Australian waters. As this species is highly migratory, the rapid change in population composition over a decade (< 1 whale shark generation) supports the hypothesis of unsustainable mortality in other parts of their range (e.g., ship strike and over-fishing), rather than the alternative of long-term abiotic or biotic shifts in the environment. As such, effective conservation of whale sharks will require international protection and collaborative tagging studies to identify and monitor migratory pathways.

1. INTRODUCTION

1.1 BACKGROUND

Whale sharks (*Rhincodon typus* Smith 1828) are the largest fish in the world (> 12 m) and the only member of the family Rhincodontidae (1994). Like the basking (*Cetorhinus maximus*) and megamouth sharks (*Megachasma pelagios*), the whale shark feeds primarily on plankton. The species is distributed circum-globally in tropical and warm temperate seas (Compagno 2001) and is easily distinguished from other sharks by its large size and unique checkerboard pattern of white or yellow spots and stripes on a dark background (Compagno 2001). Like other sharks, whale sharks have a relative slow life history (Cavanagh et al. 2003), implying that they have extended longevity, are slow to reach sexual maturity and invest their reproductive effort in producing relatively few, large and well-developed offspring, (MacArthur & Wilson 1967). These life history traits can often signify low productivity and poor recovery potential following over-exploitation (Smith et al. 1998, Walker 1998, Bradshaw et al. 2007).

Another trait that confounds the issue of a slow life history is the highly migratory nature of whale sharks (Cavanagh et al. 2003). Whale sharks migrate thousands of kilometres (Eckert et al. 2002), which means there is the potential for this species to travel from waters where they are protected from harvesting to places where they are targeted by fisheries (Meekan et al. 2006). Whale sharks leaving the aggregation that occurs annually at Ningaloo Reef, Western Australia have been found to travel into Southeast Asian waters (Wilson et al. 2006), where fishing harvest occurs. While the harvesting of whale sharks is now prohibited in many countries (e.g., Belize, Honduras, Maldives, Philippines, Thailand, India, USA and Australia; Chen & Phipps 2002), it is probable that past fisheries have contributed to the current Vulnerable (IUCN Red Listing) status of this species. Whale sharks are still targeted for their fins and flesh in many regions, especially in Southeast Asia and southern China (Joung et al. 1996) where the demand for their products is high. In Taiwan, where there was until recently a fishery and market for whale shark flesh, the government has introduced a moratorium; however, monitoring of illegal trade in developing regions is often difficult so that the degree of compliance with regulation may be uncertain.

Whale sharks are known to aggregate annually in nearshore waters in a number of regions around the world including north-western Australia, Djibouti (Rowat et al 2007) India, the Maldives, Seychelles (Rowat & Gore 2006), Galápagos Islands, Mozambique and Mexico (Burks et al. 2006). Many of these locations support lucrative tourism industries where tourists can swim with whale sharks. As a result, thousands of photographs of these animals are taken each year, which has led to the establishment of several image libraries. Given that the spot and stripe marking patterns of animals are individually unique and temporally stable (Meekan et al. 2006), these image libraries have enabled whale shark populations to be monitored via photo-identification studies (Arzoumanian et al. 2005, Meekan et al. 2006), some of which have already provided valuable information on population size and structure, survival and population trends (Meekan et al. 2006, Bradshaw et al. 2007). However, the growth of these libraries has

meant that available photographs have exceeded the number that can be reliably compared by eye, thereby necessitating an automated system of matching. Two such systems have now been developed (Arzoumanian et al. 2005, Van Tienhoven et al. 2007b).

The rarity and limited biological information available for whale sharks has led the World Conservation Union (www.iucnredlist.org; Cavanagh et al. 2003) to list the species as 'Vulnerable' to extinction. Whale sharks are also listed on Appendix II of the Convention of Migratory Species (CMS) and Annex I (Highly Migratory Species) of the UN Convention on the Law of the Sea (UNCLOS) CMS 2005. Key issues that have been identified for research include the need to describe migratory pathways of these animals and to obtain estimates of demographic rates (e.g., survival, fertility) that are based on high-quality data that have been collected using a variety of reliable and comparable techniques. At present, demographic studies of whale sharks have only been done using information gathered from photo-identification databases (Meekan et al. 2006, Bradshaw et al. 2007), where validations of resights were made by eye.

To minimize potential errors inherent in photographic methods, multiple tagging techniques that are relatively non-subjective are required. To date, conventional tags and unique scarring patterns are the only other techniques that have been used to individually identify whale sharks, usually in conjunction with photographs of spot and stripe patterns. These techniques have a number of inherent problems such as tag loss and alteration of scarring patterns through time that might seriously bias estimates of demographic parameters. 'Genetagging' (Stevick et al. 2001) offers an alternative approach and uses the microsatellite DNA profile of a fish as a life-long indelible tag. This type of tagging is currently in a developmental phase in Australia and requires validation of critical elements for use in a standard monitoring protocol including firstly, laboratory work verifying that microsatellite sequences can be retrieved from small samples of whale shark tissue. Secondly, a humane technique is required to remove reliably small samples of tissue. This latter point is essential if the technique is to achieve broad acceptance by all involved in the conservation of whale shark populations in Australia, including ecotourism operators. Once these techniques are established, researchers can begin to harvest tissue and genetically tag sharks. Ultimately, it might be possible to fingerprint the majority of the Ningaloo population of sharks (approximately 200-300 individuals). This would allow validation of photo-identification techniques and also enable it to be determined if sharks visiting Ningaloo are being harvested to supply markets in Asia. Furthermore, the technique has the added benefit of providing additional individual- and population-level information (e.g., genetic diversity, parent-offspring relationships, etc, Palsboll et al. 1997).

The project on which this report is based is an international collaboration led by Dr Mark Meekan of AIMS and involving staff from Charles Darwin University, CSIRO, NOAA, Hubbs Seaworld, the University of Texas and the University of Perpignan (France). The results described here have been obtained from field work undertaken at Ningaloo Reef, Western Australia during April-May in 2004-2007. This project is ongoing with the next scheduled field work in April-May 2008.

This report reviews current monitoring methods, highlight viable data collection and analysis techniques, and develop new protocols for genetic analysis to assist in understanding the population structure of whale sharks at Ningaloo Reef. Outcomes from demographic analysis based on photo-identification will be presented, along with new techniques for individual identification and validation. We also describe ongoing results and analysis of satellite tagging that describes migration pathways and behaviour of whale sharks participating in the Ningaloo aggregation. Finally, we place these results in context by analysing historical records of whale sharks sightings provided by the ecotourism industry that describe patterns in abundance in relation to climatic and oceanographic phenomena and track decadal trends in population size and composition. Our over-arching aim is to provide researchers and managers with the necessary context, information and tools to manage the Australian population of whale sharks on a regional and global scale.

1.2 AIMS

The specific aims of this report are to:

1. Review current monitoring methods and highlight viable data collection and analysis techniques.
2. Develop new protocols for genetic analysis to assist in understanding the population structure of whale sharks at Ningaloo Reef.
3. Use photo-identification techniques as a basis for mark-recapture and demographic analyses of population and stock structure.
4. Use satellite tagging techniques to document migration and diving patterns and to compare these to environmental variables such as water temperature and ocean productivity
5. Analyse historical databases of whale shark sightings provided by ecotourism operators to determine how abundances of sharks are influenced by oceanographic phenomena and trends in population composition and abundance through time.

1.3 FORMAT OF THE REPORT

This report deals with the abovementioned aims as separate chapters, which are followed by a conclusions and recommendations chapter. The focus is on whale shark populations in north-western Australia; however, the techniques discussed can potentially be applied to whale shark populations worldwide. Each chapter contains information that has either been published or is being prepared for publication in international, peer-reviewed journals. The titles and co-authors of these publications have been identified at the beginning of this report. Note that field work and data analysis for the project is ongoing. The overview section at the beginning of each chapter highlights major findings to date and details ongoing work and analysis to fulfil the aims mentioned above.

2. SAMPLING METHODS FOR MONITORING WHALE SHARKS IN AUSTRALIAN WATERS

The most common techniques used for monitoring whale shark populations are variants of capture-mark-recapture/resight (CMR/S) approaches, where animals are individually recognisable so that they can be followed through time for the calculation of demographic rates (Lebreton et al. 1992). Individual recognition can be achieved by applying an artificial mark to an animal or by using an animal's natural markings (Neumann et al. 2002). The former technique is pervasive in ecological studies, ranging from the purely theoretical (Booth 2004) to the highly applied (Kohler & Turner 2001) and has been used in both marine and terrestrial environments on taxa ranging from insects (Auckland et al. 2004) through to whales (Watkins et al. 1993).

Though successful in many situations, the physical marking or tagging of animals is not without drawbacks. For example, the application of artificial marks to wildlife can alter natural behaviour and reduce individual performance (Gauthier-Clerc et al. 2004). The marking process itself may also be disruptive (Bateson 1977) due to the necessity of handling and restraining for mark application (Ogutu et al. 2006) and the loss of marks over time (Bradshaw et al. 2000), and the non-reporting of retrieved marks (Schwarz & Seber 1999) may cause severe bias in parameter estimates (Stevick et al. 2001). Additionally, there are often a host of ethical and welfare issues that can arise from the application of permanent or semi-permanent marks (McMahon et al. 2006, Wilson & McMahon 2006). The artificial marking of individuals may also be costly and impractical when dealing with large populations (Kelly 2001).

Due to the vulnerable status of whale sharks, it is essential that sampling techniques are as benign as possible to ensure minimal impact on the remaining individuals. The size of whale sharks also limits sampling techniques to those that do not require the physical restraint of the animals for mark application. The aim of this chapter is to describe the techniques trialled for individual identification of whale sharks at Ningaloo Reef.

2.1 STUDY SITE AND SAMPLING

Whale sharks frequent Ningaloo Reef, WA (22° 50' S, 113° 40' E) between March and July each year (Figure 2.1). Due to their cryptic nature, light planes are used to locate animals. Once an animal is spotted at the surface, the light plane circles above while the research vessel (Figure 2.2.) is directed towards vicinity of the shark. When alongside an animal, researchers are able to swim to the shark from the boat to collect data (Figure 2.3).

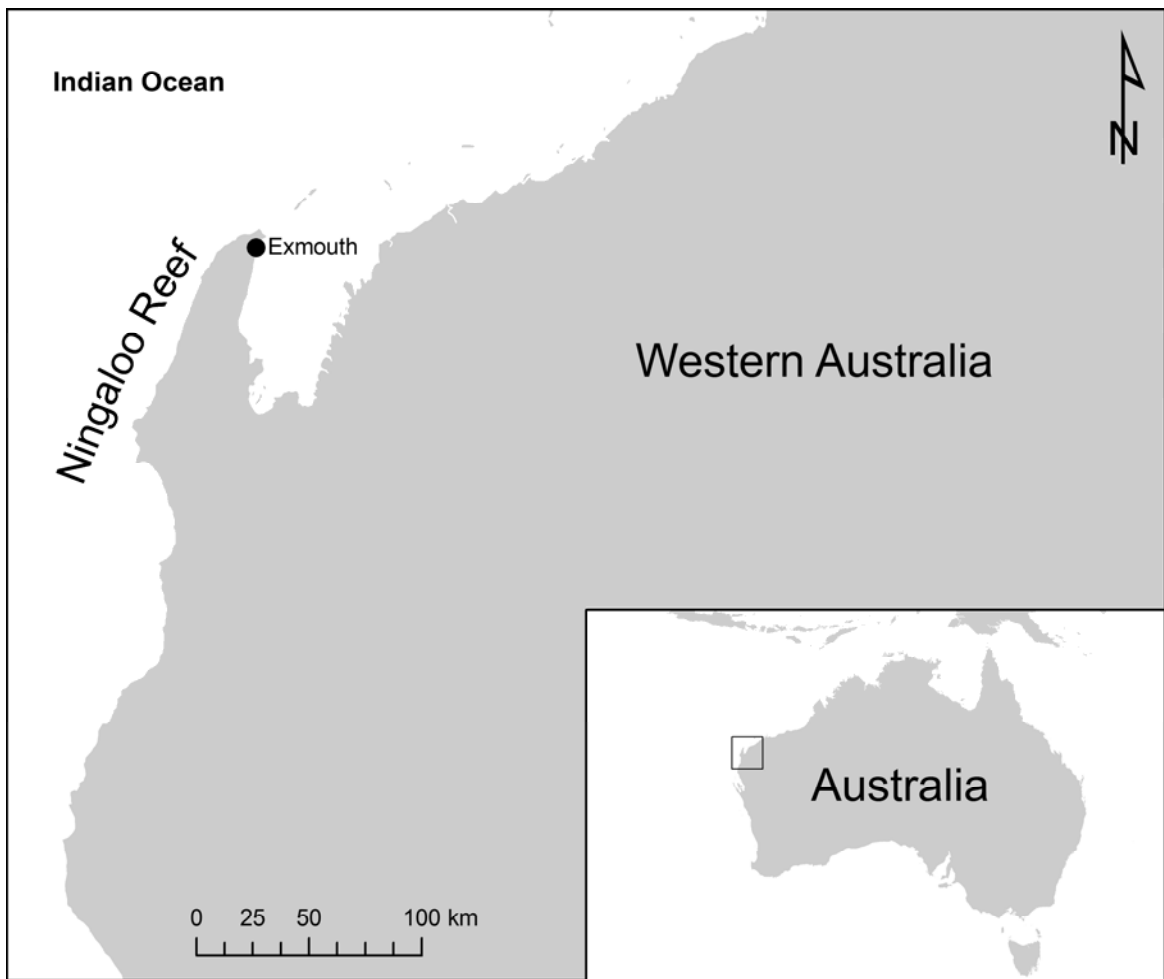


Figure 2.1. Map of study site, Ningaloo Reef, WA.



Figure 2.2. Research vessel used for whale shark work during 2005-7. (Photo – © C. Speed).



Figure 2.3. A) Researchers exiting vessel in pursuit of whale shark. B) Researcher positioning in relation to whale shark for photo-id (far) and satellite tag attachment (close) (Photos – © F. Baronie).

2.2 CONVENTIONAL TAGS

Prior to the 1990's there was relatively little reliable information on the abundance and distribution of whale sharks. At Ningaloo, the only available information was based on direct counts of sharks from boat and aerial surveys (Taylor 1996). Taylor (pers. comm.) attempted to tag whale sharks using conventional fish tags, which were numbered plastic spaghetti-shaped tags inserted by a speargun below the dorsal fin (Fig. 2.4).



Figure 2.4. The left flank of a whale shark tagged using a conventional fish tag (yellow dart below dorsal fin). (Photo – © G. Taylor).

These tags allowed researchers to recognise immediately whether a shark was a new individual or a resight, and also acted as a form of double tagging when used in conjunction with identification photographs (Geoff Taylor, pers. comm.). The physical tagging of whale sharks using standard tags has been discontinued at Ningaloo Reef due to tag loss and advances in photo-identification and satellite tagging technology; however, similar tags are still being used to assist with individual identification of whale sharks in other aggregations such as in the Seychelles (Taylor 1996, Rowat 1997).

2.3 PHOTO-IDENTIFICATION

Photo-identification is one of the most effective and popular methods of recording natural markings of an animal. It permits individual identification, which can then allow the study of

animal movement patterns, site fidelity, population size and other parameters (Karlsson et al. 2005), with the only field requirement being a suitable camera. In addition to the other benefits of non-intrusive 'marking' of individuals, this method allows storage of photos in a library for cross-matching and generation of capture-history matrices (Fujiwara & Caswell 2001, Meekan et al. 2006, Bradshaw et al. 2007). There have been an increasing number of photo-identification studies of long-lived animals that rely on natural markings, including predatory cats (Kelly 2001, Karanth & Nichols 1998, Maffei et al. 2004, Ogotu et al. 2006), cetaceans (Hammond et al. 1990), and elasmobranchs (Arzoumanian et al. 2005, Domeier & Nasby-Lucas 2006, Meekan et al. 2006, Van Tienhoven et al. 2007b).

Image capture techniques vary among studies largely due to the accessibility and ease of observation of study animals. In recent photo-identification studies, most images have been captured using digital or video cameras. Images may be captured directly on land (Kelly 2001), remotely by camera trap (Karanth, 1998 #270; Maffei, 2004 #293}), by aerial photography (Hiby & Lovell 2001), on the surface of the ocean (Hiby & Lovell 2001, Langtimm et al. 2004, Parra et al. 2006), as well as underwater (Corcoran & Gruber 1999, Arzoumanian et al. 2005, Castro & Rosa 2005, Domeier & Nasby-Lucas 2006, Meekan et al. 2006, Van Tienhoven et al. 2007b). Underwater photography has a host of problems that are not associated with standard photographic techniques (Meekan et al. 2006) in terrestrial environments, such as light refraction and backscatter from particulate matter in the water. These issues, as well as the complicating factor of maintaining the line of sight of animals being photographed, can make collection of underwater images for photo-identification particularly challenging.

The standard method of photographing whale sharks for photo-identification captures images while swimming along the flank of the animal. The area on the flank of sharks directly behind the 5th gill slit is typically chosen for use for identification of whale sharks (Figure 2.5) for a variety of reasons, including consistency with past studies, the lack of contortion of this part of the animal during swimming and also because of the ease with which photographers can focus on this area (Arzoumanian et al. 2005, Meekan et al. 2006). In addition to the host of problems associated with underwater photography, whale sharks swim at a speed of approximately 2 knots, which makes taking clear photographs exceedingly difficult, especially in rough weather (Meekan et al. 2006).

Photo-identification studies of whale sharks are relatively new in comparison to photo-identification of marine mammals. Nevertheless, similar problems associated with the manual identification and matching of individuals by eye have emerged. Image libraries can be examined manually (by eye) to build a history of individual matches (Meekan et al. 2006); however, as the number of photos in a library increases beyond a person's capacity to process the potential candidate matches reliably, the development of faster, automated techniques to compare new photographs to those previously obtained is required (Mizroch et al. 1990, Arzoumanian et al. 2005). Several automated matching algorithms have been trialled with some success (e.g., Mizroch et al. 1990, Wilkin et al. 1998, Evans 2003, Hillman et al. 2003, Arzoumanian et al. 2005, Lapolla 2005, Urian 2005), but these are often highly technical, species/morphological feature specific, or unavailable for public use.

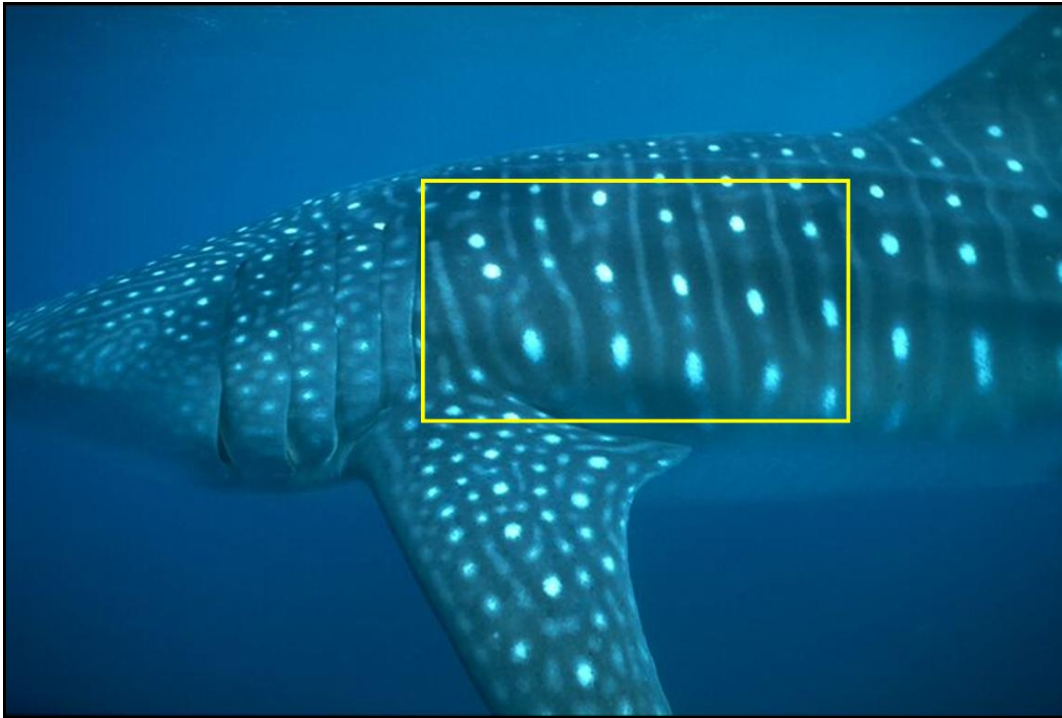


Figure 2.5. Standard reference area use for photo-identification of whale sharks (Photo – © G. Taylor).

The methods of computer-assisted image matching currently used for photo-identification of whale sharks are: 1) a method adopted from a stellar-pattern recognition software by NASA (Arzoumanian et al. 2005), and 2) a program developed for matching the spot-patterns of grey nurse (*Carcharias taurus*) sharks called Interactive Individual Identification System (I³S) (Van Tienhoven et al. 2007b) Van Tienhoven et al. 2007a. The first method is currently being employed to match images in the online Ecocean database (repository), where the public can submit photos taken while swimming with whale sharks (Arzoumanian et al. 2005). The matching algorithm incorporated into the software is insensitive to image magnification, rotation, and inversion via the use of triangulated triplets of coordinates, which can then be used to match similar patterns from the database (Arzoumanian et al. 2005). This method is almost completely automated, but like other such methods, the final validation process involves a manual by-eye component. This software has been used successfully to identify individual whale sharks; however, the program is of little use to researchers as the software is not open-access so its limitations and biases cannot be investigated. The inaccessibility of the software also means that matching cannot be done by individual researchers. In contrast, the I³S program can be freely downloaded from the internet (see www.reijns.com/i3s) and can successfully identify and match individual sharks (Speed et al. 2007). Furthermore, a validation technique using information theory has been developed to aid this program, providing the user with a relatively non-subjective means of confirming individual matches (Speed et al. 2007). The limitations, protocol and use of this matching software is discussed in Chapter 4.

Until recently, data collection for photo-identification studies of the whale shark population at Ningaloo Reef had been done largely in an *ad hoc* manner. Photographs were taken by various researchers, tourists and ecotourism operators and libraries were held separately. Recently, a new initiative to encourage collaboration and standardise effort has been implemented by the Western Australia Department of Environment and Heritage (DEC), where all photographs and measurements taken by researchers and tour operators are submitted to DEC at the end of each whale shark season. This has vastly increased the size of the library of photographs available for researchers.

2.4 TISSUE SAMPLING – COLLECTION TECHNIQUES

2.4.1 Faecal material

As an alternative to traditional tagging methods and photo-identification, individual animals can be also be identified using genetic information from nuclear microsatellite markers (Palsboll et al. 1997). Within the field of ecology, a number of methods have been trialled for obtaining tissue samples such as biopsies, sloughed skin, shed hair and faecal material collection (Palsboll et al. 1997). The collection of scat/faecal samples from animals for individual identification and mark-recapture purposes has been used in a number of circumstances (see review by Lukacs & Burnham 2005). Indeed, one such sample was collected from a whale shark during the 2007 research trip (Figure 2.6). This collection technique has been used successfully to identify prey species of whale sharks (Jarman & Wilson 2004); however it is unlikely that this would be viable for individual identification of sharks due to the relatively rare observation of the deposition of faecal matter, as well as the rapid dispersion of faeces by currents.



Figure 2.6. Whale shark faecal sample collected at Ningaloo Reef (photo – © F. Baronie)

2.4.2 *Biopsy Spear*

During April and May of 2005-2007 genetic samples were collected using a Hawaiian-sling pole that had a biopsy tip fastened to the end of the spear (Figure 2.7A). The tip was made by Ceta-Dart (Virum, Denmark – Finn Larsen fl@difres.dk), constructed of stainless steel and was 40 mm in length and 27 mm in diameter (Figure 2.7B). Samples were taken from the sub-dermal layer of either the upper-left or the upper-right flank of the sharks. Samples were then placed in vials of 10 % salt-saturated dimethylsulfoxide (DMSO) for genetic analysis (Figure 2.7C). The biopsy tip was cleansed with bleach after each use to avoid cross-contamination of samples.

This method of obtaining tissue samples from whale sharks proved to be successful, once the researcher had mastered the spearing technique. One major disadvantage of the technique was that once speared, sharks rarely remained in the immediate vicinity for further observations. For this reason, genetic samples were taken after length and sex information was collected and identification images had been captured.

2.4.3 *Microplanes*

Microplanes were trialled as an alternative and possibly less intrusive sampling technique than the biopsy probe. Two types of microplanes were trialled that had differing gauges of blade:

1. Coarse Grater – stainless steel, 12.4 × 5 cm grating area, 27.5 cm length and 6.88 cm width (Figure 2.8A).
2. Medium Ribbon grater – stainless steel, 12.4 × 5 cm grating area, 27.5 cm length and 6.88 cm width (Figure 2.8B).



Figure 2.7. A) Hawaiian-Sling pole spear with biopsy tip attached, B) .Biopsy tip for tissue sampling of whale sharks, C) Biopsy tip and whale shark tissue sample being placed in vial of DMSO (Photos A & B – © C. Speed & photo C – © F. Baronie).

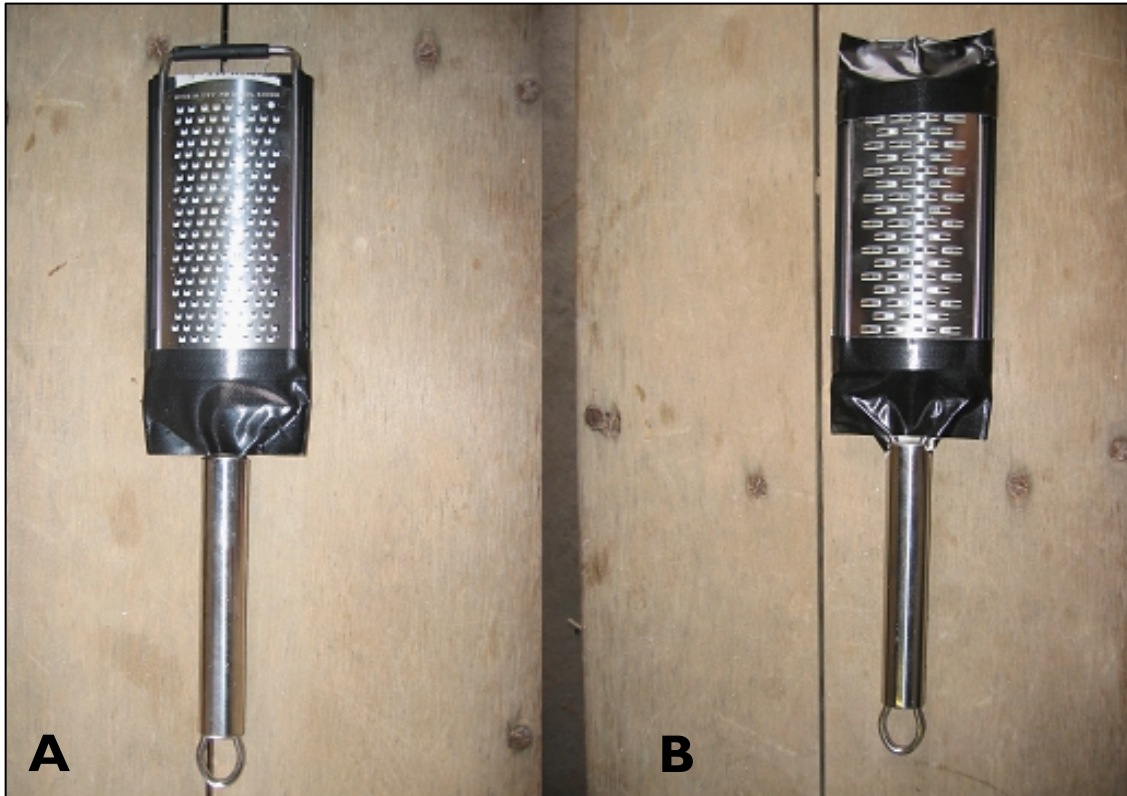


Figure 2.8. Microplanes trialled for taking skin samples from whale sharks. A) Coarse grade, B) medium ribbon grade. (Photos – © C. Bradshaw).

Electrical tape was used to seal the underside of the microplanes, so that skin samples would be retained. While swimming along side the animals, microplanes were used to remove skin from the flank by scraping in a forward motion (the opposite direction to which the denticles face). A number of potential issues arose with this technique: 1) inadequate amounts of skin were removed by the micro plane due to the toughness of whale shark skin, 2) the convoluted nature of the microplanes meant that sterilization between sampling occasions was laborious, 3) samples may be contaminated by oxidation due to prolonged contact with sea water, over multiple sampling occasions and 4) whale sharks appeared to respond negatively to the scraping sensation, often more noticeably than their reaction to the biopsy spear.

To surmise, the ineffectiveness of the microplanes to collect skin samples, coupled with other logistical problems, meant that this technique was not suitable for collecting genetic samples for individual identification of whale sharks. The toughness of whale shark skin limits the use of scraping devices for skin collection purposes. For this reason, biopsy spears provided the most appropriate means to collect tissue samples for genetic studies.

2.5 SATELLITE TRACKING OF WHALE SHARKS

Satellite tracking to monitor large- and small-scale movement patterns of animals commenced during the mid- to late 1980's (Fancy et al. 1988). It was not until the early to mid- 1990's however that this technology was used successfully to monitor the movement patterns of whale sharks (Eckert & Stewart 2001). The success of this study subsequently led to numerous other tracking studies of the horizontal and vertical movements of whale sharks (see Eckert et al. 2002, Rowat & Gore 2006, Wilson et al. 2006). While this method of monitoring is more expensive than using conventional tags or photo-identification, satellite tags allow researchers to observe horizontal and vertical movement patterns over shorter time scales and at higher spatial resolution. A summary of the number and type of satellite tags that have been deployed on whale sharks by our study is given in Appendix 2.

2.5.1 Satellite tags

The satellite tags used to track movement patterns of whale sharks at Ningaloo Reef were made by Wildlife Computers (Redmond, Washington, USA) with custom tag housings and an applicator developed by the Marine Technology Group at the Australian Commonwealth Scientific and Industrial Research Organisation (CSIRO) Marine and Atmospheric Research (Figure 2.9).

The satellite transmitters were contained in a torpedo-shaped float that was attached to the shark's dorsal fin via a one-metre tether and fin clasp. Fin clasps were covered with neoprene to reduce the risk of infection caused by friction of the clasp rubbing on the fin. Tags transmitted location, depth and water temperature information to polar-orbiting satellites fitted with Argos receivers (Myers et al. 2006).



Figure 2.9. A) Applicator & bolt, B) Applicator, fin clasp and satellite tag and C) Satellite tag ready for deployment (Photos A & C © – C. Bradshaw, B © – C. Speed).

Each tag was coated with an antifouling agent prior to attachment to minimise algal growth that can increase drag. The tags were attached to the base of the leading edge of the first dorsal fin by the custom designed applicator that fired a stainless-steel bolt through the fin clasp and fin (Figure 2.9 & Figure 2.10). A snorkeler attached tags while swimming alongside the shark.

A total of 6, 5 and 4 towed Splash satellite tags were attached to sharks during the April/May field trips to Ningaloo Reef in 2005, 2006 and 2007 respectively. Tags were retained for up to 4 months in 2005, however in 2006 and 2007 towed tags were removed by the animals after only a few weeks (2006) or months (2007). The application of satellite tags was relatively successful; however, the trigger mechanism of the applicator misfired on a few occasions. The lower retention time of the towed tags in 2006 and 2007 were most likely due to a combination of sharks actively trying to dislodge the tags on the reef and weak attachment to the dorsal fin due to problems with the applicator.



Figure 2.10. A double-tagged whale shark showing fin clasp on leading edge of 1st dorsal fin and satellite tag (above left pectoral fin) and 2 PSATs below dorsal fin on left and right flanks (Photo – © Department of Environment and Conservation). * Note: The orange material below the satellite tag is biofouling, most likely a species of brown algae.

2.5.2 Fin tags

As with the satellite tags, fin tags were attached with the same applicator and to the same position on the shark (i.e., the base of the leading edge of the first dorsal fin). Unlike the satellite tags, fin tags did not have a tether that connected the clasp and the transmitter. Rather, fin tags housed the attachment device and transmitter in one unit (Figure 2.11). As with the fin clasps used to attach satellite tags, fin tags also had a neoprene covering to minimise friction.



Figure 2.11. Fin tag without neoprene cover (Photos – © C. Speed).

The aim in placing the satellite tag in the fin clasp was to avoid issues of fouling of the towed tag by weed and flotsam (see Fig. 2.10) and to attempt to prevent the shark catching the tether on the reef and pulling the tag off. In both 2006 and 2007 all fin tags deployed on sharks failed to report position data to satellites and this approach has now been discarded. These tags were adapted from an approach in common and very successful use in other species such as great white and salmon sharks. Likely reasons for failure in whale sharks was due to the dorsal fin not clearing the water surface for periods of time sufficient for contact with a satellite to be made by the transmitter.

2.5.3 Pop-up Archival Satellite Tags (PSAT)

Both Wildlife Computers and model PTT-100, Microwave Telemetry, Inc., Columbia, MD, USA PSAT tags were deployed on whale sharks at Ningaloo Reef. (Figure 2.12). These tags measure and store light, depth and temperature at pre-determined intervals, and then later transmit raw data (Microwave tags) or data summaries (Wildlife Computer tags) to Argos satellites when tags have detached and floated to the surface (Wilson et al. 2006). In the case of Wildlife Computer tags, if the tag is retrieved after pop-off the entire archive can then be downloaded.



Figure 2.12. PTT-100, Microwave Telemetry Pop-up archival tag showing titanium dart and tether. (Photo - © S. Wilson)

Prior to deployment, each tag was coated with an antifouling agent to help minimise the settlement of algae and other micro-organisms. PSATs were connected to a titanium dart by a tether of either monofilament or nylon-coated stainless steel (Wilson et al. 2006). PSATs were deployed using a Hawaiian-sling polespear (Figure 2.13), with each dart being embedded into either the left or right flank of sharks below the first dorsal fin. Darts were implanted several centimetres into the sub-dermal tissue on the dorsal surface of the animal near the first dorsal fin (Wilson et al. 2006) (Figure 2.14).

A total of 15, 9, 5 and 1 PSATs were deployed during the 2004, 2005, 2006 and 2007 field trips at Ningaloo respectively. The lower number of deployments in 2007 reflects the fact that very few whale sharks were seen in this year, probably as a result of El Nino effects on oceanographic phenomena in the Ningaloo Reef region (see Chapter 6 for a detailed analysis of whale shark abundance patterns in relation to climatic events). PSATs were also deployed at Ningaloo in 2002 and 2003. For analysis and discussion of the track and diving information obtained from these earlier deployments, see Wilson et al. 2006.



Figure 2.13. Application of Pop-up Archival Tag (PSAT). (Photo - © C. McLean)



Figure 2.14. PSAT tag embedded in sub-dermal layer of whale shark flank/dorsal fin. (Photo- ©C. McLean)

3. GENETIC SAMPLING OF WHALE SHARKS

3.1 OVERVIEW

The development of microsatellite markers for genetic tagging has been a key aim of the project. Unfortunately, the protocols to refine markers and develop libraries proved to be a far greater technical challenge than was originally anticipated. Rather than taking the 8 months of laboratory work, this took 24 months to be completed. Below we detail the laboratory protocol and results to date. We have completed the microsatellite libraries and aim to publish this work in late 2008. Despite these technical problems, we also contributed to a worldwide study of the genetics of whale sharks. To assess the global genetic relationships of whale sharks, the collaboration sequenced complete mitochondrial DNA control regions from sharks in all ocean basins. We observed 55 polymorphic sites and 28 haplotypes in 50 individuals and found high haplotype ($h = 0.95 \pm 0.02$) and nucleotide diversity ($\pi = 0.013 \pm 0.007$). The control region had the largest length variation yet reported for an elasmobranch (1,143 - 1,332 bp). Phylogenetic analyses revealed no geographic clustering of lineages. The most common haplotypes were detected from the western Atlantic Ocean and the eastern Pacific Ocean. The absence of population structure across the Indian and Pacific oceans indicates that oceanic expanses and land barriers in Southeast Asia are not impediments to whale shark dispersal. We did, however, find population structure (AMOVA, $F_{ST}=0.153$, $P<0.001$) between the Atlantic and Indo-Pacific ocean basins. Though there may be undetected fine-scale population structure within ocean basins, in contrast to other sharks that have global distributions, we think it is unlikely that there are cryptic evolutionary divisions in this species. Discovery of the mating and pupping areas of whale sharks is key to further population genetics studies. In any event, the global pattern of shared haplotypes in whale sharks is a compelling argument for development of broad international approaches for management and conservation of whale sharks.

3.2 MICROSATELLITE MARKERS

3.2.1 Introduction

Genetic tagging of individuals is emerging as a potential alternative to standard tagging techniques that allows researchers to ask questions in relation to contemporary patterns of genetic divergence, population size, and gene flow (Palsboll 1999). Unlike many tagging methods, genetic markers (tags) have the added benefit of existing in all animals and being permanent (Palsboll et al. 1997), which is a vital assumption of capture-mark-recapture (CMR) techniques (Seber 1982). Thus, microsatellite data lend themselves to abundance estimation in a similar fashion to traditional identification methods (Palsboll et al. 1997).

Tissue samples are required prior to DNA extraction and analysis, which can be obtained either using intrusive or non-intrusive techniques. A number of intrusive techniques were detailed in Chapter 2 of this report; however, non-intrusive methods can also be used under certain conditions (e.g., Lukacs & Burnham 2005). Obtaining consistent samples using non-intrusive methods in the ocean can be problematic and often in these situations the DNA in samples may be degraded, which can in turn lead to analysis problems such as 'allelic drop out' (Palsboll 1999). Non-intrusive sampling may also lead to an insufficient quantity of DNA to carry out analysis (Bilgmann et al. 2007). To avoid these potential problems, the use of biopsies (Lambertsen 1987) have been adopted for tissue sample collection of large marine animals (Parsons et al. 2003) and are recommended for whale sharks (Chapter 2)

Tissue sampling and molecular analysis have not been attempted to date for whale sharks, therefore information pertaining to gene flow between whale shark populations and parent-offspring relationships are unknown. Additionally, microsatellite markers provide a validation technique for current photo-identification analyses, strengthening demographic estimates. The aim of this section is to describe the methods used to isolate microsatellite-containing fragments from whale sharks DNA collected at Ningaloo Reef.

3.2.2 Methods

3.2.2.1 Construction of enriched microsatellite library

We employed the strategy used by (Kandpal et al. 1994) to isolate microsatellite-containing fragments (Figure 3.). In this procedure, genomic DNA fragments containing the desired repeats are hybridized to a repeat probe that has been biotinylated. These hybrid fragments are subsequently captured by a solid matrix to which avidin is covalently bound. Non-specifically DNA fragments are eliminated by washes, and the repeat-containing fragments are eluted and cloned to produce a library. This library should contain 20-90% repeat-containing fragments.

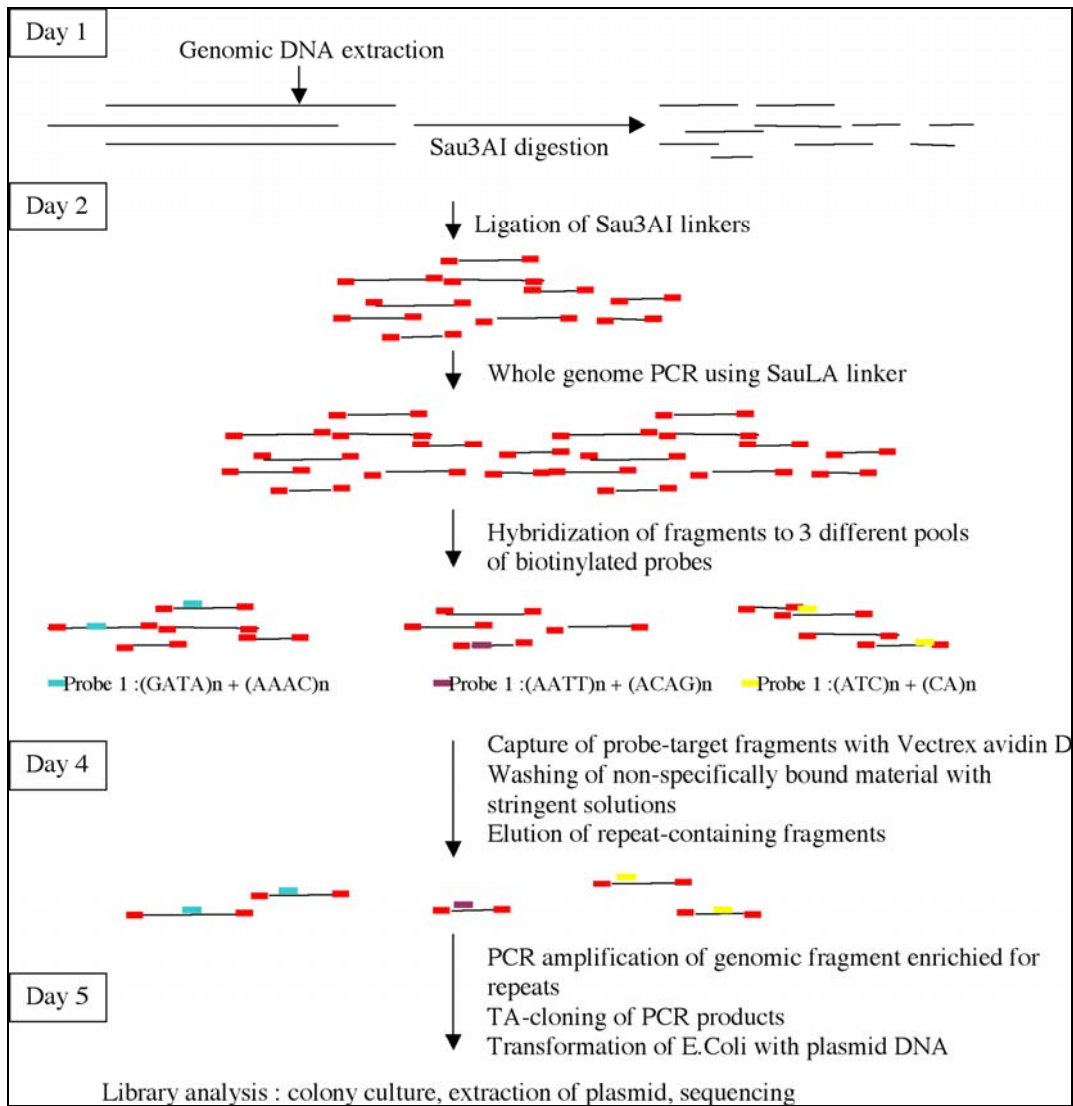


Figure 3.1. Steps followed to isolate microsatellite-containing fragments.

3.2.3 Results

First attempts to use this technique did not give any interpretable results (Figure 3.2). It appeared as if all the whale shark DNA, with or without any biotinylated probe, had been fixed non-specifically to the Vectrex avidin D matrix. For this reason, we decided not to clone PCR product and to make a second attempt with fresh DNA (Figure 3.3). We also decided to change the Vectrex avidin protocol and use a different buffer and try a second elution at 85°C. Thus, we extracted DNA from 4 individuals and pooled the DNA to obtain 5µg of fresh DNA.

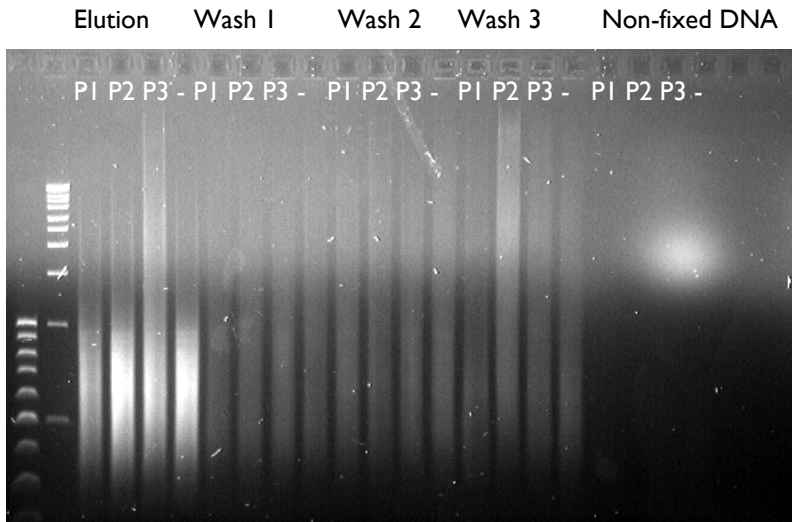


Figure 3.2. Last PCR results before cloning P1, P2, P3: probe 1, 2 or 3 - : control without probe.

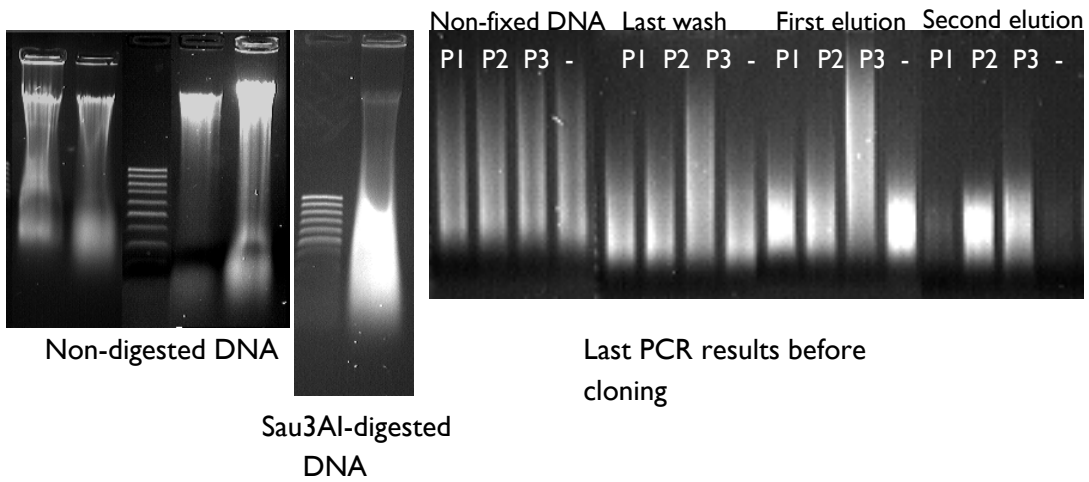


Figure 3.3. Second trial to analyse whale shark DNA.

These were encouraging and we attempted enrichment for twelve different microsatellite motifs: CA-, AAC-, TACA-, TAGA-, GA-, ATG-, AAAC-, CATC-, AAG-, AAT-, AAAG- and CAGA-. The libraries yielded microsatellites as follows:

- CA- seven out of eight sequences contained a microsatellite
- AAC- one out of nine sequences contained a microsatellite
- TACA- zero out of nine sequences contained a microsatellite
- TAGA- four out of nine sequences contained a microsatellite
- GA- six out of nine sequences contained a microsatellite
- ATG- one out of eight sequences contained a microsatellite
- AAAC- one out of nine sequences contained a microsatellite
- CATC- zero out of nine sequences contained a microsatellite
- AAG- one out of nine sequences contained a microsatellite
- AAT- zero out of nine sequences contained a microsatellite
- AAAG- one out of nine sequences contained a microsatellite
- CAGA- three out of eight sequences contained a microsatellite

Based on these results we obtained sequences from an additional set of 64 clones, drawn from three of the libraries that yielded microsatellites as follows:

- CA- 20 out of 20 sequences contained a microsatellite
- TAGA- 11 out of 21 sequences contained a microsatellite
- GA- 17 out of 22 sequences contained a microsatellite

Sequences were then examined to identify duplicates that might be present in opposite orientation, or which had not been noted upon examination of the electropherograms. In total, we identified 73 different microsatellite-containing clones from the three libraries. We designed PCR primers for 54 microsatellite-containing clones that were designed using DesignerPCR version 1.03 (Research Genetics, Inc.).

The final microsatellites selected for the library and provided with design-tested primers are shown in Appendix I.

3.2.4 Conclusion

Despite initial problems, the laboratory analysis protocols and microsatellite libraries have now been established for genotyping of whale sharks. It now remains to collect biopsy samples from large numbers of both the Ningaloo and other Indian Ocean populations firstly to validate photo-identification techniques and secondly, to begin to establish patterns genetic divergence, population size, and gene flow of whale sharks in the Indian Ocean region.

3.3 POPULATION GENETIC STRUCTURE OF THE WHALE SHARK (*RHINCODON TYPUS*)

3.3.1 Introduction

The vastness of Earth's oceans may often conceal regional biological processes particularly for pelagic and highly migratory species. For example, many sharks and tunas mature and forage far from shore. Other species like pinnipeds and sea turtles may approach continental or island shores only occasionally to breed or rest. Moreover, many large marine vertebrates often have complex migratory behaviours that vary with age and sex (Brown et al. 1995, Craig & Herman 1997, Hughes et al. 1998, Bowen et al. 2005, James et al. 2005, Carlsson et al. 2007).

Though the natural histories of many pelagic migrants have become better known during the past few years, little is still known about the biology and biogeography of whale sharks (*Rhincodon typus*). Whale sharks appear to be widely distributed in tropical and warm temperate seas (30°N and 35°S) except, perhaps, in the Mediterranean (Compagno 2001). Most information about general distribution, however, is either from seasonal sightings in scattered locations or anecdotal observations (Colman 1997). Aggregations of whale sharks have been routinely reported off Ningaloo Reef (Australia), Gladden Spit (Belize), Yucatan peninsula, Baja California (Mexico), India, Taiwan, Japan, and the Philippines (Taylor 1996, Clark & Nelson 1997, Colman 1997, Taylor & Pearce 1999, Heyman et al. 2001, Wilson et al. 2001a, Stewart & Wilson 2005, Wilson et al. 2006). Some aggregations occur year-round while others may be associated with seasonal abundance of prey. Most known aggregations are immature sharks and segregation by size and sex may occur in some areas (Colman 1997, Compagno 2001). Even though recent studies have demonstrated the remarkable ability of this species to migrate long distances (e.g., Colman 1997, Compagno 2001, Eckert & Stewart 2001, Wilson et al. 2006) it is not clear whether whale shark populations are panmictic or composed of reproductively isolated subpopulations. Recent indication for tolerance of cold water when diving (Wilson et al. 2006) suggests that temperate and perhaps even sub-polar waters may not be impediments to movements of whale sharks across thermal boundaries. Here, we present the results of a study of the population genetics of this widely distributed marine megavertebate using sequences from the mtDNA control region (CR) to assess the potential population relationships among ocean basins.

3.3.2 Materials and methods

3.3.2.1 Sample collection and laboratory procedures

Skin biopsy samples were collected from 50 whale sharks (Figure 3.4) when they aggregated seasonally in the Gulf of California or Western Australia or were found stranded ashore from 1995 through 2005 at other sites and then preserved in either salt saturated DMSO solution or 95% ethanol and stored at room temperature.

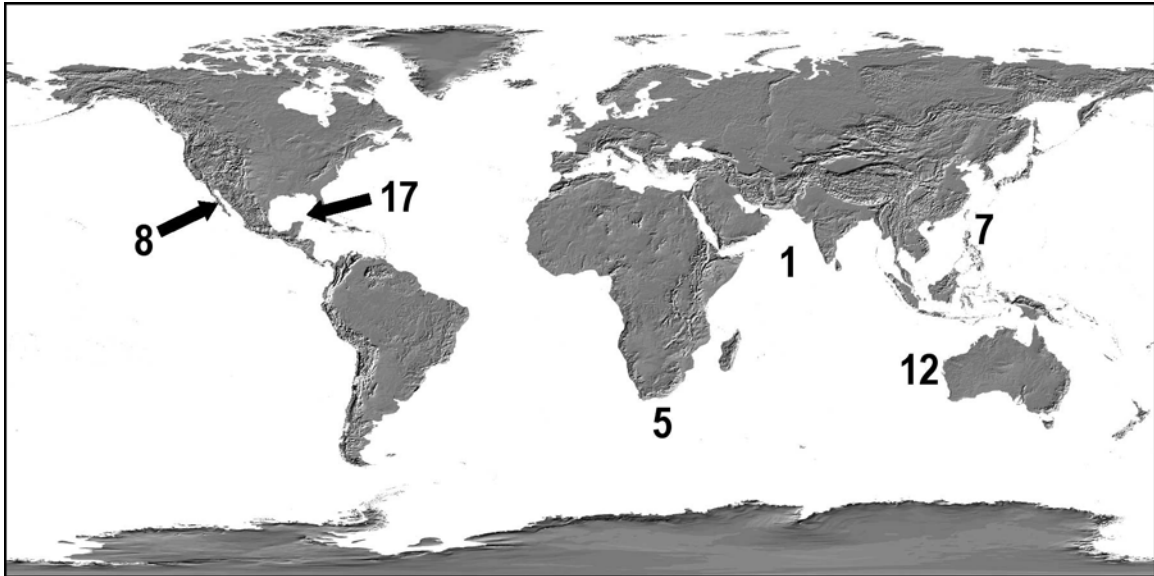


Figure 3.4. Geographic distribution and number of whale shark skin biopsy samples obtained for each geographic location.

We extracted total genomic DNA using a phenol-chloroform-isoamyl alcohol protocol (Sambrook et al. 1989) or 5% Chelex non-boiling protocol (Walsh et al. 1991). The mitochondrial CR was amplified using primers developed within the tRNA^{Pro} (WSCRI-F: 5'-TTGGCTCCCAAAGCCAAGATTCTTC-3') and tRNA^{Phe} (WSCRI-R: 5'-TTGTAACCAAATTATACATGC-3'). Because of the large size of the CR (~1,100 – 1,325 nucleotides), two internal primers were designed to facilitate sequencing of the whole region. Primer WSCR2-R (5'-CTTAATATTTATTGTTCTGGTTTCAGTT-3') was paired with WSCRI-F, and primer WSCR2-F (5'-CTATAATTGATTTAAACTGACATTTG-3') was paired with WSCRI-R producing two, overlapping fragments approximately 950 and 700 bp respectively. Amplification reactions were carried out in 50 µL volumes consisted of 1X Promega buffer (Promega, Madison, WI, USA), 1.25 U of IDProof™ DNA polymerase (ID Labs Inc., Ontario, Canada), 0.8 mM dNTPs, 2 mM MgCl₂, 0.5 µM of each primer, 6.0 µg bovine serum albumen, and 1 – 3 µL of template. Cycling conditions for all primer pairs consisted of 95°C 1 min, 35-40 cycles of 95°C 45 sec, 58°C 60 sec, and 72°C 90 sec with a final extension at 72°C for 7 min. Amplicons were purified with QIAquick kit (Qiagen, Valencia, CA, USA) following the manufacturer's instruction. Both strands were sequenced using an ABI 3730XL Genetic analyzer (Applied Biosystems, Inc., Foster City, CA, USA).

3.3.2.2 Data analysis

Control region alignments were optimized in Sequencher 4.1 (Gene Codes, Ann Arbor, MI, USA) and gaps were introduced to maximize sequence similarity. Analyses were done both including and excluding ambiguous bases and missing data (i.e., gaps). In some analyses, contiguous gaps were treated as single events by omitting all but one of the gaped bases, and gaps were weighted as transitions. In the case of substitutions within gaps, variable positions were retained and gaps were weighted as transversions. The Akaike Information Criteria within ModelTest v3.06 (Posada & Crandall 1998) was used to determine the best-fit model of

evolution. Phylogenetic analyses were done using PAUP* 4.0b10 (Swofford 2003). Gene tree reconstruction was performed using neighbor-joining algorithm (Saitou & Nei 1987), with the optimal distance model identified with ModelTest. Statistical support for the nodes was estimated with 100 non-parametric bootstrap replicates (Felsenstein 1985).

Summary statistics (number of haplotypes, haplotype frequencies, number of polymorphic sites, number of transition and transversions, and nucleotide composition) were estimated in ARLEQUIN 3.0 (Excoffier et al. 2005). Individuals were binned into five groups defined by geographical region: Gulf of Mexico/Florida ($N = 17$) in the northwestern Atlantic; South Africa (5) and Australia (12) in the Indian Ocean; Philippines/Taiwan (7) in the northwestern Pacific; and Gulf of California (8) in the northeastern Pacific. Genetic diversity within localities was measured as the number of DNA mitochondrial haplotypes, haplotype diversity (h), and nucleotide diversity (π) estimated with Nei's corrected average genetic divergence (Nei 1987) incorporating Tamura & Nei's (1993) model of sequence evolution with ARLEQUIN.

We used mismatch distributions for each sample to distinguish between population growth models, especially those invoking past exponential growth and historical population stasis (Slatkin & Hudson 1991, Rogers & Harpending 1992). Population parameters τ , θ_0 , and θ_1 were obtained from ARLEQUIN, where τ is the mutational timescale, and θ_0 and θ_1 are the expected pairwise differences before and after a change in population size (growth or contraction), respectively (Harpending 1994). The mutational timescale is $\tau = 2\mu t$, where t is measured in generations and μ is the mutation rate per generation for the entire sequence ($\mu = m_T\mu$, where m_T = number of nucleotides and μ = mutation rate per nucleotide). The expected pairwise differentiation is $\theta = 2N_f\mu$ where N_f is the effective female population size. Tests for selection also can indicate population expansion and here we apply the algorithms of Tajima (1989) and Fu (1997).

Population subdivision and structure were estimated using an analysis of molecular variance (AMOVA, Excoffier et al. 1992), and pairwise population Φ_{ST} significance test (Cockerham & Weir 1993) as implemented in ARLEQUIN. Significance of Φ_{ST} was determined via nonparametric permutation (Excoffier et al. 1992) with 1,000 data permutations. For AMOVA analyses, we used the distance matrix generated by the model selected with ModelTest (HKY85+I). Population differentiation also was tested using the Raymond and Rousset test based on haplotype frequencies (Raymond & Rousset 1995).

3.3.3 Results

The mitochondrial CR from a total of 50 individuals ranged from 1,143 to 1,332 bp with a mean of 1,236 bp. Nearly all of this size variation was due to indels composed of repeated sequence blocks (Figure 3.5). Considering just the repeat unit structure (i.e., ignoring site substitutions) there were 11 different repeat motifs in the whale shark. Repeated blocks ranged in size from 9 bp (block A) to 64 bp (block E) long. All haplotypes had regions A₁ to D₁, E₂, F₂ E₃, and F₃ to J₃ and this was the motif for the smallest haplotype, H18. The largest haplotype, H9, had all the common repeats, some less common ones, and was the only haplotype to have block I₁. Haplotypes H10 and H11 were similar to H18 except they

possessed blocks E₁ and F₁ (totaling 103 bp) making H10 and H11 the second largest haplotypes.

We also found substitutions between repeated blocks within the same sequence. For example, repeat A₁ differed from A₂ by a substitution of one nucleotide in haplotype H22. Other examples include substitutions shared between different haplotypes like block B, which was repeated twice in nearly all haplotypes. For some haplotypes these were perfect repeats whereas there were single transitional changes in others. Clearly, both larger indel changes and smaller substitutional changes are common in the evolution of whale shark CR.

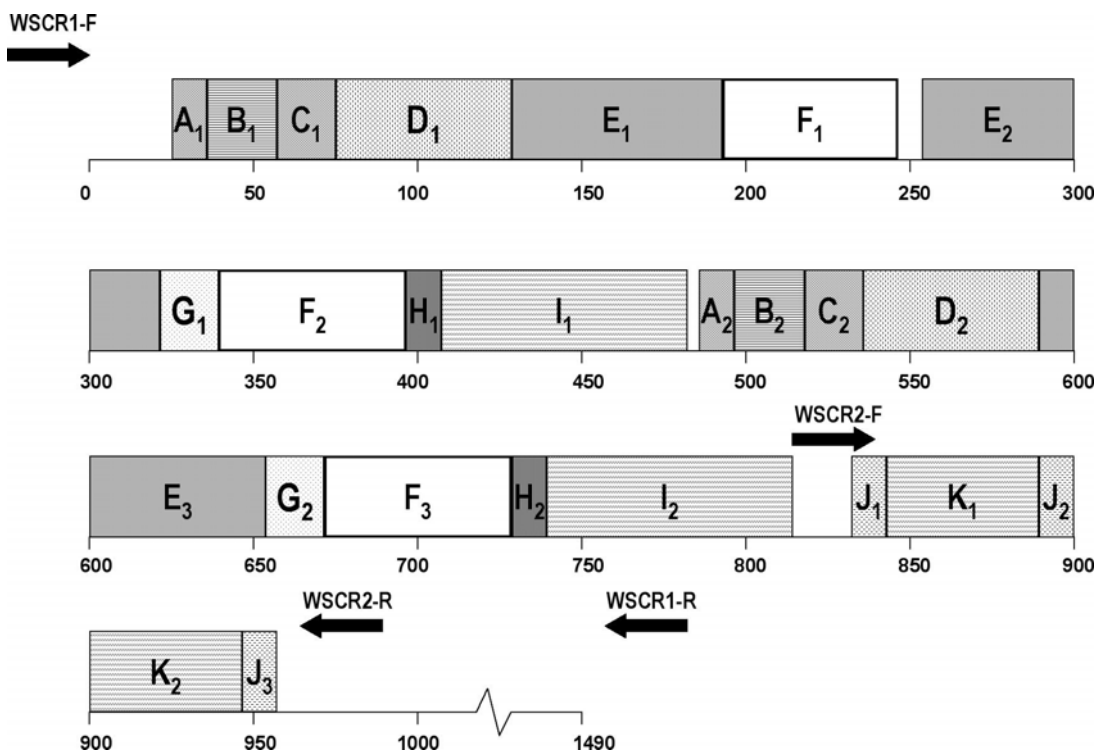


Figure 3.5. Schematic diagram showing the consensus of all 28 haplotypes for the complete CR sequences of the whale shark. Blocks with different patterns represent repeated fragments along the CR sequence. Arrows represent primers used in PCR amplification.

To maximize sequence similarity among all sampled sharks, the complete DNA sequence alignment required multiple gaps of sizes ranging from 1 to 163 bp. There were 55 polymorphic sites, with 35 substitutions (32 transitions and 3 transversions) and 27 gaps resolving 28 haplotypes. Fifteen of those gaps were coded as single nucleotide transitions, while the other 12 were coded as transversions due to substitutions in those regions. Of the fifty-six evolution models tested by ModelTest using the Akaike Information Criteria (AIC), the HKY85+I model (Hasegawa et al. 1985) was selected as the best fit with the proportion

of invariable sites $I = 0.9292$, and base frequencies of A: 0.3487, C: 0.1991, G: 0.1102, and T: 0.3421. Overall, the haplotype diversity (h), and nucleotide diversity (π) were relatively high with $h = 0.90 - 1.0$ and $\pi = 0.007 - 0.016$ (Table 3.1). Among the 28 observed haplotypes, only seven occurred in more than one shark (Table 3.2). Three of those shared haplotypes occurred in a single geographic region and four occurred in four of the regions. Except for some of the Gulf of Mexico haplotypes, there appears to be no phylogenetic clustering (Figure 3.6). AMOVA with HKY85+I distances assigned 87.05% of the genetic variability within and 12.95% among locations. There is statistically significant structure in whale shark populations, with overall $\Phi_{ST} = 0.13$ ($P < 0.005$). The Atlantic population appears to be significantly different from all but the South Africa population (Table 3.3). Moreover, there appears to be divergence only between the Atlantic and the Australian and the Atlantic and northwestern Pacific populations using a test of exact population differentiation based on haplotype frequencies (Raymond & Rousset 1995).

Table 3.1. Location, numbers of individuals (N), number of haplotypes (n), haplotype (h) and nucleotide (π) diversity estimates and standard deviations observed on the CR of the whale shark within five major geographic locations.

Location	N	n	h	π
Atlantic	17	10	0.92 ± 0.05	0.008 ± 0.004
South Africa	5	4	0.90 ± 0.16	0.007 ± 0.005
Australia	12	9	0.91 ± 0.08	0.008 ± 0.004
NW Pacific	7	7	1.00 ± 0.08	0.007 ± 0.004
NE Pacific	8	7	0.96 ± 0.08	0.016 ± 0.009
TOTAL	50	28	0.95 ± 0.02	0.013 ± 0.007

Table 3.2. Geographic distribution of haplotypes found in 50 whale sharks. Sample locations were grouped by geographic proximity (SA – South Africa, NW Pac – Northwestern Pacific, NE Pac – Northeastern Pacific).

Haplotype	Geographic location					Total
	Atlantic	SA	Australia	NW Pac	NE Pac	
H1	3	1	1	—	2	7
H2	—	—	4	1	1	6 ¹
H3	1	1	1	—	1	4
H4	4	—	—	—	—	4
H5	3	—	—	—	—	3
H6	—	2	—	—	—	2
H7	1	—	—	1	—	2
H8	—	—	—	1	—	1
H9	—	—	—	—	1	1
H10	—	—	—	—	1	1
H11	—	—	—	—	1	1
H12	—	—	—	—	1	1
H13	—	—	—	1	—	1
H14	—	—	1	—	—	1
H15	1	—	—	—	—	1
H16	—	—	1	—	—	1
H17	—	—	1	—	—	1
H18	—	—	1	—	—	1
H19	—	—	1	—	—	1
H20	—	—	1	—	—	1
H21	—	1	—	—	—	1
H22	—	—	—	1	—	1
H23	—	—	—	1	—	1
H24	—	—	—	1	—	1
H25	1	—	—	—	—	1
H26	1	—	—	—	—	1
H27	1	—	—	—	—	1
H28	1	—	—	—	—	1
TOTAL	17	5	12	7	8	50

¹ One individual with H2 was sampled in the Maldives but not included here

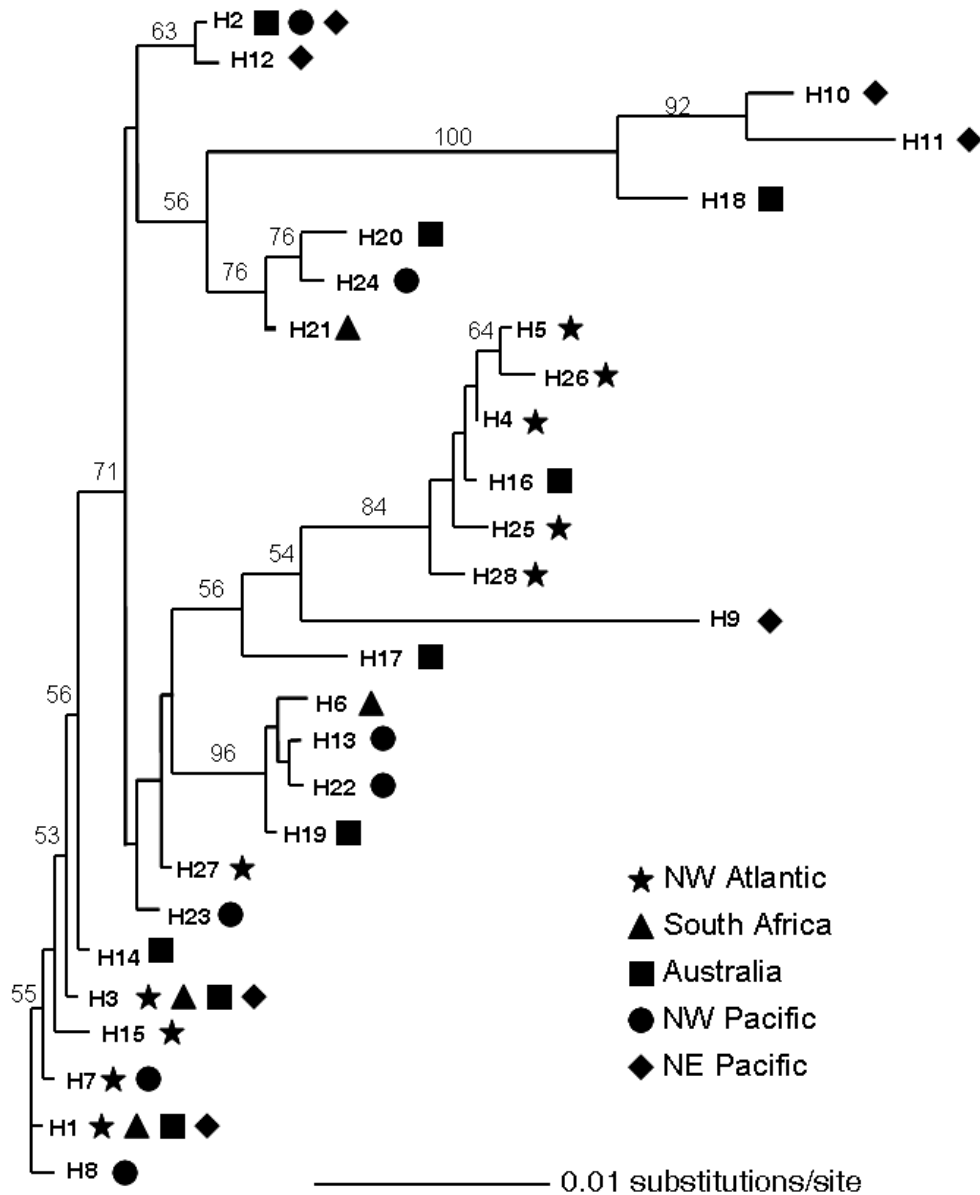


Figure 3.6. Neighbour-joining tree of the phylogenetic relationships of 28 haplotypes. Maximum likelihood distances were estimated using the HYK85+I model of molecular evolution. Bootstrap values greater than 50 are indicated above nodes.

Table 3.3. Estimate of pairwise Φ_{ST} values using both HKY85+I (below diagonal) and Tamura & Nei's (above diagonal) genetic distances. Bolded values were significant ($P = 0.05$) after Bonferroni correction.

Populations	Atlantic	SA	Australia	NW Pac	NE Pac
Atlantic	—	0.238	0.191	0.244	0.241
SA	0.259	—	0.041	0.055	0.080
Australia	0.193	0.018	—	0.048	0.096
NW Pac	0.268	0.120	0.032	—	0.051
NE Pac	0.216	0.007	0.051	0.013	—

The observed haplotype mismatch distribution is significantly different from expectations under constant population size ($P = 0.02$; Figure 3.7). Haplotype H9 (Northeast Pacific), however, was distinct from all other haplotypes (see phylogenetic analysis in Figure 3.6). Forty-four out of 47 pairwise comparisons with > 10 differences included haplotype H9. Most nodes within the phylogenetic tree were moderately to well supported in bootstrap analysis. There was no clear geographic clustering, however, and several haplotypes were shared among regions. Indeed, we detected haplotypes H1 and H3 in virtually all regions.

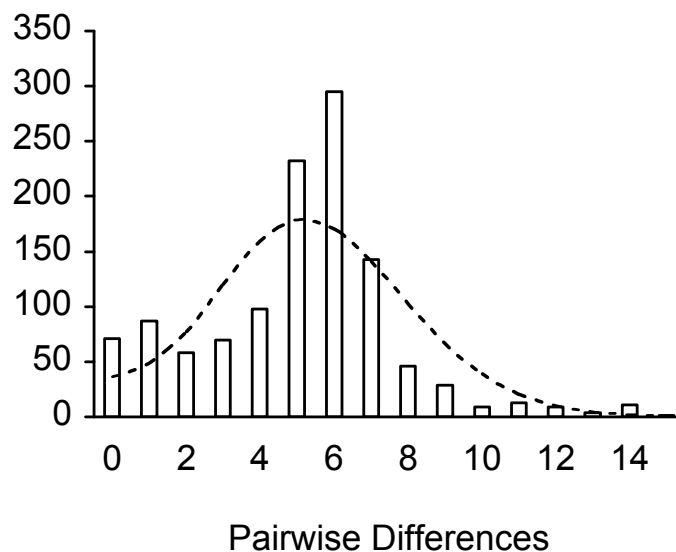


Figure 3.7. Haplotype mismatch distribution. Note that all comparisons with 10 or greater differences between the sequences involve haplotype H9. Dotted line is the expected frequency given a demographically stable population.

The mutational timescale $\tau = 2\mu t$ can be used to estimate coalescence times for populations if generation time and mutation rate (μ) are available. Moreover, the initial and current effective population sizes (N_{f0} and N_{f1}) can be estimated from the pairwise differences θ_0 and θ_1 , if mutation rate is available or estimated. Based on the observation of an adolescent female with an osteological age estimate of 20 years (Wintner 2000), we provisionally apply a generation estimate of 25 years. The control region clock for hammerhead shark, *Sphyrna lewini*, is 0.8% divergence between lineages per million years (Duncan et al. 2006) and is similar to a rate derived from lemon sharks control regions (*Negaprion brevirostris*; J. Schultz, pers. comm.). In contrast, Keeney and Heist (2006) report a rate of 0.4% per million years for control region in the blacktip shark *Carcharhinus limbatus*. We provisionally apply both rates to whale sharks, with the caution that these three species are tens of millions of years divergent from *R. typus*. Results in Table 3.4 indicate coalescence times on the order of 630,000 – 1,250,000 years ago (early Pleistocene), founding effective population sizes of $N_{f0} = 9 - 17$ individuals, and current effective population size $N_{f1} = 145,200 - 290,600$ individuals.

Table 3.4. Population size and age estimates for whale sharks globally.

Parameter		Divergence Rate	
		0.8% per my	0.4% per my
τ	5.878	628,500 yrs	1,258,100 yrs
θ_s	7.850 ± 2.506	33,600	67,200
θ_π	5.150 ± 2.817	22,000	44,100
θ_0	0.002	9	17
θ_1	33.936	145,200	290,600

3.3.4 Discussion

Our survey of whale sharks indicates unusual size polymorphism in the CR, significant population structure between Atlantic and Indian-Pacific ocean basins, and coalescence times on the order of 1 my. Before interpreting these results, we address two prominent caveats:

1) *Sample size is small and lapses in coverage include the South Atlantic, Central Pacific, and South Pacific.* Sample size clearly limits inference. Consequently, we have tempered our corresponding conclusions. There are no directed oceanic surveys for whale sharks, as there are for tunas, billfish, and sea turtles, and the species occurs at low density even in regional aggregates. The sample size of 50 represents ten years of directed effort on our part, and is the only genetic evaluation of this rare and enigmatic species. Nonetheless, though a larger sample size and more complete global sampling may increase the number and frequency of haplotypes, the sharing of haplotypes (H1 and H3) among multiple sharks at the extremes of the geographic range (NW Atlantic and NE Pacific) will not change.

2) *Estimates of coalescence times and effective population sizes are based on tenuous calibrations of generation time and mutation rate, and the latter are derived from distantly-related sharks.* The mutation rate and generation time are simple estimates based on few data, and should therefore not be interpreted quantitatively. Shark mtDNA evolution, however, appears to evolve about an order of magnitude slower than for bony fishes (Martin et al. 1992), which is consistent with our clock estimates used here. Consequently, we think that corresponding estimates are useful in a qualitative sense for determining whether (for example) population histories coalesce at 10^4 , 10^5 , or 10^6 years.

3.3.4.1 Control region morphology

The CR in whale sharks (1,143 - 1,332 bp) is larger than observed in most elasmobranchs. Stoner *et al.* (2003) amplified this region in 52 species of elasmobranchs and products were 1030-1050 bp long except for the barn door skate, *Dipturus laevis*, which was ~1200 bp long. Other studies revealed a CR smaller than the whale shark (*Squalus acanthias* – 1080 bp, Rasmussen & Arnason 1999; *Mustelus manazo* – 1,068 bp, Cao *et al.* 1998; *Heterodontus francisi* – 1,068 bp, Arnason *et al.* 2001; *Scyliorhinus canicula* – 1,050 bp, Delarbre *et al.* 1998), or comparable to the smallest whale shark CR; *Carcharodon carcharias* – 1,146 bp, (Pardini *et al.* 2001). Variation in size in the CR of whale sharks is also higher than reported for other sharks (Kitamura *et al.* 1996, Pardini *et al.* 2001, Keeney *et al.* 2005), with a 189 bp difference between the largest and the smallest amplicon.

Variation in the size of the control region has been reported for a substantial number of bony fishes (Lee *et al.* 1995, Brown *et al.* 1996, Fujii & Nishida 1997, Bentzen *et al.* 1998, Hoarau *et al.* 2002, Rokas *et al.* 2003, Tsaousis *et al.* 2005). It is typically comprised of tandem repeats, as we observed in whale sharks (Figure 3.5). Our initial attempts to PCR amplify the CR of whale sharks using a variety of published shark primers failed, probably due to the highly duplicated nature of the CR. Because the rate and pattern of these mutations is unknown, most studies have not used size variants as population markers. Insertions and deletions of repeat blocks may be relatively common, and homoplasy (convergence on the same number of repeats) is likely to confound any genealogical analysis.

3.3.4.2 Genetic diversity and effective population size

Despite an apparent decline in both catch rates and sighting of whale sharks in various regions (e.g., Stewart & Wilson 2005, Theberge & Dearden 2006, Bradshaw *et al.* 2007), there is still relatively high genetic diversity in the species. Threatened and endangered species are expected, however, to retain historical levels of genetic diversity if the decline has occurred only recently (Roman & Palumbi 2003, Bowen *et al.* 2006). In the only other global surveys of shark CRs, the blacktip shark yielded $h = 0.75 - 0.81$ and $\pi = 0.0020 - 0.0021$ (Keeney *et al.* 2005), and the scalloped hammerhead sharks had $h = 0.80$ and $\pi = 0.013$ (Duncan *et al.* 2006), compared to $h = 0.90 - 1.00$ and $\pi = 0.007 - 0.016$ for whale sharks. These values are low compared to teleost fishes, but such low values of haplotype and nucleotide diversity are observed among many shark species and when using a variety of mtDNA assay methods (cf. Heist 1999, 2004).

The relatively high diversity in whale sharks is surprising, given that the other two globally distributed sharks are common and abundant coastal species, whereas whale shark aggregations are generally small and uncommon. Two general processes might contribute to the relatively high haplotype and nucleotide diversity observed in whale sharks: 1) secondary contact between divergent allopatric lineages or 2) large stable populations. Except perhaps for haplotype H9, the mtDNA phylogeny reveals no evidence of distinct evolutionary lineages that now occur in sympatry. Hence the inference of a large, historically stable population ($N_f \sim 200,000$) deserves special attention. Although the population size of whale sharks is unknown,

though suspected to be declining, it is possible that whale sharks have maintained demographically stable populations until the active fishing for them began very recently. Our coalescence analysis, although tentative, indicates that the most recent common ancestor was around 1 my ago and that genetically effective population size of females was approximately an order of magnitude larger than the current estimate (Table 3.4). This outcome is further supported by the mismatch distribution indication of relatively stable, large populations. Moreover, new whale shark habitats continue to be discovered; in recent years a number of seasonal feeding aggregations have been documented near continental coastline and island habitats (e.g. Rowat & Gore 2006).

The large effective population size may mean that the transient surface feeding aggregations that are most often observed are not the principle habitats of adult whale sharks. Recent studies have demonstrated that at least some whale sharks spend most of each year distant from those coastal sites and often at relatively great depth in cold water (Wilson et al. 2006, Wilson et al. 2007). Although whale sharks appear to lack the anatomical, physiological and behavioral adaptations to conserve heat, the large body mass of adults may provide sufficient thermal inertia to allow extended cold-water exposure (Sims 2003, Wilson et al. 2006). Regardless of the extent of geographic and vertical population movements, it is clear that much of the habitat for this species is still unknown, and population sizes may indeed be considerably larger than expected ($N_f = 22,000 - 67,200$).

3.3.4.3 Population structure

Recent satellite tracking has discovered substantial vagility in whale sharks (Gunn et al. 1999, Eckert & Stewart 2001, Eckert et al. 2002, Wilson et al. 2006). Like traditional tag-recapture studies, satellite tracking provides generally only short-term data and allows limited inference about movements, habitat range, and inter-population exchanges during the shark's life span and is not conclusive about the boundaries of stocks or evolutionary significant units (Moritz 1994, Vogler & Desalle 1994, Waples 1995). Assessing patterns of genetic variation can supplement, enhance, and extend an understanding of population movements, illuminate cryptic evolutionary partitions, and inform management plans. Our studies of mtDNA of whale sharks indicates a population partition between Atlantic and Indian-Pacific ocean basins that might not be easily discovered by electronic tracking of small numbers of sharks.

Our genetic studies indicate that whale shark aggregations from some ocean basins are substantially interconnected. Because our samples were collected from seasonal feeding aggregations, we cannot yet say, however, whether this pattern is due to interbreeding and gene flow among populations or just physical mixing of sharks from different populations in feeding areas. In any event, the high haplotype diversity that we detected is unexpected for multiple sampling of the same evolutionary unit.

Whale shark population structure is low, even against the standards of large migratory fishes. Bluefin tuna (*Thunnus thynnus*) show subtle ($\Phi_{ST} = 0.013$) but significant population structure between western Atlantic (Gulf of Mexico) and the Mediterranean, separated by ~11,000 km (Carlsson et al. 2007). The sailfish (*Istiophorus platypterus*) also is divided among ocean basins

with additional significant population structure also within the Pacific Ocean (Graves & McDowell 2003). Blue marlin lack subdivision within ocean basins, but are clearly divided among ($\Phi_{ST} = 0.217$, Buonaccorsi *et al.* 2001). Marine mammals show similar patterns of inter-ocean differentiation. Humpback (*Megaptera novaeangliae*, Baker *et al.* 1994), minke (*Balaenoptera acutorostrata*, van Pijlen *et al.* 1995), fin whales (*Balaenoptera physalus* Berube *et al.* 1998), and Cuvier's beaked whales (*Ziphius cavirostris*, Dalebout *et al.* 2005) all have pronounced inter-ocean subdivision and some division within an ocean basin between hemispheres. An interesting contrast to these examples is the sperm whale (*Physeter macrocephalus*); a true cosmopolitan species found in all ocean basins including polar regions. Population structuring in the sperm whale ($G_{ST} = 0.03$) is markedly less than that seen in the previously mentioned fish, whales, and whale shark and was only statistically significant among ocean basins. Interestingly, this was only true for the mtDNA but not for nuclear DNA presumably due to inter ocean migration by males. Barriers to movement between ocean basins generally appear to be stronger for marine mammals and large, pelagic fishes than for whale sharks. These comparisons indicate that large pelagic domains can be population barriers to many highly mobile fishes, whereas the only apparent barriers to whale sharks may be geographic and possibly thermal (see below).

3.3.4.4 Marine phylogeography

In recent years there has been renewed interest in the biogeographic barrier between the Indian and Pacific Oceans, apparently due to substantially lower sea levels during glacial maxima (Barber *et al.* 2000). While this barrier is consistent with evolutionary separations in small marine invertebrates (Barber *et al.* 2002), it is a less substantial (albeit significant) population barrier to marine fishes (Bowen *et al.* 2001, Chenoweth & Hughes 2003, Craig *et al.* 2007), including sharks (Duncan *et al.* 2006, Keeney & Heist 2006). Whale shark dispersal ability appears to be unimpeded by this intermittent barrier. This suggests that migratory routes may be flexible enough to accommodate newly-submerged habitats, or that connectivity can be quickly re-established after a barrier of several tens of thousands of years. Regardless of where they are going, whale sharks commonly migrate over large areas and reestablishment of connections across newly removed barriers is likely.

The last tropical connection between the Atlantic and Indo-Pacific ended with the rise of the Isthmus of Panama, about 3.5 MY ago (Coates & Obando 1996). In contemporary biogeography, the southern extensions of Africa and South America are regarded as formidable impediments to tropical connectivity. Yet tropical faunas of the Atlantic and Indo-Pacific, including whale sharks, share connections on a scale shorter than 3.5 MY, indicating dispersal around southern Africa (Bowen *et al.* 1997, Bowen *et al.* 2001). Recent research indicates that such events are rare, being measured on a scale of 10^5 - 10^6 years (Roberts *et al.* 2004, Rocha *et al.* 2005, Bowen *et al.* 2006).

The cold Benguela Current along western South Africa represents a formidable barrier to the dispersal of tropical fishes into the Atlantic (Gibbons & Thibault-Botha 2002). In a compilation of whale shark stranding and sightings in South Africa, Beckley *et al.* (1997) confirmed the occurrence of whale sharks along this frigid Atlantic coast. They suggest, however, that sharks

arriving from the Indian Ocean succumb to the cold upwelling water and quickly perish. Here the observations on thermal tolerance are pertinent to discussions of inter-oceanic dispersal. Wilson *et al.* (2006) noted that whale sharks could inhabit cold water, but certainly not indefinitely. A deep cold-water grazing opportunity in the tropics can be balanced with a quick return to warm surface waters. In the Benguela upwelling system, however, surface waters are as cold as deep and no such relief from cold-water excursions is possible in this region, resulting death. Nonetheless, the sharing of haplotypes between Atlantic, Indian, and Pacific locations indicates a relatively recent connection. Whale sharks could have moved between Atlantic and Indian Ocean during hiatuses of Benguela upwelling that occurred between Pleistocene glacial epochs (Chang *et al.* 1999, Flores *et al.* 1999). Immediately following each ice age (100K to 400K years, but most recently 10K –20K years ago), tropical plankton appear in sediment cores off southwestern African, indicating an avenue of warm water into the South Atlantic (Peeters *et al.* 2004). Contemporary movement also is possible. Warm-core gyres from the Indian Ocean occasionally become entrained in the northward moving Benguela Current, feeding into the Central Atlantic (Flores *et al.* 1999, Penven *et al.* 2001). In either case, historical or ongoing gene flow is apparently limited, as indicated by the moderate and statistically significant global $\Phi_{ST} \approx 0.13$.

Finally, the sharing of haplotypes may simply be due to the retention of ancestral polymorphisms. We consider this unlikely, given the low phylogeographic signal, multiple shared haplotypes, and pattern of high connectivity. Even so, retention of ancestral polymorphisms is characteristic of large, stable populations, a possibility raised by coalescence analyses.

3.3.4.5 Conservation implications

This first genetic survey of whale sharks indicates significant population structure throughout their global range. Management units for whale sharks may encompass 8,000 km in the Atlantic, and over 16,000 km in the Indian-Pacific ocean basins. Regardless of the potential for cryptic population subdivision, any management plan for whale sharks must consider that feeding aggregations drawn from a broad geographic range area in a single location. Unilateral management in any political jurisdiction will be inadequate for a highly mobile species that may travel through several political jurisdictions. Indeed, data from tracking studies of shark movements and our mtDNA survey both indicate that management plans for the Earth's largest fish will require ocean basin-wide cooperation. Multinational coordination on that scale has proven challenging for tunas and billfish, very difficult for whales, and will likely be very difficult for whale sharks. Given the increase in fishing pressure and the evidence for population declines, the only effective conservation measure may be threatened species status under IUCN guidelines.

4. PHOTOGRAPH MATCHING TECHNIQUES AND DEMOGRAPHIC MODELS

4.1 OVERVIEW

The use of photo-identification techniques are a central part of our studies of the ecology of whale sharks. At Ningaloo, our photographic libraries date back to 1992 and have recently expanded with access to images provided by the ecotourism industry via the Western Australian Department of Environment and Conservation. With large databases, some form of automatic comparison of images using computer software is essential. This has recently become possible using the open-access, image matching software I3S. However, before the software can be routinely applied some knowledge of accuracy, precision and limitations of matching is required. These issues were addressed using the Ningaloo photo-identification database. We developed an information criterion (IC) algorithm that resulted in a parsimonious ranking of potential matches of individuals in an image library. Automated matches were compared to manual-matching results to test the performance of the software and algorithm. Validation of matched and non-matched images provided a threshold IC weight (approximately 0.2) below which match certainty was not assured. Most images tested were assigned correctly; however, scores for the by-eye comparison were lower than expected, possibly due to the low sample size. The effect of increasing horizontal angle of sharks in images reduced matching likelihood considerably. There was a negative linear relationship between the number of matching spot pairs and matching score, but this relationship disappeared when using the IC algorithm. The software and use of easily applied information-theoretic scores of match parsimony provide a reliable and freely available method for individual identification of whale sharks, with wide applications and the potential to improve mark-recapture studies without resorting to invasive marking techniques.

Given that we had an automated matching technique, we could use this software and our photo-identification library to examine demographic patterns. Precise estimates of demographic rates are key components of population models used to predict the effects of stochastic environmental processes, harvest scenarios and extinction probability. We used the 12-year photographic identification library of whale sharks from Ningaloo Reef to construct Cormack-Jolly-Seber (CJS) estimates of survival within a capture-mark-recapture (CMR) framework. Estimated survival rates, population structure and assumptions regarding age at maturity, longevity and reproduction frequency were combined in a series of age-classified Leslie matrices to infer the potential population trajectory of the population. Using data from 111 individuals, there was evidence for time variation in apparent survival (ϕ) and recapture probability (p). The null model gave a $\hat{\phi}$ of 0.825 (95% CI: 0.727 – 0.893) and $\hat{p} = 0.184$ (95% CI: 0.121 – 0.271). The model-averaged annual $\hat{\phi}$ ranged from 0.737 to 0.890. There was little evidence for a sex effect on survival. Using standardized total length as a covariate in the CMR models indicated a size bias in ϕ . Ignoring the effects of time, a 5 m shark has a

$\hat{\phi} = 0.59$ and a 9 m shark has $\hat{\phi} = 0.81$. Of the 16 model combinations considered, 10 (63%) indicated a decreasing population ($\lambda < 1$). For models based on age at first reproduction (α) of 13 years, the mean age of reproducing females at the stable age distribution (\bar{A}) ranged from 15 to 23 years, which increased to 29 to 37 years when α was assumed to be 25. All model scenarios had higher total elasticities for non-reproductive female survival ($E(s_{nr})$) compared to that for reproductive female survival ($E(s_r)$). Assuming relatively slow vital rates ($\alpha = 25$ and biennial reproduction) and size-biased survival probabilities suggest the Ningaloo Reef population of whale sharks is declining, although more reproductive data are needed to confirm this conclusion. Our work shows that combining relatively precise survival estimates from CMR studies with realistic assumptions of other vital rates provides a useful heuristic framework for determining the vulnerability of large oceanic predators for which little direct data exist.

Given modelled and observed (see Chapter 4) declines in whale shark numbers we interrogated the photo-identification data bases focusing on potential threats to this species. We recorded scars on whale sharks in three Indian Ocean aggregations (Australia, Seychelles and Mozambique), and examined whether scarring (mostly attributed to boat strikes and predator attacks) influences apparent survival rates using these photo-identification libraries. Scarring was most prevalent in the Seychelles aggregation (67 % of individuals). Predator bites were the most frequent source of scarring (aside from minor nicks and abrasions) and 27 % of individuals had scars consistent with predator attacks. A similar proportion of sharks had blunt trauma, laceration and amputation scars, the majority of which appeared to be caused by ship strike. Predator bites were more common (44 % of individuals) and scars from ship collisions were less common at Ningaloo Reef than at the other two locations. In all aggregations, scars occurred most often on the caudal fin, which may result from the fin being the body part closest to the surface when boats pass over or as a large target for predators. We found no evidence for an effect of scarring on apparent survival (ϕ) for the Ningaloo (not scarred $\phi = 0.858 \pm 0.033$; scarred $\phi = 0.929 \pm 0.033$) or Seychelles populations (not scarred $\phi = 0.502 \pm 0.060$; scarred $\phi = 0.538 \pm 0.070$). The lower apparent survival of the Seychelles population may be attributed to a high number of transient sharks in this aggregation that might bias estimates. We conclude that while scarring from natural predators and smaller vessels appears to be unrelated to whale shark survival, the effects of deaths related to ship strike need to be quantified to assist in future management of this species.

Ongoing work aims to quantify the extent of interchange among three major whale shark aggregations, Ningaloo Reef in Australia and Tofo Beach in Mozambique and Mahe Island, Seychelles. Ningaloo Reef and Tofo Beach are approximately 7,900 km apart, representing the eastern- and western-most extent of the distribution of whale sharks within the Indian Ocean, respectively, providing the best possible opportunity for differentiating putative stocks in whale sharks on a regional scale. This study will be the first major photographic database comparison of whale shark aggregation sites.

4.2 VALIDATION OF COMPUTER-AIDED MATCHING

4.2.1 Introduction

As previously outlined in Chapter 3, photo-identification is being used to identify individuals in the whale shark population at Ningaloo Reef, Western Australia. This method also allows the collection of additional information to assist in estimating demographic parameters. The aim of this section is to validate computer-aided matching of individual whale sharks. The results from trials of the pattern-matching software and an information-theoretic validation technique will also be presented. Finally, the results from population size estimates based on the computer matched and validated images are presented.

4.2.2 Methods

4.2.2.1 Matching software, fingerprint creation and image matching

Prior to 2006, images of whale sharks were matched manually (by eye) in order to establish resights and population estimates (Meekan et al. 2006). As mentioned in Chapter 2, the software currently employed for matching photographs of whale sharks is Interactive Individual Identification System (I³S). This software, originally designed to match natural variation in spot patterns of grey nurse sharks (*Carcharias taurus*), was used to create 'fingerprint' files and match individuals. Fingerprint files are used to identify individual whale sharks based on their spot pattern, in a fashion analogous to the concept of human fingerprint recognition. The area on the flank of sharks directly behind the 5th gill slit was selected as the most appropriate area to use for identification of whale sharks. This area was chosen based on consistency with past studies, and due to the ease that photographers can focus on this area (Arzoumanian et al. 2005, Meekan et al. 2006). The positioning of spots in this area was also less likely to be distorted due to undulation of the caudal fin, which may affect the matching success of I³S.

The initial procedure once an image was entered into the database was to create a fingerprint file. Three reference points were required by I³S, points that could be easily and unambiguously identified in each photo were chosen: 1) the top of the 5th gill slit, 2) the point on the flank corresponding to the posterior point of the pectoral fin and 3) the bottom of the 5th gill slit (Figure 4.1).

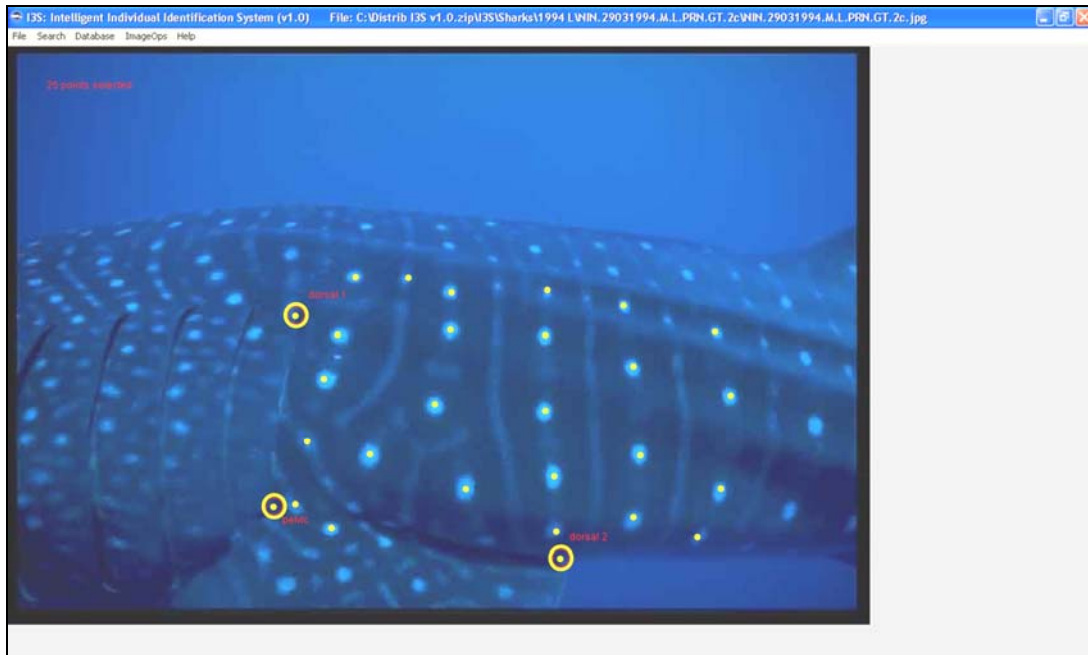


Figure 4.1. Fingerprint file creation (reference points and spot highlighting shown).

After the initial reference points for each image were entered, the centres of the most obvious spots within and slightly posterior to the reference area were highlighted by the operator. The reference area includes the spots behind the 5th gill slit, below the uppermost longitudinal ridge, and in front of the start of the dorsal fin. IIS requires a minimum of 12 spots to be highlighted to form a fingerprint, and a maximum of 40 spots. Highlighting spots outside of the immediate reference area can affect the ability of the IIS matching algorithm Van Tienhoven et al. 2007a; therefore, highlighted spots were kept roughly within the reference area for fingerprinting.

The requirement of all three reference points to be visible in the photograph for a fingerprint to be created meant that not all 797 photos in our database could be used. As such, 433 (54 %) of the original photographs could be used, of which 212 were of the left side (LS) and 221 were of the right side (RS) of the shark. To compare fingerprints, a common reference system is required, which is achieved by using a two-dimensional affine transformation Van Tienhoven et al. 2007a.

The transformation is calculated as follows:

$$M \begin{pmatrix} x \\ y \end{pmatrix} = \begin{pmatrix} m_{11} & m_{21} \\ m_{12} & m_{22} \end{pmatrix} \begin{pmatrix} x \\ y \end{pmatrix} + \begin{pmatrix} t_1 \\ t_2 \end{pmatrix} = \begin{pmatrix} m_{11}x + m_{21}y + t_1 \\ m_{12}x + m_{22}y + t_2 \end{pmatrix} \quad \text{Equation 1}$$

where M is the affine transformation matrix of x and y , and m_{11} , m_{21} , m_{12} , m_{22} , t_1 and t_2 are unknown variables (Van Tienhoven et al. 2007b).

The search function in I³S compares the new fingerprint file against all of the other fingerprint files in the database by using a two-dimensional linear algorithm. The algorithm calculates the sum of the distances between spot pairs divided by the square of the number of spot pairs (Hartog & Reijns 2004). The matching algorithm is calculated as follows:

$$\frac{\sum d}{n^2}$$

Equation 2

Where d is the distance between matching spot pairs and n is the number of matching spot pairs. The matched spot pairs with the minimum overall sum of the squared distances between them is the most likely match, and given a score from 1 to 0 (0 being a perfect match). The program also lists the next 49 most likely spot pair matches, which it ranks in decreasing order of likelihood (Figure 4.2). The next step is to look at the most likely match, which is ranked as the top of the list of 50 matches. I³S provides a visual match of the unknown image and the image with which it was matched (Figure 4.3). A visual display of the matching spot pairs called a ‘spot cloud’ is also available to assist in matching individuals (Figure 4.4).

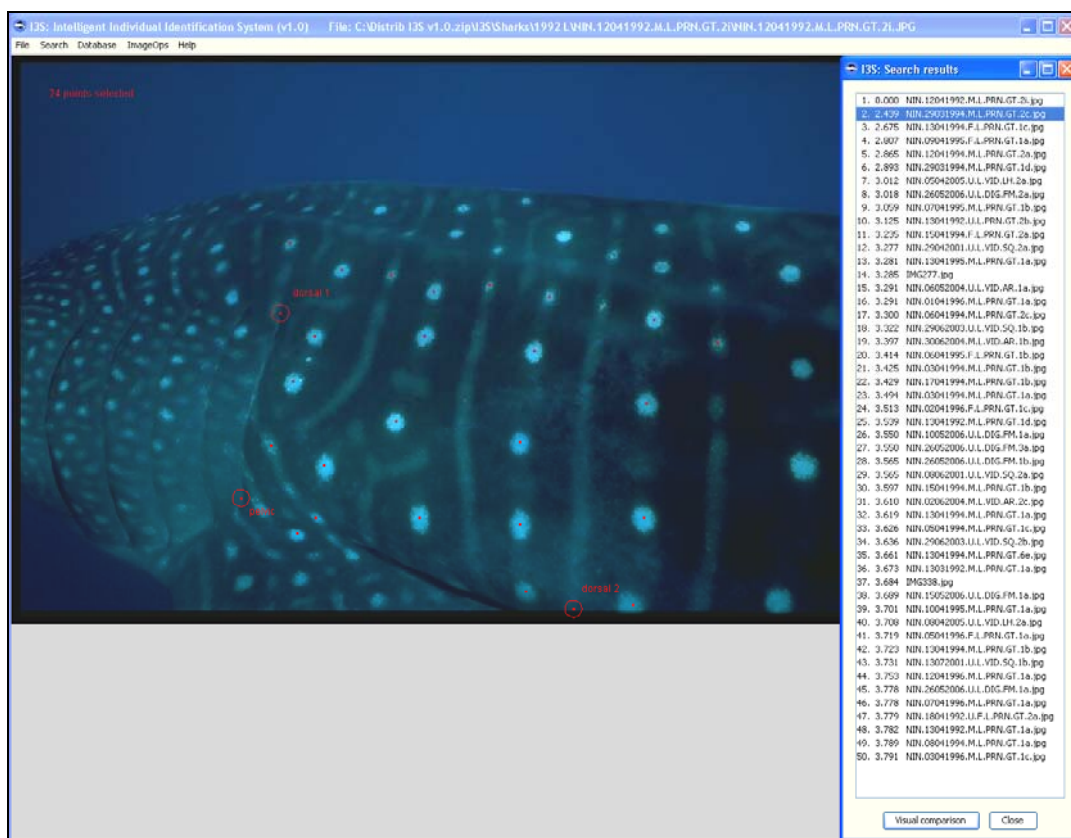


Figure 4.2. Results of searching an unknown image in I³S, showing unknown image and the top 50 ranking of the most likely matches (right side of the screen). Note. Because this example image was already present in the database, it was matched with itself (ranked number 1 in the list). Therefore, the image ranked in the second position is the most likely match in this situation.

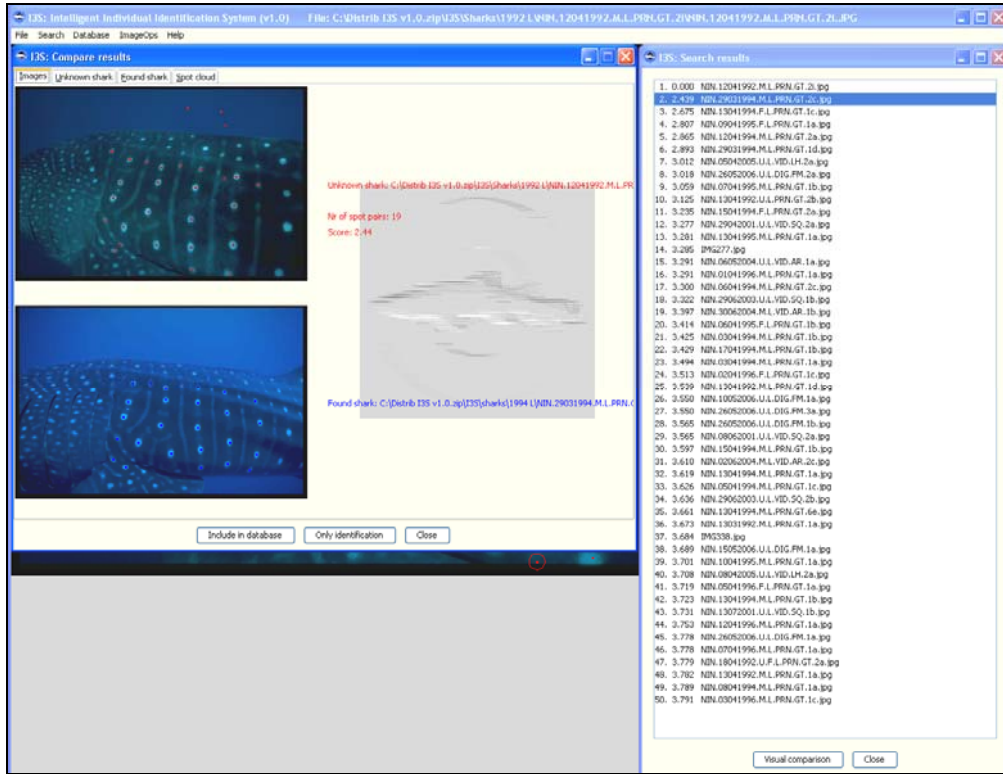


Figure 4.3. Visual comparison of unknown individual and matched individuals (left side of the screen). The top image is unknown, and the bottom image is the matched image from the database.

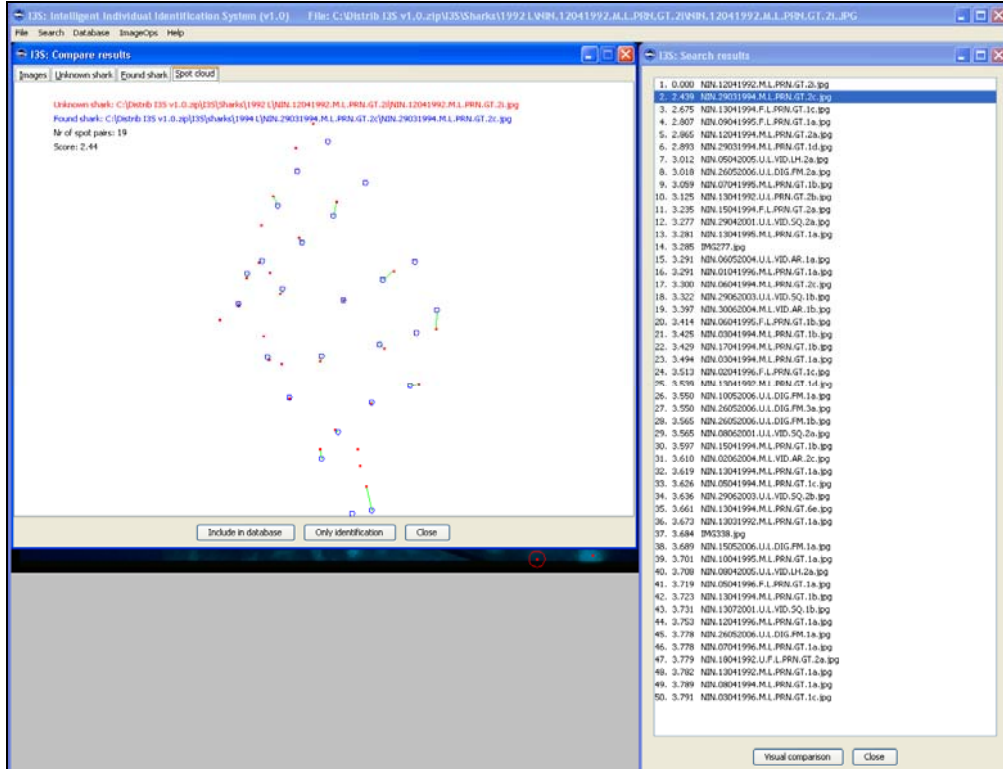


Figure 4.4. Spot cloud of matching spot pairs (left side of the screen). The red spots are the fingerprint from the unknown shark, and the blue spots are the fingerprint from a shark found in the database. The green lines denote the distance between match spot pairs.

4.2.2.2 I³S matching validation

I³S provides the user with a matching score (>0); however; this score does not take into account the uncertainty in the system, nor does it provide a relative score to all other images considered. A non-subjective validation technique is essential to assess the relative strength of matches, which has not been provided to date for automated photo-identification studies. Without a validation of image matches, the final decision is subjective, and may affect the quality of data used for parameterisation of demographic models.

To provide a measure of match parsimony based on the philosophy of information theory and to compare possible image matches in a multi-model inferential framework Burnham & Anderson 2002, the match score was modified in the following manner: (1) the spot-averaged sum of squares was back transformed to a residual sum of squares, which was simply the spot score (*SS*) multiplied by the square of the number of matching spots (*n*); (2) an information criterion (IC) analogous to the Akaike Information Criterion (Akaike 1973) or Bayesian Information Criterion (Link & Barker 2006) was developed as follows:

$$IC = 2k + n' \log_e \left(\frac{SS \cdot n^2}{n'} \right) \quad \text{Equation 3}$$

where *k* = an assumed number of parameters under a simple linear model (set to 1 for all models) and the $n' = 100/n$ and accounts for the fact that an increasing number of spots automatically leads to a higher *SS* (the 100 multiplier scales the term to be > 1);

(3) the IC weight (*w*) was calculated as:

$$w_i = \frac{e^{-0.5 \cdot \Delta IC_i}}{\sum_{i=1}^m \Delta IC_i} \quad \text{Equation 4}$$

where $\Delta IC = IC - IC_{min}$ for the *j*th image (*i*th 'model') 1 through *m* (where *m* = 49);

(4) finally, the evidence ratio (*ER*) was calculated as:

$$ER_1 = \frac{w_1}{w_2} \quad \text{Equation 5}$$

This IC algorithm was applied to a sample of 200 images; 25 matching pairs from the LS and RS databases and 25 non-matching pairs from the LS and RS databases. The LS and RS images were analysed separately using text outputs from I³S showing image name, I³S matching score

and number of pairs matched by I³S (Appendix 1). The analysis was done using the R Package (R Core Development Team 2004); the code for the IC algorithm, (including w and ER), is given in appendix 2.

4.2.2.3 Assessing 'by-eye' matches using I³S

Thirty-three sharks were re-sighted inter-annually during the manual 'by-eye' analysis of the raw photo library (Meekan et al. 2006). Of any two by-eye matched images, one of the pair was entered into either the LS or RS database and searched. A match using I³S was successful if the by-eye matched images were ranked as the most likely match (as with the validation test) and confirmed using the IC algorithm (i.e., $w_1 \geq 0.2$).

4.2.2.4 Horizontal angle (yaw)

Video footage of 10 different sharks (5 LS and 5 RS) was used to capture sequences of five images per shark, where subjects were on differing horizontal angles (0° , 10° , 20° , 30° and 40° – Figure 4.5). The angles of yaw were estimated using Screen Protractor™ software. Fingerprints were created for each image with 20 spots highlighted per fingerprint. The 10° images were searched against the 0° images and 10 non-matching images. This process was repeated, substituting images where subjects were on angles of 20° , 30° and 40° for both LS and RS image sequences. Five random, non-matching pairs were also searched against 0° and 10° images, and then repeated for 20° , 30° , and 40° images. This allowed for a comparison between matching and non-matching pairs while testing for the effects of horizontal angle in images. Results were analysed using the same IC algorithm applied to the match validation and by-eye comparison tests.

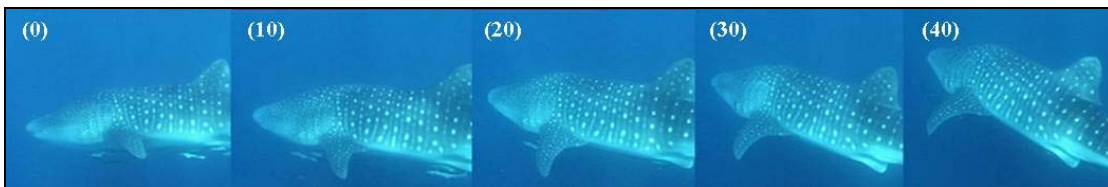


Figure 4.5. - An individual whale shark at differing angles of yaw (A: 0° , B: 10° , C: 20° , D: 30° , E 40°). This type of sequence was used to determine the effect of horizontal angle on the I³S matching process.

4.2.2.5 Number of spot pairs

Fifty known-matching pairs were compared to one another using I³S. Only the matching pairs that were successfully confirmed during validation of I³S matches were included in this test. I³S scores were compared against the number of spot pairs matched in I³S. The w_1 for each image was also compared against the number of spot pairs matched by the I³S algorithm. A complementary log-log transformation (clog-log) was applied to normalize the distribution of I³S scores and w_1 , and a \log_{10} transformation was used to normalize the distribution of spot pairs. We tested for a linear relationship between the transformed variables using least-squares regression and information-theoretic evidence ratios. Goodness-of-fit was tested using the least-squares R^2 value.

4.2.2.6 Population Size Analysis

The initial population size estimates for this study were calculated using a capture matrix based on I³S matches. The capture matrix consisted of all individuals with both sides fingerprinted, and RS only fingerprinted. Individuals which had LS fingerprinted only, were excluded to reduce the potential error of double counting individuals. Only inter-annual sightings of individuals were included within the capture matrix. Population size estimates were further refined by repeating the experiment using the capture matrix consisting of only I³S matches that had been validated using the IC algorithm. Images that received IC *w* scores above the IC *w* threshold were considered to be validated. All resights that were not validated were removed from the capture matrix prior to reanalysis. Similarly, this capture matrix only consisted of inter-annual sightings of individuals.

Population estimates using a series of closed population models (assuming no net immigration or emigration) were initially calculated using the program CAPTURE, and examined variants of the Lincoln-Petersen (LP) model (Meekan et al. 2006). Due to the sensitivity LP estimates to temporary emigration and the low power associated with databases comprising a low rate of recapture (resighting), an open-population Cormack-Jolly-Seber model (Schwarz & Arnason 1996) was also applied using the POPAN option in the program MARK (White & Burnham 1999) to estimate population abundance (Table 4.1).

Table 4.1. Open-population models for whale shark population re-assessment using MARK

Model Name	Model Equation
<i>Constant (null)</i>	$\phi(.)p(.)\beta(.)N(.)$
<i>Capture probability-time variant</i>	$\phi(.)p(t)\beta(.)N(.)$
<i>Apparent survival-time variant</i>	$\phi(t)p(.)\beta(.)N(.)$
<i>Probability of entry-time variant</i>	$\phi(.)p(.)\beta(t)N(.)$

Note: ϕ = apparent survival, p = capture probability, β = probability of entry to population per occasion and N = super-population size.

Time intervals were set according to years sampled between 1992 and 2006 which were yearly from 1992-1996, 2001, then again yearly from 2003-2006). As such, the number of years elapsed between resighting events (years) was 1, 1, 1, 1, 5, 2, 1, 1 and 1. All models were fitted using the logit link function for ϕ and p , the identity link function for N , and the multinomial logit link function (MLogit [1]) to constrain the β parameters to be ≤ 1 (White & Burnham 1999). Parameters counts (k) for each model were adjusted to account for the fact that not all were estimable due to low recovery rates in some years. Akaike's Information Criterion corrected for small sample sizes (AIC_c) was adopted to give a model comparison and model-averaged estimates of N (Burnham & Anderson 2002). AIC_c was calculated as follows:

$$AIC_c = -2\log L + 2k + \frac{2k(k+1)}{n-k-1} \quad \text{Equation 6}$$

Goodness-of-fit was calculated using the program RELEASE implemented in MARK. The coefficient of variation (CV) was also calculated for each model as a measure of parameter precision for abundance estimates:

$$CV = \frac{Sd}{\bar{\chi}} \times 100 \quad \text{Equation 7}$$

4.2.3 Results

4.2.3.1 I³S (Interactive Individual Identification Software) matching validation

The Information Criterion weights (w) for the most parsimonious matches (w_1) for the 50 matched pairs were broadly distributed between 0.05 and 0.85, while w_1 for non-matched pairs were highly right-skewed (Fig. 4.6a,b). All w_1 for non-matched pairs were < 0.18 . The median w_1 for matched pairs was $0.32 (\pm \text{SE } 0.05)$, which was much greater than the median for non-matched pairs (0.06 ± 0.01). Evidence ratios for the best-matched relative to the next-highest matched images (ER_1) for known matched pairs were also highly right-skewed and ranged from 0.73 to 51.92, with a median of $7.36 (\pm 2.45)$ (Fig. 4.6c). ER_1 values for non-matched pairs were all < 3.5 (median = 1.21 ± 0.09) (Fig. 4.6d). Evidence ratios for the second best-matched relative to the next-highest matched images (ER_2) for known matched pairs ranged from 0.73 to 114.18, with a median of $7.57 (\pm 3.82)$. ER_2 values for non-matched pairs were also all < 3.5 (median = 1.42 ± 0.12).

Overall, 93 images out of the 50 known-matched pairs were matched correctly using I³S. w_1 for the correctly assigned matches ranged from 0.05 to 0.85 (median = 0.36 ± 0.05), and their ER_1 ranged from 0.73 to 51.92 (median = 8.82 ± 2.56) (Figure 4.7 a & b). Known-matched photographs that I³S failed to match (7 images) had w_1 that ranged from 0.05 to 0.14 (median = 0.07 ± 0.02), with their ER_1 ranging from 0.95 to 2.28 (median = 1.23 ± 0.36).

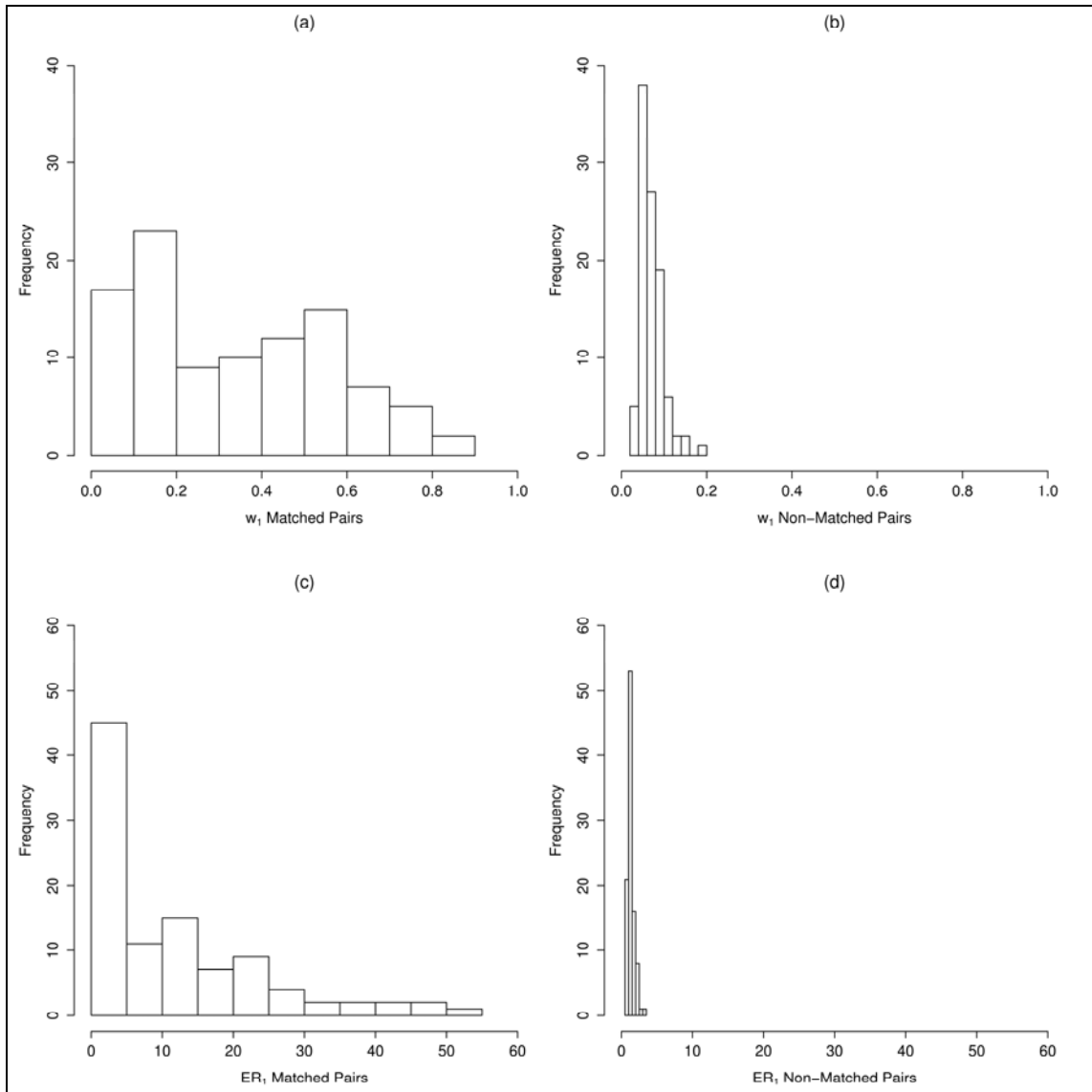


Figure 4.6. ^{13}S matching validation IC weights (w_1). Distribution of IC weights for known matched (a) and non-matched pairs (b), and ^{13}S matching validation evidence ratios (ER_1) for known matched (c) and non-matched pairs (d) are shown.

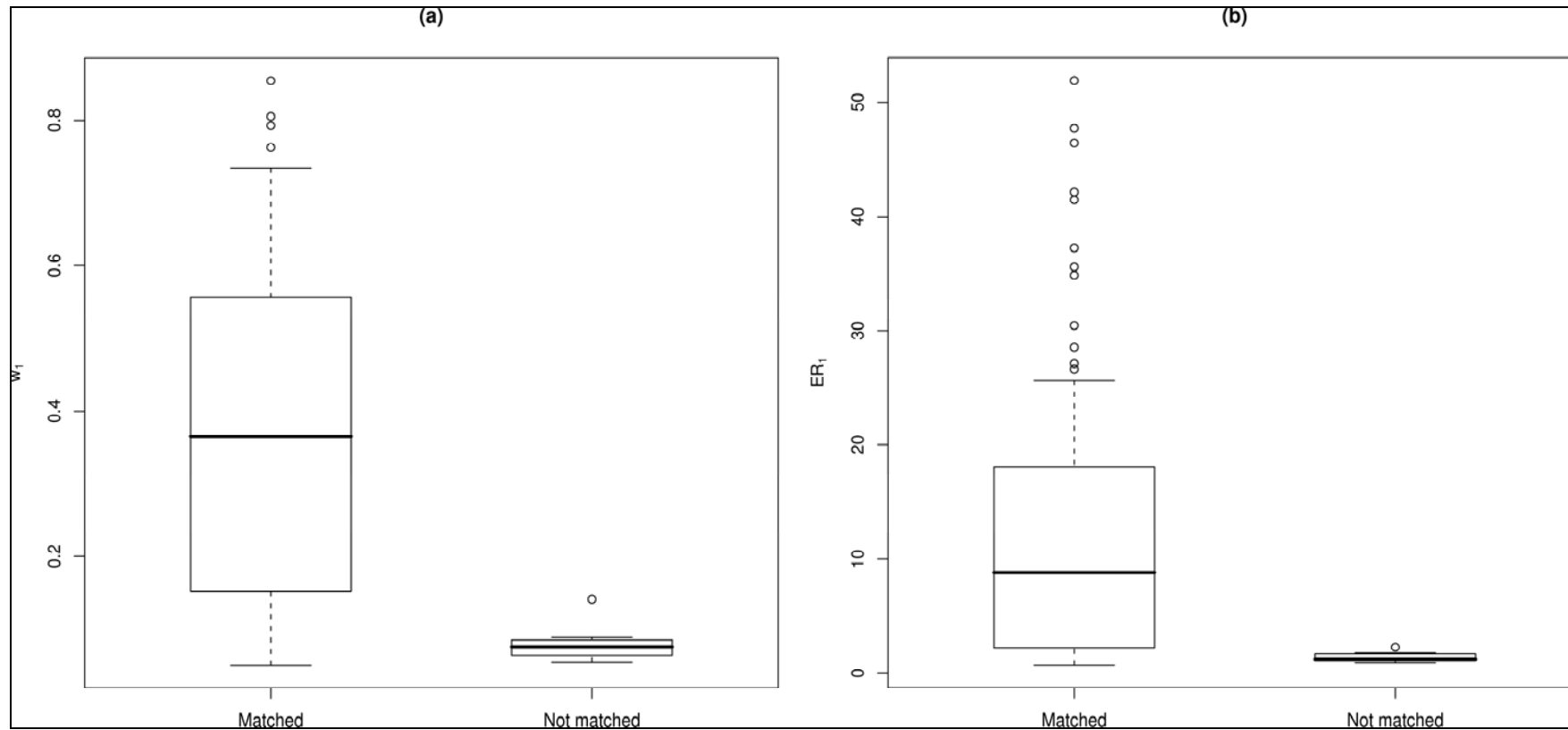


Figure 4.7. Median (a) IC weights (w_1) for known matched pairs showing images matched and not matched with I³S; (b) Median evidence ratios (ER_1) for known matched pairs showing images matched and not matched using I³S.

4.2.3.2 Assessing 'by-eye' matching using I³S

Ten of the 33 individuals re-sighted between years in the database used by Meekan et al. (Meekan et al. 2006) could not be matched with I³S because their images were not amenable to I³S fingerprinting (absence of reference points), or their match was not present in the database. This was because the Meekan et al. (2006) study also used images from a separate database and included scar-identified individuals that were not available for photographic matching using I³S. Therefore, we could only re-assess 23 of these by-eye matches that included 13 LS matches and 16 RS matches (58 images total).

Forty-eight of the 58 images (83 %) from the 23 individuals were matched correctly using I³S. w_1 for the correctly assigned by-eye matches ranged from 0.05 to 0.53 (median = 0.16 ± 0.04) (Fig. 4.8a), and their ER_1 were between 1.04 and 24.57 (median = 2.33 ± 1.58) (Fig. 4.8b). Incorrectly assigned by-eye matches had w_1 ranging from 0.04 to 0.13 (median = 0.06 ± 0.01) and their ER_1 ranged from 0.67 to 2.76 (median = 1.04 ± 0.37). I³S also identified two images that were false positives (i.e. sharks that were incorrectly matched with other photographs) in the by-eye matching process. Neither of these images was matched with other known images of the identified sharks.

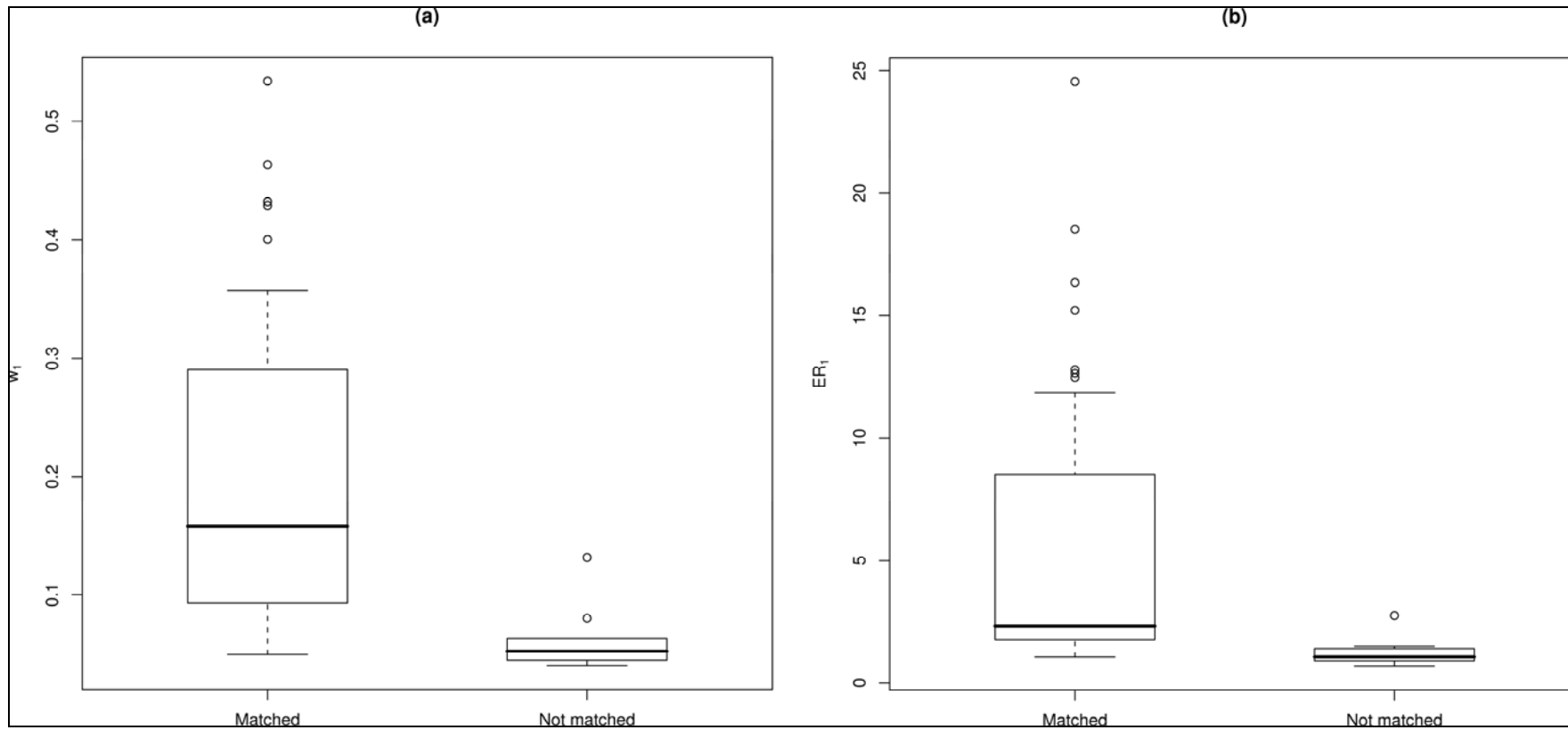


Figure 4.8. By-eye versus I3S matching Results. (a) Median IC weights (w_1) for by-eye matched images that were matched and not matched using I3S; (b) Median evidence ratios (ER_1) for by-eye matched images that were matched and not matched using I3S.

4.2.3.3 Horizontal angle

Mean w_1 scores decreased linearly as the horizontal angle of subjects within images increased (Figure 4.9 a). Mean w_1 scores ranged between 0.88 (± 0.06) for angles of 10° , to 0.30 (± 0.13) for angles of 40° . Standard errors for w_1 were relatively low for angles of 10° and 20° ; however, these increased noticeably for angles of 30° and 40° . The images of subjects at 30° approached mean w_1 scores for non-matching pairs, and mean w_1 scores for images of subjects at 40° overlapped mean w_1 scores for non-matching pairs.

There was an exponential decline of mean ER_1 with increasing angle (Figure 4.9b). Mean ER_1 ranged from 89.42 (± 52.23) for images of subjects at 10° to 4.06 (± 2.80) for images of subjects at 40° . The images of subjects at 30° approached mean ER_1 for non-matching pairs, and mean ER_1 for images of subjects at 40° overlapped mean ER_1 for non-matching pairs.

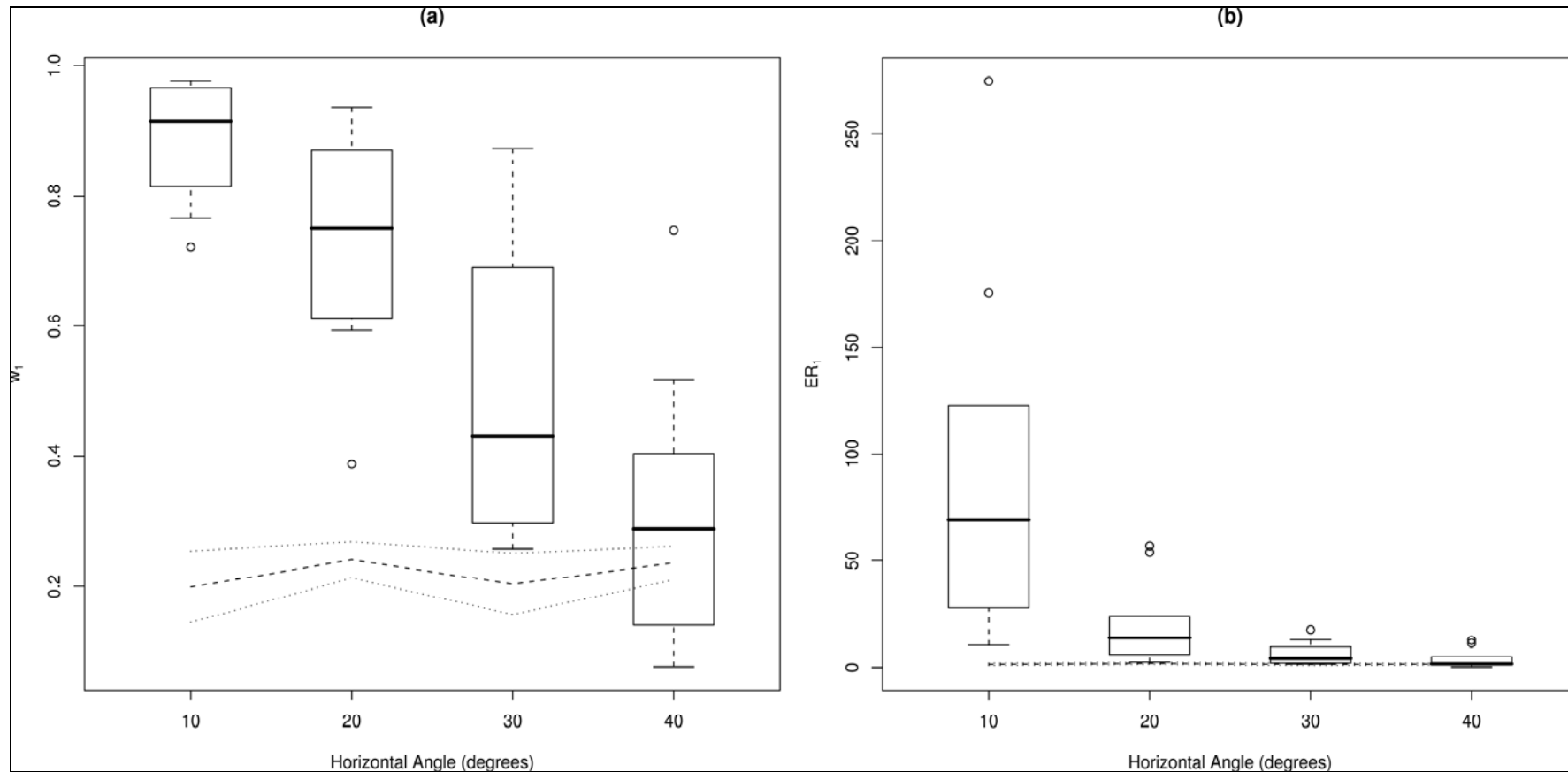


Figure 4.9. Effect of angles of yaw. (a) Mean IC weights (w_1) for horizontal angle categories, where images at 0° were matched against images skewed by 10° , 20° , 30° and 40° . Dotted lines show results for non-matching pairs; (b) Mean evidence ratios (ER_1) for horizontal angle categories, where images at 0° were matched against images skewed by 10° , 20° , 30° and 40° .

4.2.3.4 Number of spot pairs

There was evidence for a negative relationship between the transformed $\delta^{13}\text{S}$ scores and spot pairs ($ER = 9.94 \times 10^5$, adjusted $R^2 = 0.26$; Figure 4.10 a), but no evidence for a relationship between transformed w_1 and the number of spot pairs ($ER < 1$; Figure 4.10 b).

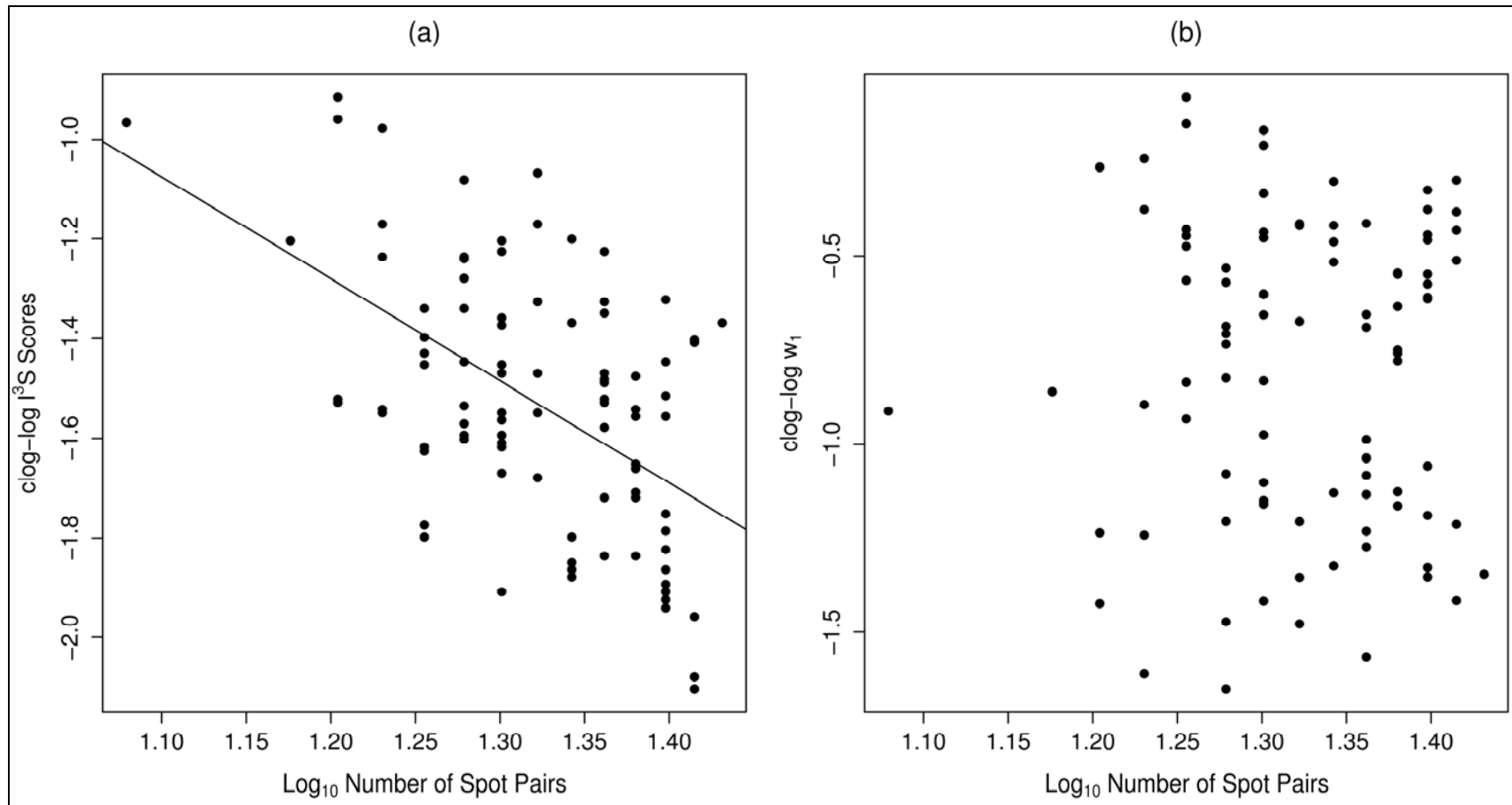


Figure 4.10. Effects of spot-pair number. (a) Relationship between complementary log-log-transformed (clog-log) I³S scores and log₁₀-transformed number of spot pairs. The fitted line illustrates the correlation observed using a linear regression; (b) Comparison of clog-log-transformed w₁ with log₁₀-transformed number of spot pairs.

4.2.3.5 Whale shark population size using I³S matches

After the removal of multiple images of the same individual, a total number of 208 individual sharks were identified for the period between 1992 and 2006 (excluding 1997, 1998, 1999, 2000 and 2002). Eighty-four of these individuals had both RS and LS fingerprints, 73 had RS fingerprints only and 51 had LS fingerprints only. We therefore excluded individuals with LS only fingerprints to avoid double counting the same individual, which left a total of 157 individuals suitable for use in population estimates. From a total of 157 individuals, there were 30 individuals that were resighted inter-annually. Twenty-six of these were included in the population analysis because they either had the right side or both sides fingerprinted.

Ten capture sessions (excluding years where sampling did not occur) including 157 individuals with fingerprints, seen in 187 separate sightings over the study period, enabled the estimation of population size using differing models and estimators. The model that provided the best fit under the model selection criteria provided by CAPTURE was the time-variant and heterogeneity model (M_{th} , model selection criterion = 1.0). Tests for closure ($z = -1.886$, $P = 0.029$) and closure by frequency of capture ($z = -3.825$, $P = 0.00007$) both violated the assumption of homogeneity of capture probabilities (i.e., the population was not closed). The M_{th} model using the Chao estimator provided time-variant capture probabilities (p_t) ranging between 0.01 (2005) and 0.08 (1994). No trend was observed over time. Population estimates are summarised in (Table 4.2).

Table 4.2. Summary of population size estimates from closed and open populations for I³S resights

Model		Goodness of Fit	N Range	CV (%)
<u>Closed</u>				
M_{th} (1992-2006)			367-780	20
M_{cb} (1992-2006)	Chao	$\chi^2_7 = 34.64$ $P = <0.001$	189-5216	150
M_t	Chao	$\chi^2_{58} = 71.95$ $P = 0.102$	347-628	15.5
<u>Open (Jolly Seber)</u>				
$\phi(.)p(.)\beta(.)N(.)$		$\chi^2_1 = 0.28$ $P = 0.60$	265-363	8.2
$\phi(.)p(.)\beta(t)N(.)$		$\chi^2_1 = 0.28$ $P = 0.60$	265-363	8.2

Note: ϕ = apparent survival, p = capture probability, β = probability of entry to population per occasion and N = super-population size.

Only one of the parameters for time-variant models converged using the POPAN open-population Jolly-Seber model structure, which was the time-variant probability of entry model ($\phi(.)p(.)\beta(t)N(.)$). The reason that many of the time variant models did not converge was due to some parameters being inestimable from a low number of resights in particular years. The constant model ($\phi(.)p(.)\beta(.)N(.)$) converged with an AIC_c of approximately 100 % (Table 4.3) and provided a super-population size of 265-363 individuals (Table 4.2).

Table 4.3. Results for model analysis using non-validated (unvalidated) I^3S dataset - Small sample size corrected Akaike Information Criterion (AIC_c), change in AIC_c (ΔAIC_c), AIC_c weights (w_{AIC_c}), number of parameters (k) and deviance.

Model	AIC_c	ΔAIC_c	w_{AIC_c}	NP (k)	deviance
$\phi(.)p(.)\beta(.)N(.)$	16252.9491	0.0000	0.99841	3	15420.6390
$\phi(.)p(.)\beta(t)N(.)$	16265	12.8868	0.00159	9	15420.6390

4.2.3.6 Whale shark population size using validated I^3S matches

Using the w_i threshold of 0.2 determined from the validation tests, only 14 of the 26 individuals resighted inter-annually were validated. w_i for validated resights ranged between 0.21 and 0.77, with a mean of 0.41 (S.E \pm 0.08) (Figure 4.11). w_i for non-validated (unvalidated) resights ranged between 0.05 and 0.14, with a mean of 0.06 (S.E \pm 0.02).

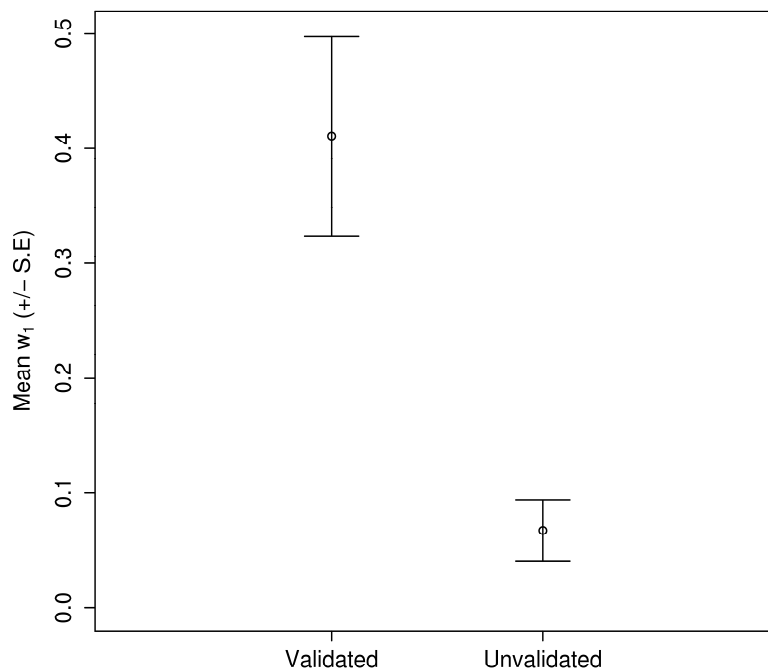


Figure 4.11. Mean validated and unvalidated (< 0.2) w_1 for inter-annual resights used for population modelling.

The ten capture sessions included 145 individuals with fingerprints seen in 161 separate sightings over the study period. These were used to create IC-validated population estimates using differing models and estimators. The model which provided the best fit under the model selection criteria provided by CAPTURE, was the time variant model (M_t) ($\chi^2_{56} = 58$, $P = 0.40$, model selection criterion = 1.0) (Table 4.4).

The test for closure ($z = -2.783$, $P = 0.002$) and closure by frequency ($z = -3.525$, $P = 0.00021$) were both violated under the null model of no heterogeneity in capture probabilities. The M_t model using the Chao estimator provided time-variant capture probabilities (p_t) ranging between 0.01 (1993) and 0.05 (1994). No trend was observed over time. Population estimates are summarised in Table 4.4.

The only time-variant model with converging parameters was the time-variant probability of entry model. The constant model using the POPAN open-population Jolly-Seber model structure implemented in MARK for 1992-2004 estimated the super-population size at between 280 and 452 individuals, with an AIC_c of approximately 90 % (Table 4.5).

Table 4.4. Summary of population size estimates from closed and open populations for validated I³S resights

Model		Goodness of Fit	N Range	CV (%)
Closed				
M_t (1992-2006)	Chao	$\chi^2_{56} = 58$ $P = 0.40$	447-1211	26.2
M_{tb} (1992-2006)	Chao	$\chi^2_7 = 27.74$ $P = < 0.001$	176-8696	203
M_{th} (1992-2006)			497-1428	28
Open (Jolly Seber)				
$\phi(.)p(.)\beta(.)N(.)$			280-453	12.4
$\phi(.)p(.)\beta(t)N(.)$			280-453	12.4

Table 4.5. Results for model analysis using validated I³S dataset - Small sample size corrected Akaike's Information Criterion (AIC_c), change in AIC_c (ΔAIC_c), AIC weights ($w AIC_c$), number of parameters (k) and deviance.

Model	AIC_c	ΔAIC_c	$w AIC_c$	NP (k)	deviance
$\phi(.)p(.)\beta(.)N(.)$	11517.4869	0.0000	0.89255	3	10803.5630
$\phi(.)p(.)\beta(t)N(.)$	11521.7211	4.2342	0.10745	5	10803.5630

4.2.4 Discussion

4.2.4.1 I³S Analysis & Information Criterion Algorithm

Our assessment of I³S, coupled with an incorporation of an information-theoretic algorithm was effective given that the natural spot pattern of whale sharks was well suited to this system. Validation of I³S matches using the Information Criterion algorithm provided a threshold w_1 for known matched pairs of approximately 0.2, below which w_1 for non-matched pairs fell. Known matched pairs not matched by I³S, or that were matched with low (i.e., < 0.2) w_1 , probably resulted due to poor clarity or high angles of yaw. This highlights the need to only select images of the highest quality for matching purposes (Friday et al. 2000). The validation process is necessary with most computer-aided matching algorithms because this alleviates much of the subjectivity associated with the final stage of matching

I³S (open access at www.reijns.com/i3s), was effective at confirming past matches made by eye in most instances. Images that were successfully confirmed using our Information Criterion algorithm received relatively low w_1 and ER_1 overall, most likely as a result of a considerably smaller sample size than that used for validation. I³S was also a useful tool for identifying image matches that were assigned incorrectly (i.e., both false positives and false negatives). When matching whale shark patterns by eye, the observer generally does not focus on the spots *per se*; rather, attention is usually paid to the lines and whirls (see Fig. 4.1) on the flank of the shark. I³S therefore provides an unbiased method of matching natural markings, which is relatively impervious to user subjectivity.

We found strong evidence that horizontal angle of subjects within images compromises the ability of the I³S algorithm to make reliable matches. As the horizontal angle of subjects in images increases, the matching likelihood decreases. Angles of yaw up to 30° compromise the matching process even though many of these images were still matched correctly. Conversely, images with angles of yaw $\geq 40^\circ$ will more than likely be incorrectly assigned. Due to the linear algorithm used by I³S to match spot patterns it is important to use only those photos with little or no contortion of the reference area. Likewise, the number of spots annotated in fingerprints can also potentially influence the I³S matching process. The higher the number of spot pairs matched, the lower the I³S score and hence, the higher the matching certainty. This corroborates similar findings from a study of *Carcharias taurus* (Van Tienhoven et al. 2007b) and emphasizes the benefit of using information-theoretic measures of matching parsimony because the updated algorithm takes relative match certainty into account.

The number of suitable images from our database for use in I³S was considerably reduced due to the absence of reference points, poor image quality and oblique angles of subjects. The rejection rate is inflated particularly by the use of photographs taken without the explicit aim of photographic matching because many are derived from ecotourism operations. However, the efficiency and reliability of matching with I³S more than compensated for the reduced sample size. The number and size of images in an I³S database can potentially slow down the program's operating speed; therefore, it is ideal to scale down the size of photographs and only include the best image of a particular animal. In addition to horizontal angle, roll and pitch

of sharks in images may affect the matching process. Pitch seems likely to be only a minor problem, because digital photos can be rotated so that the animal is aligned with the horizontal. We had few images of the same individual at varying angles of roll, so we were unable to examine this potential problem.

4.2.4.2 Estimating population size

The first population estimates for the aggregation of whale sharks at Ningaloo Reef were based on a dataset of images collected between 1992 and 2004, from which 184 individuals were identified manually (Meekan et al. 2006). Data from 2005 and 2006 were included in this analysis, in which an additional 24 individuals were identified (a total of 208 individuals). The first population estimates were based on 159 individuals, where either images for both sides or the right side were present (i.e., left side-only images were discarded to remove the possibility of double-counting individuals). There were a similar number of individuals (157) identified for population assessment in this study. Meekan et al. (2006) identified 33 individuals which were resighted between 1992 and 2004, which compared to 30 individuals identified by I³S in this study between 1992 and 2006. Despite the Meekan et al. (2006) study having fewer sampling occasions, fewer individuals were identifiable in this study due to a large number of images being incompatible for matching with I³S.

Population estimates based on data obtained via I³S matches were similar to the initial open population estimates found by Meekan et al. (Meekan et al. 2006) – the Ningaloo super-population (i.e. the population of individuals that visit Ningaloo Reef) is between 300 and 500 individuals based on open population models, with closed population estimates providing a much wider range (176-8696). This provides evidence to support the hypothesis that initial population estimates made by eye were a reasonable approximation. The relatively high number (12 of 26) of known inter-annual resights that were not validated using information criteria weights was most likely due to oblique horizontal angles of subjects in images found in the I³S validation tests (Fig.4.1). The resights that had information criteria weights below the pre-determined certainty threshold (0.2) were removed from the capture matrix prior to population re-analysis to remove any uncertainty in resights. The information criteria weights and evidence ratios provide a measure of match parsimony based on the strength of matches, which can be misleading if the quality of images compared are poor (see Friday et al. 2000). Therefore, rather than dismissing resights completely based on low information criteria weights or evidence ratios, it is more appropriate to make the final decision by manual inspection under these circumstances.

The use of validated images for population estimation has provided a measure of certainty in resights and resultant estimates of population parameters such as abundance and vital rates (e.g., survival and population trajectories; Bradshaw et al. 2007). The validation of image matches also assists in reducing identification errors which are common in photo-identification, such as false-positives and false-negatives. These types of errors can greatly inflate population estimates (Stevick et al. 2001), which can have serious implications for the management of threatened populations. Population estimates for whale sharks at Ningaloo Reef are based on the assumption that their spot and stripe patterns remain stable through

time. Therefore, if ontogenetic changes in spot patterns do occur, the number of individuals resighted will likely be underestimated and estimates of population size would be upwardly biased (Meekan et al. 2006).

In addition to data quality, sampling effort has the potential to affect estimates if it has varied over sampling periods. Sampling effort varied between the periods of 1992-2003 and 2004-2006 in this study. This variation in sampling effort may be a contributing factor to the few resights seen in recent years; nevertheless, population estimates should be viewed tentatively until enough image matches are obtained to reduce uncertainty (Meekan et al. 2006). Future estimates of population size should be facilitated by the recent policy of photo sharing implemented by the Western Australian Department of Environment and Conservation (DEC), described in Chapter 2.

4.3 MODELLING OF DEMOGRAPHY: INFERRING POPULATION TRENDS FOR THE WORLD'S LARGEST FISH FROM MARK-RECAPTURE ESTIMATES OF SURVIVAL

4.3.1 Introduction

Demographic data are useful for determining the effects of stochastic processes on abundance (Sibly & Hone 2002), the type and strength of regulation operating on a population (Bradshaw et al. 2005, Sibly et al. 2005), and extinction risk faced by populations under various environmental scenarios (Fagan & Holmes 2006). However, demographic data alone cannot always divulge the mechanisms responsible for population trajectories, which is especially inconvenient when management actions are required to mitigate decline (McMahon & Burton 2005). Population viability analyses (PVA) have provided a means to examine the relative contributions of competing factors on rates of population change (Cochran & Ellner 1992, Caswell et al. 1999), and have given useful heuristic direction in managing the processes threatening species of conservation concern (Brook & Bradshaw 2006). Despite this advance, most PVA models rely on detailed life history data (Ellner et al. 2002) and researchers are forced to make profligate assumptions when such data are missing or based on small samples. As such, the estimation of high-precision demographic parameters like age- or stage-specific survival and fertility rates should be a major aim of any study attempting to elucidate the mechanisms driving population decline and persistence.

The world's largest fish, the whale shark (*Rhincodon typus* Smith 1828), is also one of the least-studied and poorly understood shark species. No data on survival rates are available, and the reproductive data that do exist are based on extremely small sample sizes (Joung et al. 1996, Colman 1997). Even basic parameters such as growth, age at first reproduction, longevity, and population size are unknown for the majority of populations. However, some data exist for growth rates of captive juveniles (Chang et al. 1997), size and age at first reproduction (Pai et al. 1983, Satyanarayana Rao 1986, Wintner 2000), size distributions (Pravin 2000, Meekan et

al. 2006), and abundance estimates for particular aggregations (Heyman et al. 2001, Meekan et al. 2006).

The predictable aggregation of whale sharks that occurs each year from March to June at Ningaloo Reef, Western Australia (Taylor 1996, Wilson et al. 2001a) has been the site of a large and lucrative eco-tourism industry where extensive photo-identification has been done over the last 15 years (Meekan et al. 2006). Recent studies have examined the potential to identify individuals over time using automated (Arzoumanian et al. 2005) or manual (Meekan et al. 2006) approaches, with the mark-resight data used to predict the size of the super-population participating in the Ningaloo aggregation at 300 to 500 individuals (Meekan et al. 2006). The photo-identification dataset can also be used within a capture-mark-recapture (CMR) modelling framework to estimate demographic parameters such as survival and capture probability.

Good estimates of whale shark demographic rates are essential components for assessing their conservation status. The species is listed as vulnerable according to World Conservation Union criteria (IUCN 2005) based on its rarity and reduction in catch rates in the regions where they are fished to supply meat throughout Asia (CITES 2002, IUCN 2005). Satellite tagging studies have verified that whale sharks attending the Ningaloo aggregation regularly migrate into Southeast Asian waters (Wilson et al. 2006; J. Polovina *et al.*, unpubl. data), with anecdotal evidence suggesting that some tagged animals have fallen victim to fishing in this region (J. Polovina *et al.*, unpubl. data). Additionally, Meekan *et al.* (2006) reported a decline in the proportion of large whale sharks seen between 1992 and 2004, which may indicate human-mediated changes in the age-class distribution of this population.

In this study we use the photo-identification database described in Meekan *et al.* (2006) to estimate apparent survival and capture probabilities for the Ningaloo Reef aggregation. We assess variation in survival over time, between the sexes, and as a function of an individual's total length. These survival estimates and other available demographic data reported in the literature are then incorporated into a series of age-classified Leslie matrix population models to assess the long-term persistence probability of the aggregation. Our overall aim is to provide a heuristic assessment of the possible population trajectory given our mark-recapture estimates of survival probability for this aggregation. This general template can be used to derive information on population assessments when demographic, abundance, and other key data are missing for species of conservation concern.

4.3.2 Materials and Methods

4.3.2.1 Study area and population

Our study was done at Ningaloo Reef (21° 32.4' S, 114° 6.0' E) off the coast of Exmouth in Western Australia from 1992 to 2004. Whale sharks aggregate predictably here from March to June each year (Taylor 1996, Wilson et al. 2001a) and their presence supports a highly profitable ecotourism industry (Davis et al. 1997, Davis 1998). Observers have taken

photographs of sharks attending this aggregation for over 12 years for the purposes of photo-identification (Arzoumanian et al. 2005, Meekan et al. 2006).

4.3.2.2 Data collection

A total of 581 photographs were taken of whale sharks between March and July from 1992 to 2004 (Meekan et al. 2006). Photographs were made using an underwater still camera or digital video camera while snorkelling with the animal. Still images of sharks were captured from videotape for analysis. Total length (TL - tip of snout to end of caudal fin) and dorsal fin height (DIH) were recorded using a measuring tape after animals were photographed. In cases where only DIH was measured, we used a previously established equation to predict TL (Meekan et al. 2006):

$$TL = 1.059 + 10.348 DIH$$

Animal gender was determined whenever possible by distinguishing males based on the presence of claspers on the pelvic fins (Taylor 1994a). It was often difficult to discern claspers in relatively small (< 4 m TL) sharks, so those animals were recorded as indeterminate gender (Meekan et al. 2006).

4.3.2.3 Mark-recapture analysis

We used Cormack-Jolly-Seber (CJS) capture-mark-recapture (CMR) models (Cormack 1964, Jolly 1965, Seber 1970) implemented in program MARK (White & Burnham 1999) to model apparent survival (ϕ) and recapture (resighting) probability (p) of whale sharks participating in the Ningaloo Reef aggregation. Our primary interest was to estimate mean survival probability for inclusion into models projecting the population through time, so we endeavoured to assess variation in this parameter due to time and size effects. Estimates of ϕ within a CMR framework confound mortality with permanent emigration from the population, so some underlying knowledge of population closure is required to assess the degree of potential bias associated with survival estimates. We established previously that closed and open population models provided similar estimates of population size at the Ningaloo aggregation (Meekan et al. 2006). This suggests that the super-population is comprised of individuals that are not infrequent transients, but are those that attend the aggregation at least semi-regularly. As such, we expect that the estimates of survival derived from the CMR provided reasonable parameters for inclusion into population models.

Our first analysis ignored the effects of size and sex and examined whether there was evidence for annual variation in ϕ and p over the course of the study (1992 – 2004). Models were compared using an information-theoretic measure of model parsimony, Akaike's Information Criterion (Akaike 1973, White & Burnham 1999) and goodness-of-fit was assessed using the simulation procedures provided in program MARK (White & Burnham 1999). A second model set was constructed to incorporate the effects of sex and time (16 models considered). Two separate analyses were done to determine whether there was a size- (length-) bias in survival using the estimates of total length. The first model set

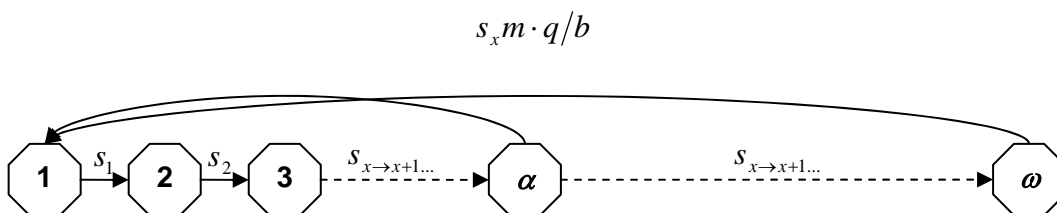
considered size as a categorical variable, where sharks < 8 m were considered immature and those ≥ 8 m as mature (Colman 1997; see also below). This size-based grouping was applied only to the apparent survival parameter, with full time dependency considered for ϕ and p (16 models). A potentially more sensitive assessment of the effects of size on survival used total length as a standardized covariate in a linear model to predict the logit of ϕ (again, with the time effect considered for both ϕ and p). Here we examined the effects of total length as potentially altering both the intercept and slope of the linear model predicting $\text{logit}(\phi)$ (12 models considered).

4.3.2.4 Population models

To examine how our estimated survival probabilities altered population projections, we constructed a series of age-based Leslie matrix population models to examine the potential population trajectory (Caswell et al. 1999). Although we have now estimated many of the demographic rates necessary to parameterize population models such as population size, sex ratio, size distribution (Meekan et al. 2006) and survival (this study), many other parameters are unknown or based on few data. As such, we defined several model scenarios that examined different assumptions with respect to the least-known parameters.

4.3.2.5 Model structure

Although stage-classified models have been used to project shark populations through time (Frisk et al. 2002, Mollet & Cailliet 2002, Otway et al. 2004), the relatively simple life history of elasmobranchs (i.e., sharks, rays and skates) coupled with the distorted elasticity patterns derived from stage-classified models (Mollet & Cailliet 2003b) argue for the use of simpler age-classified Leslie matrix models for whale sharks. We constructed a simple, deterministic and density-independent Leslie matrix (birth-pulse, post-breeding design – Caswell et al. 1999) for each of the model scenarios (described below) using the R package (R Core Development Team 2004) where the matrices were based on the general life cycle graph:



Here, s = the age-specific survival probability, x = age in years, α = the age at primiparity, ω = maximum age in years (longevity), m = litter size per female, q = pup sex ratio, and b = adult female reproduction frequency. For biennial reproduction, we calculated the discounted fertilities for every second year after α (i.e., setting the non-breeding years' discounted fertilities to 0).

4.3.2.6 Parameter estimates and assumptions

Whale sharks are live-bearers with an aplacental viviparous mode of development (Joung et al. 1996, Colman 1997). However, there is only one record of a captured female measuring approximately 11 m TL found to contain 300 embryos (Joung et al. 1996). There is no information available for the frequency of reproduction, with annual, biennial, and possibly more infrequent reproduction possible. As such, the fertility parameter was calculated as the number of potential pups (m) \times the assumed pup sex ratio (q) $0.5 \div$ the frequency of reproduction (b) taking values of one or two (see Model Scenarios below).

Age at sexual maturity for females is thought to occur at $> 8 - 9$ m total length based on two female specimens of this size captured in Indian waters found to have immature ovaries (Pai et al. 1983, Satyanarayana Rao 1986). Colman (Colman 1997) therefore suggested that sexual maturity is reached at > 9 m. We assumed that all individuals ≥ 8 m were mature given the observed peak in the distribution of whale sharks at Ningaloo was 8 m (Meekan et al. 2006), which suggests an appearance in the seasonal aggregation of a particular (potentially) reproductive class relative to immatures. Additionally, growth rates (and hence length at sexual maturity) may be lower for animals regularly visiting the relatively cooler waters of Western Australia compared to India. Thus, based on our sample of individuals for which total length was known or estimated, the proportion of individuals that were mature (≥ 8 m) was $31 \div 108 = 0.29$. However, a study of vertebral growth rings from stranded individuals recovered in South Africa (Wintner 2000) suggested that an immature 5.77 m (TL) female was 22 years old assuming annual growth rings (age not validated), although maturity could not be determined absolutely given the lack of mature animals to autopsy. Nonetheless, we repeated all model scenarios where the duration of the immature stage was doubled (i.e., 24 years). No modification was made to overall longevity (see below) given that so few individuals remained after maximum age as to make little difference to the matrix outputs.

We used the von Bertalanffy growth function (von Bertalanffy 1938):

$$L_t = L_\infty - (L_\infty - L_0)e^{-kt}$$

where L_t = predicted total length (m) at age t (in years), L_∞ = asymptotic maximum length, L_0 = length at birth and k = a rate constant in units of reciprocal time.

This growth equation has been shown to be suitable for many elasmobranch species (Aasen 1963, Cailliet et al. 1992, Van Dykhuizen & Mollet 1992, Gallucci et al. 2006) and it can be used as a means to translate size-based estimates of survival to age-based probabilities and to estimate longevity. Pauly (2002) suggested that the rate constant (k) for whale sharks was 0.031 year^{-1} with a corresponding longevity > 100 years. This gives a first-year growth of 0.39 m, a value Pauly (2002) considered to be too large. The observed growth rate of young whale sharks in captivity was 0.81 m over 120 days (corresponding to 2.46 m annual growth) (Chang et al. 1997). We speculated and assumed that first-year growth in the wild was 0.80 (approximately twice that of Pauly 2002 and one third the captive rate), yielding a von Bertalanffy rate constant $k = 0.0637 \text{ year}^{-1}$. Using a birth length (L_0) of 0.58 m (Joung et al.

1996), maximum length (L_{∞}) = 13.7 (Compagno 1984) and assuming that maturity is reached at 8 m, this predicts age at maturity is approximately 13.0 years. Using a projected longevity of $5 \log_e 2/k = 54$ years (Ricker 1979), which in this case equates to an individual achieving 97 % of L_{∞} , the duration of each stage is therefore 1 year for stage 1, 12 years for stage 2 (non-reproductive) and 41 years for stage 3 (reproductive). Finally, we set first-year survival to 0.5 based on the observed range of 0.38 – 0.65 for lemon sharks (*Negaprion brevirostris*; Gruber et al. 2001) and 0.37 – 0.82 for neonate black-tip sharks (*Carcharhinus limbatus*; Heupel & Simpfendorfer 2002). The paucity of juvenile survival data for almost all shark species prevents a more rigorous application of an evidence-based survival rate; however, we contend that given the balance of evidence, a first-year survival rate of 0.5 is a realistic mean for the heuristic purposes of inferring potential population trends.

The following sections outline various combinations of parameters and model assumptions to investigate the potential population trajectory using information derived from the CMR survival estimates. Model scenarios consider increasingly complex combinations of parameters under a deterministic framework only.

Model Scenario 1: In this scenario we constructed a simple deterministic model incorporating the mean survival estimate from the CMR models described above. Here, we maintained the first-year survival rate at 0.5 and applied the mean CMR survival rate to the remaining age classes regardless of reproductive status (non-reproductive or reproductive). We assumed a maximum invariant litter size of 300 (Joung et al. 1996) and two reproduction frequencies: annual and biennial. No density-dependent feedback mechanisms were implemented. Finally, this deterministic scenario considered both short (12 years) and long (24 years) non-reproductive stage durations.

Model Scenario 2: In this deterministic scenario we set the survival for the non-reproductive ages (years 1 to 12) to the mean probability of survival derived from the linear prediction based on total length over the size classes found at the Ningaloo Reef aggregation (4 to < 8 m). The reproductive female ages (13+) survival rate was likewise estimated as the mean survival for the size classes considered to be reproductive at Ningaloo (8 to 10 m). All other parameters and assumptions were maintained as in Scenario 1. Both short and long non-reproductive stage durations were examined.

Model Scenario 3: This deterministic matrix included an incrementing survival up to the age of 13 years, after which time survival was held constant. Age-specific survival probabilities were calculated from combination of the total length, survival and von Bertalanffy growth relationships described above. Short and long non-reproductive stage durations were considered separately, as well as annual and biennial reproduction frequencies.

Model Scenario 4: This matrix included incrementing survival up to the age of 25 years, with both non-reproductive stage durations considered separately and annual and biennial reproduction frequencies.

4.3.2.7 Elasticities of λ to changes in matrix parameters

For each deterministic base matrix, we identified the most important demographic parameters influencing the rate of population change. This type of perturbation analysis is achieved by calculating the sensitivity of the dominant eigenvalue of a matrix to changes in its elements, where the sensitivity of matrix element a_{ij} is the local slope of λ as a function of a_{ij} (Caswell et al. 1999). Elasticities (proportional sensitivities) were calculated for each matrix entry (survival, fertility) and summed to provide total elasticities for non-reproductive ($E(s_{nr})$) and reproductive female survival ($E(s_r)$), and adult fecundity ($E(m)$). This process requires taking into account the discounted fertilities (because survival is included in the first-row matrix entries in a post-breeding design) and then normalizing the elasticities for non-reproductive females, reproductive females and fertility so that they sum to 1 (Mollet & Cailliet 2003b). We also calculated the mean age of reproducing females at the stable age distribution (\bar{A}) for each matrix considered:

$$\bar{A} = \langle w, v \rangle$$

where w = left eigenvector of the matrix (age structure) and v = right eigenvector (reproductive values) when $w_1 = v_1 = 1$ (Mollet & Cailliet 2003b). Elasticities can then be calculated from \bar{A} (Mollet & Cailliet 2003b):

$$\begin{aligned} E(m) &= 1/(\bar{A} + 1) \\ E(s_{nr}) &= (\alpha)/(\bar{A} + 1) \\ E(s_r) &= (\bar{A} - \alpha)/(\bar{A} + 1) \end{aligned}$$

In the case of biennial reproduction frequency, elasticities must be calculated differently because the projection interval does not agree with the reproductive cycle (Mollet & Cailliet 2003b). Following the formulae in Appendix 1(b) of Mollet & Cailliet (2003b), \bar{A} is adjusted to $\bar{A}/2$ (i.e., in 2-year units), α becomes $(\alpha + 1)/2$.

4.3.3 Results

4.3.3.1 Survival and capture probabilities

The base CJS analysis estimating apparent survival (ϕ) and capture probability (p) using data from 111 individual sharks demonstrated the saturated model (time-variant ϕ and p) fit the data reasonably well (probability of observing the model deviance as large = 0.464 based on 1000 iterations). Therefore, no adjustment to the AIC scores for over-dispersion (\hat{c}) was required (White & Burnham 1999). The most parsimonious model had time-invariant ϕ and p (Table 4.6); however, there was some evidence for time variation in both parameters based on AIC weights (Table 4.6). The null model gave an apparent annual survival of 0.825 (SE = 0.042; 95 % CI: 0.727 – 0.893; CV = 5.1 %) and capture probability of 0.184 (SE = 0.038; 95 % CI: 0.121 – 0.271; CV = 20.7 %). The model-averaged annual estimates of ϕ are shown in Table 4.7 (range: 0.737 – 0.890).

4.3.3.2 Sex differences in survival

There were 100 individuals of known sex in the database (81 males, 19 females). The saturated model with a sex effect in survival and capture probability fit the data reasonably well (probability of observing the model deviance as large = 0.969 based on 1000 iterations). However, the top five models accounting for over 97 % of the AIC weight had only a *time* effect on survival and no sex effect, suggesting that there were no survival differences between the sexes. There was some support for a sex effect on capture probability $\phi(t) p(\text{sex})$ model with AIC weight = 21.4 %), but the model-averaged capture probability ranges for each sex overlapped (0.229 – 0.263 and 0.232 – 0.266 for males and females, respectively). As such, any possible sex bias in survival and recapture probabilities was ignored.

Table 4.6. Model ranking of Cormack-Jolly-Seber mark-recapture models estimating apparent survival (ϕ) and recapture probability (p) for whale sharks participating in the Ningaloo Reef (Western Australia) aggregation from 1992 to 2004. Shown are the delta Akaike's Information Criteria (ΔAIC), the AIC weight (AICwt), the number of parameters and the deviance for each model. A '(.)' denotes an invariant parameter, and '(t)' denotes a time-variant parameter.

Model	ΔAIC	AICwt	Parameters	Deviance
$\phi(.) p(.)$	0.00	0.588	2	53.459
$\phi(t) p(.)$	1.56	0.269	7	44.289
$\phi(.) p(t)$	3.07	0.126	7	45.800
$\phi(t) p(t)$	7.11	0.017	10	43.015

Table 4.7. Time-variant model-averaged estimates of apparent survival ($\hat{\phi}$) derived using Cormack-Jolly-Seber (CJS) mark-recapture models for whale sharks participating in the Ningaloo Reef (Western Australia) aggregation from 1992 to 2004. Also shown are the standard error (SE), unconditional SE and 95 % confidence interval for each model-averaged estimate.

Interval	$\hat{\phi}$	SE	Uncond SE	95 % CI
1992-1993	0.890	0.038	0.092	0.563 – 0.981
1993-1994	0.890	0.038	0.092	0.563 – 0.981
1994-1995	0.737	0.080	0.176	0.321 – 0.943
1995-1996	0.863	0.124	0.139	0.386 – 0.984
1996-2003 (annual)	0.842	0.056	0.064	0.676 – 0.931
2003-2004	0.773	-	-	-

4.3.3.3 Size differences in survival

There were size (total length) data for 75 individuals in the database (48 immature, 27 mature). Mean total length was 7.2 m and ranged from 4.4 to 9.7 m. In the size-class analysis, the saturated model fit the data reasonably well, although there was moderate evidence for a lack of fit to the data (probability of observing the model deviance as large = 0.052 based on 1000 iterations). The top 4 models (accounting for over 93 % of the AIC weight) had only a time effect on survival, suggesting no support for size (categorical) differences in survival.

The analysis using standardized total length as a covariate in the models demonstrated however, that there was a size bias in survival probability. The top four models all included a *length* and *time* effect on ϕ and accounted for over 92 % of the AIC weight. The most parsimonious model (AIC weight = 38 %) indicated a common intercept and time-variant slopes for the *length* effect on survival, but the second model had identical weight (38 %) and indicated both intercept and slopes were time-variant. Many of the parameters in the time-variant models were not estimable, so we chose to express the simpler relationship between length and ϕ by ignoring the *time* effect. The linear model derived was:

$$\text{logit}(\hat{\phi}) = 0.966 + 0.388 \left(\frac{TL - \overline{TL}}{\hat{\sigma}_{TL}} \right)$$

where TL is the estimated length of a whale shark, \overline{TL} is the mean total length of all sharks in the sample (7.2 m) and $\hat{\sigma}_{TL}$ is the standard deviation of total length from the sample (1.4 m). Thus, ignoring the effects of time, a 5 m shark has a predicted survival probability of 0.59 and a 9 m shark has predicted survival probability of 0.81.

4.3.3.4 Population models

The results of the Leslie matrix projection models are presented in Table 4.8 (age at first reproduction, α , = 13 years) and Table 4.9 (α = 25 years). Of the 16 model combinations considered, 10 (63 %) indicated a decreasing population ($\lambda < 1$). For models based on $\alpha = 13$, the mean age of reproducing females at the stable age distribution (\bar{A}) ranged from 15 to 23 years (Table 4.8), which increased to 29 to 37 years when α was increased 25 (Table 4.9). In all model combinations considered, the stable age distribution indicated a minority of reproductive females, but the dominance of first-year sharks or non-reproductive females varied according to particular combinations of vital rates and model assumptions. However, when survival rate was allowed to vary with age (length), the number of first-year sharks dominated the stable age distribution. All scenarios had higher total elasticities for non-reproductive female survival ($E(s_{nr})$) compared to that for reproductive female survival ($E(s_r)$) (Tables 4.8 and 4.9). $E(m)$ was inferior to $E(s_{nr})$ and $E(s_r)$ in all cases.

Table 4.8. Matrix parameters calculated for each Model Scenario considered when age at first reproduction (α) = 13, for both annual and biennial reproduction frequencies. Shown are the dominant eigenvalue of the deterministic matrix (λ), the stable stage distribution (SSD) for first-year (0 to 1 year), juvenile (1 to 12 years) and adult (13 to 54 years) sharks, respectively, the mean age of reproducing females at the stable stage distribution (\bar{A}), the combined elasticities for non-reproductive ($E(s_{nr})$) and reproductive ($E(s_r)$) survival, the ratio of elasticities for reproductive to non-reproductive survival ($E(s_r)/E(s_{nr})$) and the elasticity for fertility ($E(m)$).

Scenario	Description	λ	SSD	\bar{A}	$E(s_{nr})$	$E(s_r)$	$E(s_r)/E(s_{nr})$	$E(m)$
<u>Annual reproduction</u>								
Scenario 1	constant survival	1.2658	0.47, 0.53, 0.005	14.87	0.8191	0.1179	0.1440	0.0630
Scenario 2	average length-based survival	1.0438	0.45, 0.54, 0.004	16.53	0.7412	0.2013	0.2713	0.0571
Scenario 3	length-based survival to age 13	0.9500	0.60, 0.40, 0.005	17.12	0.7173	0.2275	0.3171	0.0552
Scenario 4	length-based survival to age 25	0.9751	0.61, 0.39, 0.005	20.61	0.6015	0.3522	0.5855	0.0463
<u>Biennial reproduction</u>								
Scenario 1	constant survival	1.2229	0.44, 0.55, 0.007	14.67	0.7798	0.1002	0.1285	0.1200
Scenario 2	average length-based survival	1.0078	0.43, 0.57, 0.006	16.73	0.6940	0.1992	0.2870	0.1068
Scenario 3	length-based survival to age 13	0.9177	0.58, 0.42, 0.008	17.52	0.6658	0.2317	0.3480	0.1024
Scenario 4	length-based survival to age 25	0.9470	0.59, 0.40, 0.008	22.38	0.5332	0.3848	0.7218	0.0820

Table 4.9. Matrix parameters calculated for each Model Scenario considered when age at first reproduction (α) = 25, for both annual and biennial reproduction frequencies. Shown are the dominant eigenvalue of the deterministic matrix (λ), the stable stage distribution (SSD) for first-year (0 to 1 year), juvenile (1 to 24 years) and adult (25 to 54 years) sharks, respectively, the mean age of reproducing females at the stable stage distribution (\bar{A}), the combined elasticities for non-reproductive ($E(s_{nr})$) and reproductive ($E(s_r)$) survival, the ratio of elasticities for reproductive to non-reproductive survival ($E(s_r)/E(s_{nr})$) and the elasticity for fertility ($E(m)$).

Scenario	Description	λ	SSD	\bar{A}	$E(s_{nr})$	$E(s_r)$	$E(s_{nr})/E(s_r)$	$E(m)$
<u>Annual reproduction</u>								
Scenario 1	constant survival	1.0508	0.31, 0.69, 0.003	28.63	0.8436	0.1223	0.1453	0.0337
Scenario 2	average length-based survival	0.9432	0.38, 0.62, 0.003	30.91	0.7836	0.1851	0.2362	0.0313
Scenario 3	length-based survival to age 13	0.8715	0.54, 0.44, 0.004	31.56	0.7679	0.2014	0.2623	0.0307
Scenario 4	length-based survival to age 25	0.9352	0.58, 0.41, 0.004	35.45	0.6859	0.2867	0.4180	0.0274
<u>Biennial reproduction</u>								
Scenario 1	constant survival	1.0295	0.29, 0.71, 0.004	28.55	0.8183	0.1162	0.1420	0.0655
Scenario 2	average length-based survival	0.9244	0.36, 0.63, 0.005	31.20	0.7531	0.1867	0.2479	0.0602
Scenario 3	length-based survival to age 13	0.8542	0.53, 0.47, 0.007	31.95	0.7364	0.2047	0.2780	0.0589
Scenario 4	length-based survival to age 25	0.9178	0.57, 0.42, 0.008	36.23	0.6540	0.2937	0.4491	0.0523

4.3.4 Discussion

The paucity of data describing the variation in vital rates in species of conservation concern is a common problem for ecological modellers (Boyce 1992, Morris & Doak 2002). Indeed, obtaining estimates of vital rates and their corresponding variances may be difficult or impossible for many species, especially for long-lived marine vertebrates (Caughley 1994, Heppell et al. 2000). As such, generalizations for predicting population persistence derived from few data or based on allometric or species-specific ecological characteristics are often sought (Beissinger & Westphal 1998, Belovsky et al. 2004, Brook et al. 2006). Although heuristically useful (Brook et al. 2002), matrix population models lacking quantitatively derived vital rates are subject to many assumptions that are difficult to test or validate. In the case of the relatively poorly studied whale shark, we have provided the first estimates of survival rates based on mark-recapture data. These estimates, combined within a series of deterministic Leslie matrix models have permitted the first quantitative appraisal of the projected long-term trends of this vulnerable population.

Although caution must be exercised in interpreting our population matrices (see below), the variants of the age-classified Leslie matrix models using different estimates of non-reproductive female and reproductive female survival and stage duration demonstrate the importance of considering biologically plausible covariates in survival analyses, especially for long-lived and slow-growing species. For example, ignoring the important effect of total length (size) on estimates of survival led to the conclusion of population increase (i.e., $\lambda > 1$) regardless of changes to age at first reproduction and frequency of reproduction. However, when we used the more parsimonious information-theoretic model predictions of length-varying survival, the importance of stage duration became much more apparent. With the shorter stage duration and age-specific survival estimates, most scenarios predicted a declining population ($\lambda < 1$), and doubling the interval between reproductive events resulted in an increased rate of decline.

Many elasmobranchs have a reproductive cycle of two years (Cortés 2002), and a few species breed more infrequently, every three years (Mollet et al. 2000, Cortés 2002). Although the reproduction interval of whale sharks is currently unknown, the precautionary principle for fisheries management (Caddy & Mahon 1995) suggests that assuming annual reproduction would be inappropriate for whale sharks. Reducing the breeding frequency further to once every three years, the estimates of λ under the most realistic Scenario 4 (length-based survival to age 25) are further depressed to 0.9325 (age at first breeding = 13) and 0.9077 (age at first breeding = 25). Despite the severe lack of demographic data for this species (especially with respect to its reproductive capacity), the models that incorporated the most biologically realistic parameter estimates and assumptions support the conclusion of a declining population visiting Ningaloo Reef each year. However, this conclusion depends on some as yet untested assumptions. The duration of the non-reproductive stage and lifespan of the species are important determinants in the projections using length-varying estimates of survival. Of these two parameters, perhaps it is more tractable to collect information on growth rates that would verify the onset of reproduction.

The super-population of whale sharks participating in the Ningaloo Reef aggregation has been estimated at 300 – 500 individuals of which approximately 16 % were identified as female (74 % male and 10 % indeterminate gender) (Meekan et al. 2006). It should also be noted that pups and yearlings have never been observed at Ningaloo Reef, so pup production is likely to occur elsewhere. It is unknown whether the female component of the Ningaloo aggregation represents a small proportion of females that normally participate in a larger, sexually segregated female population that has yet to be identified. If there is an important sexual segregation of whale sharks as has been documented for other elasmobranch species (Springer 1967, Klimley 1987, Sims et al. 2001, Sims 2006), then the small number of females observed at Ningaloo might not necessarily comprise the majority of the reproductively active females contributing new individuals to the aggregation. The embryo and juvenile sex ratio of many shark species does not depart from unity (Joung & Chen 1995, Chen et al. 1997b, Liu et al. 1999, Smale & Goosen 1999, Joung et al. 2005, Hazin et al. 2006), and Beckley *et al.* (1997) reported an equal sex ratio for stranded, immature whale sharks in South Africa. As such, we expect the low percentage (16 %) of females at Ningaloo to be the result of sexual segregation, perhaps with many females within the super-population instead spending their time farther north in Southeast Asian waters (Theberge & Dearden 2006), around the Indian coastline (Satyanarayana Rao 1986), or even in the vicinity of the Galápagos Islands (Stewart & Wilson 2005).

Our analyses also revealed some important aspects of the contribution of length- (and age-) specific survival rates to population rates of change. Elasticities from a mean matrix cannot by themselves accurately predict how λ fluctuates with variation in vital rates because of non-equality of change in these parameters, non-linearities in their relationships to λ , and differences in the coefficients of variation among matrix elements (Mills et al. 1999, Stewart & Wilson 2005). Additionally, the reported elasticities were derived from deterministic matrices, which can be poor predictors of stochastic elasticities when the environment is extremely variable or includes catastrophic mortality events (Benton & Grant 1996). Although it has been shown previously that whale shark numbers at Ningaloo Reef fluctuate in response to environmental events such as El Niño-Southern Oscillation (ENSO; Wilson et al. 2001a), we deliberately avoided using stochastic projections given the uncertainty associated with mean values of reproductive output, reproduction frequency and age at first reproduction.

With these caveats in mind, we found that the highest elasticities were for immature (i.e., non-reproductive) survival rates. This result agrees with re-assessments of elasticities for most elasmobranch species (Mollet & Cailliet 2002, 2003b). Even though others have suggested that elasmobranch population rates of change are more sensitive to adult (reproductive) survival (Colman 1997, Smith et al. 1998, Walker 1998, Frisk et al. 2001, Cortés 2002), the elasticities for many stage-classified models are calculated inappropriately (see Mollet & Cailliet 2003b). When calculated correctly (and more easily) using age-classified Leslie matrix models, we found that immature female survival was a far more important determinant of the potential population rate of change for whale sharks; therefore, estimating this parameter precisely should be a prime area of research.

The limitation of producing robust estimates of the reproductive potential of whale sharks is problematic and may ultimately prevent the construction of reliable population viability analyses. There have only been nine 'juveniles' (0.55 – 0.93 total length) recorded for whale sharks (Colman 1997), some of which have been found in the stomach of other oceanic predators (blue shark, *Prionace glauca* and blue marlin, *Makaira mazara*) (Kukuyev 1996, Colman 1997). Neither have there ever been reports of individuals between 0.93 and 3.00 m total length, suggesting that there are either extremely high predation rates on small individuals, or that reproduction occurs in the open ocean and is so dispersed that the probability of detecting young individuals is too low to quantify precisely. Another potential limitation is the likely density-related changes in vital rates used to parameterize the models, especially considering the pervasiveness of density dependence in nature (Brook & Bradshaw 2006). We deliberately avoided constructing hypothetical density-dependent relationships in our simple scenarios given the complete lack of associated data, but we acknowledge that persistence predictions and parameter elasticities are likely to vary with the inclusion of density dependence (Grant & Benton 2000, Drake 2005). However, future work on this aggregation and other whale shark populations should attempt to assess the degree to which vital rates are modified by density fluctuations. This may be achieved perhaps initially by examining the evidence for density dependence in phenomenological time series of relative abundance (e.g., sightings-per-unit-effort data; Brook & Bradshaw 2006).

Our analyses beg the questions – (1) what is the state of the Ningaloo Reef whale shark population and (2) can our analyses shed light on its persistence probability? Recent evidence from Ningaloo suggests that the population is comprised of a larger proportion of juveniles compared to previous decades (Meekan et al. 2006). However, severe declines have not been reported, so we believe that the real population trajectory lies somewhere between the extremes of our predictions. Additionally, an aggregation of juvenile whale sharks in nearby Thailand has recently declined by 96 % (sightings per unit effort from 1992 to 2001) (Theberge & Dearden 2006). These observations, in combination with our results, lend credence to the hypothesis that the regional (Australasian) population of whale sharks is declining. As such, our results have several conservation implications for this and other large oceanic shark species. The wide dispersal range and sensitivity of population growth rates to minor variation in survival makes this species particularly vulnerable to anthropogenic sources of mortality (customary and commercial fishing). Non-reproductive whale sharks aggregating at Ningaloo travel long distances (1000s km) to Southeast Asian waters (Wilson et al. 2006) where they are potentially susceptible to fishing pressure (Eckert et al. 2002; Polovina et al. unpubl. data). The low population size (300 – 500 individuals; Meekan et al. 2006), the possibility of limited mixing (Wilson et al. 2006; Polovina et al. unpubl. data), and the high elasticity of λ to non-reproductive female survival rates demonstrate the need for concerted conservation efforts to span national boundaries (Wilson et al. 2006).

The collection of mark-recapture databases for whale sharks has provided the first quantitative foundation for testing hypotheses regarding population persistence in one of the largest known aggregations of this species. Continued development of this database will be important for adjusting the predictions of matrix-based models, and will also provide a template for other large, oceanic marine vertebrates for which few demographic data exist.

Our combination of standard CJS mark-recapture estimates of apparent survival and age-classified Leslie matrix models allowed us to assess the biological reality of the demographic rate estimates for whale sharks. In so doing, our study has highlighted the demographic processes that conservation practitioners should aim to maximize to increase the persistence probability of this, and other large elasmobranch species.

4.4 SCARRING PATTERNS AND RELATIVE MORTALITY RATES OF INDIAN OCEAN WHALE SHARKS

4.4.1 Introduction

Declines in populations of whale sharks (*Rhincodon typus*) have been observed and predicted in many regions (CITES 2002, IUCN 2005, Theberge & Dearden 2006, Bradshaw et al. 2007, Bradshaw et al. In press). This species, the world's largest fish and one of the most wide-ranging marine vertebrates (Wilson et al. 2006, Bradshaw et al. 2007, Castro et al. 2007), is known to be susceptible to a variety of mortality sources including direct harvest, ecosystem modification and collisions with ocean-going vessels (Bradshaw et al. 2007) that may be the cause of these declines. The prospect of losing such a large and iconic species is of both conservation and economic concern. For example, the disappearance of the species could precipitate annual losses in the order of US\$47.5 million generated from whale shark tourism globally (Graham 2004).

Although potential sources of population decline have been recognised for many years (Colman 1997), their relative importance remains largely unquantified. The large size (> 12 m total length), slow swimming speeds (between 1 and 3 km h⁻¹) (Gunn et al. 1999, Eckert & Stewart 2001, Eckert et al. 2002, Hsu et al. 2007) and tendency to spend a large proportion of their time at the surface (Wilson et al. 2006) renders this species particularly vulnerable to ramming by vessels (Gudger 1940), artisanal and commercial fishing (Colman 1997) and predation by large sharks and some cetaceans (Fitzpatrick et al. 2006). Additionally, these animals make annual long-distance migrations through international and national waters (Wilson et al. 2006). This means that whale sharks may experience protection by legislation and management in some areas, while being exploited in other parts of their range (Bradshaw et al. In press), a problem common to other wide ranging marine species such as North Atlantic right whales (*Eubalaena glacialis*) (Ward-Geiger et al. 2005). Thus, identifying mortality sources and areas where these pose a risk to whale sharks are important steps in formulating global initiatives for conservation.

Legal and illegal fishing of whale sharks is often suggested to be a central driver of population declines (Chen & Phipps 2002, CITES 2002, Bradshaw et al. 2007). This mortality is relatively easy to quantify because animals are brought to shore by fishermen and sold in markets. However, other factors such as predation and boat strike may be equally important, but are far more difficult to estimate reliably because they are thought to occur principally in the open

ocean. Despite the lack of direct observation, where whale sharks survive predatory attacks or collisions with ships, some evidence of these events may be left in the form of scars or injuries on the body. Analysis of scarring patterns may thus provide an insight into the relative importance and source of mortality afflicting whale sharks, as is the case for other large marine species such as manta rays, manatees, whales, dolphins and seals (e.g., Kraus 1990, Hiruki et al. 1993, Angliss & DeMaster 1997, Heithaus 2001b, Laist et al. 2001, Naessig & Lanyon 2004, Rommel et al. 2007).

Each whale shark has a unique pattern of spots and stripes (Meekan et al. 2006) that can be used to identify individuals (Speed et al. 2007). Photographic databases are now used worldwide in mark-recapture studies to document population trends and estimate demographic rates (Fujiwara & Caswell 2001, Stevick et al. 2001, Bradshaw et al. 2003, Meekan et al. 2006, Speed et al. 2007). A combination of information on rates and source of scarring in conjunction with mark-recapture data may provide a means to quantify relative mortality rates among whale shark populations experiencing different direct and indirect human impacts. Similar analyses of the survival implications of scarring and injuries have been made in other taxa (e.g., Iberian lynx *Lynx pardinus*, North Atlantic right whale *Eubalaena glacialis*, Hawaiian monk seals *Monachus schauinslandi* – Kraus 1990, Garcia-Perea 2000); however, no study to date has combined photo-identification with scarring to test the hypothesis that scarring is indicative of higher mortality rates.

This study documents the severity, positioning and likely causes of scars observed on whale sharks participating in three Indian Ocean aggregations: 1) Ningaloo Reef, western Australia, 2) Mahe, Seychelles and 3) southern Mozambique. Using capture-mark-recapture (CMR) models and quantified scarring patterns, relative apparent survival rates were estimated between two of the study sites (Ningaloo and Seychelles) and compared to shipping traffic rates to estimate the potential high risk boat-strike areas for this species.

4.4.2 Materials and methods

4.4.2.1 Scarring databases and image matching

Scarring image libraries were constructed from larger whale shark photo-identification databases for Ningaloo Reef, western Australia (22° 50' S, 113° 40' E), Mahe, Seychelles (4°6' S, 55° 26' E) and southern Mozambique (23° 52' S, 35° 33' E). (Fig. 4.12). The Ningaloo scarring library consisted of images of individuals with scars taken over 10 capture sessions (years) between 1992 and 2006 (not including 1997-2000 and 2002). The Seychelles library consisted of images taken over 6 capture sessions between 2001 and 2006 and also included scarring information obtained from a tagging database. The Mozambique scarring library consisted of images taken during one capture session over the 2004/2005 season.

Images were matched using the software I³S (Van Tienhoven et al. 2007b) and visual confirmation following guidelines for use on whale sharks outlined in Speed *et al.* (2007). Where images did not lend themselves to the fingerprinting process required for I³S, images were matched manually by an experienced photo-archivist (Meekan et al. 2006) using not only the pattern of natural pigmentation, but also other individually unique identifiers such as scars and tags.

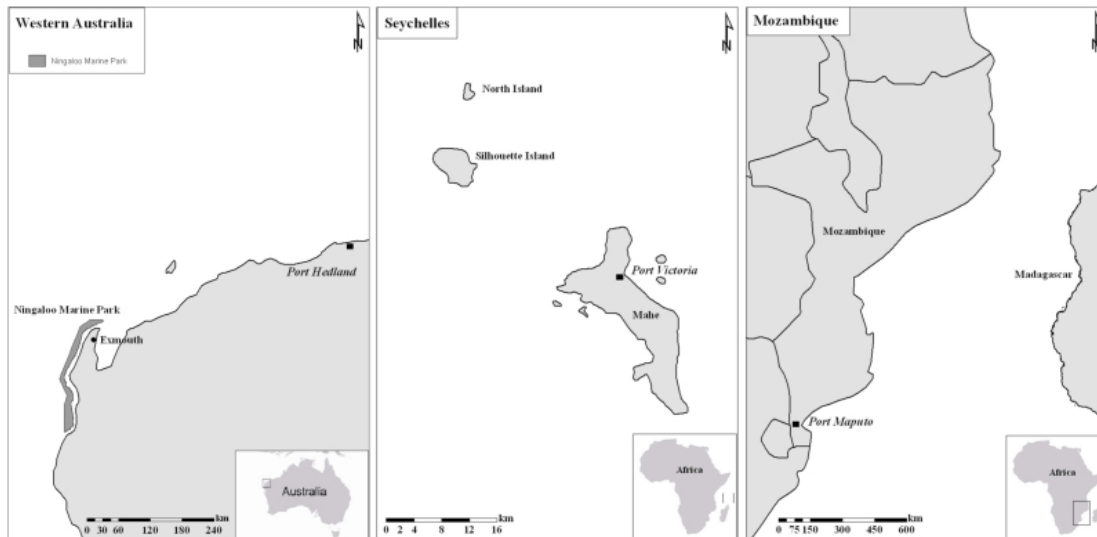


Figure 4.12. Indian Ocean whale shark aggregation sites – Ningaloo Reef (Western Australia), Seychelles and Mozambique.

4.4.2.2 Scarring categories

Seven scarring categories were created based on images present in the libraries for each region: (1) abrasions, (2) lacerations, (3) nicks, (4) bites, (5) blunt trauma, (6) amputations and (7) 'other' (Appendix 1). Each image was assigned to one or more of the seven categories by visual inspection. The severity of scarring was classified into two groups: 'major' or 'minor'. Major scars were considered to be potentially life-threatening and included complete or near-complete amputation of the first dorsal, pectoral or caudal fins, lacerations penetrating the sub-dermal layer, blunt trauma around the head or gills and large shark bites (> 30 cm in length) (Fig. 4.13A - C). Minor scars were considered to be superficial and included abrasions, partial amputations, small bites, nicks, and 'other' (Fig. 4.13D - F).

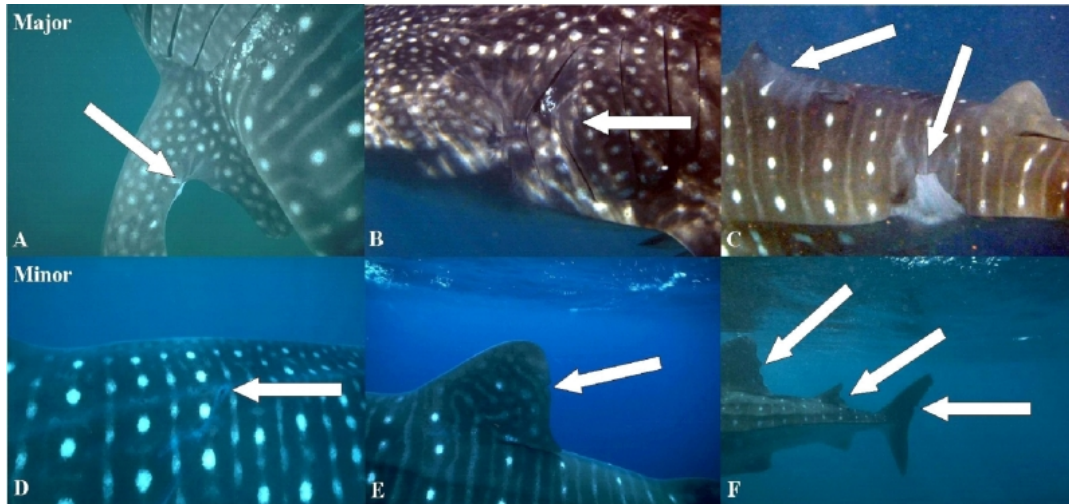


Figure 4.13. Classification of scar severity. Images A – C show examples of ‘major’ scarring; A) (Photo© G. Taylor) A large bite taken out of the left pectoral fin, B) (Photo© A. Richards) Blunt trauma to the left side of head and C) (Photo© A. Richards) Bites taken out of dorsal fin and left flank. Images D – F (Photos© G. Taylor) show examples of ‘minor’ scarring; D) Abrasion on the right flank, E) Small nick taken out of the trailing edge of the dorsal fin and F) Nicks and small bites taken out of the first and second dorsal fins and caudal fin.

4.4.2.3 Database comparisons

The frequency of individuals with scars per capture session was initially calculated for each database and then combined to give total numbers of scarred individuals per aggregation. Due to differing numbers of sample periods among databases, estimates were standardised for cross-database comparisons by dividing the number of scarred individuals by the total number of individuals photographed for each aggregation. The total number of sharks scarred per database was also recalculated with the scarring categories ‘nicks’ and ‘abrasion’ omitted for two reasons: (1) the scar categories are unlikely to affect survival rates given that they are by definition superficial wounds, and (2) minor scars were often not photographed on individuals at Ningaloo Reef. The proportion of individuals with differing scar types were calculated for each aggregation (with minor scars omitted). A randomised multinomial contingency analysis (10000 iterations) was constructed to test the hypothesis that the distribution of animals in each scar category differed among aggregations. Scar categories were combined into three main classes to avoid low-frequency classes dominating results: bites, blunt trauma, and lacerations/amputation (ignoring other categories). Scar positions on the body of each shark were also recorded to compare among aggregations and to determine the most commonly scarred areas of the body.

4.4.2.4 Effects of scarring on apparent survival

Capture histories consisting of inter-season resights from Ningaloo and Seychelles were initially constructed using matches identified by I³S as well as tags deployed in Seychelles. The capture history for the Mozambique aggregation was unable to be included because there were too few sample sessions. To avoid double-counting, individuals with only the left side photographed were removed from the Ningaloo capture history (because there were fewer

left-side photographs than right-side), while individuals with only the right side photographed were removed from the Seychelles capture history (fewer right-side photographs there) (Meekan et al. 2006). Capture histories included (1) whether the individual was scarred or not (three categories: major, minor and none), (2) the putative source of scarring (anthropogenic, bite, unknown, none) and (3) the body position of the scar (fin, body or none). Cormack-Jolly-Seber (CJS) CMR models were used and executed in the program MARK (White & Burnham 1999) to model apparent survival of (ϕ) and resighting probability (p) (Bradshaw et al. 2007). The major focus of this analysis was to assess whether the apparent survival rate for whale sharks with scars differed from whale sharks without scars.

The initial analysis examined whether there was evidence for time variance in ϕ or p over the study period (1992-2006) at Ningaloo, which was analogous to the approach adopted by Bradshaw *et al.* (2007), although the current analysis included two additional capture sessions (2005 & 2006). This process was then repeated for the Seychelles aggregation. The second analysis included scarring as an additional group effect on ϕ or p . Scar type and severity were examined to assess whether they influenced ϕ or p . Models were compared using Akaike's Information Criterion corrected for small sample sizes (AIC_c) (Burnham & Anderson 2002) and goodness-of-fit was estimated using the bootstrap GOF function in program MARK (White & Burnham 1999).

4.4.2.5 Shipping activity around aggregations

Due to limited availability of spatial shipping data for the east coast of Africa, shipping density was unable to be modelled around the three whale shark aggregations. Consequently, the number of commercial ships (i.e., container ships and bulk carriers) calling in at the largest and nearest port to each aggregation was obtained through associated port authorities as a proxy for shipping intensity. Where available, statistics on smaller vessel traffic were also noted. Ship-calling data were obtained for the fiscal year from 01 July 2005 through to 30 June 2006 from Port Hedland (Australia), Port Victoria (Seychelles) and Port Maputo (Mozambique) authorities.

4.4.3 Results

The Seychelles aggregation had the highest percentage of scarred individuals (67 %, 534 of 797), followed by Mozambique (37.2 %, 67 of 180) and Ningaloo (27 %, 84 of 311). After the removal of minor scars (nicks and abrasions), the total percentages of scarred individuals per aggregation dropped to 45.3 % (361 of 797) for Seychelles, 22.7 % (41 of 180) for Mozambique, and 20 % (62 of 311) for Ningaloo Reef.

Nicks were the most abundant scar category in all aggregations (Table 4.10). After the removal of these minor scars (nicks and abrasions), bites were the most common scars (Table 4.10; Fig. 4.14).

Table 4.10. Percentage of individuals within scar type and body location category among three Indian Ocean aggregations observed.

	Aggregation		
	Ningaloo	Seychelles	Mozambique
Scar Type (%)			
abrasions	21.4	14.6	40.3
lacerations	8.3	34.5	7.5
nicks	11.9	48.6	14.9
bites	44.0	21.4	14.9
blunt trauma	8.3	5.1	7.5
amputations	15.5	21.4	26.9
other	2.4	4.4	10.4
Scar Location (%)			
head	9.5	11.6	30
dorsal fin	30.0	38.5	20.9
caudal fin	25.0	62.2	31.3
pectoral fin	22.6	14.4	22.4
flank	25.0	25.2	34.3

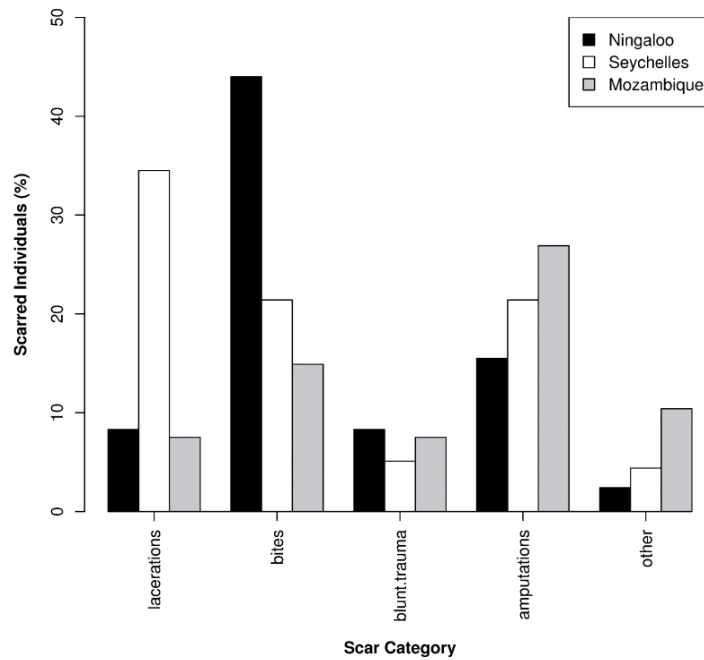


Figure 4.14. Percentage occurrence of individuals within scar categories by location.

The randomised contingency analysis demonstrated that the probability of generating the same among-site differences in the distribution of individuals within the three major scar categories (bites, blunt trauma, lacerations/amputations) was = 0.0007 (based on 10000 iterations). Observed and expected frequencies were similar for Seychelles and Mozambique animals, but Ningaloo had more bites and fewer amputations/lacerations than expected (Fig. 4.15). Caudal fins were the most commonly scarred body part (Fig. 4.16A) at all locations (Fig. 4.16B).

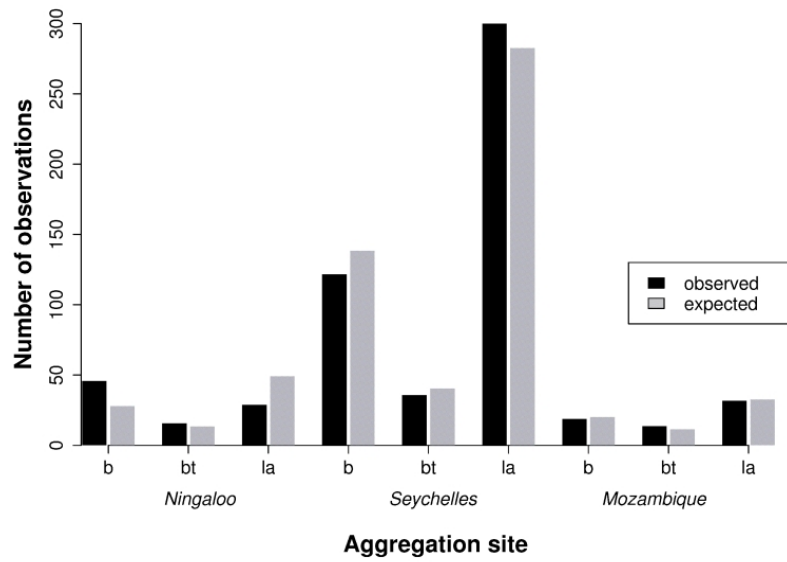


Figure 4.15. Observed and expected numbers of sharks in each scarring category among aggregation sites. *b = bites, bt = blunt trauma and la = lacerations and amputations.

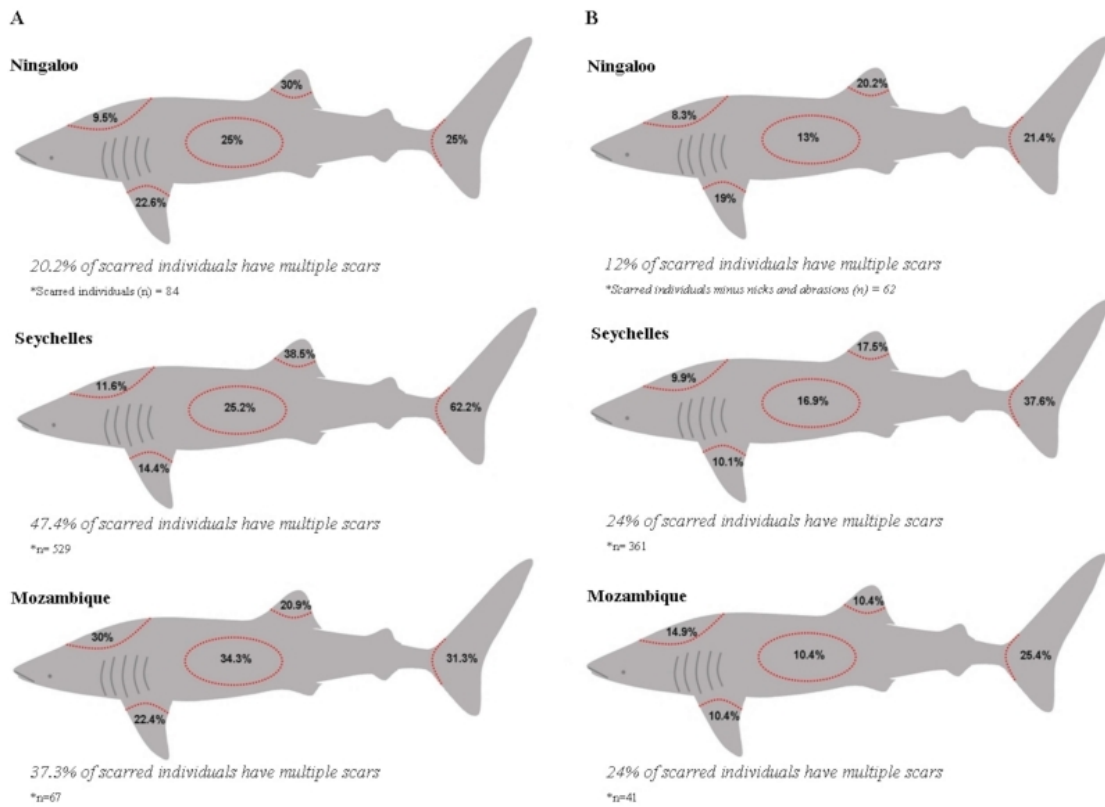


Figure 4.16. A) Position of scars on body by aggregation site B) Position of scars on body by aggregation site (nicks and abrasions omitted).

The saturated Cormack-Jolly-Seber capture-mark-recapture model $\phi(t^*s) p(t^*s)$ relating time (t) and scarring (s) to apparent survival (ϕ) and resight probability (p) for the 221 individual sharks seen at Ningaloo fit the data reasonably well (probability of observing the model deviance as large = 0.134 based on 1000 iterations). Therefore, no adjustment to AIC_c was made for over-dispersion (White & Burnham 1999). Most parameters were inestimable using the t^*s interaction for ϕ and p , so these group factors were considered separately in all subsequent model comparisons. The most highly ranked model ($wAIC_c = 0.84$) had scar effects on apparent survival and time-variant resighting probability $\phi(s) p(t)$ (Table 4.11); however, confidence intervals for scarred and not-scarred individuals overlapped substantially (Table 4.11).

There was no over-dispersion detected for the Seychelles dataset, and the most highly ranked model ($wAIC_c = 0.99$) demonstrated time variance in ϕ and p (Table 4.11). However, many of the interval estimates of ϕ were inestimable, so the second-most highly ranked model was used to test for scarring effects. Again, there was considerable overlap in the confidence intervals between scarred and non-scarred individuals (Table 4.12), suggesting little evidence for an effect on apparent survival. Apparent survival rates were considerably lower in the Seychelles (~ 0.50) compared to Ningaloo Reef (~ 0.90).

Table 4.11. Five most highly ranked Cormack-Jolly-Seber models testing the effects of scarring (s) and time (t) on apparent survival (ϕ) and resight probability (p) of whale sharks participating in the Ningaloo Reef aggregation between 1992 and 2006, and at Seychelles between 2001 and 2006. Shown are the difference in Akaike's Information Criterion corrected for small sample sizes between the current and top-ranked model (ΔAIC_c), AIC_c weight ($wAIC_c$), the number of model parameters (k), and model deviance. '(.)' indicates a constant parameter.

Model	ΔAIC_c	$wAIC_c$	k	Deviance
Ningaloo Reef				
$\phi(s)p(t)$	0.000	0.842	10	133.021
$\phi(.)p(t)$	3.381	0.155	10	136.402
$\phi(.)p(.)$	58.406	0.000	2	208.329
$\phi(t)p(.)$	58.114	0.000	10	191.135
$\phi(t)p(t)$	12.535	0.000	17	129.777
Seychelles				
$\phi(t)p(t)$	0.000	0.999	8	31.894
$\phi(s)p(t)$	25.201	0.000	7	61.233
$\phi(.)p(t)$	23.491	0.000	6	61.580
$\phi(.)p(.)$	57.842	0.000	2	104.074
$\phi(t)p(.)$	28.918	0.000	6	67.006

Table 4.12. Apparent survival estimates for whale sharks with and without scarring at Ningaloo Reef and Seychelles based on Cormack-Jolly-Seber mark-recapture models.

Model		ϕ	SE	Lower 95 % CI	Upper 95 % CI
Ningaloo Reef					
$\phi(s)p(t)$	Not Scarred	0.858	0.033	0.781	0.911
	Scarred	0.929	0.033	0.830	0.972
Seychelles					
$\phi(s)p(t)$	Not Scarred	0.502	0.060	0.386	0.618
	Scarred	0.538	0.070	0.402	0.669

ϕ = apparent survival, s = scarred or not, p = sighting probability, t = time.

The number of commercial ships that called in to Port Hedland during the fiscal year of 2005/2006 was 925 (excluding fishing vessels). The intended destinations after departure for the majority of these ships were Asia. The number of commercial vessels calling in to Port Victoria during the same period was 510; however, there was also a notably high number of fishing vessels (628), both purse-seine and long-line, whose next destination was the high seas. For commercial vessels, the next port of call was largely South East African and Indian Ocean island ports or European or Asian ports. The number of commercial ships that docked at Port Maputo during this period was 674, with the final destination of most of these vessels also being Asia.

4.4.4 Discussion

The prevalence and origin of large scars on whale sharks leads to the hypothesis that activities other than direct over-exploitation from fishing may also contribute to observed and modelled population declines of whale sharks in the Indian Ocean. Of the 1288 individuals identified in this study, 36 % bore prominent scars (i.e., excluding nicks and abrasions). Bite marks were the most common form of major scar (27 % of scarred individuals) followed by lacerations/amputations (19 %) and blunt trauma (7 %). Bite scars were probably the result of attacks by large predators such as sharks and killer whales. Non-lethal attacks by a large (> 4 m) predatory shark on a whale shark have been recorded at Ningaloo Reef (Fitzpatrick et al. 2006) and a fatal attack on an 8-m whale shark by killer whales (*Orcinus orca*) was observed in the Gulf of California (O'Sullivan & Mitchell 2000). None of the bite scars found on whale sharks in this study could be unambiguously attributed to killer whales, as virtually all were healed wounds that lacked the distinctive teeth rake marks that are definitive of attacks by these predators (Naessig & Lanyon 2004).

Many whale sharks bore the evidence of collisions with boats and this phenomenon was probably responsible for the majority of lacerations, amputations and blunt trauma injuries. The parallel rows of deep lacerations found on the backs of many sharks were clear evidence of strikes by ship propellers (Rommel et al. 2007), while the large blunt trauma injuries on the head and flanks of sharks were probably mostly due to ramming by ship bows (Laist et al. 2001). In the case of amputations, some of these injuries may have also have been due to predatory attacks, albeit most could be distinguished from ship strike by the circular edge of the wound (see Fig. 4.13A).

Ramming of whale sharks by ocean-going vessels was well-recognised as a threat to whale sharks in the early years of the 20th century (Gudger 1940), but such deaths of sharks are rarely recorded today. Due to relatively thin sub-dermal fat layers, whale shark carcasses may sink quickly in comparison to whales (Ward-Geiger et al. 2005) so that most mortalities due to collisions probably go unnoticed (Stevens 2007). However, boat collisions are likely still to reduce the survival probability of whale sharks, particularly since shipping traffic along coasts and in the open oceans has more than tripled since the 1940s (Lloyd's Register of Shipping 1939-2005), and today's cargo vessels are larger and travel at much greater speeds. Mortalities due to shipping have been recorded in recent times; for example, a whale shark was struck and killed by a large vessel off the coast of the Seychelles in 2000 (Fig. 4.16). Other possible

evidence of ship strikes comes from Pop-up Archival Tag (PSAT; Wilson et al. 2006) deployments on whale sharks at Ningaloo Reef. These tags are designed to release and float to the surface once an animal remains at a constant depth and temperature for more than two days. During one deployment, a 4-m whale shark travelling at the surface along the Northwest Shelf, one of Australia's busiest shipping routes, suddenly descended to 900 m and remained there for 12 hours (Wilson et al. 2006). Given diving records of other animals and the water temperature at that depth (2°C) this behaviour may represent mortality due to a ship strike, although other causes (e.g., predatory attacks) cannot be excluded.

The proportion of sharks bearing predator bite scars and those with laceration/amputation and blunt trauma scars were similar (27 versus 26% of individuals, respectively). However, this does not necessarily mean that they translated into a similar number of deaths. Lacerations and blunt trauma scars generally appeared more severe than bite scars because the former covered larger areas of the body and in the case of lacerations, propellers often left multiple scars on the same animal. Furthermore, bite scars tended to be most common on the fins, and evidence from Ningaloo suggests that animals can recover from even total fin amputation by bites (Fitzpatrick et al. 2006). Thus, ship collisions may be responsible for greater mortalities of whale sharks, even if rates of scarring from this source are similar to bites.

Although minor scars (nicks and abrasions) are unlikely to alter individual survival probability, they may act as warning signs of other threats. Three of the Mozambique sharks possessed abrasions similar to those described from net-entangled cetaceans (Angliss & DeMaster 1997). Tuna purse-seine fisheries in the western Indian Ocean catch small numbers of whale sharks (Romanov 1998), while gill-net fisheries also occasionally catch whale sharks (Stevens 2007). Five Mozambique sharks had minor abrasions or lacerations characteristic of small boat propeller strikes (Rommel et al. 2007). Similar scars have been noted at other aggregation sites (Graham & Roberts 2007, Rowat et al. 2007) and in some cases, were possibly caused by vessels used to view sharks (Rowat et al. 2007). 'Go-slow' areas within aggregation sites, already used for some other slow-moving marine species (Laist & Shaw 2006) and regulated through the whale shark code of conduct in Western Australia, may reduce the probability and severity of ship strikes.

The caudal fin was the area most commonly scarred. This is not surprising, given that these animals spend most of their lives in < 100 m of water and much time swimming at the surface (Wilson et al. 2006). For this reason, the caudal fin will be the body part most likely to be struck by a boat. The caudal fin may also be an attractive target for predators because it may be easier to grip with teeth and sever in contrast to the body trunk (Long & Jones 1996).

Whale sharks at Ningaloo Reef had more bites (44 % of individuals) and fewer lacerations and blunt trauma scars than those at either the Seychelles or Mozambique. Although this suggests that there may be higher rates of predation at Ningaloo and lower numbers of boat strikes, it needs to be recognised that these animals are highly migratory (Eckert & Stewart 2001, Eckert et al. 2002, Rowat & Gore 2006, Wilson et al. 2006) and that the healed scars observed at the study sites may have been accrued in distant parts of their range. Despite the incongruence of shipping activity and relative scarring rates among sites (e.g., there were more commercial

vessels near Ningaloo despite a lower incidence of ship-related injuries), there is some evidence that small boat traffic at Ningaloo may be lower than at either the Seychelles or Mozambique. Ningaloo Reef is largely protected by an expansive marine park in a remote area of Western Australia, whereas the coastal areas around Mozambique and Seychelles are heavily populated and have a strong fishing presence. Furthermore, tiger sharks (*Galeocerdo cuvier*) and other large species of requiem (*Carcharhinidae*) sharks (Fitzpatrick et al. 2006) are regularly sighted by spotter planes during the peak whale shark season at Ningaloo Reef, and are also temporarily abundant in other areas immediately to the south such as Shark Bay (Heithaus 2001a). In contrast, large, predatory sharks are rarely spotted during aerial surveys during whale shark season in the Seychelles (D. Rowat, unpubl. data).

The hypothesis that observed rates of scarring were indicative of relative mortality rates at two widely separated aggregations on opposite sides of the Indian Ocean experiencing different intensities of shipping traffic was not supported. The lack of a scarring effect on apparent survival may indicate that individuals surviving ship strike and predator attack are no more susceptible to premature mortality than their unscathed counterparts, but the relative contribution of different shipping rates to explain regional variance in survival patterns still cannot be ruled out. Despite the observation there appears to be fewer commercial vessels around whale shark aggregation sites in the western Indian Ocean (Seychelles and Mozambique), large fishing vessels may still pose threats to whale sharks in this region. Whale shark mortalities related to ship-strikes from commercial and fishing vessel may contribute to the lower apparent survival rates observed in the Seychelles; however, better and longer-term mark-recapture data are required to confirm this. Indeed, even individuals with major scarring returned repeatedly to their aggregation sites, indicating that scarring itself is unlikely to alter survival or migration patterns. Whether scars are naturally or anthropogenically derived, whale sharks appear to be resistant to the hypothetical negative effects of injuries on survival, but may still demonstrate reductions in maturation time or reproductive ability (Hiruki et al. 1993).

It must also be assumed that estimates of apparent survival between the Ningaloo and Seychelles aggregations are comparable based on equal probabilities of permanent emigration. Capture histories analysed in the Cormack-Jolly-Seber framework provide estimates of apparent survival that are confounded with permanent emigration (White & Burnham 1999), so a higher proportion of transients in one population will bias apparent survival estimates downward. Nonetheless, the large difference in apparent survival between Ningaloo and Seychelles is suggestive of true differences in survival rates and requires longer-term data to verify this adequately.

This analysis of three Indian Ocean whale shark populations based on photo-identification provided little evidence that major or minor scarring affects survival rates, despite the prevalence of injuries and scarring among the individuals examined. However, the magnitude of shipping-related deaths remains unquantified and may only be revealed with dedicated large-ship surveys near known aggregation sites. Due to their apparent resilience to scarring, it is true that whale sharks may not fear shark, man or ship; however, current trends in population status suggest they are not as impervious to these threats as previously thought.

5. SATELLITE TAGGING

5.1 OVERVIEW

Satellite tagging of whale sharks has aimed to determine not only the migratory pathways of whale sharks, but to also understand the mechanisms by which these long distance voyages take place. As animals were tagged with different types of tags (Splash and PSAT) that use different techniques to produce estimates of geo-location, an essential first step in the study was to validate location estimates. To assess the accuracy of raw and refined estimates of locations from PSATs, we attached two PSAT and one Argos satellite-linked transmitter (SAT tag) to one whale shark at Ningaloo Reef. The root mean square error (RMSE) in raw estimates of location provided by the PSATs was 5.16° latitude and 2.00° longitude. Estimates were more accurate after processing the data with a Kalman filter (RMSE = 2.97° latitude and 0.78° longitude) and most accurate after processing with a Kalman filter model that integrates SST measurements (RMSE = 1.84° latitude and 0.78° longitude). We also assessed the precision of the PSAT-derived locations, and depth and temperature measurements by comparing the data from the two PSATs. Our findings support the use of archival tag data to reconstruct the large-scale movements of marine animals and demonstrate the significant improvements that may result from two refinement techniques.

Long distance migrations of sharks from Ningaloo were recorded by Splash tags in 2005, 2006 and 2007. In 2005, one animal was tracked from Ningaloo to the Indian Ocean in the vicinity of the longitude of Sri Lanka. A second animal travelled from Ningaloo to the Indonesian Archipelago and spent some weeks in Indonesian coastal waters. A third animal travelled from Ningaloo along the edge of the continental shelf to Indonesian islands to the east of Timor. These tracks show that the Ningaloo population of sharks is part of a wider Indian Ocean stock that is likely to encompass much of the south eastern Indian Ocean and the waters of South East Asia. We combined these data sets with tracks from earlier tagging work using Splash tags to investigate how migratory patterns of whale sharks were influenced by geostrophic surface currents. This was done by utilizing a passive diffusion model parameterised with observed whale shark starting positions and weekly maps of surface current velocity and direction (derived from altimetry). Map outputs from the passive diffusion model and maps of Chlorophyll-*a* concentration (SeaWiFs/MODIS) for corresponding weeks were compared to actual whale shark tracks with the use of GIS and generalised linear mixed-effects models (GLMM). The GLMM indicated very little support for passive diffusion by currents as a factor influencing whale shark distributions in the north eastern Indian ocean with Chlorophyll-*a* having only a very weak influence in their distributions. The seven whale sharks included in this analysis had average swimming speeds comparable with those recorded in other satellite tracking studies of whale sharks. Swimming speeds were up to 3 times greater than the maximum surface current velocities that whale sharks encountered during their migration into lower southerly latitudes (towards the equator). Our results indicate that whale sharks departing from Ningaloo are likely to use active locomotion in their migration,

rather than surface currents to passively drift, particularly given that they probably spend the majority of their time in the upper surface water / mixed layers. Active swimming locomotion is likely to have high metabolic costs for whale sharks.

Splash tags also record and transmit information about diving behaviour by whale sharks. This allowed us to investigate how whale shark dive patterns during long distance migrations were linked with ocean temperatures and dissolved oxygen levels by overlaying 3-dimensional satellite tracks of tagged sharks (Splash tags) with oceanographic data (NOAA-World Ocean Atlas 2005). Frequency distribution histograms of temperature and dissolved oxygen were compared throughout the Indian Ocean region (within which all the whale sharks were observed) and within the specific waters occupied by each whale shark during their dives. Results reveal that while the majority of the ocean temperatures and dissolved oxygen levels within the region are low, whale sharks appear to selectively dive within water bodies of warm temperatures ($24.01 < 30^{\circ}\text{C}$) and high levels of dissolved oxygen ($4 < 5 \text{ ml/l}^{-1}$) for the majority of dives (usually $>60\%$). This pattern of habitat selection may relate to physiological limitations of large aquatic poikilotherns and energetic conservation mechanisms.

Ongoing work includes analysis of Splash tag tracks from tags deployed in 2006 and 2007. In two instances, Splash tags were recovered from beaches at Ningaloo after they had detached from the animal. This allowed the detailed (every 2 sec) records held in the archive of the tag to be downloaded (while attached the tags only transmit summary information to satellites). These are now being compared with oceanographic data collected by Acoustic Doppler Current Profilers and water temperature loggers deployed by AIMS at Ningaloo. Also currently in preparation is a summary of the records of migration tracks and diving behaviour obtained from the 43 PSAT deployments on sharks from 2002-2007. A PhD student will commence a detailed analysis of the dive records from these tags in April 2008.

5.2 PSAT TAG VALIDATION

5.2.1 Introduction

Measurements of ambient light levels and derived estimates of time of civil twilight (i.e. sunrise and sunset) and local apparent noon have been used by humans to navigate for several centuries (e.g. Bowditch 1802, Stanford 1927, Nautical Almanac Office 1989). Hunter *et al.* (1986) first proposed that archived measurements of light levels could be used to provide location estimates of marine animals at sea. DeLong *et al.* (1992) and Stewart and DeLong (1995) subsequently developed and tested archival tags that used light level data to document the movements of northern elephant seals (*Mirounga angustirostris*). The technique has since been used to study the movements of a variety of marine vertebrates, including tunas (e.g. Gunn *et al.* 1994), billfishes (e.g. Gunn *et al.* 2003), sharks (e.g. West & Stevens 2001), mola (Seitz *et al.* 2002), eels (Jellyman & Tsukamoto 2002), penguins (e.g. Wilson *et al.* 1995) and albatrosses (e.g. Tuck *et al.* 1999). Several tag configurations exist, including pop-up satellite archival tags (PSATs) that jettison on pre-programmed dates and transmit their stored

information to earth-orbiting, Argos satellites. In addition to light levels, the tags can also measure, store and transmit other data like water depth and temperature and so provide valuable insights into the vertical movements of marine animals and the physical oceanographic properties that influence them. PSATs offer several advantages over traditional satellite tags (SAT tags) that use Argos or Global Positioning Satellite systems to determine location. Though SAT tags provide very accurate location estimates, they have limited use on species that remain submerged for long periods because the tag's antenna must breach the sea surface for a signal to reach an orbiting satellite. Moreover, the large size (owing to large power supplies) of those tags and resulting drag can interfere with long term retention of the tag by the animal. Raw estimates of locations are derived from archived light levels using astronomical algorithms provided by tag manufacturers. However, these raw estimates are often very inaccurate. Sources of error include equinoxes, light attenuation, water turbidity, weather, resolution of the light sensor, clock error and diving behavior of the fish (Musyl et al. 2001). Estimates of latitude using ambient light levels are generally less accurate than estimates of longitude because variation in estimates of civil twilight (and consequently day length) has greater influence on determination of latitude than does variation in estimates of local apparent noon on determination of longitude. Moreover, estimates of latitude from ambient light measurements have extreme variation and uncertainty near the vernal and autumnal equinoxes when daylength is similar at all latitudes. Researchers have used several techniques to improve the accuracy of these raw estimates, including (1) filtering outliers (e.g. Schaefer & Fuller 2002), (2) using smoothing procedures like moving averages (e.g. Matsumoto et al. 2005), (3) processing raw estimates of location using state-space movement models like the Kalman filter (Sibert & Nielsen 2003) or the particle filter (Royer et al. 2005), and (4) matching sea surface temperatures (SST) from tags with remotely sensed SSTs (e.g. Delong et al. 1992). Despite the widespread use of light-based archival tags, there have been few studies to determine the accuracy of their raw or refined estimates of location. We addressed this important issue by attaching two PSATs and one SAT tag to a free-ranging whale shark (*Rhincodon typus*) to validate the accuracy and precision of the data from the PSATs and to quantify improvements in estimates of locations from processing with Kalman filter and SST models. Because these data were collected in the most challenging conditions (i.e. at low latitudes on a species that may dive deeply and spend little time at the sea surface), we think that these results have general relevance to studies conducted under more favorable conditions.

5.2.2 Methods

5.2.2.1 Tagging

We attached two PSATs (model PTT-100, Microwave Telemetry, Inc., Columbia, Maryland, USA) and one SAT tag (model SPLASH, Wildlife Computers, Inc., Redmond, Washington, USA) to a whale shark at Ningaloo Reef, Western Australia, in 2005 (Table 5.1). The PSATs were deployed using methods described by Wilson et al. (2006) and both were attached to the shark just below its first dorsal fin (PSAT 1 on the right side, PSAT 2 on the left side). The PSATs recorded measurements of ambient light levels, depth and temperature every 15 min and then later transmitted those archived data to Argos satellites after they detached and

reached the sea surface. The SAT tag, embedded in a buoyant, hydrodynamic housing, was attached to the leading edge of the first dorsal fin of the whale shark using a Ramset HD200 powder actuated fastening tool (Ramset Fasteners, Mooroolbark, Victoria, Australia). This 'pistol' fires a pin that joins the two ends of a U-shaped collar positioned at the base of the anterior side of the fin. A 1-m nylon-coated stainless-steel tether connected the tag to the collar. Geographic locations of the shark were determined by Doppler-shift calculations made by the Argos Data Collection and Location Service whenever a passing satellite received two or more signals from a tag.

5.2.2.2 Data processing

We processed the PSAT data on three levels: (1) Raw estimates of location were computed from recovered light level data by Microwave Telemetry, Inc. (Columbia, Maryland, USA) using a proprietary algorithm derived from standard celestial algorithms (Bowditch 1802, Nautical Almanac Office 1989); (2) The raw estimates were further processed using a state-space Kalman filter model (KF) to estimate movement parameters and provide a most probable trackline for each shark (Sibert & Fournier 2001, Sibert & Nielsen 2003); (3) Alternatively, the raw estimates were processed using a Kalman filter model (KFSST) that integrates SST measurements (Nielsen & Sibert 2005, Nielsen et al. 2006). Mean daily tag SSTs were calculated from those temperature records where depth = 0. Level 3 MODIS Aqua (night) 8 d composite SST data (resolution = 4 km) were used for reference. Prior to KFSST processing, the SST fields were smoothed by local polynomial regression (Loader 1999) using a nearest neighbor fraction of 5%. KF and KF-SST processing were both run in the R statistical environment (R Core Development Team 2004). The investigator that conducted the PSAT data processing was blinded to the SAT tag locations. We calculated mean daily Argos locations from the SAT tags using all locations with location class (LC) > 1 (i.e. accuracy < 1 km). We assumed that these were the true locations of the shark.

5.2.2.3 Accuracy and precision

Accuracy is a measure of reliability and defined as the closeness of a measured or computed value to its true value (Sokal & Rohlf 1981). We compared estimates of 7 locations derived from light level and SST data from PSATs with mean Argos locations (LC > 1) from SAT tags for the corresponding day to estimate accuracy of the PSAT locations. We used several statistics to characterize the accuracy of locations estimated from each level of processing of the PSAT data. The mean absolute error (MAE) and the root mean square error (RMSE) both indicate the magnitude of the average error. The MAE is always < the RMSE, though the two statistics are usually of similar magnitude. The RMSE gives more weight to large errors than small ones and provides a measure of error variance (i.e. high error variance would be indicated by a RMSE that is >> the MAE). We also present the error range and mean error (ME) for the estimates of latitude and longitude. Because positive errors cancel negative ones, the ME is not a good measure of accuracy. It does show, however, the magnitude and direction of bias in the error (positive = north or east, negative = south or west) owing to faulty measuring instruments or procedures (Walther & Moore 2005). We did not compare the depth and temperature data from the PSATs with those from the SAT tag because (1) the

PSAT and SAT tag datasets were in different formats (raw data vs. summary histograms), and (2) the SAT tag measurements are not true. Because the geographic coordinate system is not isometric (i.e. the length of 1° of longitude varies with latitude), we also calculated the mean great-circle error (MGCE) between estimated locations of PSATs computed at each level of data processing and corresponding true (Argos) locations. Great-circle distances are the shortest distances between any two points on the surface of a sphere (Zar 1989). Precision is a measure of repeatability and defined as the closeness of multiple measurements of the same quantity (Sokal & Rohlf 1981). We determined precision by 8 comparing replicate estimates of location (computed from each level of data processing), depth and temperature recorded by the PSATs. To facilitate comparisons with the statistics on accuracy, we calculated the MAE, RMSE, error range, and ME.

5.2.3 Results

The PSATs detached at the same time 50 d after they were attached (Table 5.1).

This premature detachment occurred because the shark descended below a fail-safe depth threshold (1200 m) which triggered the release (P. Howey, Microwave Telemetry, Inc., pers. comm.). The SAT tag remained attached and continued transmitting for another 97 d.

Table 5.1. Accuracy of location estimates resulting from 3 levels of data processing

Parameter	PSAT	N	MAE ± SD	RMSE	Error range	ME ± SD
Raw light-level latitude (°)	1	39	4.28 ± 3.83	5.71	-5.71 to 19.06	0.00 ± 5.79
	2	32	3.82 ± 2.24	4.41	-6.19 to 9.06	-2.09 ± 3.94
	Both	71	4.07 ± 3.20	5.16	-6.19 to 19.06	-0.94 ± 5.11
KF latitude (°)	1	39	2.54 ± 1.45	2.92	-4.60 to 0.87	-2.41 ± 1.67
	2	32	2.90 ± 0.90	3.03	-3.94 to -1.12	-2.89 ± 0.90
	Both	71	2.70 ± 1.24	2.97	-4.60 to 0.87	-2.63 ± 1.39
KF-SST latitude (°)	1	37	1.78 ± 0.57	1.87	-2.73 to -0.47	-1.78 ± 0.57
	2	23	1.72 ± 0.47	1.78	-2.79 to -0.94	-1.72 ± 0.47
	Both	60	1.76 ± 0.53	1.84	-2.79 to -0.47	-1.76 ± 0.53
Raw light-level longitude (°)	1	39	1.29 ± 1.55	2.00	-2.79 to 6.18	0.72 ± 1.89
	2	32	0.93 ± 1.11	1.43	-2.81 to 4.73	0.29 ± 1.43
	Both	71	1.12 ± 1.37	1.77	-2.81 to 6.18	0.53 ± 1.70
KF longitude (°)	1	39	0.64 ± 0.59	0.86	-0.32 to 2.37	0.59 ± 0.63
	2	32	0.52 ± 0.41	0.66	-0.20 to 1.62	0.49 ± 0.44
	Both	71	0.58 ± 0.52	0.78	-0.32 to 2.37	0.55 ± 0.55
KF-SST longitude (°)	1	37	0.80 ± 0.43	0.91	-0.38 to 1.84	0.75 ± 0.51
	2	23	0.42 ± 0.28	0.51	-0.28 to 1.04	0.34 ± 0.38
	Both	60	0.66 ± 0.42	0.78	-0.38 to 1.84	0.60 ± 0.50

N, number of corresponding PSAT location estimates and SAT tag Argos locations used to validate accuracy; MAE, mean absolute error; SD, standard deviation; RMSE, root mean square error; ME, mean error.

5.2.3.1 Locations from light levels

The PSATs provided 39 (PSAT 1) and 32 (PSAT 2) daily estimates of location during the 50 d they were attached. Incomplete transmission of depth and temperature data reduced the number of daily locations computed by KF-SST processing to 37 and 23. The SAT tag provided 3.41 ± 2.43 locations d⁻¹ (mean \pm SD, LC > 1) during the 50 d that the PSATs were attached. Overall, the estimates of locations derived from light level data were the least accurate (latitude: RMSE = 5.16°; longitude: RMSE = 2.00°; Table 5.1, Fig. 5.1a).

The estimates from the KF model were closer to the locations from the SAT tag (latitude: RMSE = 2.97°; longitude: RMSE = 0.78°; Table 5.2, Fig. 5.1b). The estimated locations computed by the KF-SST model were the most accurate (latitude: RMSE = 1.84°; longitude: RMSE = 0.78°; Table 5.2, Fig. 5.1c). The computed locations of the PSATs were consistently biased to the southeast of the true location of the shark. ⁹ In great-circle distances, overall mean errors (MGCE \pm SD) were 484 ± 247 km for raw estimates of locations, 317 ± 124 km for KF computed estimates, and 213 ± 54 km for KF-SST computed estimates (Table 5.2). Errors in estimates from KF processing were significantly less than those of raw estimates (paired t-test: $t_{70} = 3.97$, $P = 0.00017$) and errors from KF-SST processing were significantly less than those either raw estimates (paired t-test: $t_{59} = 5.63$, $P = 0.000001$) or KF processed estimates (paired t-test: $t_{59} = 5.39$, $P = 0.000001$).

Precision, as measured by comparing the location estimates of the PSATs, was not clearly improved by processing the raw estimates further (Table 5.3).

Raw estimates of location were the least precise for latitude (RMSE = 1.16°) and most precise for longitude (RMSE = 0.27°). KF processing resulted in more precise estimates of latitude (RMSE = 0.76°) and less precise estimates of longitude (RMSE = 0.34°) and KF-SST processing resulted in the most precise estimates of latitude (RMSE = 0.60°) and the least precise estimates of longitude (RMSE = 0.43°).

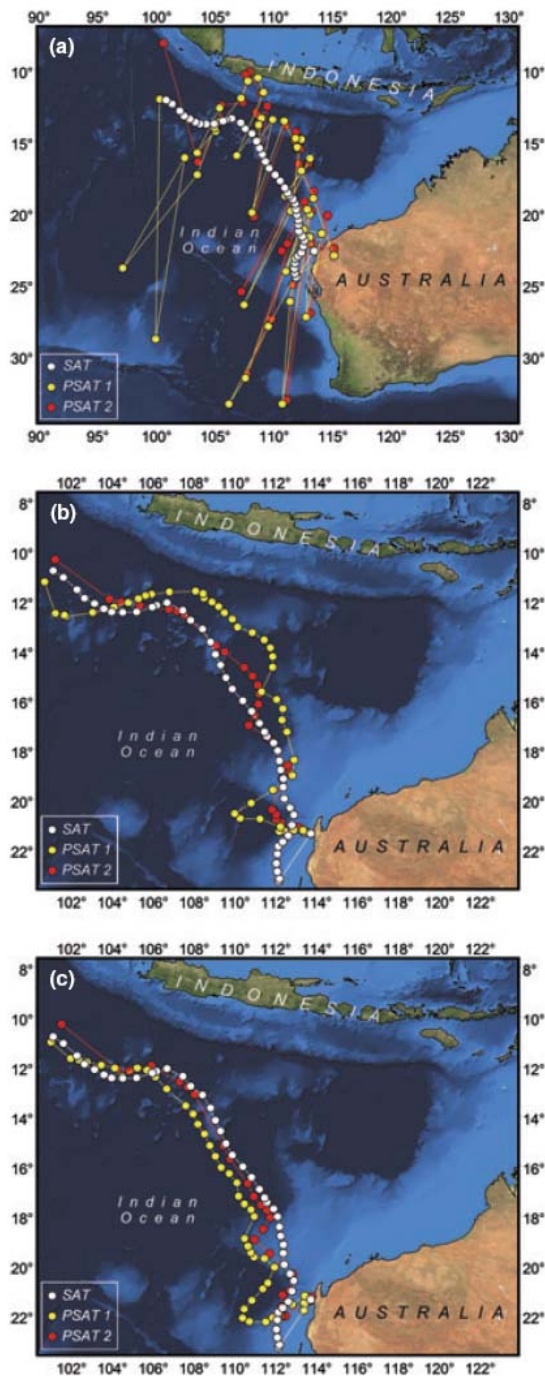


Figure 5.1. Sat tag track vs location estimates from PSATs 1 and 2 derived from 3 levels of data processing (a) raw light level (b) Kalman filtered (c) Kalman filtered with SST integration.

Table 5.2. Accuracy of location estimates resulting from 3 levels of data processing

Parameter	PSAT	N	MGCE ± SD
Raw light-level location (km)	1	39	512 ± 431
	2	32	450 ± 247
	Both	71	484 ± 359
KF location (km)	1	39	307 ± 140
	2	32	329 ± 102
	Both	71	317 ± 124
KF-SST location (km)	1	37	223 ± 55
	2	23	199 ± 51
	Both	60	213 ± 54

N, number of corresponding PSAT geolocation estimates and SAT tag Argos positions used to validate accuracy; MGCE, mean great circle error.

Table 5.3. Precision of location estimates resulting from 3 levels of PSAT data processing and depth and temperature data from PSATs 1 and 2

Parameter	n	MAE ± SD	RMSE	Error range	ME ± SD
Raw light-level latitude (°)	32	0.75 ± 0.90	1.16	-2.59 to 0.41	-0.61 ± 1.01
KF latitude (°)	32	0.64 ± 0.42	0.76	-2.34 to 0.69	-0.19 ± 0.75
KF-SST latitude (°)	21	0.51 ± 0.33	0.60	-0.87 to 1.42	-0.04 ± 0.61
Raw light-level longitude (°)	32	0.21 ± 0.17	0.27	-0.29 to 0.73	0.07 ± 0.27
KF longitude (°)	32	0.29 ± 0.17	0.34	-1.00 to 0.42	0.05 ± 0.34
KF-SST longitude (°)	21	0.36 ± 0.23	0.43	-0.94 to 0.47	-0.24 ± 0.37
Depth (m)	1634	3.01 ± 7.11	7.72	-75.31 to 64.55	-0.91 ± 7.67
Temperature (°C)	1320	0.10 ± 0.24	0.26	-2.80 to 2.56	0.05 ± 0.26

N, number of corresponding PSAT records used to validate precision, other abbreviations as in Table 2.

5.2.3.2 Depth and temperature

We matched the dates and times of 1634 depth records and 1320 temperature records from the archived PSAT data (Table 5.3, Fig. 5.2a,b). Of the 1634 replicate depth records, 1174 (71.8%) were identical. The precision of the depth records, as quantified by the RMSE of repeat measures, was 7.72 m. Of the 1320 replicate temperature records, 850 (64.4%) were the same and the RMSE was 0.26°C.

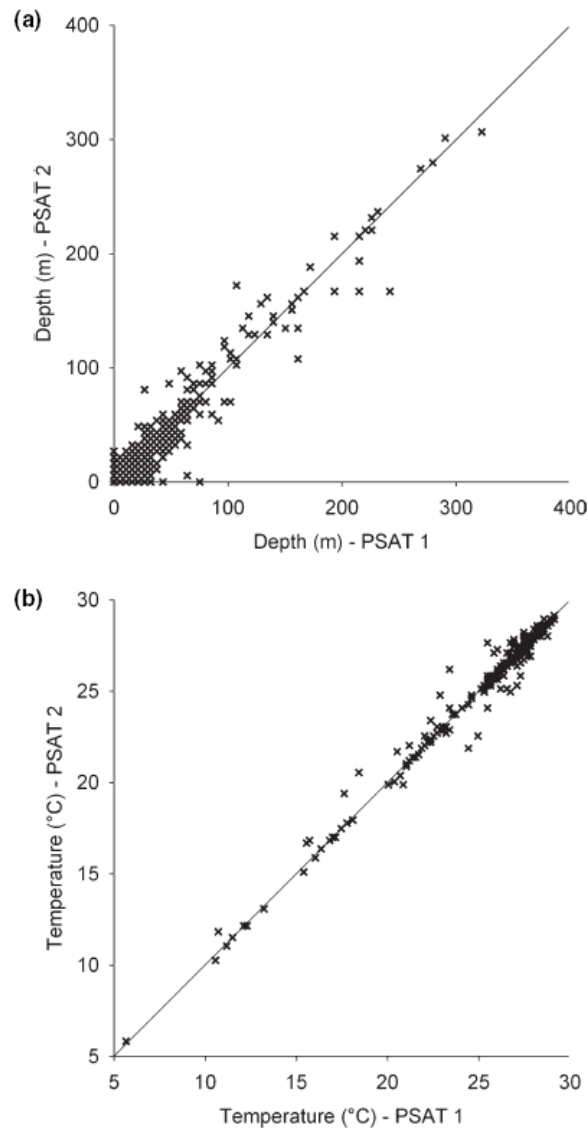


Figure 5.2. Scatterplots of replicate measurements of: (a) depth (n=1634 pairs); and (b) temperature (n=1320 pairs) from PSATs 1 and 2. Line is provided for reference only.

5.2.4 Discussion

5.2.4.1 Locations from light levels

Our primary objective was to evaluate the accuracy and precision of estimates of locations from PSATs derived from three levels of data processing. The raw estimates of location from the PSATs were not very accurate (latitude: RMSE = 5.16°; longitude: RMSE = 2.00°), though they were relatively precise (latitude: RMSE = 1.16°; longitude: RMSE = 0.27°). Indeed, despite significant differences between locations of the PSATs and the SAT, the distances between matched locations of the PSATs were consistently small (Fig 5.1a). We think this means that factors external to the tags, such as vertical behavior or data processing, were the principal sources of location error. Application of the state-space KF model greatly improved the accuracy of estimates of locations of the PSATs (latitude: RMSE = 2.97°; longitude: RMSE = 0.78°). The KF model has been applied in a variety of studies including analyses of fish movements (e.g. Sibert et al. 2003, Wilson et al. 2005, Wilson et al. 2006). We found additional improvements in the accuracy of estimates of PSAT locations using a KF-SST model that matched tag SST records with remotely sensed SSTs (latitude: RMSE = 1.84°; longitude: RMSE = 0.78°). Several studies have similarly used tag SST data to refine estimates of locations from archived, light level data (e.g. DeLong et al. 1992, Stewart & DeLong 1995, Block et al. 2001, Inagake et al. 2001, Beck et al. 2002, Teo et al. 2004, Domeier et al. 2005, Nielsen et al. 2006). The raw estimates of location that we present here are less accurate than those we reported in a previous study of whale sharks in the same area (Wilson et al. 2006; RMSE = 1.44°; longitude: RMSE = 0.68°). In that study, we compared raw estimates of locations from PSATs just before the tags detached with the locations of those tags as determined by Argos just after detachment. Teo *et al.* (2004) noted, however, that errors determined from last on-fish estimates of location can be very low. A few studies have attempted to assess location error in PSATs. Gunn *et al.*, (1994) compared raw estimates of locations from archival tags attached to southern bluefin tuna (*Thunnus maccoyii*) being towed in a sea cage to known locations of the cage. They reported mean absolute errors of 1.52° latitude and 0.54° longitude. However, that experiment was in early January, when errors in latitude are lowest, and the cage restricted the vertical movement of the fish. That eliminated two major sources of error: variation around the equinoxes and deep diving behaviour. In other studies, archival tags were attached to moving vessels and fixed moorings and the estimated locations were then compared with known locations of the vessels and moorings (Welch & Eveson 1999, Musyl et al. 2001). Reported errors ranged from 1-4° latitude and 0-1° longitude. Until now, only one study has compared estimates of PSAT locations with locations from SATs in free-ranging fishes (Teo et al. 2004). Those researchers double-tagged salmon sharks (*Lamna ditropis*) and blue sharks (*Prionace glauca*) in the temperate Pacific Ocean. They analyzed the accuracy of raw (smoothed) estimates of latitude and longitude and SST-refined estimates of latitude. The RMSE of raw estimates of latitude was 9.87° for salmon sharks and 4.00° for blue sharks whereas the RMSE of raw estimates of longitude was 0.89° for salmon sharks and 0.55° for blue sharks. SST refined estimates of latitude had an RMSE of 1.47° for salmon sharks and 1.16° for blue sharks. Some of the improved accuracy in the raw estimates of location may be due to the smoothing procedures used on the light-based location estimates (i.e. the removal of 12 outliers through the use of an iterative forward and backward averaging filter;

McConnell et al. 1992). Furthermore, temperate waters typically have stronger gradients in SST than tropical waters and thus are more conducive areas for refining estimates of locations with SST. That benefit may be moderated, however, by greater water turbidity in temperate regions. Stewart and DeLong (1995) double-tagged a northern elephant seal with a SAT tag and an archival light level tag and found that estimates of location differed, on average, by $67 + 31$ km. Beck et al. (2002) double-tagged free-ranging gray seals (*Halichoerus grypus*) in the North Atlantic Ocean and found MGCEs (+ SE) of $1026 + 292$ km in raw estimates of locations from light level data and $94 + 8$ km in estimates adjusted by SST. Two recent studies compared estimates of location from light-based archival tags with locations from SAT tags in free-ranging albatrosses (*Thalassarche melanophrys*, *Phoebastria immutabilis* and *P. nigripes*). Phillips et al. (2004) reported an MGCE (+ SD) of $186 + 114$ km in raw estimates of location and Shaffer et al. (2005) reported errors of $400 + 298$ km in raw estimates of location and $202 + 171$ km in estimates in latitude from SST refinement. The consistent southerly bias in error in latitude might be due to the features of the proprietary algorithm used to calculate the raw estimates of location. If the estimates of civil twilight were consistently incorrect, it might account for this bias. An easterly bias in the error in longitude might be due to a slow clock. Adjustments correcting for such systematic error can be made in cases where the amount of clock error is known (e.g. when the archival tag is recovered after deployment; Musyl et al. 2001).

5.2.4.2 Depth and temperature

The PSATs that we used transmitted depth and temperature data at a resolution of 5.38 m and 0.18°C , respectively. The precision of the depth and temperature measurements (RMSE = 7.72 m and 0.26°C , respectively) slightly exceeded those values. Though the replicate depth and temperature data had identical dates and times, they were not necessarily recorded simultaneously. The PSAT manufacturer advised us that these readings should have been made within 144 s of each other. Therefore, some of the observed differences between the depth and temperature records of the PSATs might be explained by vertical movements of the shark that occurred during that time. We conclude that using ambient light levels as the basis for estimating the locations of free-ranging marine animals can be a relatively robust method if the raw estimates of location are processed further to improve their accuracy. The errors associated with these processed estimates will likely vary, however, among species, tags, and regions (Teo et al. 2004). Because fishes do not need to surface to breathe, we predict that errors in estimates of their locations will be greater than those of air-breathing marine vertebrates because of the ability to more accurately estimate civil twilight for the latter. Consequently, we recommend continued efforts to calibrate and validate these methods as central components of future studies. We expect that SST refinement of estimates of location from light level based instruments will be most effective in areas with strong SST gradients. The satellite SST product selected for reference in KF-SST processing might also have a significant impact on the accuracy of the resulting estimates of location. For example, we used a night SST product because the study area consisted of tropical waters that are prone to solar heating during the day. Satellites sense only emissive radiation from the top few micrometers of the sea surface (the skin SST). At 14 night, the skin SST is more indicative of the top few meters of the water column (the bulk SST).

5.3 SAT TAG TRACKS AND GEOSTROPHIC CURRENTS

5.3.1 Introduction

It has been hypothesized that migratory marine species assist their navigation by using geophysical directional clues such as the Earth's magnetic field or thermoreception of large water temperature gradients associated with fronts and eddies (Montgomery & Walker 2001, Sims 2003). For example, the basking shark (*Cetorhinus maximus* Gunnerus) is another filter-feeding migratory shark that exhibits selective foraging behaviour by swimming 100s to 1000s of km to productive continental-shelf edge habitats and remaining within temporally discrete productivity 'hotspots' associated with frontal features (Sims 2003). Likewise, the broad-scale migration of various marine turtle species is affected by oceanographic processes; for example, olive ridley (*Lepidochelys olivacea*) and leatherback (*Dermochelys coriacea*) turtles use major surface currents and eddies to assist migration to feeding areas (Polovina et al. 2000, Luschi et al. 2003, Sims 2003, Polovina et al. 2004).

Whale sharks (*Rhincodon typus* Smith) are the world's largest fish and are broadly distributed throughout the world's tropical oceans. These migratory animals occur seasonally in a few regions throughout the world, although our understanding of the drivers of these annual migrations is rudimentary. This is largely because tracking studies have generally been able to provide data describing only short-term movements given limitations in satellite technology and tag attachments (Gunn et al. 1999, Eckert & Stewart 2001, Eckert et al. 2002, Graham et al. 2006, Rowat & Gore 2006, Wilson et al. 2006, Hsu et al. 2007). In a few exceptional cases, tags attachments have persisted for several months, allowing the tracking of broader-scale movements across entire ocean basins (1000s of kilometres) (Eckert & Stewart 2001, Eckert et al. 2002). These studies demonstrate that whale sharks travel on average around 1.0 km h⁻¹ (Eckert & Stewart 2001, Eckert et al. 2002).

While whale sharks aggregate seasonally in richly productive areas (Taylor 1996, Clark & Nelson 1997, Gunn et al. 1999, Eckert & Stewart 2001, Heyman et al. 2001, Duffy 2002, Wilson et al. 2006), it is unknown how they navigate to and from these areas and whether they use active locomotion or they are assisted via passive drifting in currents. Here we examine how whale shark movements are influenced by surface geostrophic currents at weekly time scales to and from one of the most well-known and studied of the larger whale shark aggregations at Ningaloo Reef in north-western Australia. Using satellite tracking data from seven whale sharks tagged off Ningaloo Reef in 2002 and 2005, we test the hypothesis that movement patterns mimic satellite-derived geostrophic currents determined via an agent-based passive diffusion model. Specifically, we examine (i) whether whale shark movements agree with the those produced from the passive diffusion model to determine the role of currents in assisting migration, and (ii) whether whale sharks residency patterns can also be explained in part by local productivity measures (i.e., remotely assessed chlorophyll-*a* concentration).

5.3.2 Methods

5.3.2.1 Tagging

Splash Tags (Wildlife Computers, Redmond, USA) were attached to the dorsal fin of a 7-m (total length) female whale shark on the 22 April 2002, a 7-m male on 28 June 2002, and five individuals (2 female, 1 male, and 2 of undetermined sex) ranging in total length from 4.2 to 7.5-m from the 1st to 6th May 2005 off Point Cloates, Ningaloo Reef (113° 36' E, 22° 42' S) in Western Australia (Fig. 5.3).

Whale sharks were initially spotted from the air by the pilot of a single-engine, high-wing aircraft who relayed their relative positions to an awaiting vessel below via UHF radio (see also Wilson et al. 2006). A snorkeller attached the tag to the whale shark using a handheld, pressure-driven applicator (RAMSET) that secured the tether by a stainless steel pin and plastic saddle. Application techniques were developed at CSIRO Marine and Atmospheric Research in accordance with methods to minimize tag loss and in adherence to strict animal ethics regulations. Tags consisted of a small buoyant torpedo-shaped housing that was attached to the shark's dorsal fin via a one-metre tether. When a tagged shark surfaced, the tag within the housing transmitted location and archived histogram diving (depth, temperature) information every 45 seconds to Argos satellites.

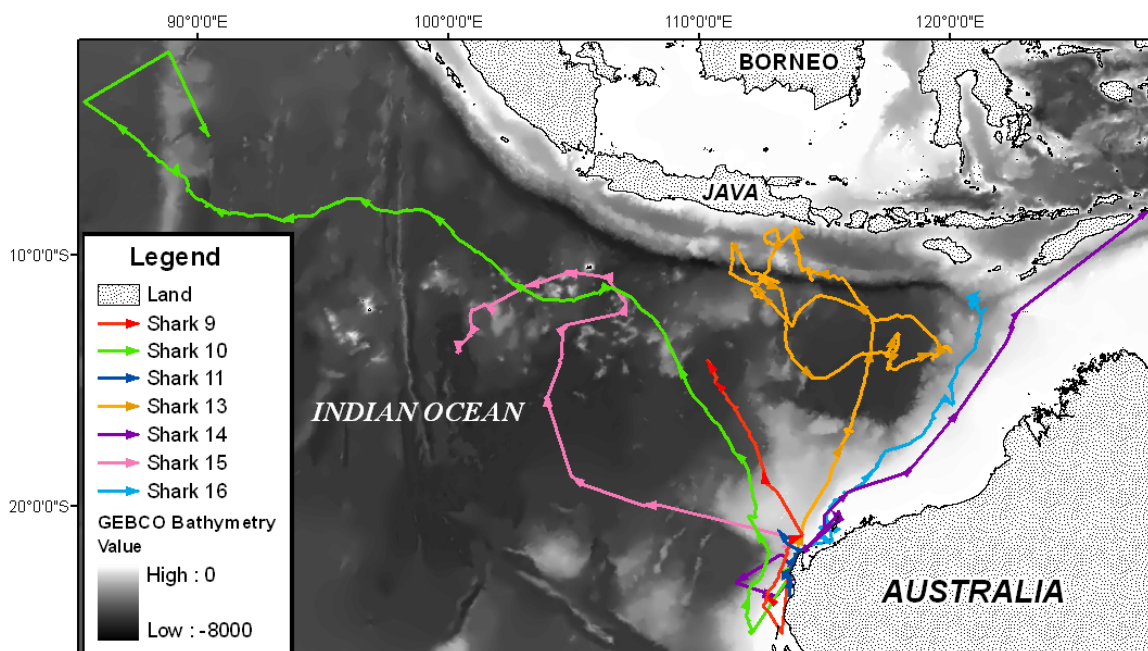


Figure 5.3. Distribution of whale shark tracks throughout the Indian Ocean and bathymetry.

Location data were filtered to remove invalid locations or location classes errors > 1000 m (i.e., we retained classes 1, 2 and 3). The filter threshold was deemed appropriate to include locations that were well within the scale (at least 5 times smaller) (O'Neill et al. 1996) of the minimum resolution of corresponding environmental data (see below). Point location data were checked for anomalous locations to determine when the tags separated from whale sharks and became surface drifters. Locations were divided into weekly intervals that corresponded with environmental data of similar periods and time-frames. Point data were imported into ArcGIS v9.1 (ESRI, Redlands, USA) and interpolated (assuming linear movement between points) into track lines where points were used as vertices. The average accuracy of interpolated locations from Argos tagged marine animals have been found to be unaffected by various interpolation methods and were always within the precision of the tracking technique used Tremblay et al. 2006b. For each shark we calculated length of track (km) between weekly points, the time (hours) of travel between points, and the travel speed (km/hr), and joined these data to a vector grid (with cell sizes of 0.1 degree [latitude/longitude] or ~ 36 km, equal to geostrophic current data) using the Hawth's Tools ArcGIS extension. By summing the time spent within each vector grid cell we created an observed probability density time series grid for each whale shark.

5.3.2.2 Environmental data

Geostrophic surface currents are generated by differences in horizontal pressure gradients associated with sea surface topography and the Coriolis force. To estimate weekly surface geostrophic currents for locations corresponding to the whale shark tracks, we obtained altimetry data (www.aviso.oceanobs.com) with a spatial resolution of 0.1 degrees (latitude/longitude). Using a raster calculator in ArcGIS, we multiplied mean sea level anomalies by their formal mapping errors (variance in sensor signal) to estimate minimum and maximum mean sea level height per grid cell. These limits were added to a mean dynamic topography grid based on an improved geoid model (Rio & Hernandez 2004). The resulting absolute dynamic topography maps were reprojected into a mercator equal-area projection and east-west (dz/dx) and north-south (dz/dy) gradients were calculated using a filter in ArcView 3.2 (ESRI). Gradient maps were exported in geographic coordinates to calculate the geostrophic current components of U and V (Polovina et al. 1999) and these were decomposed into compass direction (degrees True North) and velocity (cm/s^{-1}) (Fig. 5.4).

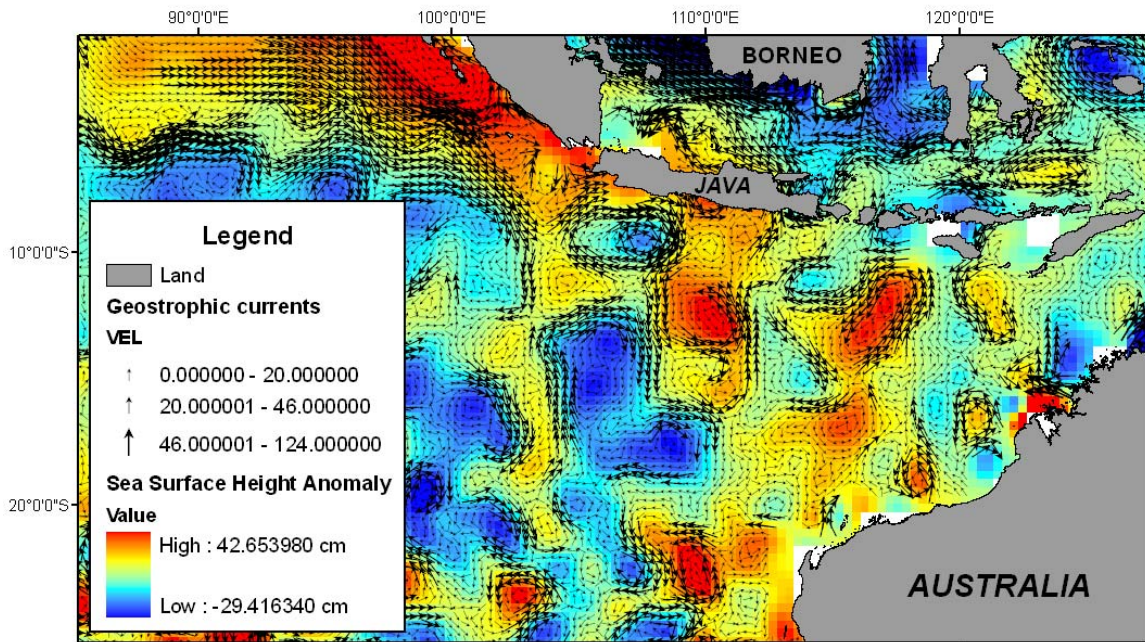
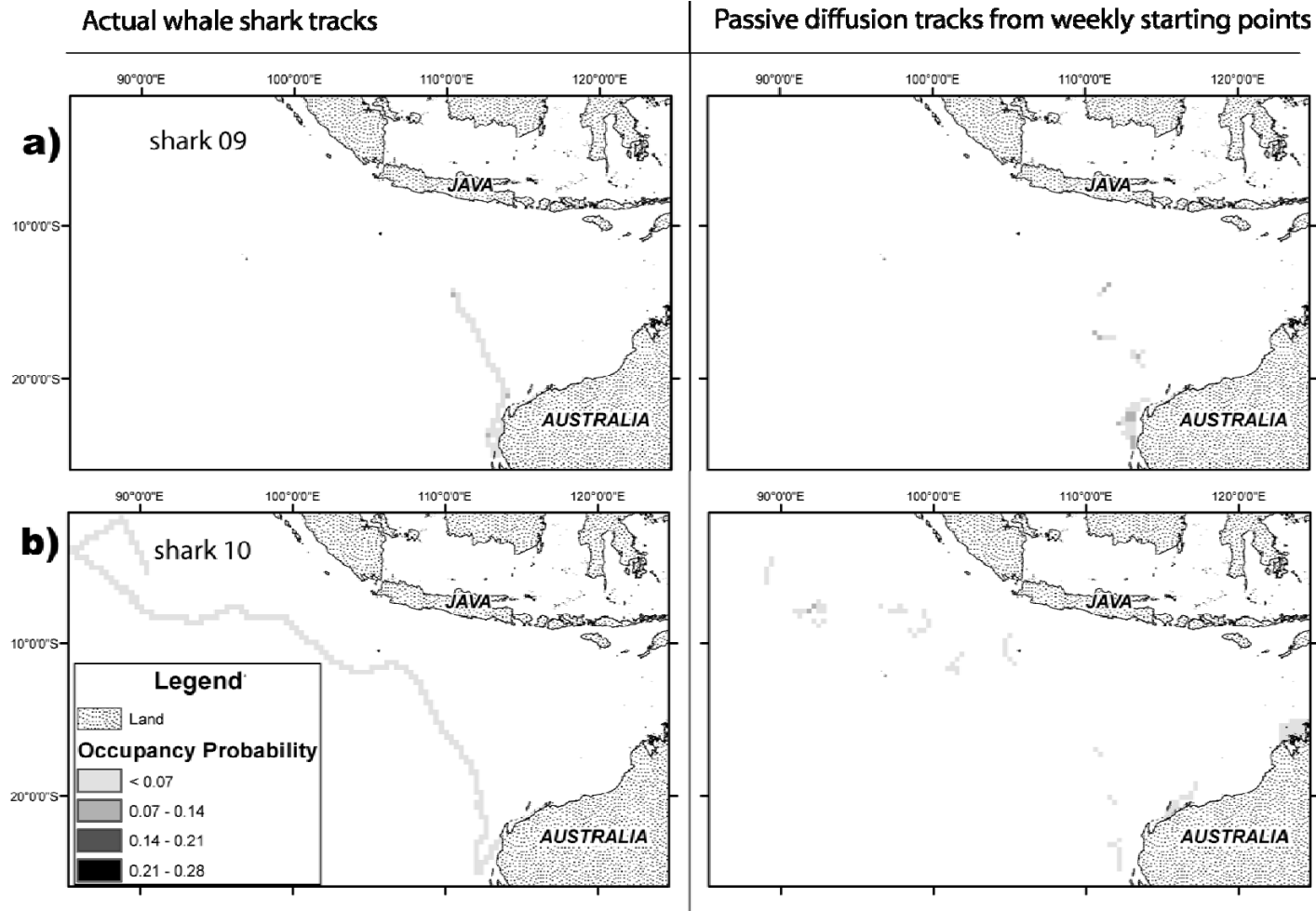
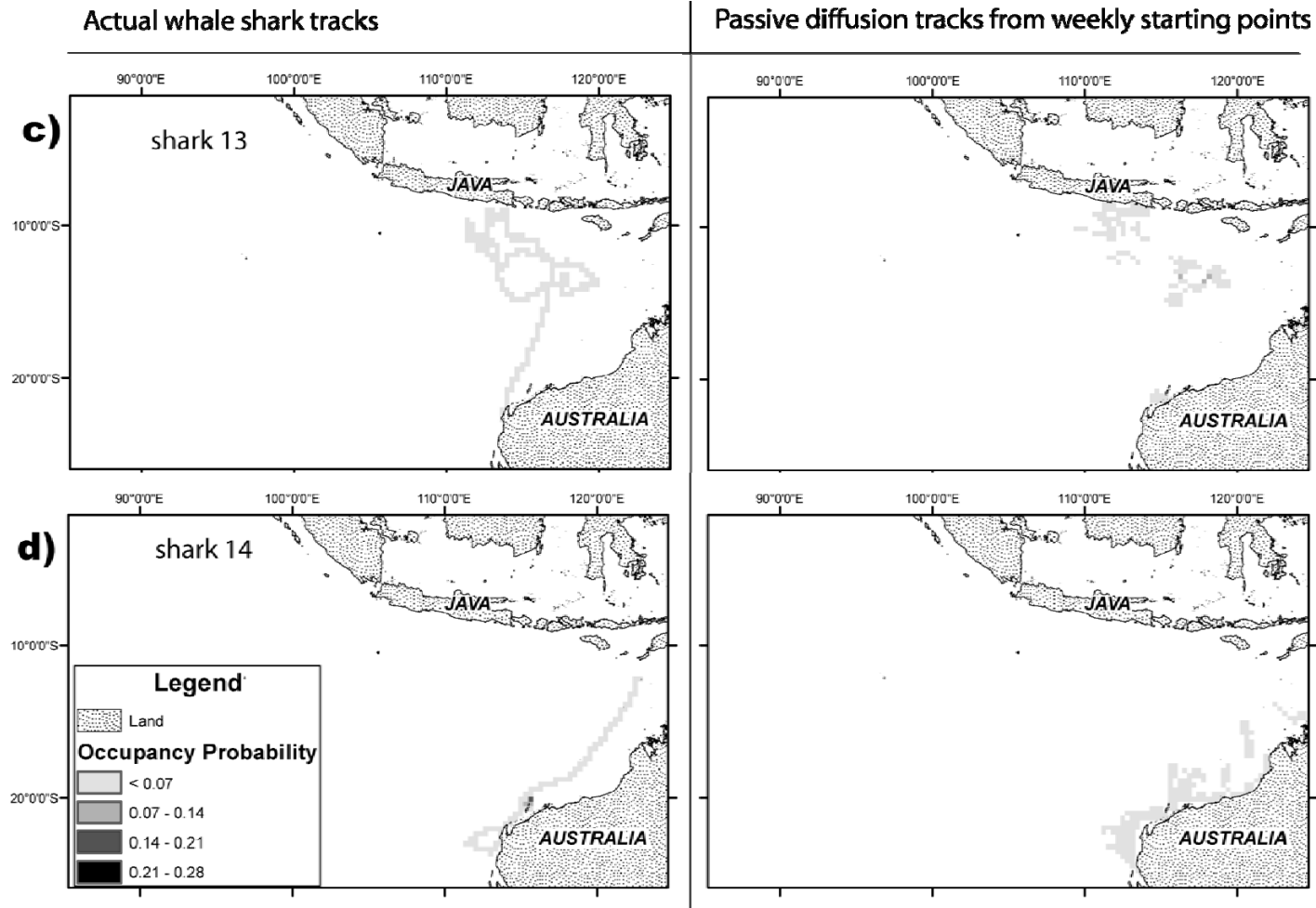


Figure 5.4. Example of geostrophic current map for the mid Austral winter period (June 2005).

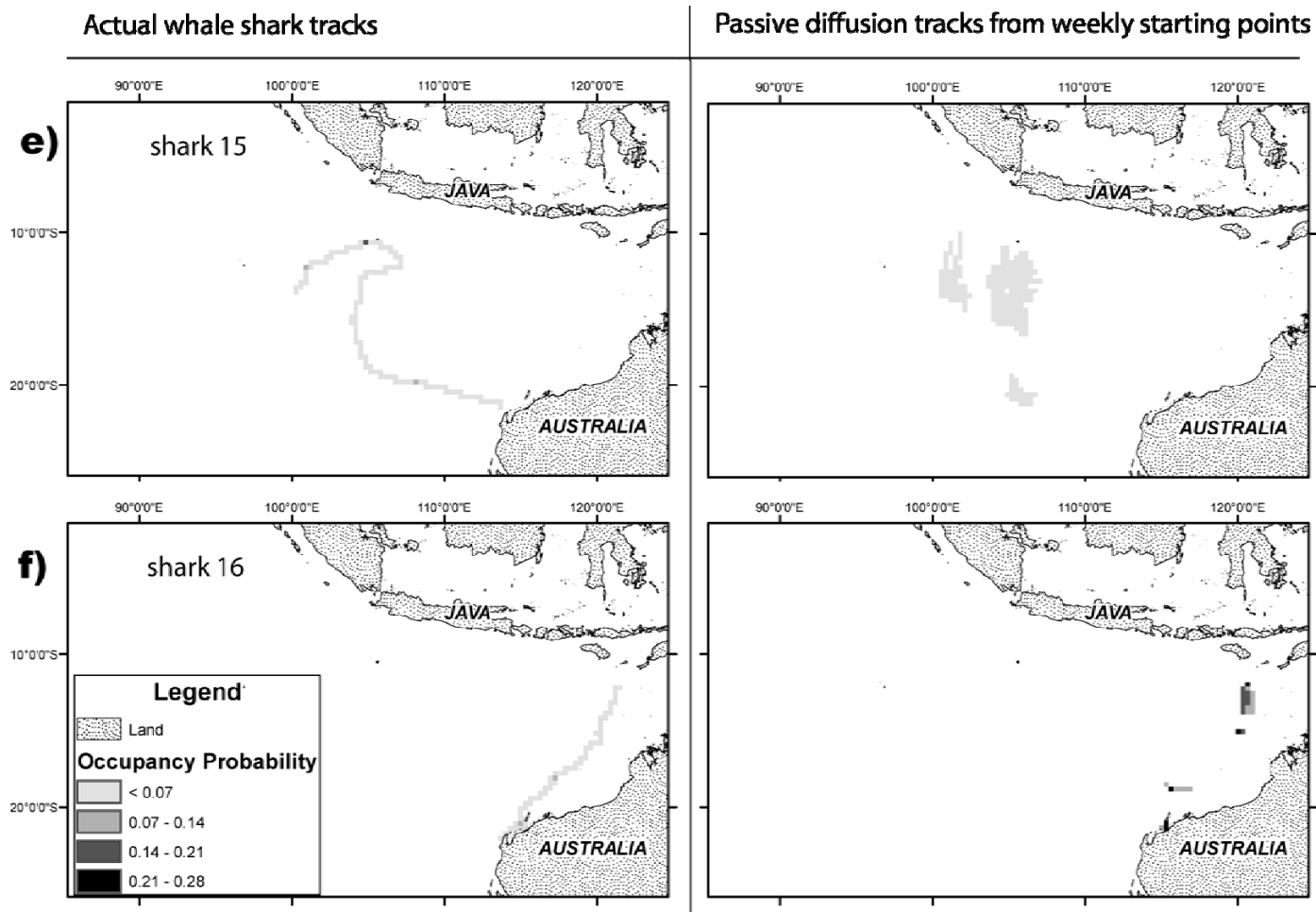
Maps of chlorophyll-*a* concentration were used as an index of surface water productivity around whale shark tracks. Weekly chlorophyll-*a* maps with 9-km spatial resolution were derived from Sea-viewing Wide Field-of-view Sensor (SeaWiFS) level 3 (version 5.1) Global Area Coverages (GAC). SeaDAS 4.8 ocean colour software (developed by the US National Aeronautics and Space Administration - NASA), was used to georeference and subset chlorophyll-*a* imagery for the entire region within which whale sharks tracks occurred (Fig. 5.5).



Figures 5.5 a-f. Actual cumulative tracks of individual whale sharks (left) compared with probability distribution maps based on modelled passive diffusion by geostrophic currents (right). The modelled maps are parameterised with weekly starting points of whale sharks.



Figures 5.5 a-f. Actual cumulative tracks of individual whale sharks (left) compared with probability distribution maps based on modelled passive diffusion by geostrophic currents (right). The modelled maps are parameterised with weekly starting points of whale sharks.



Figures 5.5 a-f. Actual cumulative tracks of individual whale sharks (left) compared with probability distribution maps based on modelled passive diffusion by geostrophic currents (right). The modelled maps are parameterised with weekly starting points of whale sharks.

5.3.2.3 Passive diffusion model

We developed an agent-based, passive current diffusion model using the R Package (R Core Development Team 2004). The model was based on weekly minimum and maximum geostrophic current velocity and direction maps and a land-mask map as inputs. Starting x and y coordinates were based on the start locations of the measured whale shark tracks as the inputs for each weekly model scenario. We filtered some of the starting locations to remove weekly tracks that remained outside of the region within which geostrophic currents could be evaluated (i.e., these areas were typically within ~36 km from the coast).

The model simulated movement of an agent through a grid-based environment where each daily time step (within a weekly interval) was evaluated on the basis of the grid cell length (distance) according to the velocity and direction values of geostrophic currents in neighbouring cells and whether the cells were could be occupied or not (based on the land mask). Geostrophic map data were reprojected into an Albers equidistant conic projection prior to input to ensure that simulated agent movements into adjacent cells were standardised in both the east-west and north-south directions. The model was coded as a stochastic process where variation of geostrophic current estimates (associated with formal mapping errors) was incorporated as 100 iterations of daily steps for each weekly interval and randomly sampling velocity and direction values within their error ranges (coefficient of variation for velocity and direction set at 0.25). A cumulative cell occupancy output map was generated following 100 iterations to generate a passive agent surface occupancy probability density. We then extracted surface current probability values and average chlorophyll- a concentrations at cell locations that corresponded to the observed probability distributions of sharks using GridSampler (CSIRO Sustainable Ecosystems, Canberra, Australia).

5.3.2.4 Analysis

To test for a correlation between current speed and direction and the productivity surrogate on shark movement patterns, we constructed a set of five generalized linear mixed-effects models (GLMM) that incorporated these terms. We first assessed the amount of temporal autocorrelation between weekly values of the observed probability of occupying a grid cell. We applied the `acf` function in the R Package (R Core Development Team 2004) to each of the observed cell probability time series for each shark. All `acf` lag probabilities fell within the 95 % confidence interval for the uncorrelated series for each shark except one – Shark 14 demonstrated a possible temporal autocorrelation at a lag of two weeks (data not shown). However, the lack of any strong evidence for important lags in these time series suggests that the assumption of independence was not violated.

We transformed the observed and passive-movement predicted probabilities accordingly using the complementary log-log transformation, and chlorophyll- a values with a \log_{10} transformation to normalise non-Gaussian distributions. Passive-movement predicted probabilities were somewhat problematic given the large number of zero values; however, subsequent verification of the quantile-quantile plots indicated only minor departure from normality. We therefore constructed five *a priori* GLMM with the term *individual* coded as a

random effect to account for repeated measurements (weekly values) per individual tracked. The response variable was the observed cell occupation probability, with model variants combining the chlorophyll-*a* concentration, passive-movement probability, and their interaction (see Results).

Models were contrasted using an index of Kullback-Leibler (K-L) information loss which assigns relative strengths of evidence to each model Burnham & Anderson 2002. We used the Akaike's Information Criterion corrected for small sample sizes (AIC_c) to contrast models. AIC_c provides measures of model parsimony to identify those model(s) from a set of candidate models that minimize K-L information loss (Burnham & Anderson 2004), with the relative likelihoods of candidate models assessed using AIC_c weights. We also applied the dimension-consistent Bayesian Information Criterion (BIC) because the K-L prior used to justify AIC weighting can favour more complex models when sample sizes are large (Burnham & Anderson 2004, Link & Barker 2006). Thus, the weight ($wAIC_c$ and $wBIC$) of any particular model varies from 0 (no support) to 1 (complete support) relative to the entire model set. Model goodness-of-fit was assessed by calculating the per cent deviance explained (%DE) by a model relative to the null.

5.3.3 Results

Whale sharks had varied movement patterns but generally migrated into lower southerly latitudes (towards the equator) (Fig. 5.3). When leaving Ningaloo Reef, whale sharks 9 and 10 headed south for approximately 270 km (near Dirk Hartog Island in Shark Bay) before swimming in north-west arcs along the shelf edge. When in pelagic waters (distances greater than ~100km from the coast) most sharks (with the exceptions of shark 13 and 15) maintained fairly consistent weekly directional headings with few deviations. Shark 13 displayed widely deviating movement patterns across weeks, moving north towards the southeast coast of Java in Indonesia (an area high in productivity as indicated by high chlorophyll-*a* levels) (see Fig. 5.6), then circling around the shelf edge to return to the mid ocean basin between Java and northwestern Australia. When almost 1500 km northwest of Ningaloo, shark 15 deviated from its path and headed east towards sea-mounts adjacent to Christmas Island, Australia (Fig. 5.3).

Individual whale shark tracks had poor correspondence with the probability distribution maps outputted from the passive diffusion model using geostrophic currents (Figs. 5.5a-f).

Geostrophic current velocities throughout the northeast Indian Ocean ranged between 0 and 206 cm/s^{-1} yet whale sharks occurred in waters where currents did not exceed speeds greater than 50.3 cm/s^{-1} (Table 5.4). Average speeds of whale sharks ranged between 1.2 and 3.2 km/hr^{-1} , with greater (up to 3 times) speeds than the maximum geostrophic current velocities they encountered during their migrations (Table 5.4).

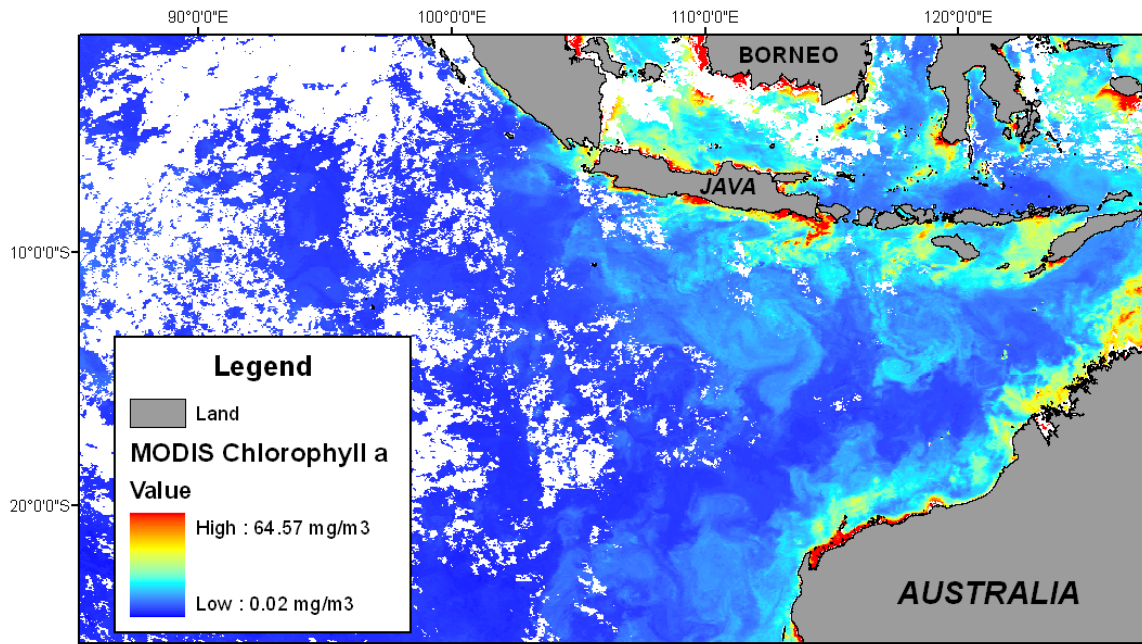


Figure 5.6. Example of chlorophyll-*a* concentration map for the mid-winter period (June 2005).

While geostrophic current directions varied widely throughout time across the region, there were regular appearances of cyclonic eddy systems (spiraling in clock-wise directions) and large anti-cyclonic eddies adjacent to these (usually around 350 km to the west of cyclonic eddies) in the mid ocean basin between Java and Western Australia (see Fig. 5.4). These eddies generally corresponded to visible regions of productivity as indicated by moderate chlorophyll-*a* concentrations (0.2-0.5 mg/m³, see Fig. 5.6).

The generalized linear mixed-effects models demonstrated that the terms considered (passive-movement predicted cell occupancy probability and chlorophyll-*a* concentration) accounted for only a small amount of the deviance in observed cell occupancy probabilities (Table 5.5).

Table 5.4. Comparison of tagged whale sharks, sex (F = female, M = male, ? = unknown), total track length (km) and the average movement speeds of whale sharks (km/hr⁻¹) with average, mode, minimum and maximum of geostrophic current velocities (km/hr⁻¹) within their observed migration routes.

Shark ID	Sex	Total track length (km)	Average speed of sharks (km/hr ⁻¹)	Average velocity of geostrophic currents (km/hr ⁻¹)	Mode of geostrophic current velocity (km/hr ⁻¹)	Minimum geostrophic current velocity (km/hr ⁻¹)	Maximum geostrophic current velocity (km/h ⁻¹)
09	F	2003.84	2.41	22.43	41.73	5.48	82.06
10	M	6384.76	1.74	47.44	58.89	4.17	151.20
11	?	1209.02	1.17	35.11	32.32	32.32	81.53
13	F	6595.08	1.89	51.48	38.82	3.16	181.39
14	?	3944.63	1.36	47.75	74.81	19.87	134.87
15	F	3441.76	1.63	44.41	52.72	2.81	160.34
16	M	2681.19	3.19	31.57	27.27	3.39	160.34

Table 5.5. Model comparison using Akaike's Information Criterion corrected for small sample size (AIC_c) and Bayesian Information Criterion (BIC). Shown are the model terms (PMP = passive-movement cell occupancy probability; CHL = chlorophyll-a concentration), number of parameters (*k*), maximum log-likelihood, deviance in criterion scores from top-ranked models (ΔAIC_c and ΔBIC), information criteria weights (*w*AIC_c and *w*BIC) and the per cent deviance explained by each model.

No.	Model	<i>k</i>	LL	ΔAIC_c	<i>w</i> AIC _c	ΔBIC	<i>w</i> BIC	%DE
1	~PMP+CHL	5	-581.557	0.000	0.432	4.146	0.086	0.99
2	~CHL	4	-582.726	0.306	0.371	0.000	0.686	0.79
3	~PMP+CHL+PMP*CHL	6	-581.552	2.026	0.159	10.618	0.003	0.99
4	~PMP	4	-585.219	5.292	0.031	4.986	0.057	0.37
5	~I (null)	3	-587.380	7.589	0.010	2.824	0.167	0.0

Although there was reasonable support for a weak effect of chlorophyll-*a* (Table 5.1, Model 2 $wAIC_c = 0.371$, $wBIC = 0.686$), this term only accounted for 0.8 % of the deviance in the response. The addition of passive-movement probability was supported only by AIC_c ($wAIC_c = 0.432$); however, the extra deviance explained by this addition was minimal (~ 0.2 %), and $wBIC$ for this model was low (0.086). Examination of the partial residual plots for both terms (Fig. 5.7) showed a weak relationship with chlorophyll-*a*, but due to the highly skewed distribution (i.e., zero-dominated) of passive-movement probabilities, the correlation with observed cell occupancy probabilities was equivocal.

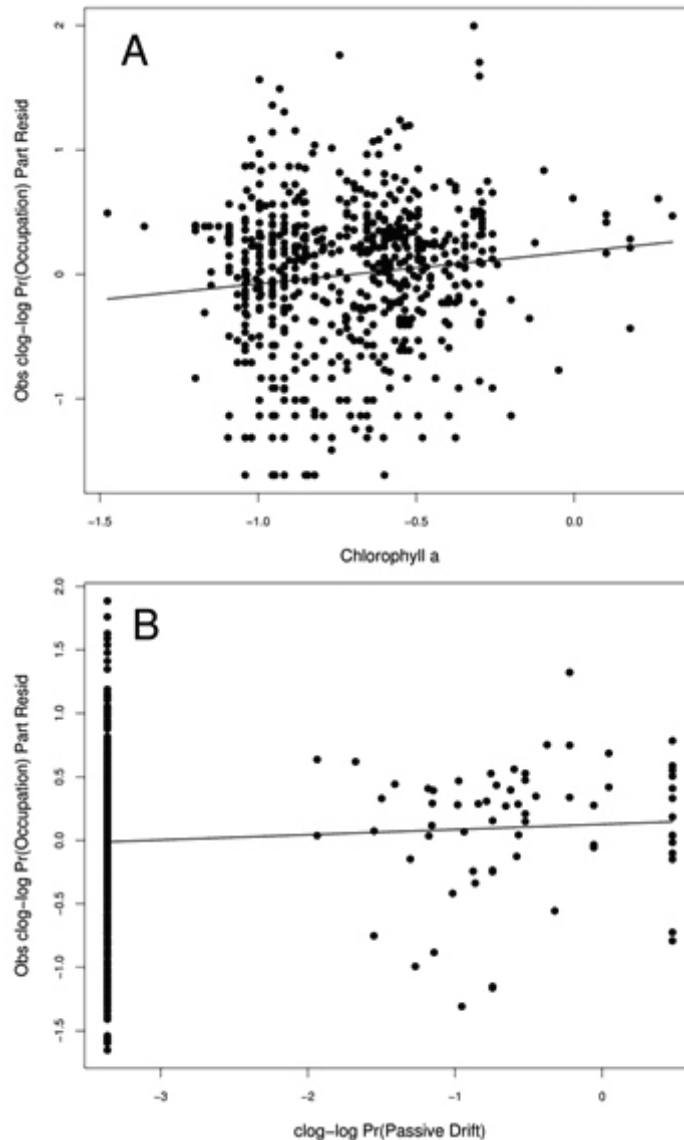


Figure 5.7. Partial residual plots of the relationship between the complementary log-log (clog-log) of the observed cell occupancy probability and the (A) log of chlorophyll-*a* concentration and (B) the clog-log of the passive-movement predicted cell occupancy probability.

5.3.4 Discussion

Despite evidence that some marine species exploit surface flow characteristics to assist in migratory movements (Polovina et al. 2000, Luschi et al. 2003, Polovina et al. 2004), we found that surface geostrophic currents explained only a small proportion of the variation in the distribution of tracked whale sharks tagged at Ningaloo Reef. Indeed, the swimming speeds we recorded are comparable to those of other whale sharks tracked from Ningaloo (Gunn et al. 1999), the eastern Pacific (Eckert & Stewart 2001), the South China Sea (Eckert et al. 2002), the Red Sea (Rowat et al. 2007), and the northwest Pacific (Hsu et al. 2007). Whale shark tracking studies have also found that some individuals move at high speeds (3.9 - 13.6 km/h) for relatively short periods (less than a day) (Gunn et al. 1999, Eckert & Stewart 2001, Hsu et al. 2007). Further, our tracked individuals swam generally much faster than average or maximum geostrophic current velocities they encountered. The combined current speed and direction data embedded within the stochastic passive diffusion model confirms quite clearly that whale sharks are capable of swimming effectively against prevailing currents and that they show little selection for current-assisted movement.

Active swimming against currents will likely entail higher metabolic costs during their migration from Ningaloo. Whale sharks at Ningaloo are commonly observed to engage in surface feeding behaviour such as open-mouthed lunging and swimming in close circles through the water (Taylor 1994b, Gunn et al. 1999). This index of foraging suggests that energy acquisition necessary for the outward winter migration to the north is a fundamental reason for the existence of the seasonal aggregation at Ningaloo Reef.

The lack of a strong correlation between whale shark movement patterns and surface productivity as measured by chlorophyll-*a* concentrations suggests either (i) they exhibit little selective foraging behaviour or (ii) that chlorophyll-*a* is poor proxy for zooplankton biomass due to potential disparities between the distributions and life histories of particular types of phytoplankton and zooplankton assemblages (McKinnon & Duggan 2001, Rossi et al. 2006). Indeed, satellite data limitations associated with the depth of light penetration in sea water may have biased this index of chlorophyll-*a* through omission or under-representation of phytoplankton biomass at increasing depth. Hydroacoustic sampling along Ningaloo Reef during summer has demonstrated that the deep chlorophyll maximum layer lies between depths of 60 to 100 m, whereas the SeaWiFS and MODIS data only account for chlorophyll-*a* in the layer between 0 and ~45 m from the surface, depending on atmospheric and bio-optical effects in the water column (Yan et al. 2001, Wilson et al. 2002). This disassociation may indicate that whale sharks are foraging on subsurface productivity that is not directly evident from remotely sensed data.

In their migration from Ningaloo, whale sharks appear to adopt generally consistent directional headings into lower southerly latitudes along the continental shelf of north western Australia. While the routes taken varied among individuals, each shark tended to remain on an approximately consistent course. This suggests that whale sharks do not adopt random searching behaviours to maximize prey encounters, but may instead be responding to some larger-scale stimulus such as directed travel. Elasmobranchs are thought to rely on olfactory

stimuli for middle-scale navigation and orientation, but they may also use these senses to navigate over long distances (Montgomery & Walker 2001). For instance, sharks may respond to variability in the apparently featureless middle depths of the ocean where there is likely to be considerable vertical fine structure in relation to temperature and odour (Montgomery & Walker 2001). Noise and geomagnetic cues may also play a role (Klimley 1993, Lohmann & Lohmann 1996, Montgomery & Walker 2001, Myrberg 2001).

Future studies of whale shark movements and migration will require longer tag retentions to increase the proportion of the life cycle tracked, with additional information on ontogenetic shifts in movement patterns (e.g., Field et al. 2005). Further, better tracking technology should allow for the collection of more behavioural data that will help to distinguish feeding behaviours from other activities (Robinson et al. 2007). Such additional information will provide a framework for prioritizing areas of whale shark habitat necessary to enhance existing conservation management arrangements at regional (Conservation and Land Management Act 1984), national (Commonwealth EPBC Act 1999) and international scales (IUCN and CITES).

Overall, our study found little support for geostrophic currents acting as passive dispersal mechanisms to whale sharks in the northeast Indian Ocean, with the caveat to this being that we have used broad-scale (0.1 degree grids @ weekly intervals) data that may mask potential influences of these currents on whale shark distributions at smaller scales (i.e. km's @ daily intervals). Alternately, inherent limitations associated with tag (i.e. geolocation/triangulation algorithms) and/or geostrophic data (i.e. generalisation of values within 0.1 degree grid cells) may have contributed to the lack of support for geostrophic transport in whale shark migration paths. Other studies have indicated lack of correspondence between historical ship drift and geostrophic currents, particularly in equatorial waters and suggest that additional information on wind stress and vertical viscosity can help improve, but not necessarily approximate a model to explain surface current drift (Arnault 1987). While there are no remotely sensed data available for measuring vertical viscosity of the north east Indian Ocean, new models approximating wind stress (from altimetry) could be included in future investigations.

Regardless of the accuracy of available surface current data, whale sharks in the northeast Indian Ocean are likely to be actively foraging rather than simply transiting through areas of ocean. This premise is supported by results of PSAT tag studies showing diurnal and nocturnal vertical migration, characteristic of feeding behaviour (Wilson et al. 2006). Given that this is the case, we need to more closely identify and analyse the relationships between dive locations and biophysical parameters within the water column, across whale shark migration routes.

5.4 WHALE SHARK DIVE PATTERNS AND OCEANOGRAPHY

5.4.1 Introduction

Spatial and temporal variation in the physical, chemical, and biological structure of the ocean environment can influence the distribution of biological productivity. Inherent physiological limitations of particular organisms, coupled with the spatial variability of productivity, can influence the distribution and space (habitat) utilization of foraging marine animals.

The world's largest fish, the whale shark (*Rhincodon typus* Smith) has an extensive migratory distribution throughout the tropical oceans of the world yet very little is known about their dive habits. The development of microwave and satellite telemetry technology has enabled scientists to better understand the horizontal and vertical movements of whale sharks (Gunn et al. 1999, Eckert & Stewart 2001, Eckert et al. 2002, Graham et al. 2006, Wilson et al. 2006, Hsu et al. 2007, Rowat et al. 2007). Typically researchers have used 'Pop-up' archival tags (PSAT tags) which store a continuous stream (1-hour interval logs) of record data about dive depth until they detach from the fish and float to the surface. In contrast, newer technology of Splash Tags enables the transmission (via Argos satellites) of compressed depth histograms at intervals set at 1 or 12-hours.

Despite the superior 'continuous' vertical data resolution of PSAT tags (compared to Splash Tags) these tags utilize ambient light-level data to calculate daily estimates of latitude and longitude which have shown to have variable accuracy. For instance, the mean latitude and longitudinal error in PSAT tags has shown to range between 0° - 5.65° depending on the timing/seasonality (presence of equinoxes) and proximity to the equator, light attenuation, water clarity, weather conditions, light sensor resolution, clock error, and diving behaviour (Musyl et al. 2001, Teo et al. 2004, Seitz et al. 2006, Wilson et al. 2006).

In this study we examine the interaction between whale-shark dive locations (determined by basic interpolation from satellite geo-location of Splash Tags) and oceanographic variables of dissolved oxygen and temperature, (derived from objectively analysed water column profiles). We hypothesize that as large poikilotherms, whale sharks will conduct dives within the upper temperature limits and will occupy water within the upper limits of dissolved oxygen levels.

5.4.2 Methods

5.4.2.1 Tag Data

Four whale sharks (referred to hereafter as sharks 10, 11, 12 and 13) were tracked throughout the Indian Ocean (for up to 3-months) from Ningaloo Reef (113° 36' E, 22° 42' S) in Western Australia (Figure 5.8 a & b). Between the 1st and 6th of May 2005, Splash tags (Wildlife Computers, Redmond, USA) were fitted to the dorsal fins of the whale sharks following their initial spotting from the air by the pilot of a single-engine, high-wing aircraft who relayed their relative positions to an awaiting vessel below via UHF radio (see also

Wilson et al. 2006). Once the shark was located by the surface vessel, a snorkeller attached the tag connected to 1-meter tether using a handheld, pressure-driven applicator (RAMSET) that secured the tether by a stainless steel pin and neoprene saddle to the shark fin. Tag application techniques were developed at CSIRO Marine and Atmospheric Research in accordance with methods to minimize tag loss and adherence to strict animal ethics regulations.

At intervals of 1-minute the Splash tags recorded maximum dive depth (m) for 14 histogram bins (15, 25, 50, 75, 100, 125, 150, 175, 200, 250, 300, 500, 1000, >1000), dive duration (seconds) for 12 histogram bins (300, 600, 900, 1200, 1800, 2400, 3000, 3600, 5400, 7200, 9000, >9000), time-at-temperature (°C) for 14 histogram bins (4, 8, 12, 16, 20, 22, 23, 24, 25, 26, 27, 28, 29, >29) and time-at-depth (m) for 14 histogram bins (15, 25, 50, 75, 100, 125, 150, 175, 200, 250, 300, 500, 1000, >1000).

When sharks visited shallow water whereupon tags broke the surface, geographic location and archived histogram data were transmitted every 45 seconds to Argos satellites. Upon download and inspection of different histogram data sources, most variables including; maximum dive depth, dive duration, time-at-temperature were found to have incomplete and inconsistent temporal coverages (i.e. erroneous and missing values). Consequently, 'time-at-depth' was the only histogram variable with adequate data coverage to be used for analysis.

Initially, we filtered surface reading to remove invalid locations or location class errors > 1000 m (i.e., we retained classes 1, 2 and 3). The filter threshold was deemed appropriate to include locations that were well within the scale (at least 5 times smaller) (O'Neill et al. 1996) of the minimum resolution of corresponding environmental data (see below). Point location data were checked for anomalous locations to determine when the tags separated from whale sharks and became surface drifters.

Surface point locations were imported as point data into ArcGIS v9.1 (ESRI, Redlands, USA) and a mid-point (centroid) between each location was interpolated (assuming linear movement between points).

We ordered the time-at-depth data chronologically to correspond with the surface location data, converted the histogram bin data into raw data and summarised the mean depth between each surface location point. We considered a dive as the averaged depth (derived from a series of histogram depth bins) that fell within two surface (transmission) locations. We use the basic assumption that between two surface transmission points all dives are relatively equal and can be summarized as a single averaged dive value. We justify this generalisation technique on the grounds that the dive intervals between surface transmissions were typically short (<3 days) and within these intervals the majority (~80%) of dives did not vary more than 20 m.

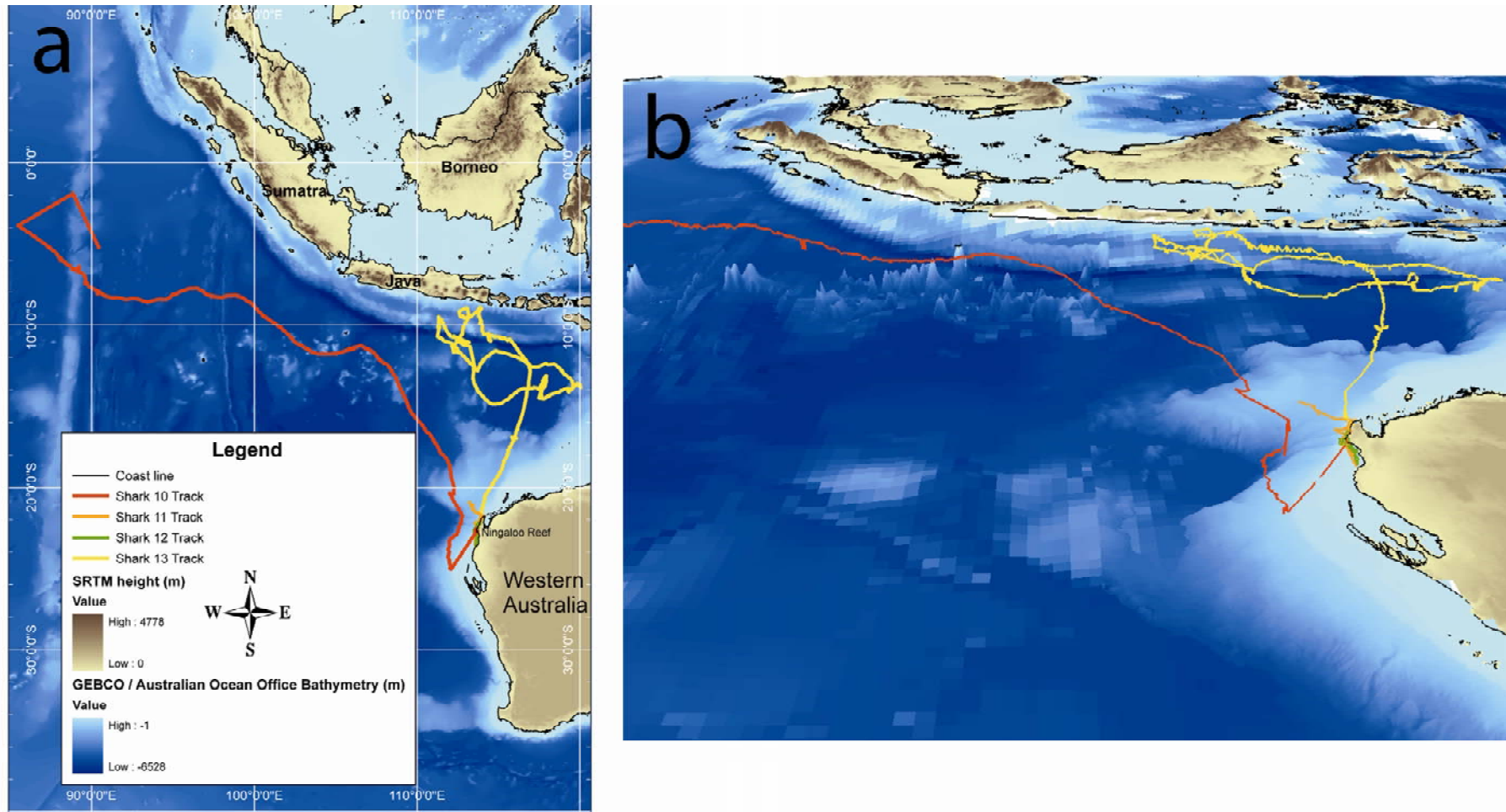


Figure 5.8. a) Track locations of tagged whale sharks (b) 3-dimensional dive tracks of whale sharks in relation to bathymetry.

The mean depth values (representing dives) were joined in chronological order to the mid-point shapefile in ArcGIS v9.1. A 3-dimensional track line was created for each shark using the surface location points and the mid-points with mean depth values.

The average accuracy of track lines interpolated from Argos tagged marine animals have been found to be unaffected by various interpolation methods and are always within the precision of the tracking technique used (Tremblay et al. 2006a).

Mean dive depth values were later rounded to the nearest depth bin corresponding with the oceanographic data layers.

5.4.2.2 Oceanographic Data

We used monthly objectively analysed oceanographic data of temperature and dissolved oxygen from the World Ocean Atlas 2005 (WOA05) (supplied by the U.S. National Oceanographic and Atmospheric Administration –NOAA) to describe the Indian Ocean environment within the region occupied by the four whale sharks.

Oceanographic data was stored as individual comma delimited files for each variable (temperature and dissolved oxygen) and month and for each of the 22 depth levels (20, 30, 50, 75, 100, 125, 150, 200, 250, 300, 400, 500, 600, 700, 800, 900, 1100, 1200, 1300, 1400, 1500 and 1750 m). These data were imported as point files into ArcGIS v9.1 and converted to raster layers with grid cell sizes of 1-degree latitude and longitude. Histograms were used to summarise the overall distribution of temperature and dissolved oxygen values that were available to the whale sharks during their presence in the region.

We selected temperature and dissolved oxygen depth layers that corresponded temporally (monthly) and spatially (depth) with mean dive depth point files and subsequently extracted the values for these variables using GridSampler software. Using the extracted variables we made histograms displaying the distribution of temperature and dissolved oxygen values within which each whale shark was observed.

5.4.3 Results

The majority (> 67%) of the ocean area available to the whale sharks had low temperatures ranging between 0 and 18°C (Figure 5.9 a). More than 60% of the ocean area available to whale sharks had low ranges (0 - 3 ml/l⁻¹) of dissolved oxygen (Figure 5.9 b).

Every shark except for shark 13 made at least 60% of their dives in areas of the ocean containing high temperatures (24.01 < 30°C) (Figure 5.10a). Shark 13 conducted all of its dives in medium to high water temperatures (12.01 < 30°C) (Figure 5.10a).

Greater than 70% of dives by sharks 10, 11 and 12 were in waters rich in dissolved oxygen ($4 < 5 \text{ ml/l}^{-1}$) (Figure 5.10b). While the majority of shark 13 dives were in waters rich in dissolved oxygen ($4 < 5 \text{ ml/l}^{-1}$), at least a third of the dives occurred in waters with moderate levels of dissolved oxygen ($\sim 3 \text{ ml/l}^{-1}$) (Figure 5.10b).

Sharks 10 and 11 conducted the largest proportion ($< 60\%$) of their dives in depths less than 100 m (Figure 5.11). Around 30% of dives by sharks 12 and 13 were in depths greater than 300 m (Figure 5.11).

Overall sharks 10, 11 and 12 appeared to have preference for warmer waters that were also rich in dissolved oxygen, despite the fact that shark 12 exploited deeper areas of oceans. Shark 13 didn't appear to display a high preference for warmer waters, rich in dissolved oxygen and had the greatest variation in depths exploited whilst diving.

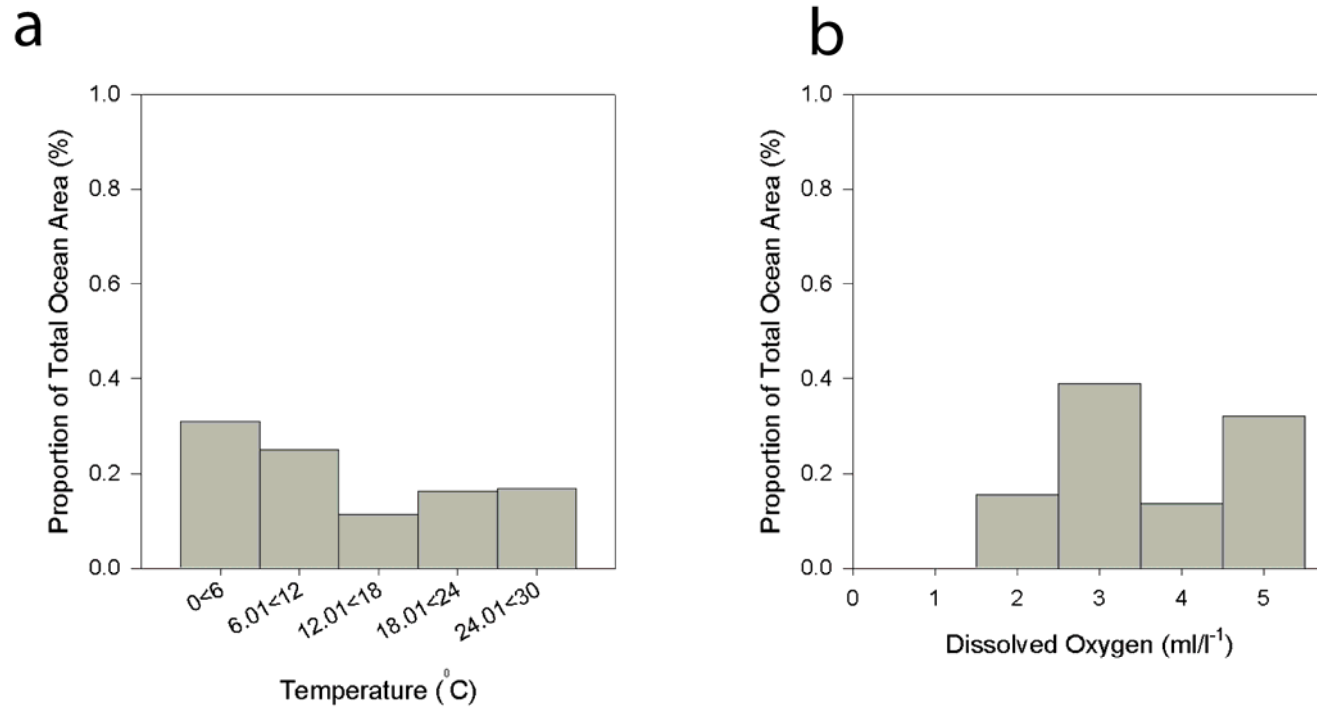


Figure 5.9. a) distribution of temperature and (b) distribution of dissolved oxygen levels throughout the Indian Ocean in which the whale sharks were observed.

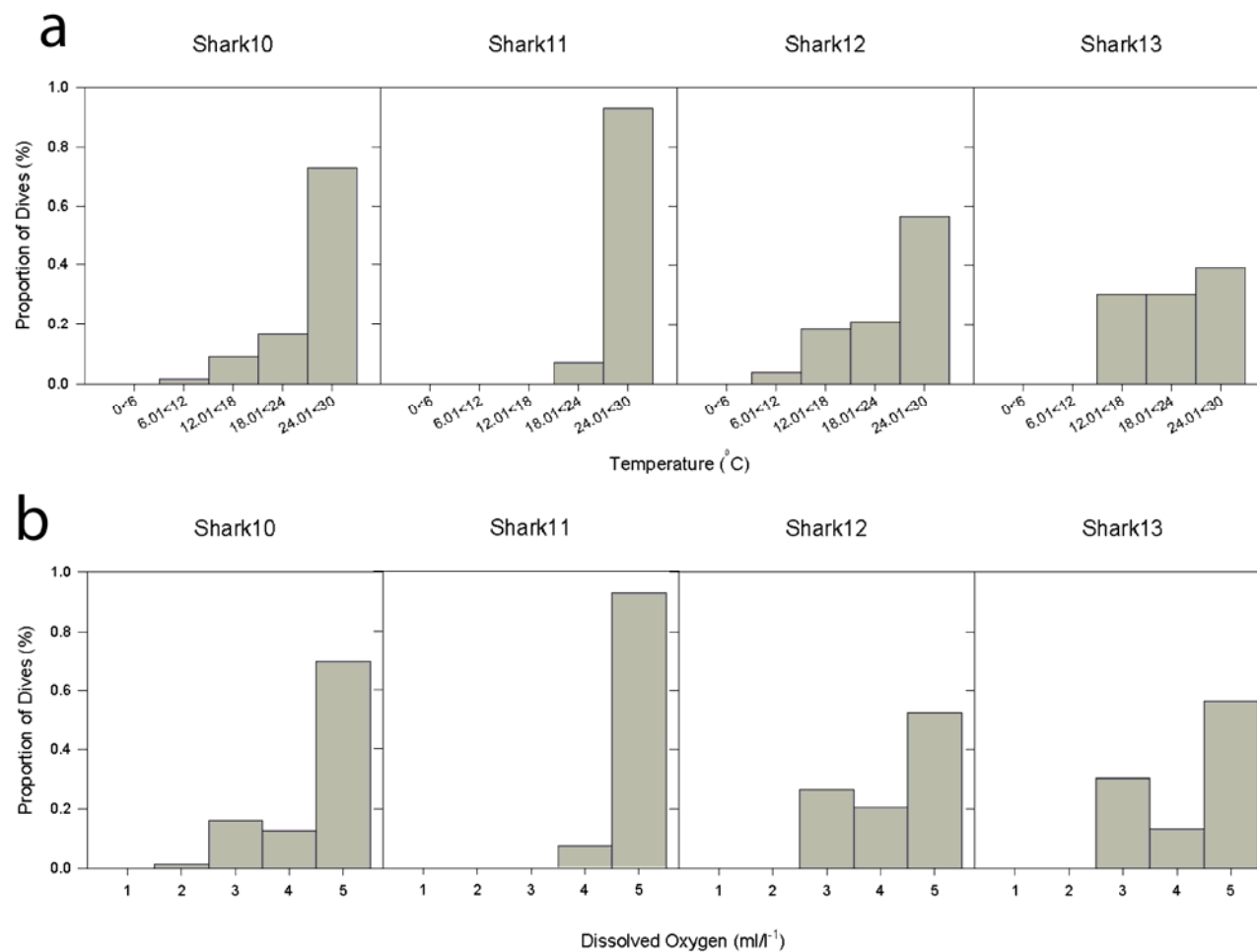


Figure 5.10. a) frequency distribution of temperatures and (b) dissolved oxygen levels corresponding to dives by whale sharks

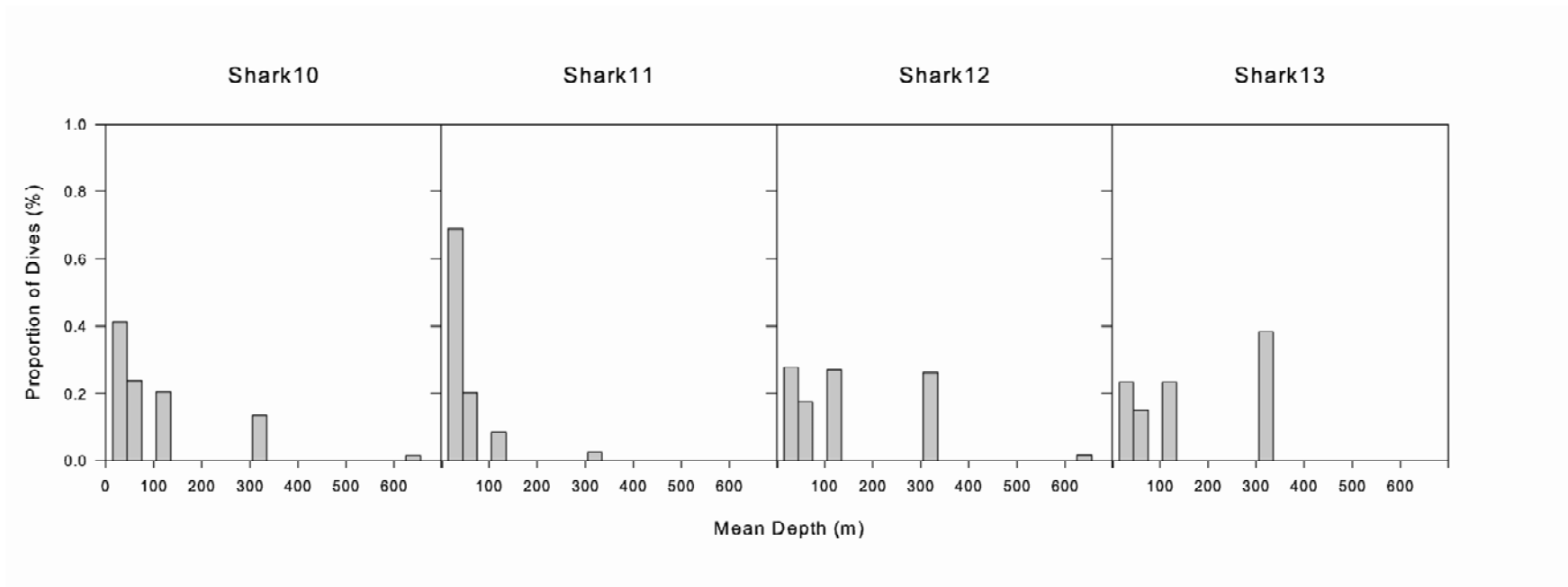


Figure 5.11. Frequency distribution of depths occupied by whale sharks during dives.

5.4.4 Discussion

When conducting dives and migrating from Ningaloo Reef in 2005, at least three of the four tagged whale sharks appeared to be actively (rather than passively) selecting for areas of ocean with higher temperatures and dissolved oxygen levels. This is based on the apparent lack of correspondence between water temperatures/dissolved oxygen levels within which whale sharks occurred and the overall pattern of cooler water temperatures (0 – 18°C) and low dissolved oxygen levels (0 - 3 ml/l⁻¹) found throughout a large proportion (>60% of the area) of the North-East Indian Ocean environment between the months of April and September.

Temperature and oxygen are important for regulating metabolic processes in all animals. Animals such as sharks are poikilotherms meaning they are affected by thermal changes in their external environments (Vas 1990). Typically metabolic rates of animals decrease with increasing body mass, yet in poikilotherms these increase with ambient temperature (Makarieva et al. 2005). As such large terrestrial poikilotherms tend to occur in the warmer (tropical) environments where metabolic processes are faster and more oxygen is available for respiration (Makarieva et al. 2005). In aquatic environments, the amount of oxygen available to animals is several orders of magnitude lower than in terrestrial environments and is dependant on temperature (and salinity and pressure) (Weiss 1970), such that oxygen solubility (dissolved oxygen) decreases with increasing temperature. According to this logic we would expect to find the largest aquatic poikilotherms such as whale sharks (the world's largest fish) in shallower/warmer waters as demonstrated in our findings.

Being large poikilotherms, whale sharks are likely to avoid diving into areas of low dissolved oxygen and low temperature particularly when foraging, as exposure to these conditions may be metabolically expensive. Graham et al. (2006) believes that whale sharks may be able to tolerate low temperatures for short periods due to their layer of subcutaneous fat.

Studies of whale shark dive behaviours in the Sea of Cortez, Mexico, at Ningaloo Reef in Western Australia and in the Northwestern Pacific near Taiwan have shown complimentary patterns as we have shown here with sharks spending the majority of their time (mostly >80%) in shallow water (<10 m depth) and occurring within warm water temperatures of (20 - 32°C) (Gunn et al. 1999, Eckert & Stewart 2001, Hsu et al. 2007). Other studies have shown whale sharks to mainly undertake diurnal dives and remain in shallow water during the night (Vas 1990, Graham et al. 2006, Hsu et al. 2007). In the Gladden Spit Marine Reserve, Belize (Meso-America) Graham et al. (2006) recorded 3 whale sharks to dive as deep as 979.5 m where temperatures were below 7.6°C with most sharks spending the majority (> 80%) of their time in waters 25–30°C. Graham et al. (2006) proposed that deeper diving behaviour was likely a response to reduction in availability of prey items and rapid ascents made by sharks were presumably a thermoregulatory behaviour, to re-oxygenate the gills following time spent in low oxygen layers of the water column.

Overall the results of this study give further weights of evidence to suggest that whale sharks prefer to occupy shallow depths and warm waters, rich in dissolved oxygen. Whether this preference is related to minimising physiological stress or is simply a beneficial strategy for enhancing prey capture, remains to be tested in further detail.

It may be that whale sharks use diving as a secondary (alternative) strategy only to evade predators and enhance prey capture when search effort yields poor results in shallower water.

6. ANALYSIS OF HISTORICAL DATA SETS

6.1 OVERVIEW

Seasonal observations of whale shark abundance recorded by ecotourism operators at Ningaloo Reef from 1995-2004 provide a historical data set that can be used to investigate temporal patterns in abundance of whale sharks in relation to oceanographic phenomenon and decadal trends in population composition and size. These records were compared with regional and global oceanographic and atmospheric variables, including average weekly sea surface temperatures (SST), along-shelf wind shear (WS), sea level (SL) and the Southern Oscillation Index (SOI). Estimates of these physical variables were derived from either ground-based data or from remote-sensing instruments. We applied generalised linear mixed-effects models (GLMM) with random sampling and model simulation to determine the relationships between the number of whale sharks and all model variants of the environmental parameters. Models were contrasted using information-theoretic weights of evidence. The SOI had the most support for explaining the deviance in weekly whale shark abundance at Ningaloo Reef during a season. The SOI positively influenced whale shark abundance such that during La Niña years, more sharks were sighted, and fewer were recorded during El Niño years. This may reflect changes in the strength of oceanographic processes such as the Leeuwin Current in response to the Southern Oscillation, which may act to transport sharks to the region and/or affect their prey by driving productivity events.

In addition to variation in response to oceanographic phenomena, analysis of ecotourism records shows that mean shark length declined linearly by nearly 2.0 m and relative abundance measured from ecotourism sightings (corrected for variation in search effort and environmental stochasticity) has fallen by approximately 40 % over the last decade. This population-level result confirms previous predictions of population decline based on projection models parameterised using mark-recapture estimates of survival. The majority of these changes are driven by reductions in the number of large individuals in the population. Phenomenological time series models support a deterministic (extrinsic) decline in large females, although there was some evidence for density dependence in large males. These reductions have occurred despite the total protection of whale sharks in Australian waters. As this species is highly migratory, the rapid change in population composition over a decade (< 1 whale shark generation) supports the hypothesis of unsustainable mortality in other parts of their range (e.g., overfishing), rather than the alternative of long-term abiotic or biotic shifts in the environment. As such, effective conservation of whale sharks will require international protection, and collaborative tagging studies to identify and monitor migratory pathways.

6.2 OCEANOGRAPHIC AND ATMOSPHERIC PHENOMENA INFLUENCE THE ABUNDANCE OF WHALE SHARKS AT NINGALOO REEF, WESTERN AUSTRALIA

6.2.1 Introduction

Whale sharks (*Rhincodon typus*), the largest fishes in the ocean (attaining sizes > 12 m in length), have a global tropical and warm-temperate distribution (Last & Stevens 1994). This wide-ranging species (Wilson et al. 2006, Bradshaw et al. 2007, Castro et al. 2007) aggregates seasonally at several coastal locations around the world (Clark & Nelson 1997, Gunn et al. 1999, Heyman et al. 2001, Meekan et al. 2006, Wilson et al. 2006, Rowat et al. 2007), making the species the target of lucrative ecotourism operations (Colman 1997, Davis et al. 1997). Whale sharks are suction filter feeders and their occurrence in coastal waters is believed to coincide with productivity events that provide an ample supply of zooplanktonic food (Taylor & Grigg 1991, Taylor 1996, Clark & Nelson 1997, Gunn et al. 1999, Heyman et al. 2001, Wilson et al. 2001a). Although various studies have attributed the aggregations of whale sharks off Ningaloo Reef to feeding as opposed to reproduction (given that a major proportion of the observed whale sharks are sexually immature males – Meekan et al. 2006), few studies have attempted to verify how the abundance of whale sharks is influenced by other environmental variables (Gunn et al. 1999, Wilson et al. 2001a).

A variety of oceanographic and atmospheric variables are known to influence the spatio-temporal abundance of pelagic and migratory marine organisms. The relative importance of these variables to a particular organism will depend on the spatial scale at which these processes operate and the functional importance of this scale to the organism. El Niño-Southern Oscillation (ENSO) is a global atmospheric process that is described by the Southern Oscillation Index (SOI) as the mean sea-level pressure difference between the central Pacific (Tahiti) and the north-eastern Indian Ocean (Darwin). In years when the sea-level pressure is higher in Pacific than the Indian ocean (a La Niña year), trade winds drive stronger currents and warmer sea temperatures along the north of Australia, positively influencing the southward flow of the Leeuwin Current along the west coast of Australia where whale sharks aggregate annually between March and June off Ningaloo Reef (Pearce & Phillips 1988, Caputi et al. 1996).

Wilson et al. (2001a) demonstrated that uncorrected total counts of whale sharks at Ningaloo between 1993 and 1998 were moderately correlated with the SOI, yet weakly correlated with local oceanographic variables such as sea level (SL) and sea surface temperature (SST). They concluded that inter-annual variation in the strength of the Leeuwin Current (related to the SOI rather than SL) had a greater influence on whale shark abundance than local-scale processes, presumably due to the active-transport mechanism, or directional cues provided by the Leeuwin Current. However, results of the Wilson et al. (2001a) study were potentially biased by inconsistent sampling strategies used in the collection of shark abundance data and the limited temporal extent of sampling periods. Furthermore, abundance data were not corrected for variation in sampling effort among years and they did not determine how these

oceanographic variables correlated with whale shark sightings at shorter temporal scales of months or weeks.

Here, we build on the work of Wilson *et al.* (2001a) by analysing a larger time series of whale shark observations from Ningaloo Reef that has been corrected for sampling effort (number of hours of observation). We also use a larger range of environmental variables and a more statistically rigorous method to determine how ocean and atmospheric processes may influence whale shark abundance. In addition to using a time series of SOI values, we use *in situ* measurements of sea level (SL) from a tide gauge and wind shear from a weather station situated close to those where whale shark sightings were recorded. We aim to estimate better the effect of physical oceanographic variables on whale shark abundance and understand this relationship in the context of the Leeuwin Current (Pearce & Phillips 1988).

6.2.2 Methods

6.2.2.1 Whale shark abundance data

We accessed an relative abundance dataset spanning from 1995 to 2004 of whale shark observations recorded from ecotourism vessels at Ningaloo Reef (Colman 1997). The area surveyed for whale sharks by ecotourism operators encompassed the northern and southern sections of the Ningaloo Marine Park in the Indian Ocean on the Northwest Cape of Western Australia (21° 40' S to 23° 30' S and 113° 45' E to 114° 15' E), which spans approximately 260 km of coastline from north to south. The number of whale sharks encountered by each operator each day during the months of April and May (the peak of the whale shark season) and the search time (effort) was recorded in a standardised log sheet as a licensing requirement for operators by the West Australian Department of Environment and Conservation (DEC) (formerly the Department of Conservation and Land Management). These data were used to calculate the average daily, weekly and monthly abundance of whale sharks and search effort.

6.2.2.2 Oceanographic and atmospheric parameters

Daily and monthly SOI values were acquired from the Australian Bureau of Meteorology and weekly values were subsequently calculated using running mean sea level pressure values (MSLP) between Tahiti and Darwin with the base period of 1932-1999. The temporal span of the SOI data was consistent with that of the whale shark abundance dataset. Sea level (SL) data were collected hourly from a tide gauge deployed at Milyering (21° 1.816' S and 113° 55.316' E) in the northern section of the Marine Park from 1998. The data were corrected to remove the effects of tides and inertial signals using a low-pass filtering technique where values were smoothed (averaged) over 30 hours. Daily, weekly and monthly average SL values were calculated. Sea surface temperature (SST) is known to predict biologically important changes in fish abundance (Iwasaki 1970, Fiedler & Bernard 1987). SST data were calculated from daily and weekly composites of 4-km resolution NOAA Advanced Very High Resolution Radiometer (AVHRR) satellite images of the Ningaloo region (21° S to 24° S and 112° E to

115° E). The 4 × 4 km pixel values in the composites were spatially averaged to obtain single daily and weekly SST values.

Wind shear (WS) was hypothesised to correlate with whale shark abundance because it is a good proxy for the strength and direction of wind along the shelf, and thus related indirectly to the strength of the Ningaloo Current, an inshore counter current that is believed to be important for retaining planktonic biomass along Ningaloo Reef (Taylor & Pearce 1999). Wind speed and direction data were collected half-hourly at a weather station at Milyering from 1997. These were used to calculate an along-shelf wind vector or wind shear parameter that was a length vector calculated by combining wind direction and speed and rotating the data clockwise at 60° (relative to true north). Currents and winds were also rotated to along- and cross-shelf components. The same low-pass filtering technique used for SL was also used for wind shear and the resulting values averaged on daily, weekly and monthly intervals.

We also explored the utilisation of weekly maps from a variety of remotely sensed and point-source data for determining the influences of other biophysical properties on whale shark abundance. We generated maps of weekly surface geostrophic currents (surface current estimates that relate directly to sea surface topography and the Coriolis force) using Topex/Poseidon altimetry data (www.aviso.oceanobs.com) with a spatial resolution of 0.1 degrees (latitude/longitude). Maps were made in ArcGIS 9.1 according to calculations described by (Polovina et al. 1999), where U and V vectors were calculated and then decomposed into compass direction (degrees True North) and velocity (cm/s-1). Weekly chlorophyll-*a* maps with 9-km spatial resolution were derived from Sea-viewing Wide Field-of-view Sensor (SeaWiFS) level 3 (version 5.1) Global Area Coverages (GAC) using SeaDAS 4.8 ocean color software (developed by the US National Aeronautics and Space Administration – NASA). While some of these additional data helped to illustrate general patterns in oceanographics, we refrained from including weekly maps of chlorophyll-*a* concentration (e.g., SeaWiFs) and geostrophic currents/mean sea surface height (e.g., Topex/Poseidon altimetry) in any further analysis since large areas without data were frequently present in maps due to atmospheric interference or due to coastal/land mask generalisation.

6.2.2.3 Analysis

A series of generalised linear mixed-effects models (GLMM) were used to explore relationships between oceanographic and atmospheric variables and relative whale shark abundance at Ningaloo Reef. Examination of the residuals for the saturated models determined the statistical family (i.e., Gaussian, gamma etc.) and error distribution most appropriate for each analysis. In this case, a gamma error distribution with a log link function was most appropriate. The error structure of GLMM corrects for non-independence of statistical units (relative abundance estimates) due to shared temporal structure (months), and permits the 'random effects' variance explained at different levels of clustering (months) to be decomposed. All oceanographic and atmospheric variables were modelled as fixed effects.

Model comparison was based on Akaike's Information Criteria corrected for small samples (AIC_c), (Burnham & Anderson 2002). Model AIC_c were ranked, with the most parsimonious model(s) having the lowest AIC_c values and highest model weights (Lebreton et al. 1992). From the set of *a priori* models we used a predictive model averaging procedure to determine the magnitude of the effect of some terms, keeping all other dependent variables constant (Burnham & Anderson 2002). The weights of evidence (w_{+i}) for each variable were calculated by summing the model AIC_c weights (w_i) over all models in which each term appeared. However, the w_{+i} values are relative, not absolute because they will be > 0 even if the predictor has no contextual explanatory importance (Burnham & Anderson 2002). To determine the predictors that were relevant to the data, a baseline for comparing relative w_{+i} across predictors was required. Following Burnham & Anderson (2002), we randomised the data for each predictor separately within the dataset, re-calculated w_{+i} , and repeated this procedure 100 times for each predictor. The median of this new randomized w_{+i} distribution for each predictor was taken as the baseline (null) value (w_{+0}). For each term the relative weight of evidence (Δw_{+}) was obtained by subtracting w_{+0} from w_{+i} . Predictors with Δw_{+} of zero or less have essentially no explanatory power. All statistical analyses were done using the R Package (R Core Development Team 2004).

We separated the modelling component into a hierarchy based on the extent of the time series for each environmental variable. Only SOI and SST data available for the full dataset of whale shark abundance (1995–2004), so these and all combinations of these variables were used for the initial model (all-subsets). Sea level and wind shear were only available from 1998–2004. Consequently, the second model used four environmental variables (SOI, SST, SL and WS) and all combinations of these to determine how they influenced weekly whale shark abundance from 1998 to 2004. A Spearman's correlation analysis was done for each set of variables in each model. Highly correlated ($r > 0.8$) variables were not included in the same model. The percentage of deviance explained (D) was also calculated for each model as a measure of goodness-of-fit.

6.2.3 Results

6.2.3.1 Relative abundance of whale sharks 1995-2004

Within the annual period (March to July) when whale sharks attend the area off Ningaloo Reef, the highest abundances were observed in early April 1995 and 1996, and towards the end of May in 2002 (Fig. 6.1a & b). In most years, weekly whale shark sightings were clustered between the beginning of April and the beginning of June, with few sighting occurring at the start of March or at the end of June.

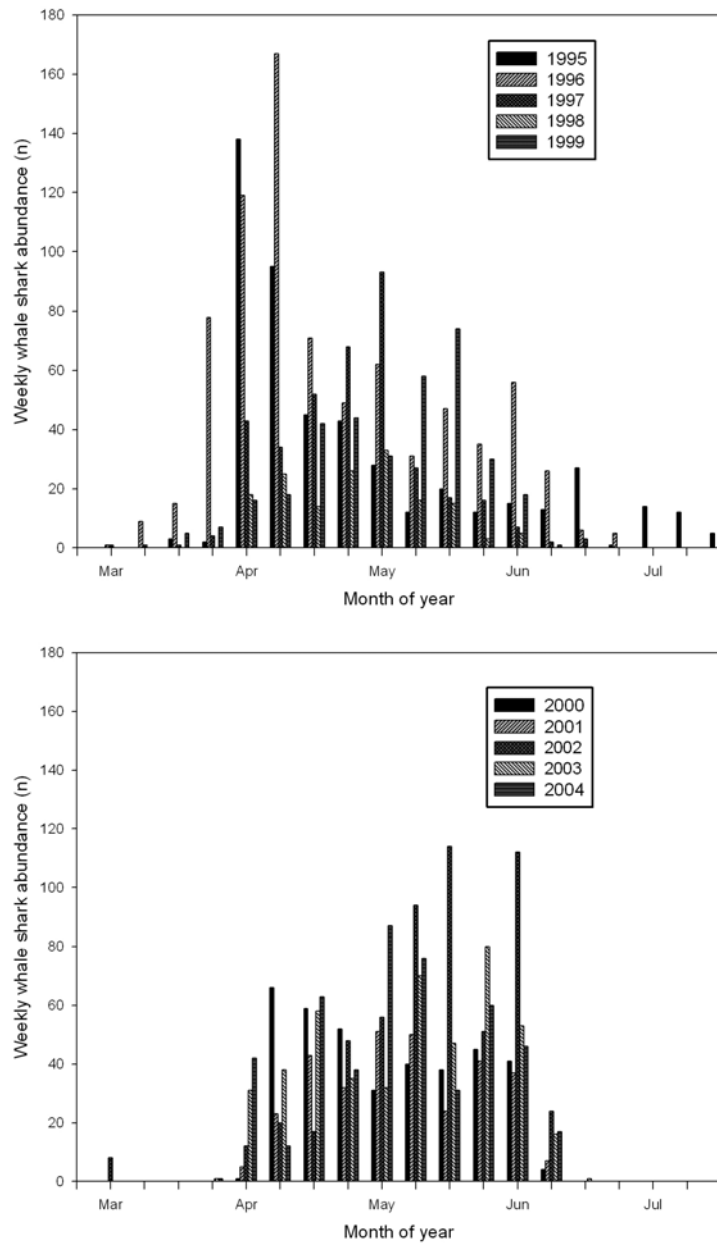


Figure 6.1. The weekly abundance of whale sharks observed off Ningaloo Reef from March to July between years (a) 1995 – 1999, and (b) 2000 – 2004.

6.2.3.2 Weekly SOI and SST from 1995-2004

SOI and SST were weakly correlated (0.28, Table 6.1). The model that included the Southern Oscillation index (SOI) was the best in the set of possible models for explaining the variation in weekly abundance of whale sharks between 1995 and 2004 (8.9 % deviance explained, Table 6.2). The weights of evidence revealed that the SOI term had the highest contribution to model fits ($\Delta w_i = 0.30$). In general, there was a positive relationship between weekly whale shark abundance at Ningaloo Reef and SOI values in 1995-2004 suggesting that more whale sharks were observed in weeks with a characteristic La Niña signal while relatively few sharks were observed in weeks with a strong El Niño signal (Fig. 6.2).

Table 6.1: Correlation matrix between Southern Oscillation index (SOI), sea surface temperature (SST), sea level (SL) and along shelf wind shear (WS) from 1998-2004.

	SOI	SST	SL
SST	0.292	-	-
SL	0.512	0.419	-
WS	0.091	0.074	0.502

Table 6.2: Generalised linear mixed-effects models and information-theoretic statistics based on the change in Akaike's Information Criterion corrected for small samples (ΔAIC_c) for model scenario 1 using Southern Oscillation index (SOI) and sea surface temperature (SST) to estimate trends in weekly whale shark abundance from 1995-2004. Notations; D = % deviance explained ΔAIC_c = change in AIC_c between models, w_i = AIC_c weight.

Model	D	ΔAIC_c	w_i
SOI	8.904	0.000	0.424
SST	3.270	1.949	0.159

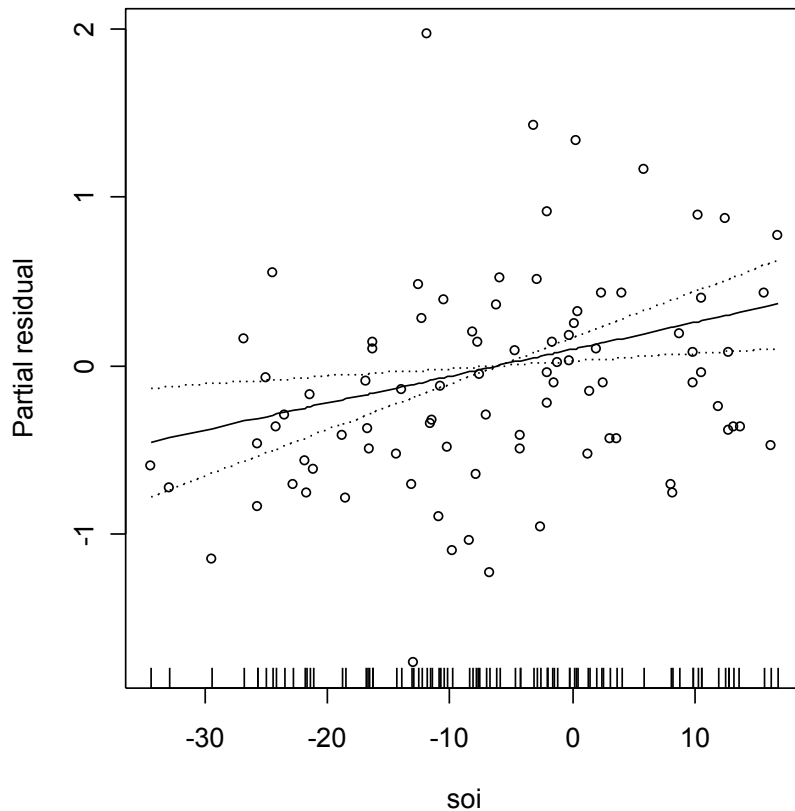


Figure 6.2. Partial residual plot generated from the most-parsimonious generalized linear model relating weekly whale shark abundance between 1995 and 2004 to the Southern Oscillation index (SOI). The solid line is the fitted linear model. The dashed lines are the approximate 95 % point-wise confidence intervals.

6.2.3.3 Weekly SOI, SST SL and WS from 1998-2004

Of all the variables, only SOI and sea level were moderately correlated (0.512, Table 6.1). Despite several competing models (Table 6.3) only SOI and SST had sufficient evidence for explaining variance in whale shark abundance ($\Delta w+ = 0.19$ and 0.15 , respectively). Both these variables were positively correlated with whale shark abundance (Fig. 6.3), yet the model that included only SOI was able to explain a larger amount of the deviance in the data compared to a model that included SST or a model that included both SST and SOI. This suggested that SOI had the best predictive capacity for explaining the weekly abundance of whale sharks at Ningaloo Reef.

Table 6.3: Generalised linear mixed-effects models and their information-theoretic statistics based on the change in Akaike's Information Criterion corrected for small samples (ΔAIC_c) for model scenario 2 using Southern Oscillation index (SOI), sea surface temperature (SST), sea level (SL) and wind shear (WS) to estimate trends in weekly whale shark abundance from 1998-2004. Notations; D = % deviance explained, ΔAIC_c = change in AIC_c between models, w_i = AIC_c weight.

Model (i)	D	ΔAIC_c	w_i
SOI + WS	26.152	0.000	0.218
SST + WS	24.585	0.343	0.183
WS	14.804	0.548	0.165
SOI + SST+WS	30.894	0.962	0.134
SL + WS	19.408	1.476	0.104

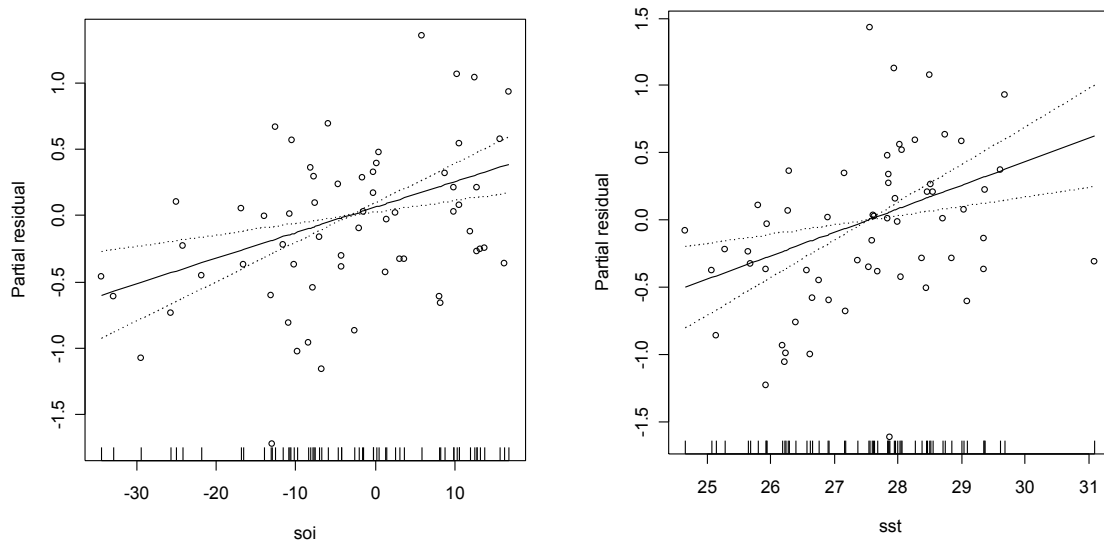


Figure 6.3. Partial residual plots generated from the most-parsimonious generalized linear model relating weekly whale shark abundance between 1998 and 2004 to the Southern Oscillation index (SOI) and sea surface temperature (SST). The solid lines represent the fitted linear models. The dashed lines are the approximate 95 % point-wise confidence intervals.

6.2.4 Discussion

Of the atmospheric and oceanographic variables that were hypothesised to influence whale shark abundance at Ningaloo Reef, only the SOI appeared to be related to shark numbers. In the analysis of the longest time series of environmental and abundance data (1995-2004), the SOI was negatively correlated with weekly whale shark abundance. The importance of the SOI did not change even when additional environmental variables were included in the models, and the weekly dataset of shark abundance was truncated (1998-2004). There was some support for SST having an influence on relative whale shark abundance, although unlike the SOI, there is likely to be high spatial variation in SST at scales of 1 to 100 km Sumner et al. 2003. Weekly AVHRR satellite image composites captured during times when whale shark abundances are peaking at Ningaloo, illustrate the presence of high SST's in the north – eastern Indian Ocean extending south past Ningaloo reef where mixing with cooler surface water occurs (Figure 6.4). A clearer analysis of the relationship between SST and whale shark abundance requires a more explicit spatial and temporal assessment which is likely to come through future tagging studies. Surprisingly, sea level had little influence on whale shark abundance, despite its strong correlation with the strength of the Leeuwin Current and SOI (Pearce & Phillips 1988).

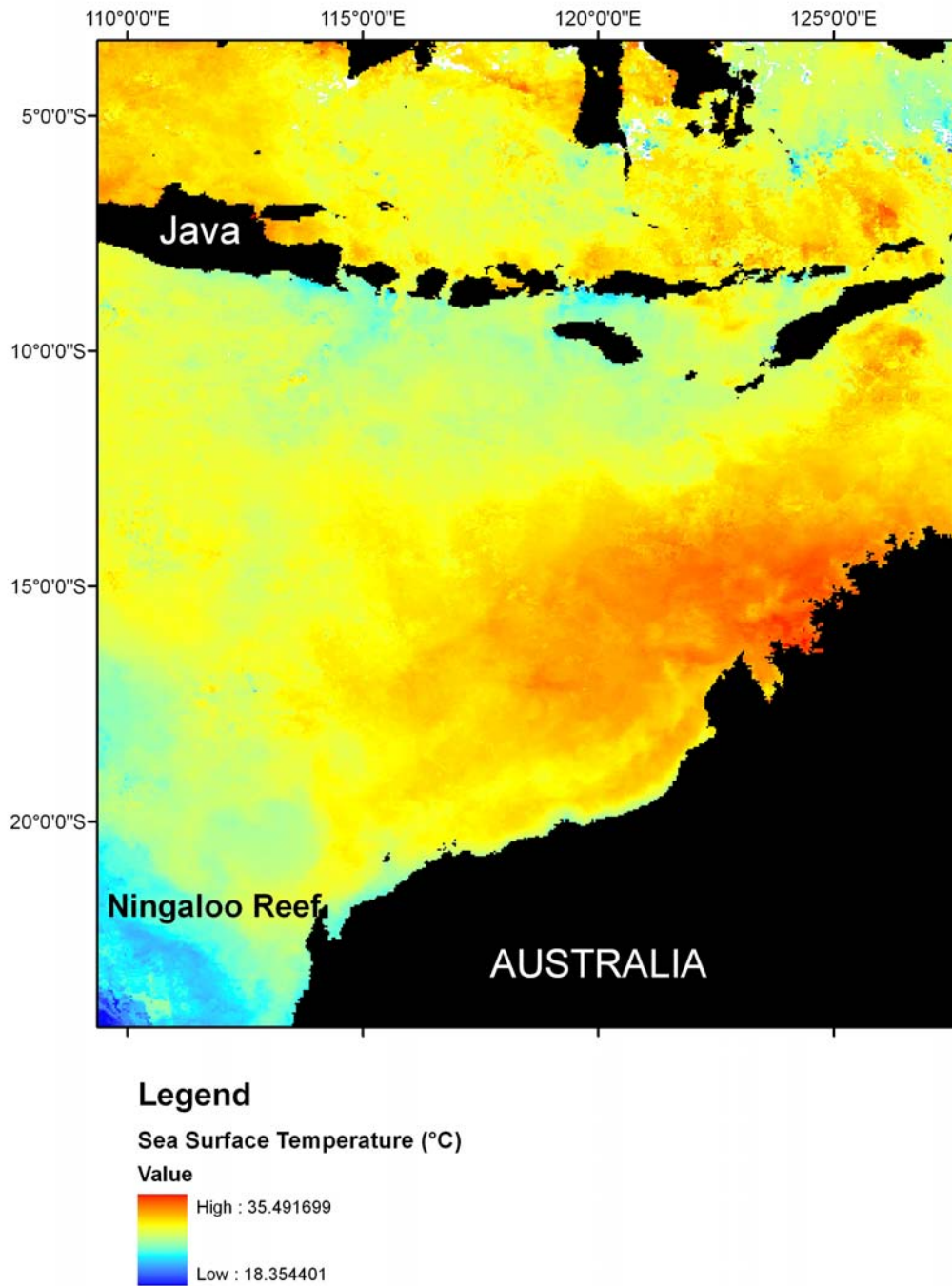


Figure 6.4. Weekly AVHRR satellite image composite of sea-surface temperature variability in the East Indian Ocean during the annual period when average whale shark abundances tend to be high (1st week of May).

Our results based on corrected data and using a rigorous multi-model inferential approach (Burnham & Anderson 2002) support the findings of Wilson *et al.* (2001a) who also suggested that SOI was an important factor influencing the abundance of whale sharks at Ningaloo Reef. The SOI is effectively a measure of ENSO, a large-scale climatic process that has two climatic phases: El Niño and La Niña. During the latter, strong Pacific trade winds and warmer sea temperatures (also known as the Walker circulation) in the ocean north of Australia act to increase the strength of a variety of ocean currents, notably the Indonesian Through-Flow and the East Gyral current and ultimately the southerly flowing Leeuwin Current (Rochford 1962, 1984) (Fig. 6.5a & b). These currents may influence the abundance of whale sharks at Ningaloo Reef in two ways; first, by providing a transport mechanism (i.e., currents - geostrophic flow) for sharks to the Ningaloo region and second, by acting as the drivers of coastal upwelling and productivity events (increased chlorophyll-*a*) that increase zooplankton abundance for filter-feeding sharks. While we cannot retrospectively determine the configuration of currents in the north eastern Indian Ocean during the times when high abundances of whale sharks were observed at Ningaloo, we can make some inferences about surface current structure through the use of Altimetry data. Geostrophic surface flow vectors (generated from Topex/ Poseidon Altimetry -Sea Surface height data) show cyclonic and anti-cyclonic circulation (eddies) present offshore during periods of high whale shark abundance (Fig. 6.6). These might influence numbers by entraining sharks and transporting them southwards toward the reef.

Ocean colour satellite imagery (SeaWiFs) indicates the presence of high chlorophyll-*a* concentrations in the surface waters in the Gulf of Exmouth (adjacent to Ningaloo) and in anomalous 'highly mixed' water bodies off the shelf from Ningaloo reef during the period when whale sharks are in peak abundance (Fig. 6.7). These relationships are intriguing, but require further investigation to determine how primary production equates spatially with secondary production and the subsequent availability of food to whale sharks.

A long-term (decadal) photo-identification study of whale sharks at Ningaloo Reef has shown that many sharks are resighted in successive years at this locality (Meekan *et al.* 2006, Bradshaw *et al.* 2007). Tagging studies using Pop-up archival tags (PSAT) show that following aggregations, whale sharks move northward from Ningaloo (Wilson *et al.* 2006). Tags that detach from whale sharks < 4 to 5 months after deployment are typically found on the continental shelf to the north, while tags that detach after this time have been found in the open ocean beyond the continental shelf. Wilson *et al.* 2006 suggested that this indicates that whale sharks could be using the directional cues of the northward-flowing current systems such as the Ningaloo Current to migrate northwards along the shelf after visiting Ningaloo and then later move offshore to take advantage of the southward-flowing Leeuwin Current to return to the reef. A weakening or strengthening of the Leeuwin Current as a result of the ENSO phenomenon might thus account for the correlation between the SOI and relative whale shark abundance.

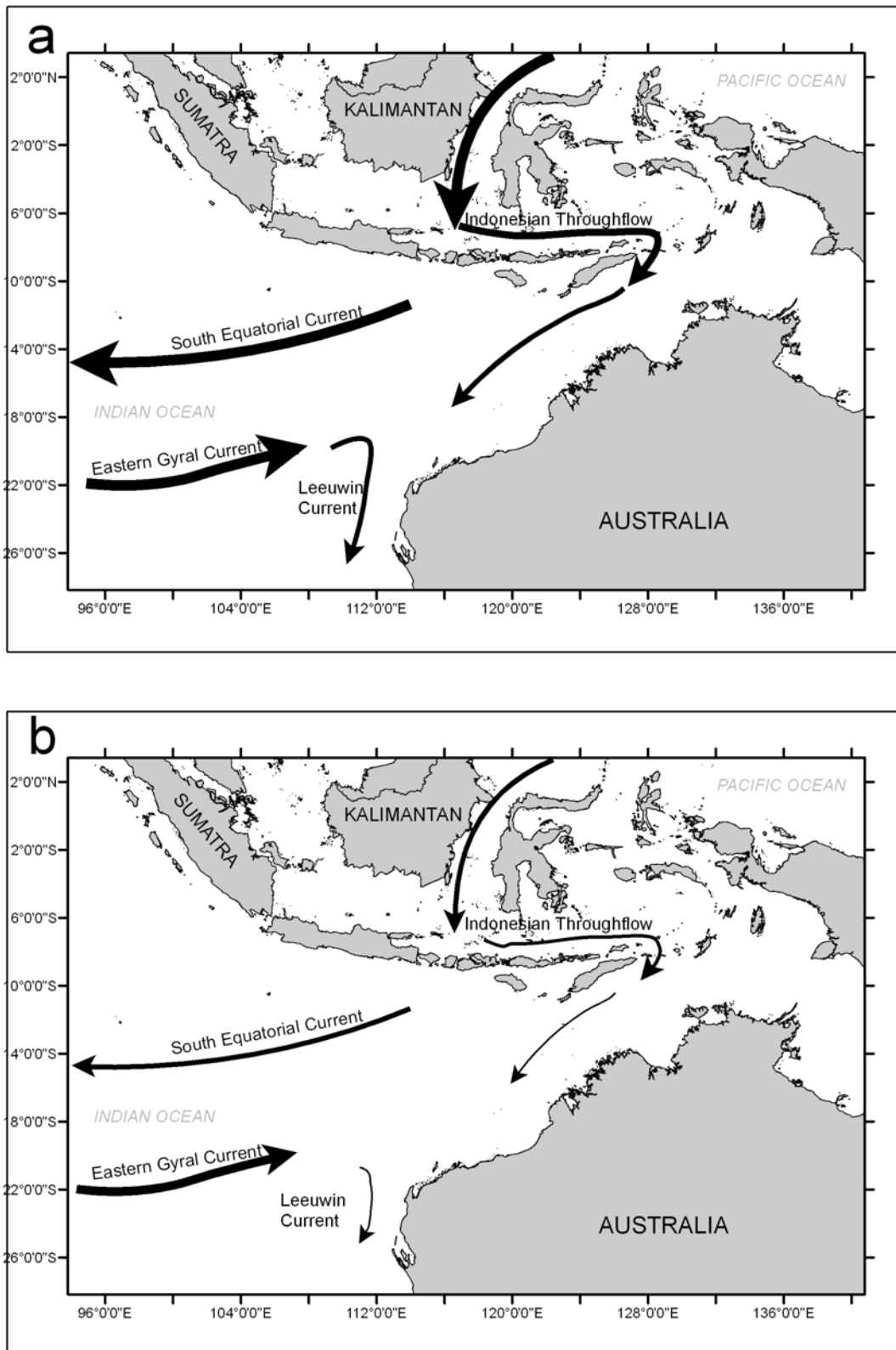


Figure 6.5. Oceanographic models indicating the relative differences in the circulation patterns and strength of major currents (as denoted by thickness of arrows) in the North East Indian Ocean during (a) La Niña and (b) El Niño climatic periods.

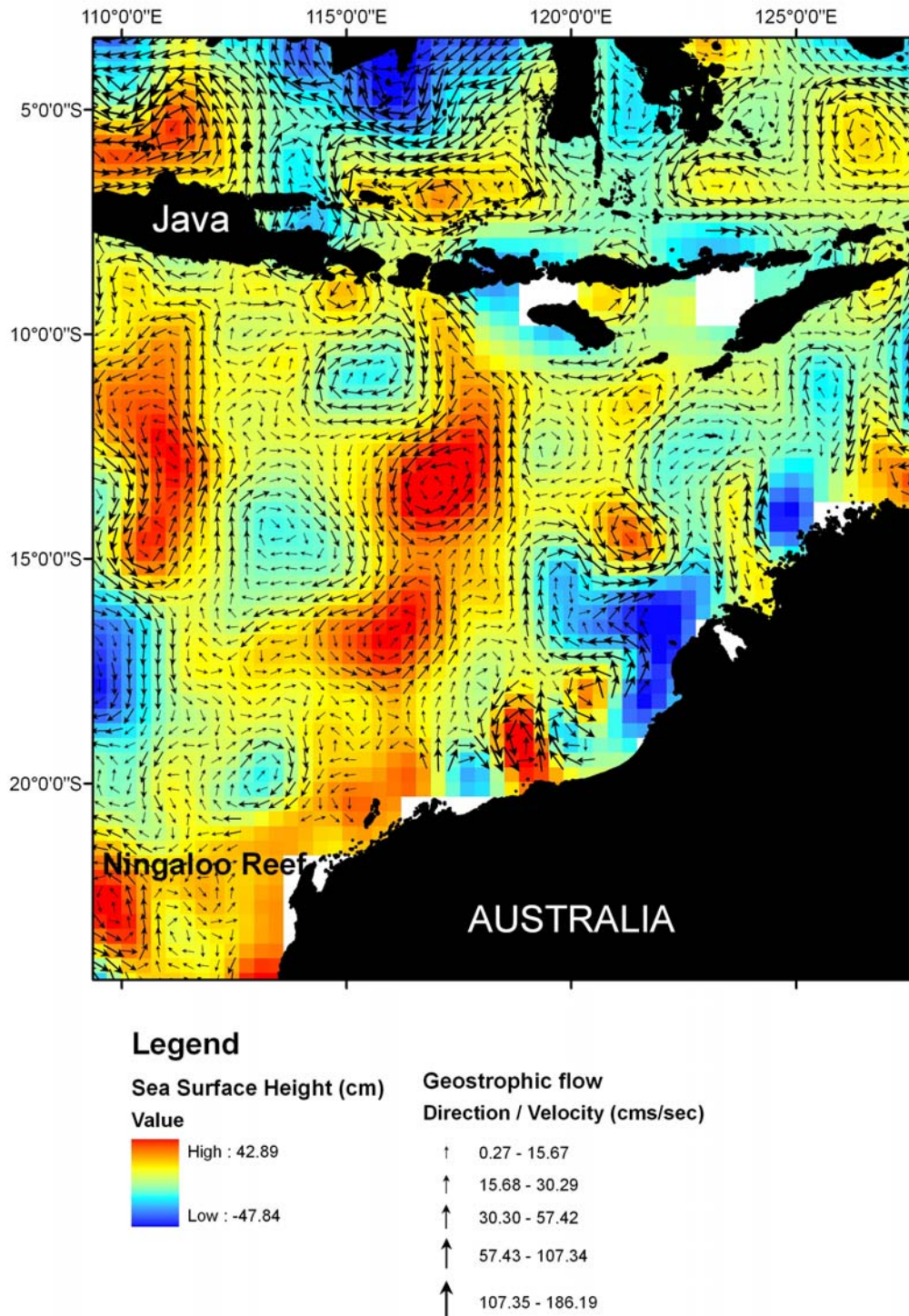


Figure 6.6. Weekly Topex/ Poseidon altimetry composite of Sea Surface height and associated geostrophic flow (direction and velocity) in the East Indian Ocean during the annual period when whale shark abundances tend to peak (1st week of May).

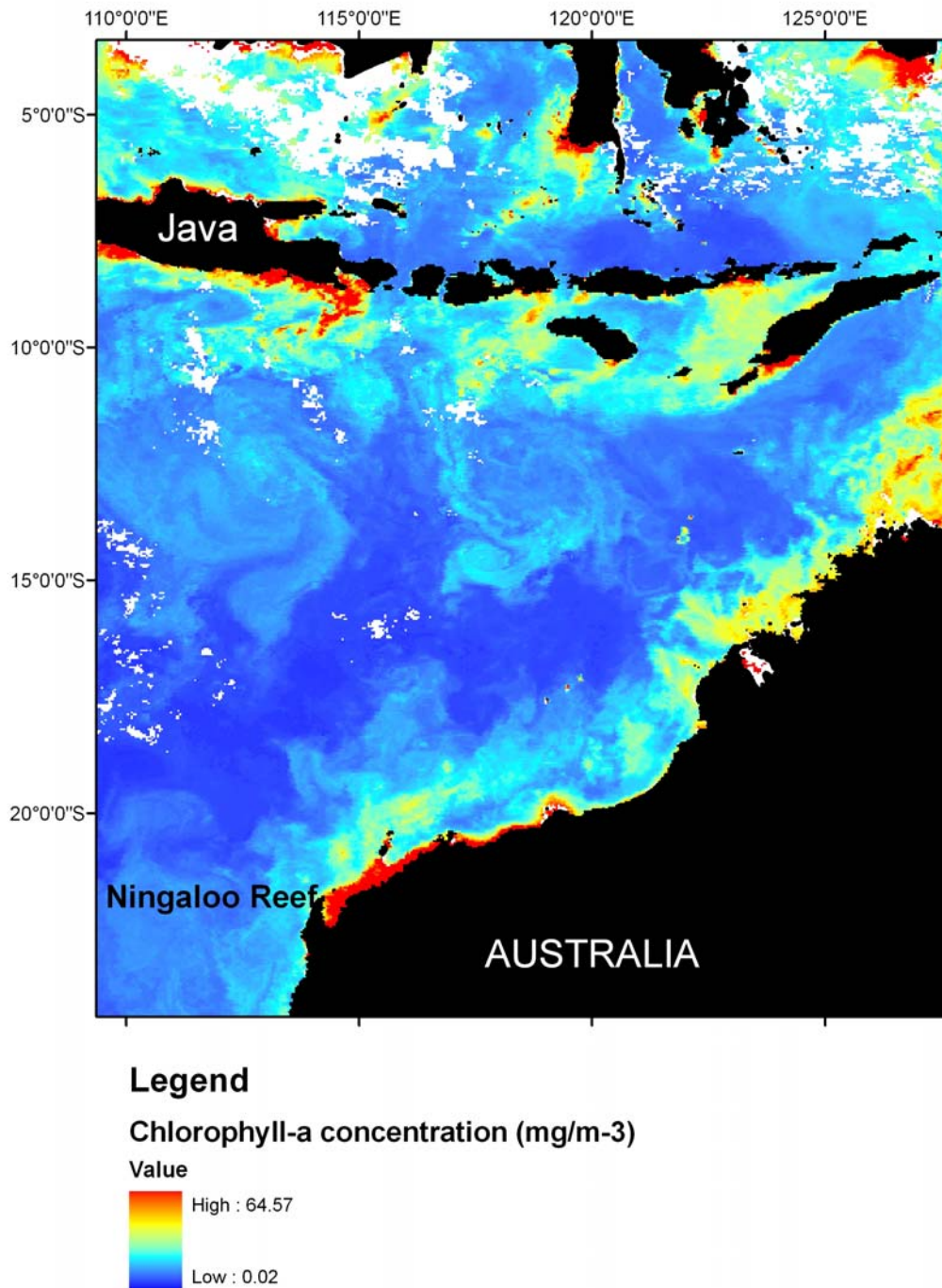


Figure 6.7. Weekly SeaWiFs satellite image composite of chlorophyll-a concentration in the East Indian Ocean during the annual period when whale shark abundances tend to peak (1st week of May).

The influence of the ENSO climatic signal is not limited to physical effects on currents. Variation in the strength, timing and path of the Leeuwin Current due to ENSO has cascading effects on the types and abundances of marine organisms that occur on the Western Australian coastline (Caputi et al. 1996). For instance, recruitment of the western rock lobster (*Panulirus cygnus*) is positively influenced, while recruitment of scallops (*Amusium balloti*) and pilchards (*Sardinops sagax neopilchardus*) are negatively influenced. These annual differences probably reflect changes in the food chains and the availability of the appropriate prey for larval or young stages. For whale sharks, it is possible that La Niña climatic episodes influence abundance on Ningaloo Reef by favouring the oceanographic conditions necessary for the proliferation of their prey. While the strong Pacific trade winds characteristic of La Niña are important for driving the warm, southerly-flowing Leeuwin Current, the strength of this current also positively influences the flow of the cooler Ningaloo counter-current. The Ningaloo Current predominates on the reef front from September to April, and is believed to influence coastal upwelling with prevailing South Westerly winds due to Ekman transport (Holloway & Nye 1985, Taylor & Pearce 1999, Holloway 2001). This upwelling determines localised productivity events along the Ningaloo coast, which may attract whale sharks to the reef (Taylor & Pearce 1999). In temperate regions there is some evidence that large-scale climatic phenomena influence the abundance of planktivorous sharks (e.g., basking sharks *Cetorhinus maximus*) by driving oceanographic events that alter productivity of coastal waters and ultimately the availability of zooplankton food (Squire 1990, Sims & Quayle 1998).

It is still a challenge to determine how changes in the strength of current systems in response to the ENSO phenomenon may act to transport sharks to the region and/or indirectly affect their prey by driving productivity events at Ningaloo Reef. This issue is currently under investigation through the deployment of satellite tags so that whale shark migrations can be linked to oceanographic processes observed from remotely sensed data. Satellite measurements of chlorophyll *a* concentrations and other potentially important parameters (e.g., SST and salinity) can be overlaid on migration pathways to determine the extent to which whale shark aggregations are related to physical transport mechanisms and productivity of Ningaloo Reef.

6.3 DECLINE IN WHALE SHARK SIZE AND ABUNDANCE AT NINGALOO REEF OVER THE PAST DECADE: THE WORLD'S LARGEST FISH IS GETTING SMALLER

6.3.1 Introduction

The effects of overfishing reach far beyond the relatively predictable reduction of yields (Food and Agriculture Organisation of the United Nations 2006); overfishing of marine species can also disrupt important biological processes by removing particular size classes (Walker 1998), thereby changing an exploited population's age structure, individual maturation times and growth rates (Myers et al. 1995, Jennings & Kaiser 1998, Jennings et al. 1998, Dulvy et al. 2003, Reynolds et al. 2005). Changes to demographic rates and the evolutionary patterns induced by size-selective fishing can increase extinction risk in harvested species (Jennings & Kaiser 1998, Jennings et al. 1998, Conover & Munch 2002, Reynolds et al. 2005), so measuring changes in size structure is an important step in identifying whether over-exploitation has occurred (Shin et al. 2005, Greenstreet & Rogers 2006).

Many large pelagic species such as tunas, billfishes and sharks that are targeted directly or are taken as bycatch in industrial fisheries have experienced substantial declines over the last century (Baum et al. 2003, Sibert et al. 2006, Myers et al. 2007). For sharks in particular, high harvest rates mainly from bycatch have resulted in rapid population declines (Baum et al. 2003, Robbins et al. 2006, Sibert et al. 2006, Myers et al. 2007), although the dynamics of the interacting drivers of decline make predictions of extinction risk difficult (Walker 1998, Stevens et al. 2000, Baum et al. 2003, Baum et al. 2005, Burgess et al. 2005a, b, Robbins et al. 2006). Additionally, these population crashes have occurred in spite of the perceived lower extinction risk of broad-ranging and wide-dispersing species (Terborgh & Winter 1980).

Although harvested to an unquantified extent (Chen et al. 1997a, Chen & Phipps 2002), the world's largest fish, the whale shark (*Rhincodon typus* Smith, 1828), also appears to have declined throughout much of its range (CITES 2002, Theberge & Dearden 2006, Bradshaw et al. 2007). These wide-ranging (Eckert et al. 2002, Wilson et al. 2006, Bradshaw et al. 2007, Castro et al. 2007) filter feeders are distributed throughout the world's tropical and warm temperate seas and are classed as *Vulnerable* under IUCN Red List criteria and listed by the *Convention on International Trade in Endangered Species of Wild Fauna and Flora* (CITES) in *Appendix II* (i.e., "species not necessarily threatened with extinction, but in which trade must be controlled in order to avoid utilization incompatible with their survival") (CITES 2002). Like most shark species, whale shark have slow growth rates, late maturity and extended longevity (Frisk et al. 2001, Bradshaw et al. 2007, Graham & Roberts 2007), and such traits are likely to limit annual recruitment and increase susceptibility to over-exploitation by humans (Smith et al. 1998, Bradshaw et al. 2007). The high degree of connectivity among aggregations at broad spatial scales (Castro et al. 2007, Graham & Roberts 2007) suggests that unsustainable fishing mortality at one locality will affect unexploited aggregations at another (Bradshaw et al. 2007).

In the late 1980s, aggregations of whale sharks were reported in coastal waters at a few locations in Australia, Southeast Asia and the Caribbean (Taylor 1996, Heyman et al. 2001). Since this time, the predictability of seasonal aggregations has fostered the development of a profitable ecotourism industry (Meekan et al. 2006, Graham & Roberts 2007). Ecotourism at Ningaloo Reef, Western Australia, one of the world's largest whale shark aggregations, began in the early 1990s and since 1995, location, sex and length data have been recorded for most individuals encountered (Meekan et al. 2006). This industry uses light aircraft to locate the sharks in surface waters and to direct vessels into their path so that paying tourists are able to swim with the slow-moving sharks (Davis et al. 1997). Whale sharks come to Ningaloo Reef from March to June, where they are found in shallow water (< 100 m) along the front of the fringing coral reef (Taylor 1996). These continuous records now span a decade, providing a large sightings dataset that offers insight into this aggregation's demography and population status.

Based on the anecdotal and catch evidence that the whale shark population has experienced (largely unmeasured) exploitation in the Indian Ocean basin (Chen et al. 1997a, Chen & Phipps 2002), we hypothesised that evidence for over-exploitation would be revealed by an observed decline in larger (older) individuals (Stergiou 2002). Previous work using photo-identification of 159 known individuals at Ningaloo Reef has provided some support for this hypothesis, with an observed increase in the proportion of small (< 6.7 m total length) sharks (Meekan et al. 2006). Here we used a much larger and independently collected dataset to test for a continuous reduction in average shark size (total length). There are three main mechanisms that may drive changes in body size of harvested populations: (1) abiotic factors affecting growth and development (e.g., large-scale climate or regime shifts); (2) biotic changes such as density-modified growth rates and (3) changes to demography and genetic composition via harvesting (Ratner & Lande. 2001). We therefore explicitly examined the form of the decline (linear, logistic or quadratic) to test for the presence of a new mean size equilibrium. We hypothesised that a rapid, deterministic mortality source of a particular size class (e.g., size-biased harvest) might induce a gradual decline in mean size followed by a tapering toward a new equilibrium size as larger individuals were systematically removed from the population. By comparison, sustained linear decline without tapering may indicate a shift by fishers to target progressively smaller individuals as larger individuals are depleted from the population (cf. Pauly et al. 1998).

A natural corollary of over-exploitation is the prediction that overall abundance of the population decreases (Food and Agriculture Organisation of the United Nations 2006); as such, we tested the hypothesis that the number of whale sharks seen at Ningaloo Reef has changed since monitoring began. This hypothesis is based on previous capture-mark-recapture model estimates of survival and matrix projections that inferred long-term decline of whale sharks visiting Ningaloo Reef (Bradshaw et al. 2007). Using the large operator-collected dataset, we tested the hypothesis of a decline directly using relative abundance data corrected for sampling effort and environmental stochasticity because whale shark abundance is known to fluctuate annually relative to local oceanographic conditions (Wilson et al. 2001a).

Our final aim was to gain insight into the relative contribution of demographic and environmental processes driving the population trends. We hypothesised that abundance time series from a declining population will demonstrate more support for an exponential model describing the relationship between the rate of change and population density compared to a stable population fluctuating around carrying capacity (see Brook & Bradshaw 2006). As such, we predicted that the exploited whale shark abundance time series will show little support for density regulation, and we test this explicitly by contrasting phenomenological density-dependent and density-independent models applied to the relative abundance time series. Although we focus on a single iconic species, our intent is to provide marine conservation biologists with a general approach for examining potential causes of decline in long-lived marine predators when detailed demographic data are rare and relative abundance time-series data are readily available.

6.3.2 Materials and methods

6.3.2.1 Tourist operator-collected data

Numbers of whale sharks at Ningaloo Reef peak in the months of April and May (Davis et al. 1997, Wilson et al. 2001a). Because sighting effort occurs sporadically outside of the peak months, our analysis was restricted to the peak period. Tour operators collected information on estimated total length (TL, visual estimation from the spotter plane and vessel; corroborated by in-water measurements) (Meekan et al. 2006) and sex (via the identification of claspers on males) (Taylor 1994a) for each shark observed. Licenses for tourist boat access to sharks are restricted by the Western Australian Department of Environment and Conservation (WA-DEC). This means that the same vessels tend to operate from year to year (Davis et al. 1997). There is however, turnover in crew, which should negate the possibility that any observed trends in size distribution are merely the result of year-by-year improvement in an operator's assessment skill and capacity. Supporting this, the same observed trends were consistent in data collected by licensees operating only from Coral Bay or Tantabiddi > 100 km away (B. M. Fitzpatrick, unpubl. data). Recently, WA-DEC implemented a training course that all employees of the whale shark tourism operations are required to attend, and records indicate that no single boat skipper, dive master or crew member has remained during the entire sample interval. In fact, most employees remain for an average of two years only. Additionally, spotting-plane pilots typically provide the first estimate of whale shark size, and pilots turnover at a similar rate to boat crews (B. M. Fitzpatrick, unpubl. data).

Spotter planes are generally shared between two or more tourist vessels with patrons sharing the same shark. Length estimates of the same shark are a combined effort between a plane pilot, one or more boat skippers, and in-water shark spotters, all with varying experience. Such repeat observations of the same shark were identified in different ship logs and removed from the dataset. Length estimates of surfaced sharks are typically made by pilots and corroborated by comparison to known-length vessels in the water; further validation is provided by in-water measurements compared to known-length snorkelers. Length measurements are only entered into the database once pilots and multiple operators agree. As

quantified corroboration, direct in-water measurements of sharks compared favourably to pilot and vessel-operator estimates of total length (Norman 1999).

There is little evidence that the presence of snorkelers influences whale shark behaviour. The interaction of tourists and vessels with sharks is tightly controlled by a code of conduct enforced by DEC (Davis et al. 1997). This ensures that patrons do not approach within 3 m of the shark while snorkelling, and vessels must remain a minimum of 30 m from the shark for a maximum of 90 minutes (Davis et al. 1997). Studies of whale sharks at Ningaloo Reef could find no detectable changes in behaviour of sharks in the presence of snorkelers (Norman 1999) that might bias our results.

6.3.2.2 Reduction in total length over time

To test the hypothesis of a continuous decline in mean shark size and to examine the form of this trend, four linear and nonlinear models of mean annual TL (over all individuals for which a TL estimate was made) against year were contrasted. Models represented four hypotheses: (1) no temporal trend (intercept: $TL \sim 1$), (2) linear decline (linear: $TL \sim year$), (3) curvilinear decline (quadratic: $TL \sim year + year^2$), and (4) sigmoidal decline (logistic: $TL \sim a/b \cdot e^{-year}$, where a and b are constants). Non-linear models were used in addition to linear models because distinct processes affecting mean size in a population may introduce different trends in size over time (see Introduction).

We used Akaike's Information Criterion corrected for small sample size (AIC_c) as an index of Kullback-Leibler (K-L) information loss to assign relative strengths of evidence to the different competing models (Burnham & Anderson 2002). One could also employ other methods to compare models such as the dimension-consistent Bayesian Information Criterion (BIC); however, BIC may only be preferable when sample sizes are approximately ≥ 20 data per parameter estimate (Burnham & Anderson 2002, Link & Barker 2006). The relative likelihoods of candidate models were calculated using AIC_c (Burnham & Anderson 2002), with the weight ($wAIC_c$) of any particular model varying from 0 (no support) to 1 (complete support) relative to the entire model set. For each model considered, we also calculated the percentage deviance explained (%DE) as a measure of goodness-of-fit. Information-theoretic evidence ratios (ER, an index of the likelihood of one model over another, calculated as the $wAIC_c$ of one model \div $wAIC_c$ of another model) (Burnham & Anderson 2002) were used to contrast specific model pairs.

The above analysis only examines the trend in mean total length over time. To incorporate uncertainty due to year, month and vessel into the test for a decline in mean total length, we also applied a series of five *a priori* general linear models (GLM) with Gaussian error distributions and identity link functions, where individual TL was set as the response and the terms *year/month* were treated as a nested term and individual factors made up the various model combinations. The term *month* was included in some models to account for possible phenology changes (e.g., temporal changes arrival patterns during the peak season) that may vary with strength of the El Niño-Southern Oscillation events each year (Wilson et al. 2001a, and see below). We also considered a second set of models replacing *month* with *day of year*

as a covariate to investigate whether more variance in *total length* could be explained. Models were contrasted using the Bayesian Information Criterion (BIC) given the large sample size ($n = 1814$) and our desire to distinguish main from tapering effects (Burnham & Anderson 2002, Link & Barker 2006). We also considered a second set of 8 models that included the sex effect (with a reduced overall sample size given that not all individuals could be sexed reliably; $n = 1333$). To test further the hypothesis that systematic changes in observers may have biased observed size trends, we constructed a series of linear mixed-effects models (GLMM) using the `lmer` command in the `lme4` library of the R Package (R Core Development Team 2004), coding year as a fixed covariate and vessel as a random factor.

6.3.2.3 Relative shark abundance and climate variation

Relative shark abundance was calculated by summing the total number of sharks seen for the months of April and May and dividing these values by the total search time for all observing vessels for these two months over each year of the study (SPUE = sightings per unit effort). The monthly interval was chosen to match available environmental data for sightability bias correction (see below). Search time was calculated only over the peak interval and not the entire year. The database was corrected so that a shark was only recorded once per day even though it may have been sighted by several tourist operators during that day. The majority of this 'effort' (> 90 %) is devoted to searching for sharks rather than transiting to one once it has been identified by another vessel. There is therefore little chance that extra time spent transiting between a single shark visited by several vessels would impart any important bias to indices of search effort. However, it was still possible that the same shark was seen on subsequent days (i.e., individual sharks were not marked). Tagged whale sharks remain near the Ningaloo coast for several weeks after tagging (Wilson et al. 2006), so repeated sampling of some sharks was probable. However, this problem is unlikely to affect overall size and abundance trends unless there was some systematic change in residence times that we could not record. Furthermore, given that individual sharks are unlikely to remain at Ningaloo Reef for more than a few weeks (at most), monthly comparisons of relative abundance should account for gross changes in abundance more appropriately than examining the trends at finer temporal scales.

Climate variation is thought to affect whale shark relative abundance at Ningaloo Reef (Wilson et al. 2001a). Critically, however, the relationship between whale shark abundance and El Niño-Southern Oscillation (ENSO) variation established by Wilson et al. (2001a) did not correct relative abundance estimates for variation in search effort. The oceanography around Ningaloo Reef is dominated by the Leeuwin Current (LC), which forms from the Indonesian Through-Flow system to the north (Morrow & Birol 1998). The LC flows south along the shelf break bringing warm, nutrient-poor water to the coast of Western Australia (Pearce & Griffiths 1991). Between the LC and the coast, cooler water upwells from depth to form the Ningaloo Current, which flows along the edge of Ningaloo Reef towards the north (Morrow & Birol 1998). The relative strengths of these current systems are strongly influenced by El Niño-Southern Oscillation (ENSO) events (Pearce & Phillips 1988). During El Niño years, the LC is weak and water temperatures along the coast of Western Australia are relatively cool, while in La Niña years the current is stronger and water temperatures are higher. This

variability in current flow is known to influence recruitment to many commercial fisheries in Western Australia (Lenanton et al. 1991, Caputi et al. 1996).

To correct the relative abundance data (sightings per unit effort – SPUE) for this annual climate variation, we used maximum likelihood estimation (MLE) to fit a linear regression between mean SPUE to the mean April and May Southern Oscillation Index (SOI) (calculated from a two-month running mean smoother). We then detrended the SPUE time series based on this relationship (subtracting fitted values from observed SPUE). Temporal comparisons of detrended SPUE assume, of course, that SPUE reflects relative changes in total abundance.

Photo-identification data of 159 known individuals suggest that that whale sharks at Ningaloo Reef have changed in age/size composition since monitoring began (Meekan et al. 2006). To expand on this preliminary work and to test the hypothesis with the much larger tourist operator dataset, we examined the SOI-detrended SPUE trends for four size-sex classes based on the median TL (6 m) observed over all sharks: small (< 6 m) or large (\geq 6 m), and male or female (median TL was not calculated for each sex separately due to the weak sex effect; see Results). We deliberately avoided using a putative size at maturity as the threshold for dividing 'small' and 'large' sharks, given the uncertainty associated with this value (Bradshaw et al. 2007). Our aim here was primarily to ensure representative samples in each size category, to test the hypothesis that different size categories of whale sharks (based on the median threshold) demonstrate different temporal trends in abundance.

6.3.2.4 Evidence of intrinsic and extrinsic control in SPUE rate of change

In addition to testing for a decline in the raw temporal trends in SOI-detrended SPUE, we examined the relative evidence for intrinsic (including both births and temporary immigration) and extrinsic (e.g., deterministic drivers such as over-harvest) control of the detrended relative abundance data. Our hypothesis in this case was that evidence for an exogenous (i.e., environmental or anthropogenic) driver of the decline, as revealed by the SPUE data, would be supported if density-independent models of the relationship between population rate of change (r) and relative abundance (SPUE) had stronger information-theoretic evidence than density-dependent models (an approach used for many other taxa to determine the relative contribution of extrinsic versus intrinsic control of population size - de Little et al. 2007, Chamaillé-Jammes et al. 2008, Yang et al. 2008). This hypothesis is based on the assumption that deterministic declines caused by harvest do not fluctuate with respect to stock density; this a fundamental tenet of fisheries management based on catch-per-unit-effort (CPUE) data (Walters 1995, Walters & Martell 2004, but see also Maunder et al. 2006 for the limitations of CPUE data interpretation).

We adopted a multiple-working hypotheses approach based on information-theoretic multi-model inference (Burnham & Anderson 2002) by applying two variants of the generalised θ -logistic population growth model (Turchin 2003) to the detrended SPUE series (averaged by year): (1) Gompertz-logistic growth –

$$\log\left(\frac{\text{SPUE}_{t+1}}{\text{SPUE}_t}\right) = r = r_m \left[1 - \left(\frac{\log(\text{SPUE}_t)}{\log(K)} \right)^\theta \right] + \varepsilon_t$$

where SPUE_t = SOI-detrended relative abundance time t , r = realised population growth rate, r_m = maximal intrinsic population growth rate, K = carrying capacity, θ is a shape parameter set to 1, and ε_t has a mean of zero and a variance (σ^2) that reflects environmental variability in r ; and (2) exponential growth (where $\sigma = -\infty$, and r_m and σ are estimated).

We used MLE to fit model parameters via linear regression, and models were contrasted using AIC_c as described above. All detrended SPUE were first standardised according to the expression $y' = y + 1.1 \max(\text{abs}(y))$ to remove negative values that can be problematic for ML estimation.

6.3.3 Results

A total of 4436 sightings provided 2411 unique (per day) sightings of whale sharks from 1995 to 2004, of which 1333 records had estimates of TL and sex. The overall length-frequency distribution showed was moderately right-skewed (Fig. 6.8A) as is expected for a largely juvenile aggregation (Meekan et al. 2006, Bradshaw et al. 2007). Comparing the length-frequency distribution from 1995-1996 (Fig. 6.8B) to that from 2003-2004 (Fig. 6.8C) shows a marked shift of the frequency distribution to one dominated by smaller (< 6 m TL) individuals with few large representatives (Fig. 6.8C).

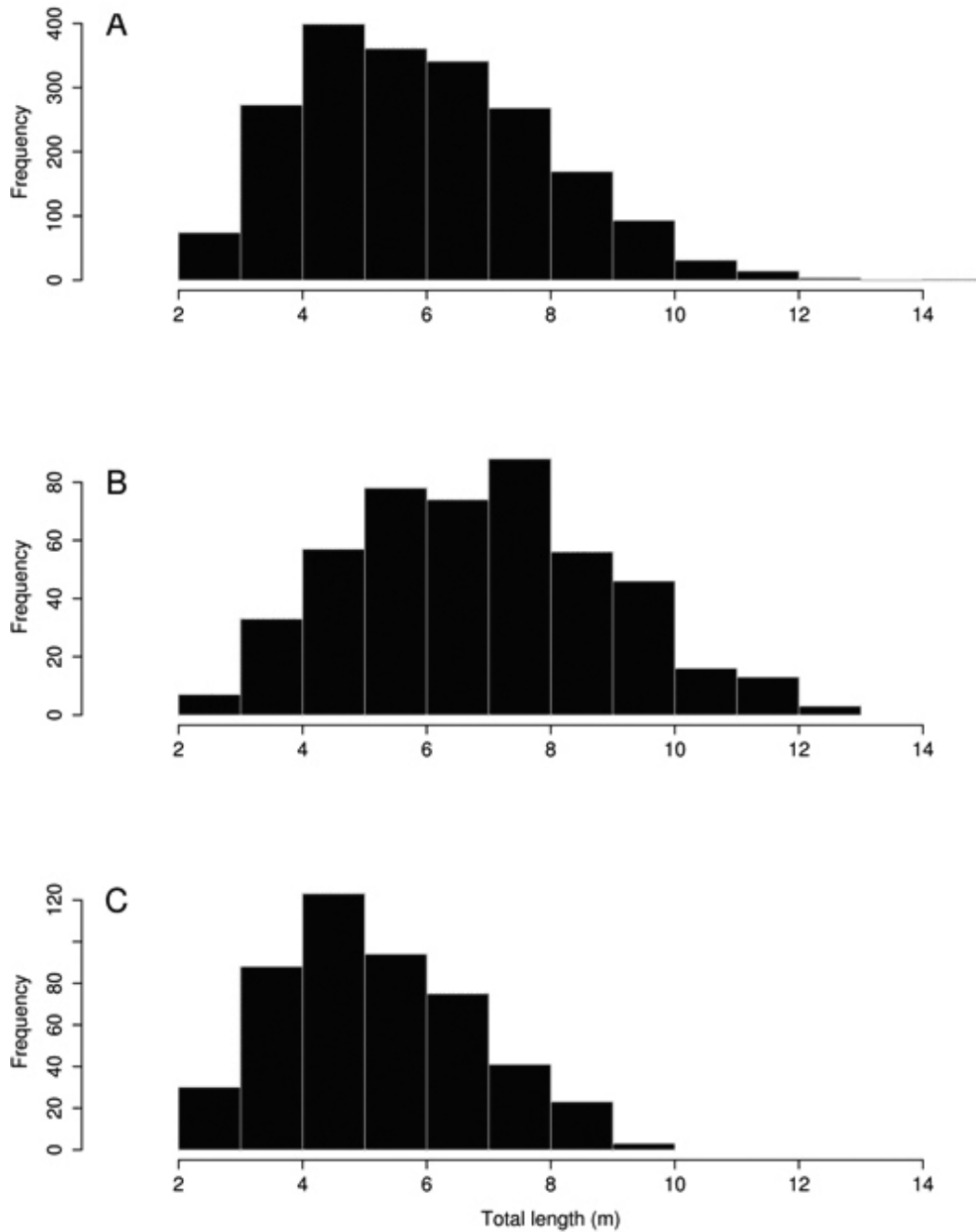


Figure 6.8. Estimated total length (TL in m) distribution for whale sharks seen at Ningaloo from A. 1995-2004, B. only 1995-1996 and C. only 2003-2004. There is a noticeable loss of larger individuals in the more recent distribution.

This can also be shown as a temporal trend; the annual mean estimates of TL showed a strong linear decline with year, explaining over 91 % of the deviance (%DE) (Table 6.4; Fig. 6.9). In 1995, whale sharks averaged 7.0 m TL (95 % 10000 iterations bootstrapped confidence interval: 6.5 – 7.4 m), but by 2004, sharks averaged only 5.4 m (5.2 – 5.6 m; Fig. 6.9). There was moderate support for the logistic model (Akaike’s Information Criterion weigh [$wAIC_c$] = 0.20); however, the increase in %DE using the logistic against the linear was minor (< 3 %; Table 6.4). This implies that the decline is being driven by the faster disappearance of the remaining largest individuals – a result consistent with hypothesis that an anthropogenic source of mortality is driving the decline.

Table 6.4. Four models applied to the relationship between mean total length (TL) and year for whale sharks from Ningaloo Reef between 1995 and 2004. Models are ranked according to Akaike’s Information Criterion corrected for small sample size (AIC_c). Shown for each model are the number of parameters (k), the maximum log-likelihood (LL), the difference in AIC_c for each model from the top-ranked model (ΔAIC_c), AIC_c weight ($wAIC_c$), and the percent deviance explained (%DE) in the response variable (TL).

Model	k	LL	ΔAIC_c	$wAIC_c$	%DE
linear	3	3.49	0.00	0.71	91.49
logistic	3	2.20	2.57	0.20	89.00
quadratic	4	4.53	3.93	0.09	93.08
intercept	1	-8.83	20.35	< 0.01	0.00

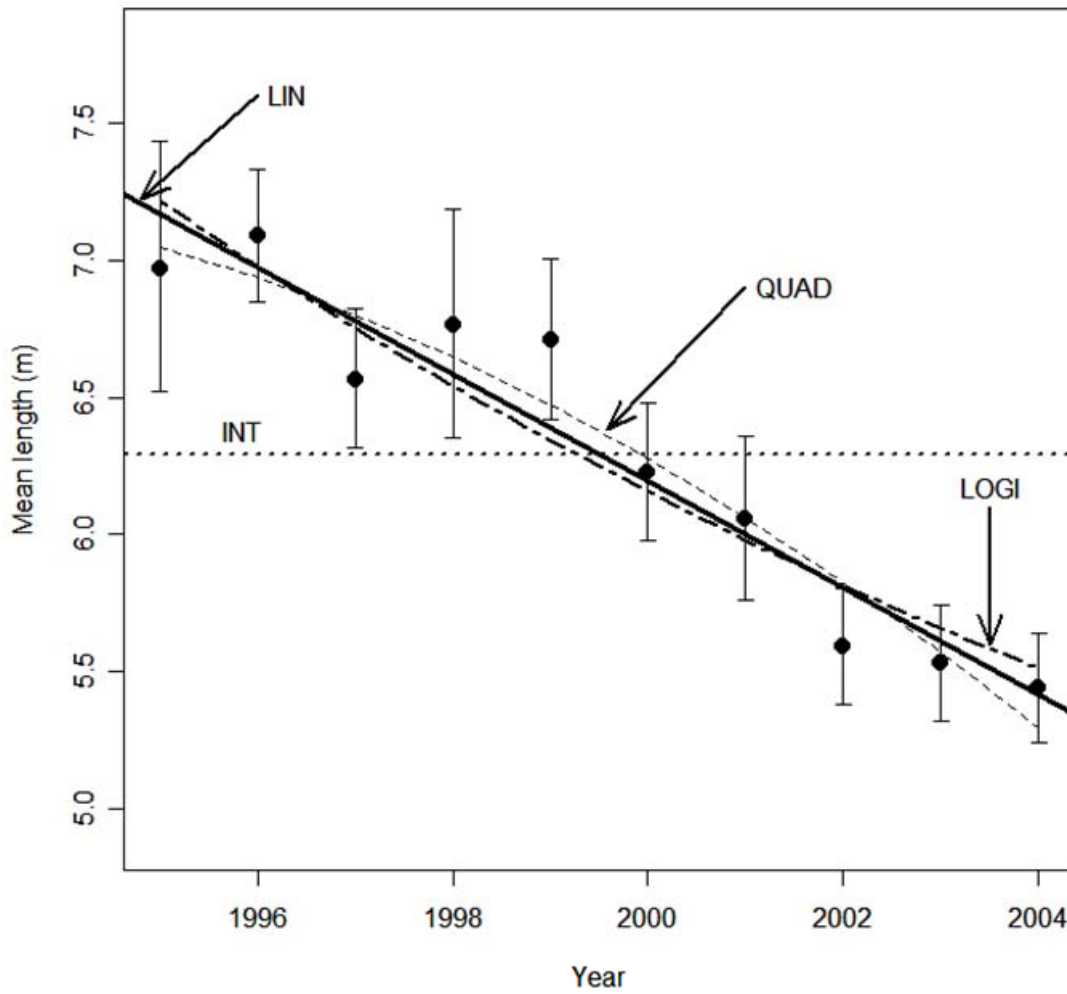


Figure 6.9. Mean length (\pm 95 % bootstrapped confidence intervals based on 10 000 iterations to account for non-normal data in some years) of all whale sharks observed at Ningaloo Reef from 1995 – 2004. Information-theoretic model rankings indicated highest support for a linear decline (LIN) against the quadratic (QUAD) and logistic (LOGI) models. Relative to any of these models of decline, the intercept model (INT), characterising a stable population, had no support.

Using all data (i.e., not just annual means), we found strong support for a nested *year/month* effect on TL, but nearly no support for a *month* effect alone on %DE (Table 6.5). Including the sex term in the reduced dataset improved model fit slightly (Table 6.5), but the relatively small improvement in the % deviance explained (1.8 %) suggested that its effect was negligible (i.e., no major size differences between males and females).

Table 6.5. Comparison of general linear models (GLM) examining the relationship between total length (TL) and temporal variables for whale sharks at Ningaloo Reef from 1995 – 2004. A. TL versus *year* and *month*, and B. Five top-ranked GLMs examining the relationship between *year*, *month* and *sex* and TL. Models are ranked according to the Bayesian Information Criterion (BIC). Shown for each model are the number of parameters (*k*), the maximum log-likelihood (*LL*), the difference in BIC for each model from the top-ranked model (Δ BIC), BIC weight (*w*BIC), and the percent deviance explained (%DE) in the response variable (TL).

Model	<i>k</i>	<i>LL</i>	Δ BIC	<i>w</i> BIC	%DE
A. Year & month only					
TL ~ <i>year/month</i>	4	-3646.06	0.00	0.72	9.99
TL ~ <i>year</i>	3	-3650.87	2.12	0.25	9.51
TL ~ I	2	-3741.51	175.90	< 0.01	0.00
TL ~ <i>month</i>	3	-3741.47	183.32	< 0.01	< 0.01
B. Year, month & sex					
TL ~ <i>sex + year</i>	4	-2676.01	0.00	0.51	11.33
TL ~ <i>sex + year/month</i>	5	-2672.44	0.07	0.49	11.80
TL ~ <i>sex + year/month + year/month*sex</i>	7	-2671.63	12.84	< 0.01	11.91
TL ~ <i>year</i>	3	-2686.35	13.49	< 0.01	9.94
TL ~ <i>sex</i>	3	-2749.52	139.83	< 0.01	0.99

Replacing the *month* factor for the *day of year* covariate changed the model rankings only marginally and overall %DE was similar (Table 6.6). The linear mixed-effects models (GLMMs) used to account for potential trends within vessels demonstrated that the model $TL \sim year/month$ remained the most highly ranked ($wBIC = 0.58$), indicating a decline in TL even after accounting for any observer bias (i.e., bias accounted for by partitioning the variance among vessels in the random effect).

Table 6.6. Comparison of general linear models (GLM) examining the relationship between total length (TL) and temporal variables for whale sharks at Ningaloo Reef from 1995 – 2004. A. TL versus *year* and *day of year (doy)*, and B. Five top-ranked GLMs examining the relationship between *year*, *doy* and *sex* and TL. Models are ranked according to the Bayesian Information Criterion (BIC). Shown for each model are the number of parameters (*k*), the maximum log-likelihood (*LL*), the difference in BIC for each model from the top-ranked model (ΔBIC), BIC weight (*wBIC*), and the percent deviance explained (%DE) in the response variable (TL).

Model	<i>k</i>	<i>LL</i>	ΔBIC	<i>wBIC</i>	%DE
<u>A. Year & day-of-year only</u>					
$TL \sim year$	3	-3650.87	0.00	0.74	9.51
$TL \sim year/doy$	4	-3648.18	2.12	0.26	9.78
$TL \sim I$	2	-3741.51	173.78	< 0.01	0.00
$TL \sim doy$	3	-3740.55	179.35	< 0.01	0.11
<u>B. Year, day-of-year & sex</u>					
$TL \sim sex + year$	4	-2676.01	0.00	0.91	11.33
$TL \sim sex + year/doy$	5	-2674.69	4.56	0.09	11.51
$TL \sim sex + year/doy + year/doy*sex$	7	-2671.90	13.37	< 0.01	11.87
$TL \sim year$	3	-2686.35	13.49	< 0.01	9.94
$TL \sim sex$	3	-2749.52	139.83	< 0.01	0.99

Total numbers of sharks observed from year to year varied by nearly an order of magnitude, with peaks in the 1996 and 2002 seasons, and lows in 1998 (Fig. 6.10A). Search effort (number of search hours by vessels) was also variable (Fig. 6.10A) and tended to increase through time. The sightings per unit effort (SPUE) appeared to decline through time, albeit with substantial annual variation (Fig. 6.10B). The relationship between SPUE and the SOI was strongly supported (AIC_c evidence ratio [ER] = 10.6; $R^2 = 0.28$; Fig. 6.10D), such that during years characterised by cooler El Niño events (low SOI; Fig. 6.10C), relatively fewer sharks were seen by tourist operators. This provides clarity on the earlier work demonstrating a possible relationship between whale shark abundance and ENSO-related climatic variation (Wilson et al. 2001b). SOI-detrended SPUE for all sharks combined demonstrated a gradual decline from 1995 to 2004 ($ER = 2.4$; $R^2 = 0.16$) – tourist operators saw approximately 40 % fewer sharks per hour of searching in 2004 than in 1995. This population-level result confirms life-history based predictions of decline at Ningaloo Reef (Bradshaw et al. 2007).

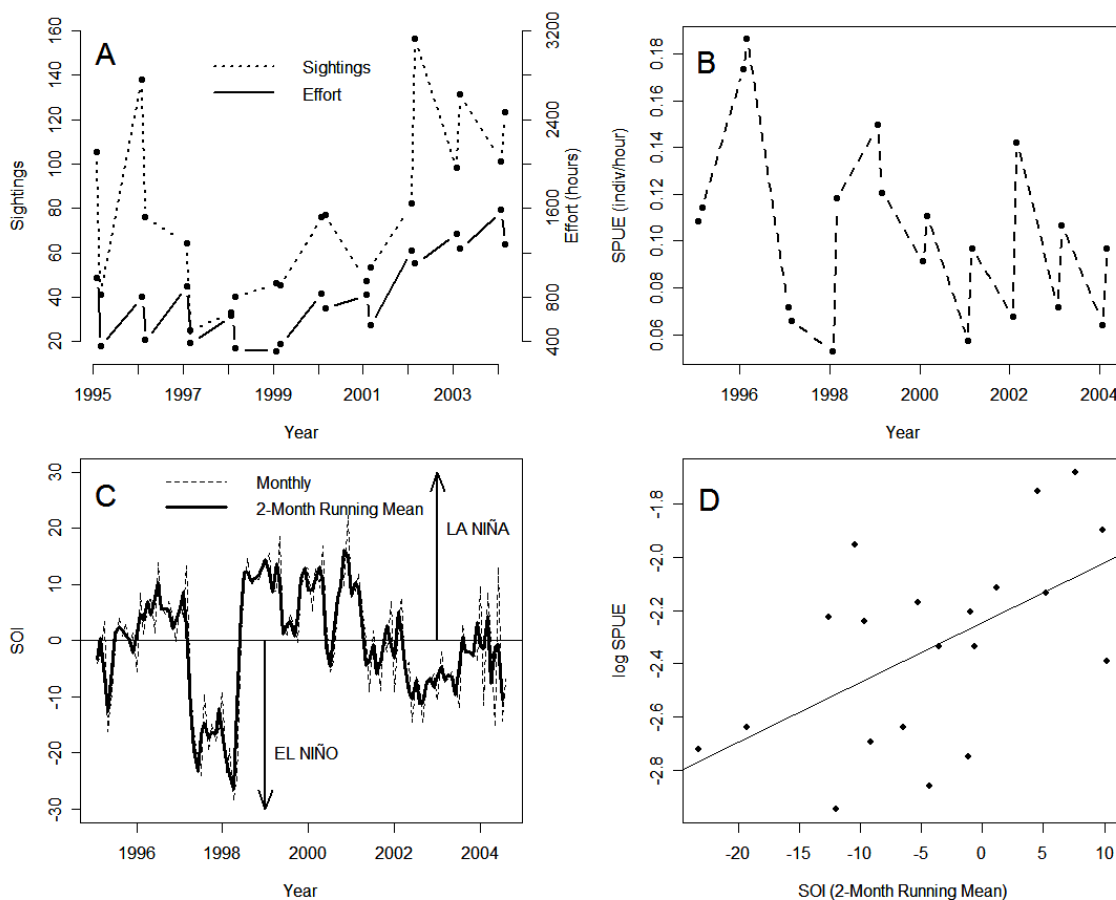


Figure 6.10. A. Total number of sharks seen at Ningaloo Reef in April and May from 1995 – 2004 after removing individuals seen more than once per day, and total vessel search time (hours) as an index of effort; B. Relative abundance corrected for effort (sightings per unit effort = SPUE); C. Monthly and two-monthly running mean of the Southern Oscillation Index (SOI) from 1995 – 2004. High positive values are indicative of La Niña conditions, whereas low negative values signal El Niño events; D. Linear relationship between the two-monthly running mean of SOI and log SPUE for all individuals combined (information-theoretic evidence ratio [ER] = 10.6 times more support than the no-change model; $R^2 = 0.28$).

There was no discernable reduction in SOI-detrended SPUE for small individuals (small males: $ER = 0.4$; $R^2 < 0.01$; small females: $ER = 0.3$; $R^2 < 0.01$; Fig. 6.11 A, C), but both large male ($ER = 6.0$; $R^2 = 0.25$; Fig. 6.11 B) and large female ($ER = 39.8$; $R^2 = 0.38$; Fig. 6.11 D) SPUE declined substantially over the study interval, suggesting that the overall decline is driven mainly by a loss of larger individuals rather than a change in the number of smaller individuals (cf. Figures 6.8 and 6.9).

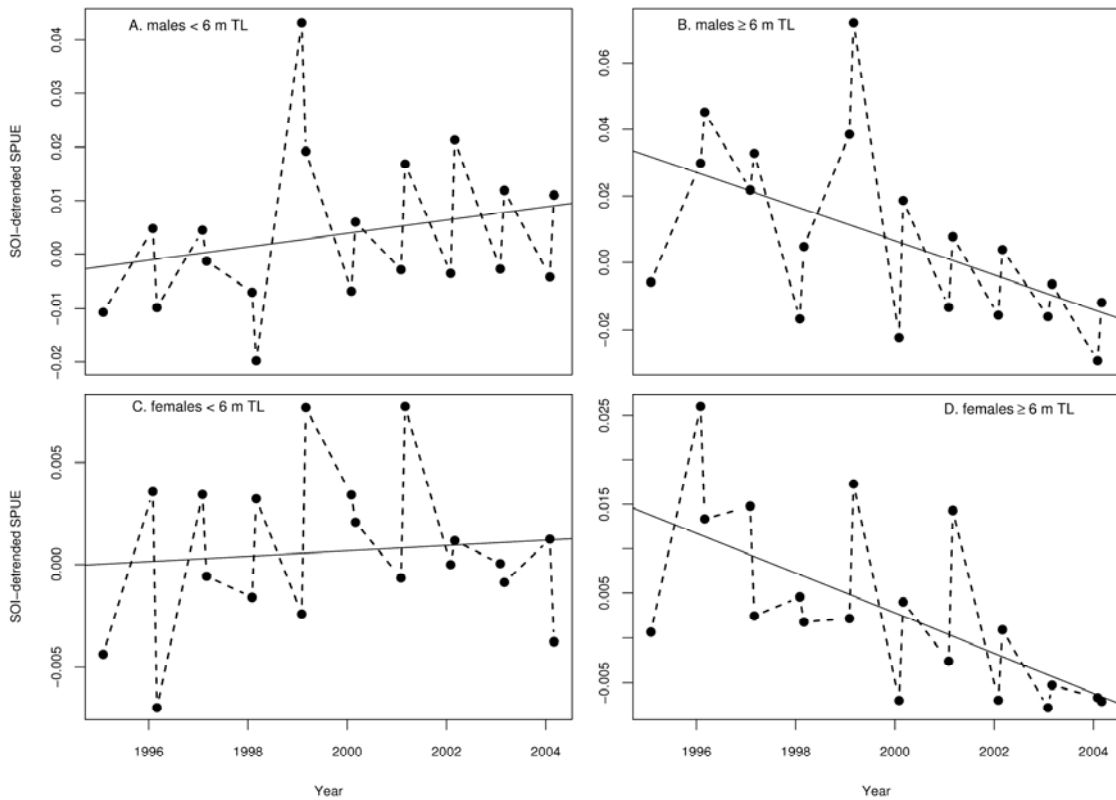


Figure 6.11. Southern Oscillation Index (SOI)-detrended whale shark sightings per unit effort (SPUE) for A. small (< 6 m total length) males (evidence ratio $[ER] = 0.4$; $R^2 < 0.01$), B. large (≥ 6 m TL) males ($ER = 6.0$; $R^2 = 0.25$), C. small females ($ER = 0.3$; $R^2 < 0.01$) and D. large females ($ER = 39.8$; $R^2 = 0.38$).

The relative contribution of intrinsic versus extrinsic control in the various age-sex classes provides insight into the possible mechanisms driving the observed decline. For all individuals combined ($\bar{r} = -0.015$, $\hat{\sigma}^2 = 0.24$), the Gompertz-logistic (GL) versus exponential (EX) model ranking was equivocal (little support for the GL versus EX models: $ER = 1.2$; Table 6.7; and mean r and estimated variance were $\bar{r} = -0.08$, $\hat{\sigma}^2 = 0.27$, respectively); however, there was moderate support for a density-dependent GL relationship ($ER = 2.7$; Table 6.7) for large males (Fig. 6.12), suggesting a possible negative feedback control. Large female SPUE had higher relative support for the EX model ($ER = 2.8$; Table 6.7), reinforcing the hypothesis of a deterministic reduction ($\bar{r} = -0.03$, $\hat{\sigma}^2 = 0.16$) in the large breeding females.

Table 6.7. Comparison of two population dynamical models (Gompertz-logistic and exponential) describing the relationship between rate of change in Southern Oscillation Index (SOI)-detrended whale shark sightings per unit effort (SPUE) for A. All individuals combined, B. large (≥ 6 m total length) males only and C. large females only. Models are ranked according to Akaike's Information Criterion corrected for small sample size (AIC_c). Shown for each model are the number of parameters (k), the maximum log-likelihood (LL), the difference in AIC_c for each model from the top-ranked model (ΔAIC_c), and AIC_c weight ($wAIC_c$).

Model	k	LL	ΔAIC_c	$wAIC_c$
<u>A. All individuals</u>				
Gompertz	3	-3.75	0.00	0.54
exponential	2	-6.31	0.31	0.46
<u>B. Large males only</u>				
Gompertz	3	-2.43	0.00	0.73
exponential	2	-5.81	1.97	0.27
<u>C. Large females only</u>				
exponential	2	-3.88	0.00	0.74
Gompertz	3	-2.51	2.06	0.26

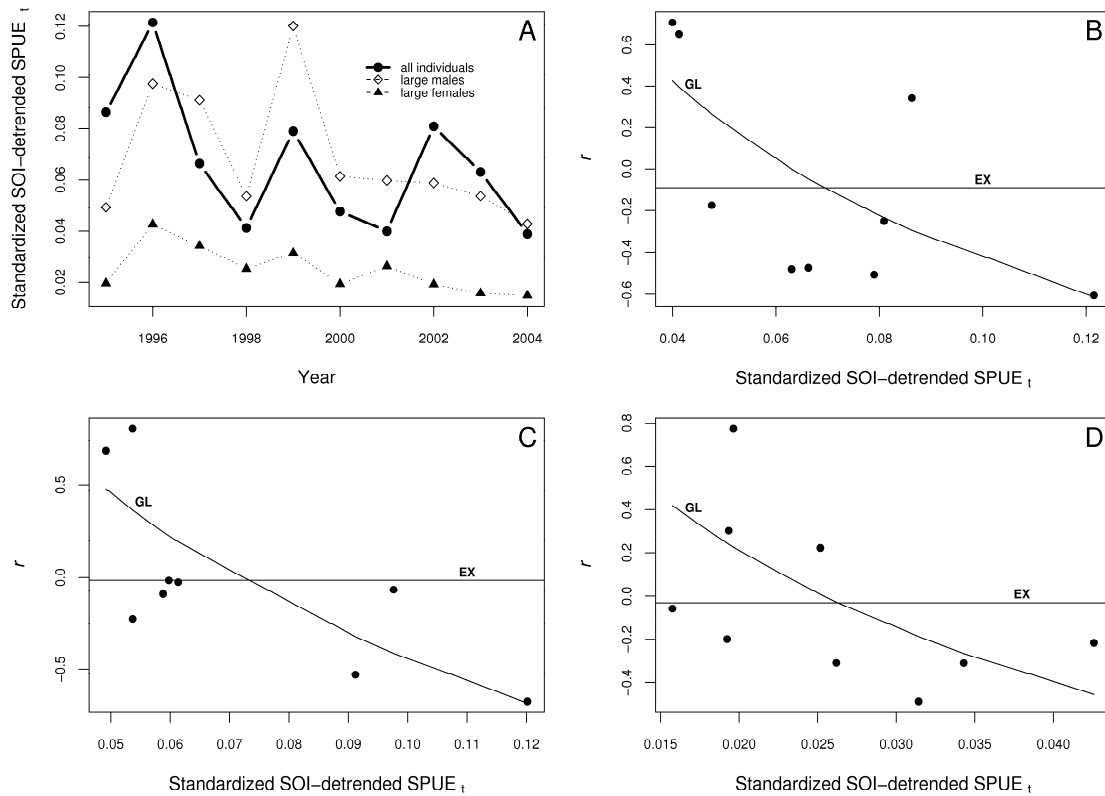


Figure 6.12. A. SOI-detrended SPUE versus year for all individuals combined, large (≥ 6 m total length) males only, and large females only; B. SOI-detrended SPUE rate of change and standardised SPUE according to the Gompertz-logistic (GL) and exponential (EX) dynamical models; C. The same relationship for large males only; D. The same relationship for large females only. Model results are presented in Table 6.6.

6.3.4 Discussion

Our results are derived from one of the largest-ever databases compiled for whale sharks. They provide empirical confirmation at the population level of the vital rate predictions of Bradshaw et al. (2007), who argued that apparent survival probability combined with plausible reproductive rates predict a declining population. While it is possible that the observed trends in mean size and relative abundance could be driven by permanent emigration of larger animals away from Ningaloo rather than an increased mortality rate, photo-identification data suggest that the Ningaloo aggregation is comprised of mainly non-transient individuals (Bradshaw et al. 2007). In other words, individuals residing at Ningaloo for a few weeks or months per year return regularly over time, at least at the decadal scale. This supports the conclusion that current survival rates are insufficient to maintain population stability or increase (Meekan et al. 2006).

The pronounced linear reduction in mean size we report here provides a robust empirical confirmation of previous results (based on a much reduced sample) that larger individuals are being lost from the Ningaloo Reef aggregation (Meekan et al. 2006). The rapid reduction in mean size we observed over a decade and the greater support for a linear model without tapering support the hypothesis of a rapid, deterministic mortality source such as harvesting. The latter evidence for exponential decline does also rely to some extent on the degree of measurement error associated with the SPUE time series. However, high measurement (observation) error tends to overinflate the evidence for density-feedback models (Brook & Bradshaw 2006), so the support of the exponential model suggests any possible bias was low. Another potential source of error is that trending populations can mask some of the evidence for endogenous mechanisms (Strong 1986), especially if the time series does not represent a large variation in densities (Speed et al. 2008). However, none of the SPUE declines measured were precipitous (\bar{r} varied from -0.015 to -0.03 for large males and females, respectively), so we expect little undue bias. Although alternative hypotheses such as an increase in ship-strike (Bradshaw et al. 2007) or entanglement rates, genetic changes and re-equilibration of population density to shifting climate patterns, cannot be rejected given the relatively short time series available, the long generation time of whale sharks (> 14 years; Speed et al. 2008) suggests that genetic and abiotic factors would likely drive much more gradual body size trends than the one we observed over a single decade. Furthermore, recent evidence that the incidence of scarring in whale sharks does not correlate well with relative mortality rates (Davis et al. 1997) suggests that non-targeted sources of anthropogenic mortality are unlikely to account for the large changes observed.

In Australia, whale sharks are protected by government legislation and are not fished or caught incidentally (Eckert et al. 2002, Wilson et al. 2006, Bradshaw et al. 2007, Castro et al. 2007). However, satellite tracking and genetic data have shown that this species has a propensity to migrate large distances (i.e., in the order of 1000s of kilometres; IUCN-SSC Shark Specialist Group 2002), implying that the geographical range of Ningaloo whale sharks is large and potentially encompasses much of Southeast Asia and the Indian Ocean. These lines of evidence – decline in relative abundance driven mainly by the disappearance of large individuals in less than a single whale shark generation, lack of evidence for a re-equilibration in mean body size, and long-distance migratory capacity – all lend support to the view that unsustainable mortality sources are occurring outside of Australian's jurisdiction. The most likely candidate is the whale shark fishery of Southeast Asia (Chen & Phipps 2002). The commercial harvest of whale sharks principally supplies markets in Taiwan, where fins (preferably from large individuals) are used for soup and the flesh is sold for human consumption (Chen et al. 1997a, Pravin 2000). Demand has driven increased fishing effort at aggregation sites throughout the Indian Ocean and Asia (Fowler 2000), although Taiwan recently announced its decision to halt commercial harvest of the species. Although many countries now have prohibited or reduced commercial harvest in recent years, there is little enforcement of regulation and it seems likely that considerable illegal and legal exploitation of whale sharks still continues throughout much of Asia (Ricker 1981, Pauly et al. 1998, Stokes & Law 2000, Tenhumberg et al. 2004).

6.3.5 *Conclusions and conservation remarks*

Our hypothesis that the trend observed is driven largely by over-harvesting throughout the species' range within Southeast Asia and the Indian Ocean is also consistent with declines in abundance and change in the size composition of other exploited animal populations worldwide (Gerrodette 1987). The support for the alternative hypothesis, that the decline results from an ocean-wide regime shift or climate change, is comparatively weak. Indeed, the long time series (relative to generation length) normally required to detect subtle changes in population trends (Bradshaw et al. 2007) leads us to conclude that the mechanisms driving the observed decline in whale sharks are particularly pronounced. The recent cessation of one of the last remaining commercial harvests of whale sharks in Taiwan will most likely increase the average survival probability of whale sharks in the region; however, it is unlikely that the benefits of this shift in policy will be manifested in whale shark abundance patterns for some time given the relatively slow vital rates of this large species (Bradshaw et al. 2007) and unquantified illegal and artisanal harvests elsewhere. We predict, therefore, that the downward trend in relative abundance and mean body size will continue for the foreseeable future.

Given the higher statistical likelihood that exploitation, rather than natural climate cycles, is the principal driver of the decline in abundance and body size of the world's largest fish, the precautionary principle argues for the adoption of more proactive and internationally directed conservation efforts. Although whale sharks are entirely protected in Australian waters, the seasonal outward migration of the Ningaloo population outside of Australian jurisdiction demonstrates that the observed population trend cannot be reversed by protection in only isolated parts of the species' range. Conservation of whale sharks will require international collaboration to reduce overall fishing mortality, potentially at the scale of entire ocean basins, and more tagging studies to identify migration pathways will be a vital part of this effort. Continued monitoring of relative abundance patterns, body size distributions and demographic parameters via capture-mark-recapture studies at all major aggregation sites are also important components of an ocean-wide approach to manage this species.

7. CONCLUSIONS AND RECOMMENDATIONS

The limited knowledge and fragile status of whale sharks necessitates the monitoring of populations with a variety of techniques to ensure that information pertinent to their survival is collected reliably and accurately. Current methods of observation are providing valuable information on the biology and ecology of whale sharks, which is essential for estimating population demographics. These studies then act as the scientific underpinning for informed and effective management strategies.

Of available techniques, mark-recapture analysis based on photo-identification is possibly the simplest and most reliable means of collecting extensive demographic data for population monitoring. We have developed an information-theoretic validation technique that can be used with open-source software (I3S) to reliably match images from large databases. With aid of this software we analysed a 12-year photographic identification library of whale sharks from Ningaloo Reef and modelled survival. Assuming relatively slow vital rates ($\alpha = 25$ and biennial reproduction), size-biased survival probabilities suggest the Ningaloo Reef population of whale sharks is declining. Furthermore, analysis of ecotourism records shows that mean shark length declined linearly by nearly 2.0 m and relative abundance measured from ecotourism sightings (corrected for variation in search effort and environmental stochasticity) has fallen by approximately 40 % over the last decade. This population-level result confirms the predictions of population decline based on projection models parameterised using mark-recapture estimates of survival.

The majority of the decline of whale sharks at Ningaloo is driven by reductions in the number of large individuals in the population, probably due to unsustainable mortality such as over-fishing in other parts of the range. Given this problem, we interrogated the photo-identification data bases focusing on potential threats to this species. We recorded scars on whale sharks in three Indian Ocean aggregations (Australia, Seychelles and Mozambique), and examined whether scarring (mostly attributed to boat strikes and predator attacks) influences apparent survival rates. Scarring was most prevalent in the Seychelles aggregation (67 % of individuals). Predator bites were the most frequent source of scarring (aside from minor nicks and abrasions) and 27 % of individuals had scars consistent with predator attacks. A similar proportion of sharks had blunt trauma, laceration and amputation scars, the majority of which appeared to be caused by ship strike. Predator bites were more common (44 % of individuals) and scars from ship collisions were less common at Ningaloo Reef than at the other two locations. We found no evidence for an effect of scarring on apparent survival for the Ningaloo or Seychelles populations. We conclude that while scarring from natural predators and smaller vessels appears to be unrelated to whale shark survival, the effects of deaths related to ship strike need to be quantified to assist in future management.

Reductions in whale shark populations have occurred despite the total protection of whale sharks in Australian waters. As this species is highly migratory, the rapid change in population composition over a decade (< 1 whale shark generation) supports the hypothesis of

unsustainable mortality in other parts of their range (e.g., overfishing), rather than the alternative of long-term abiotic or biotic shifts in the environment. A central goal of scientific research on this species must therefore be to describe migratory pathways of whale sharks that participate in the aggregation at Ningaloo Reef.

Long distance migrations of sharks from Ningaloo were recorded by Splash tags in 2005, 2006 and 2007. In 2005, one animal was tracked from Ningaloo to the Indian Ocean in the vicinity of the longitude of Sri Lanka. A second animal travelled from Ningaloo to the Indonesian Archipelago and spent some weeks in Indonesian coastal waters. A third animal travelled from Ningaloo along the edge of the continental shelf to Indonesian islands to the east of Timor. These tracks show that the Ningaloo population of sharks is part of a wider Indian Ocean stock that is likely to encompass much of the south eastern Indian Ocean and the waters of South East Asia.

Despite the vital information obtained above, satellite tagging does have drawbacks. Despite design modifications, we have not been able to deploy tags on whale sharks for more than 6 months. This period is too short to reveal the entire extent of migratory pathways; this might require tag retention on animals for 12-24 months. One means to circumvent the problem of tag retention would be to tag animals at remote localities such as Christmas Island or at Roti Island in Indonesia that our work has shown are visited by whale sharks that are part of the Ningaloo aggregation. In this way, return migrations to Ningaloo could be tracked, possibly closing the migratory loop. This should be a key aim of future tagging work.

Ongoing work that uses photo-identification libraries to compare the extent of interchange among major whale shark aggregations in the Indian Ocean is also essential. At present we are in the process of comparing libraries from Ningaloo Reef and Tofo Beach in Mozambique and Mahe Island, Seychelles. These represent the approximate eastern- and western-most extent of the distribution of whale sharks within the Indian Ocean and provide the best possible opportunity for differentiating putative stocks in whale sharks on a regional scale. It is important to note however, that such comparisons show only if sharks travel among these localities; they do not reveal the migratory pathway used by the shark to arrive at these destinations. This is important since sharks may have ventured into waters where they were at risk of fishing while on route.

Genetic information confirms the long-distance dispersal of whale sharks. The absence of population structure across the Indian and Pacific oceans indicates that oceanic expanses and land barriers in Southeast Asia are not impediments to whale sharks. There is however, significant population structure between the Atlantic and Indo-Pacific ocean basins. The development of microsatellite markers by our project will allow the genetics of whale sharks to now be studied in far greater detail.

The global pattern of shared haplotypes in whale sharks, long distance patterns of dispersal and declines in abundance of sharks at Ningaloo despite their complete protection in Australian waters are compelling arguments for development of broad international approaches for management and conservation of whale sharks.

We recommend that:

- Biopsy sampling continue at Ningaloo and commence at other localities in the Indian Ocean to provide a more detailed picture of gene flow among whale shark populations in the region
- DEC continue to collate and supply images from researchers and ecotourism operators at Ningaloo to increase the size of photo-identification libraries
- DEC allows access to ecotourism logbooks (post-2004) for researchers so that historical records of sightings of whale sharks can be updated and reanalysed and the alarming patterns of decline in size and abundance of sharks at Ningaloo can be more closely monitored
- Satellite tagging studies should be extended to nearby localities such as Christmas Island and Indonesia so that migratory pathways can be fully described
- DEWHA encourage the collaboration of research groups in the Indian Ocean region so that photo-libraries can be pooled and the extent of interchange among populations can be assessed.
- DEWHA support studies that seek to assess the extent of harvesting of whale sharks in Southeast Asia, particularly in eastern Indonesia.
- The Australian Government support initiatives by any country to protect and reduce human impacts on whale sharks throughout their range

8. REFERENCES

- Aasen O (1963) Length and growth of the porbeagle (*Lamna nasus*, Bonnaterre) in the North West Atlantic. Reports on Norwegian Fishery and Marine Investigations 13:20-37
- Akaike H (1973) Information theory as an extension of the maximum likelihood principle. In: Proceedings of the Second International Symposium on Information Theory Petrov BN, Csaki F (eds), Budapest, Hungary, p 267-281
- Angliss RP, DeMaster DP (1997) Differentiating serious and non-serious injury of marine mammals taken incidental to commercial fishing operations. Report of the Serious Injury Workshop 1-2 April 1997, Silver Spring, Maryland, p 1-53
- Arnason U, Gullberg A, Janke A (2001) Molecular phylogenetics of gnathostomous (jawed) fishes: old bones, new cartilage. *Zoologica Scripta* 30:249-255
- Arnault S (1987) Tropical Atlantic geostrophic currents and ship drifts. *J Geophys Res C* 92:5076-5088
- Arzoumanian Z, Holmberg J, Norman B (2005) An astronomical pattern-matching algorithm for computer-aided identification of whale sharks *Rhincodon typus*. *Journal of Applied Ecology* 42:999-1011
- Auckland JN, Debinski DM, Clark WR (2004) Survival, movement, and resource use of the butterfly *Parnassius clodius*. *Ecological Entomology* 29:139-149
- Baker CS, Slade RW, Bannister JL, Abernethy RB, Weinrich MT, Lien J, Urban J, Corkeron P, Calmabokidis J, Vasquez O, Palumbi SR (1994) Hierarchical Structure of Mitochondrial-DNA Gene Flow among Humpback Whales *Megaptera-Novaeangliae*, Worldwide. *Molecular Ecology* 3:313-327
- Barber PH, Palumbi SR, Erdmann MV, Moosa MK (2000) Biogeography - A marine Wallace's line? *Nature* 406:692-693
- Barber PH, Palumbi SR, Erdmann MV, Moosa MK (2002) Sharp genetic breaks among populations of *Haptosquilla pulchella* (Stomatopoda) indicate limits to larval transport: patterns, causes, and consequences. *Molecular Ecology* 11:659-674
- Bateson PPG (1977) Testing an observer's ability to identify individual animals. *Animal Behaviour* 25:247-248
- Baum JK, Kehler D, Myers RA (2005) Robust estimates of decline for pelagic shark populations in the northwest Atlantic and Gulf of Mexico. *Fisheries* 30:27-30
- Baum JK, Myers RA, Kehler DG, Worm B, Harley SJ, Doherty PA (2003) Collapse and conservation of shark populations in the Northwest Atlantic. *Science* 299:389-392
- Beck CA, McMillan JI, Bowen WD (2002) An algorithm to improve geolocation positions using sea surface temperature and diving depth. *Marine Mammal Science* 18:940-951
- Beckley LE, Cliff G, Smale MJ, Compagno LJV (1997) Recent strandings and sightings of whale sharks in South Africa. *Environ Biol Fishes* 50:343-348
- Beissinger SR, Westphal MI (1998) On the use of demographic models of population viability in endangered species management. *Journal of Wildlife Management* 62:821-841
- Belovsky GE, Botkin DB, Cowl TA, Cummins KW, Franklin JF, Hunter MLJ, Joern A, Lindenmayer DB, MacMahon JA, Margules CR, Scott JM (2004) Ten suggestions to strengthen the science of ecology. *BioScience* 54:345-351

- Benton TG, Grant A (1996) How to keep fit in the real world: elasticity analyses and selection pressures on life-histories in a variable environment. *American Naturalist* 147:115-139
- Bentzen P, Wright JM, Bryden LT, Sargent M, Zwaneburg KCT (1998) Tandem repeat polymorphism and heteroplasmy in the mitochondrial control region of redfishes (Sebastes : Scorpaenidae). *Journal of Heredity* 89:1-7
- Berube M, Aguilar A, Dendanto D, Larsen F, Di Sciara GN, Sears R, Sigurjonsson J, Urban-R J, Palsboll PJ (1998) Population genetic structure of North Atlantic, Mediterranean Sea and Sea of Cortez fin whales, *Balaenoptera physalus* (Linnaeus 1758): analysis of mitochondrial and nuclear loci. *Molecular Ecology* 7:585-599
- Bilgmann K, Griffiths OJ, Allen SJ, Moller LM (2007) A biopsy pole system for bow-riding dolphins: Sampling success, behavioral responses, and test for sampling bias. *Marine Mammal Science* 23:218-225
- Block BA, Dewar H, Blackwell SB, Williams TD, Prince ED, Farwell CJ, Boustany A, Teo SLH, Seitz A, Walli A (2001) Migratory movements, depth preferences, and thermal biology of Atlantic Bluefin Tuna. *Science* 293:1310
- Booth DJ (2004) Synergistic effects of conspecifics and food on growth and energy allocation of a damselfish. *Ecology* 85:2881-2887
- Bowditch N (1802) *The New American Practical Navigator*. E.M. Blunt for Brown & Stansbury, New York
- Bowen BW, Bass AL, Rocha LA, Grant WS, Robertson DR (2001) Phylogeography of the trumpetfishes (Aulostomus): Ring species complex on a global scale. *Evolution* 55:1029-1039
- Bowen BW, Bass AL, Soares L, Toonen RJ (2005) Conservation implications of complex population structure: lessons from the loggerhead turtle (*Caretta caretta*). *Molecular Ecology* 14:2389-2402
- Bowen BW, Clark AM, Abreu-Grobois FA, Chaves A, Reichart HA, Ferl RJ (1997) Global phylogeography of the ridley sea turtles (*Lepidochelys* spp.) as inferred from mitochondrial DNA sequences. *Genetica* 101:179-189
- Bowen BW, Muss A, Rocha LA, Grant WS (2006) Shallow mtDNA coalescence in atlantic pygmy angelfishes (Genus *Centropyge*) indicates a recent invasion from the Indian Ocean. *Journal of Heredity* 97:1-12
- Boyce MS (1992) Population viability analysis. *Annual Review of Ecology and Systematics* 23:481-506
- Bradshaw CJA, Barker RJ, Davis LS (2000) Modeling tag loss in New Zealand fur seal pups. *Journal of Agricultural, Biological, and Environmental Statistics* 5:475-485
- Bradshaw CJA, Barker RJ, Harcourt RG, Davis LS (2003) Estimating survival and capture probability of fur seal pups using multistate mark-recapture models. *Journal of Mammalogy* 84:65-80
- Bradshaw CJA, Evans K, Hindell M (2005) Mass cetacean strandings - a plea for empiricism. *Conservation Biology* 20:584-586
- Bradshaw CJA, Fitzpatrick BW, Steinberg CC, Brook BW, Meekan MG (In press) The world's largest fish is getting smaller. *Biological Conservation*
- Bradshaw CJA, Mollet HF, Meekan MG (2007) Inferring population trends for the world's largest fish from mark-recapture estimates of survival. *J Anim Ecol* 76:480-489

- Brook BW, Bradshaw CJA (2006) Strength of evidence for density dependence in abundance time series of 1198 species. *Ecology* 87:1445-1451
- Brook BW, Burgman MA, Akçakaya HR, O'Grady JJ, Frankham R (2002) Critiques of PVA ask the wrong questions: throwing the heuristic baby out with the numerical bath water. *Conservation Biology* 16:262-263
- Brook BW, Traill LW, Bradshaw CJA (2006) Minimum viable population size and global extinction risk are unrelated. *Ecology Letters* 9:375-382
- Brown JR, Beckenbach K, Beckenbach AT, Smith MJ (1996) Length variation, heteroplasmy and sequence divergence in the mitochondrial DNA of four species of sturgeon (Acipenser). *Genetics* 142:525-535
- Brown MR, Corkeron PJ, Hale PT, Schultz KW, Bryden MM (1995) Evidence for a Sex-segregated migration in the Humpback Whale (Megaptera-Novaeangliae). *Proceedings of the Royal Society of London Series B-Biological Sciences* 259:229-234
- Burgess GH, Beerkircher LR, Cailliet GM, Carlson JK, Cortes E, Goldman KJ, Grubbs RD, Musick JA, Musyl MK, Simpfendorfer CA (2005a) Is the collapse of shark populations in the Northwest Atlantic Ocean and Gulf of Mexico real? *Fisheries* 30:19-26
- Burgess GH, Beerkircher LR, Cailliet GM, Carlson JK, Cortes E, Goldman KJ, Grubbs RD, Musick JA, Musyl MK, Simpfendorfer CA (2005b) Reply to "Robust estimates of decline for pelagic shark populations in the Northwest Atlantic and Gulf of Mexico". *Fisheries* 30:30-31
- Burks CM, Driggers WB, Mullin KD (2006) Abundance and distribution of whale sharks (*Rhincodon typus*) in the northern Gulf of Mexico. *Fishery Bulletin* 104:579-584
- Burnham KP, Anderson DR (2002) *Model Selection and Multimodal Inference: A Practical Information-Theoretic Approach*. Springer-Verlag, New York, USA
- Burnham KP, Anderson DR (2004) Understanding AIC and BIC in model selection. *Sociol Meth Res* 33:261-304
- Caddy JF, Mahon R (1995) *Reference Points for Fisheries Management*. Report No. 347, FAO Fisheries, Rome, Italy
- Cailliet GM, Mollet HF, Pittinger GG, Bedford D, Ntanson LJ (1992) Growth and demography of the Pacific angel shark (*Squatina californica*), based upon tag returns off California. *Australian Journal of Marine and Freshwater Research* 43:1313-1330
- Cao Y, Waddell PJ, Okada N, Hasegawa M (1998) The complete mitochondrial DNA sequence of the shark *Mustelus manazo*: Evaluating rooting contradictions to living bony vertebrates. *Molecular Biology and Evolution* 15:1637-1646
- Caputi N, Fletcher WJ, Pearce A, Chubb CF (1996) Effect of the Leeuwin Current on the recruitment of fish and invertebrates along the Western Australian coast. *Mar Freshw Res* 47:147-155
- Carlsson J, McDowell JR, Carlsson JEL, Graves JE (2007) Genetic identity of YOY bluefin tuna from the eastern and Western Atlantic spawning areas. *Journal of Heredity* 98:23-28
- Castro ALF, Rosa RS (2005) Use of natural marks on population estimates of the nurse shark, *Ginglymostoma cirratum*, at Atol das Rocas Biological Reserve, Brazil. *Environ Biol Fishes* 72:213-221
- Castro ALF, Stewart BS, Wilson SG, Hueter RE, Meekan MG, Motta PJ, Bowen BW, Karl SA (2007) Population genetic structure of Earth's largest fish, the whale shark (*Rhincodon typus*). *Molecular Ecology* 16:5183-5192

- Caswell H, Fujiwara M, Brault S (1999) Declining survival probability threatens the North Atlantic right whale. *Proceedings of the National Academy of Sciences of the United States of America* 96:3308-3313
- Caughley G (1994) Directions in conservation biology. *J Anim Ecol* 63:215-244
- Cavanagh RD, Kyne PM, Folwer SL, Musick JA, Bennett MB (2003) The Conservation Status of Australasian Chondrichthyans: Report of the IUCN Shark Specialist Group Australia and Oceania Regional Red List Workshop, IUCN Shark Specialist Group, Queensland, Australia
- Chamaillé-Jammes S, Fritz H, Valeix M, Murindagomo F, Clobert J (2008) Resource variability, aggregation and direct density dependence in an open context: the local regulation of an African elephant population. *J Anim Ecol* 77:135-144
- Chang WB, Leu MY, Fang LS (1997) Embryos of the whale shark, *Rhincodon typus*: early growth and size distribution. *Copeia* 1997:444-446
- Chang YP, Chang CC, Wang LW, Chen MT, Wang CH, Yu EF (1999) Planktonic foraminiferal sea surface temperature variations in the southeast Atlantic Ocean: A high-resolution record MD962085 of the past 400,000 years from the IMAGES II-NAUSICAA cruise. *Terrestrial Atmospheric and Oceanic Sciences* 10:185-200
- Chen C-T, Liu K-M, Joung S-J (1997a) Preliminary report on Taiwan's whale shark fishery. *TRAFFIC Bulletin* 17:53-57
- Chen CT, Liu KM, Chang YC (1997b) Reproductive biology of the bigeye thresher shark, *Alopias superciliosus* (Lowe, 1839) (Chondrichthyes: Alopiidae), in the northwestern Pacific. *Ichthyological Research* 44:227-235
- Chen VY, Phipps MJ (2002) Management and Trade of Whale Sharks in Taiwan. A TRAFFIC East Asia Report:1-35
- Chenoweth SF, Hughes JM (2003) Oceanic interchange and nonequilibrium population structure in the estuarine dependent Indo-Pacific tasselfish, *Polynemus sheridani*. *Molecular Ecology* 12:2387-2397
- CITES (2002) CITES Appendix II nomination of the Whale Shark, *Rhincodon typus*. Proposal 12.35. CITES Resolutions of the Conference of the Parties in effect after the 12th Meeting, Santiago, Chile
- Clark E, Nelson DR (1997) Young whale sharks, *Rhincodon typus*, feeding on a copepod bloom near La Paz, Mexico. *Environ Biol Fishes* 50:63-73
- CMS (2005) Bullet Summary of the Dialogue on Whale Shark Conservation. 8th Meeting of the Conference of the Parties, Bangkok
- Coates AG, Obando JA (1996) The geologic evolution of the Central American isthmus. In: Evolution and environment in tropical America. Jackson JBC, Budd AF, Coates AG (eds). University of Chicago Press, Chicago, p 21-56
- Cochran ME, Ellner S (1992) Simple methods for calculating age-based life history parameters for stage-structured populations. *Ecol Monog* 62:345-364
- Colman JG (1997) A review of the biology and ecology of the whale shark. *J Fish Biol* 51:1219-1234
- Compagno LJV (1984) Sharks of the world, Part 1: Hexanchiformes to Lamniformes, Rome
- Compagno LJV (2001) Sharks of the world: an annotated and illustrated catalogue of shark species known to date. Volume 2 Bulhead, mackerel and carpet sharks

- (Heterodontiformes, Lamniformes and Orectolobiformes), Food and Agriculture Organization of the United Nations, Rome, Italy
- Conover DO, Munch SB (2002) Sustaining fisheries yields over evolutionary time scales. *Science* 297:94-96
- Corcoran MJ, Gruber SH (1999) The Use of Photoidentification to Study Social Organization of the Spotted Eagle Ray, *Aetobatus narinari* (Euphrasen 1790), at Bimini, Bahamas: A Preliminary Report. *Bahamas Journal of Science* 7:21-27
- Cormack RM (1964) Models for capture-recapture. *Biometrika* 51:429-438
- Cortés E (2002) Incorporating uncertainty into demographic modeling: application to shark populations and their conservation. *Conservation Biology* 16:1048-1062
- Craig AS, Herman LM (1997) Sex differences in site fidelity and migration of humpback whales (*Megaptera novaeangliae*) to the Hawaiian Islands. *Canadian Journal of Zoology-Revue Canadienne De Zoologie* 75:1923-1933
- Craig MT, Eble JA, Bowen BW, Robertson DR (2007) High genetic connectivity across the Indian and Pacific Oceans in the reef fish *Myripristis berndti* (Holocentridae). *Marine Ecology-Progress Series* 334:245-254
- Dalebout ML, Robertson KM, Frantzis A, Engelhaupt D, Mignucci-Giannoni AA, Rosario-Delestre RJ, Baker CS (2005) Worldwide structure of mtDNA diversity among Cuvier's beaked whales (*Ziphius cavirostris*): implications for threatened populations. *Molecular Ecology* 14:3353-3371
- Davis D (1998) Whale shark tourism in Ningaloo Marine Park, Australia. *Anthrozoos* 11:5-11
- Davis D, Banks S, Birtles A, Valentine P, Cuthill M (1997) Whale sharks in Ningaloo Marine Park: managing tourism in an Australian marine protected area. *Tour Manage* 18:259-271
- de Little SC, Bradshaw CJA, McMahon CR, Hindell MA (2007) Complex interplay between intrinsic and extrinsic drivers of long-term survival trends in southern elephant seals. *BMC Ecology* 7:3
- Delarbre C, Spruyt N, Delmarre C, Gallut C, Barriel V, Janvier P, Laudet V, Gachelin G (1998) The complete nucleotide sequence of the mitochondrial DNA of the dogfish, *Scyliorhinus canicula*. *Genetics* 150:331-344
- Delong RL, Stewart BS, Hill RD (1992) Documenting migrations of northern elephant seals using day length. *Marine Mammal Science* 8:155-159
- Domeier ML, Kiefer D, Nasby-Lucas N, Wagschal A, O'Brien F (2005) Tracking Pacific bluefin tuna (*Thunnus thynnus orientalis*) in the northeastern Pacific with an automated algorithm that estimates latitude by matching sea-surface-temperature data from satellites with temperature data from tags on fish. *Fish Bull* 103:292-306
- Domeier ML, Nasby-Lucas N (2006) Annual re-sightings of photographically identified White Sharks (*Carcharodon carcharias*) at an eastern Pacific aggregation site (Guadalupe Island, Mexico). *Mar Biol DOI* 10/1007/s00227-006-0380-7
- Drake JM (2005) Density-dependent demographic variation determines extinction rate of experimental populations. *PLoS Biology* 3:e222
- Duffy CAJ (2002) Distribution, seasonality, lengths, and feeding behaviour of whale sharks (*Rhincodon typus*) observed in New Zealand waters. *N Z J Mar Freshw Res* 36:565-570
- Dulvy NK, Sadovy Y, Reynolds JD (2003) Extinction vulnerability in marine populations. *Fish Fish* 4:25-64

- Duncan KM, Martin AP, Bowen BW, De Couet HG (2006) Global phylogeography of the scalloped hammerhead shark (*Sphyrna lewini*). *Molecular Ecology* 15:2239-2251
- Eckert SA (2002) Distribution of juvenile leatherback sea turtle *Dermochelys coriacea* sightings. *Marine Ecology-Progress Series* 230:289-293
- Eckert SA, Dolar LL, Kooyman GL, Perrin W, Rahman RA (2002) Movements of whale sharks (*Rhincodon typus*) in South-east Asian waters as determined by satellite telemetry. *J Zool* 257:111-115
- Eckert SA, Stewart BS (2001) Telemetry and satellite tracking of whale sharks, *Rhincodon typus*, in the Sea of Cortez, Mexico, and the north Pacific Ocean. *Environ Biol Fishes* 60:299-308
- Ellner SP, Fieberg J, Ludwig D, Wilcox C (2002) Precision of Population Viability Analysis. *Conservation Biology* 16:258-261
- Evans PGH (2003) EUROPHLUKES Database Specifications Handbook. <http://www.europhlukes.net>.
- Excoffier L, Laval G, Schneider S (2005) Arlequin ver. 3.0: An integrated software package for population genetics data analysis. *Evolutionary Bioinformatics Online* 1:47-50
- Excoffier L, Smouse PE, Quattro JM (1992) Analysis of molecular variance inferred from etric distances among DNA haplotypes - Application to human mitochondrial-DNA restriction data. *Genetics* 131:479-491
- Fagan WF, Holmes EE (2006) Quantifying the extinction vortex. *Ecology Letters* 9:51-60
- Fancy SG, Pank LF, Douglas DC, Curby CH, Garner GW, Amstrup SC, Regelin WL (1988) Satellite telemetry: a new tool for wildlife research and management. *US Fish and Wildlife Service Research Publications* 172:1-54
- Felsenstein J (1985) Confidence limits on phylogenies: An approach using the bootstrap. *Evolution* 39:783-791
- Fiedler PC, Bernard HJ (1987) Tuna aggregation and feeding near fronts observed in satellite imagery. *Continental Shelf Research* 7:871-881
- Field IC, Bradshaw CJA, Burton HR, Sumner MD, Hindell MA (2005) Resource partitioning through oceanic segregation of foraging juvenile southern elephant seals. *Oecologia* 142:127-135
- Fitzpatrick B, Meekan M, Richards A (2006) Shark attacks on a whale shark (*Rhincodon typus*) at Ningaloo Reef, western Australia. *Bull Mar Sci* 78:397-402
- Flores JA, Gersonde R, Sierro FJ (1999) Pleistocene fluctuations in the Agulhas Current Retroflection based on the calcareous plankton record. *Marine Micropaleontology* 37:1-22
- Food and Agriculture Organisation of the United Nations (2006) *The State of the World Fisheries and Aquaculture 2006*, FAO, Rome
- Fowler SL (2000) Whale shark *Rhincodon typus*. Policy and research scoping study, Nature Conservation Bureau, Newbury, United Kingdom
- Friday N, Smith TD, Stevick PT, Allen J (2000) Measurement of Photographic Quality and Individual Distinctiveness for the Photographic Identification of Humpback Whales, *Megaptera novaengliae*. *Marine Mammal Science* 16:355-374
- Frisk MG, Miller TJ, Fogarty MJ (2001) Estimation and analysis of biological parameters in elasmobranch fishes: a comparative life history study. *Can J Fish Aquat Sci* 58:969-981

- Frisk MG, Miller TJ, Fogarty MJ (2002) The population dynamics of little skate *Leucoraja erinacea*, winter skate *Leucoraja ocellata*, and barndoor skate *Dipturus laevis*: predicting exploitation limits using matrix analyses. *Ices Journal of Marine Science* 59:576-586
- Fu YX (1997) Statistical tests of neutrality of mutations against population growth, hitchhiking and background selection. *Genetics* 147:915-925
- Fujii T, Nishida M (1997) High sequence variability in the mitochondrial DNA control region of the Japanese flounder *Paralichthys olivaceus*. *Fisheries Science* 63:906-910
- Fujiwara M, Caswell H (2001) Demography of the endangered North Atlantic right whale. *Nature* 414:537-541
- Gallucci VF, Taylor IG, Erzini K (2006) Conservation and management of exploited shark populations based on reproductive value. *Can J Fish Aquat Sci* 63:931-942
- Garcia-Perea P (2000) Survival of injured Iberian lynx (*Lynx pardinus*) and non-natural mortality in central-southern Spain. *Biological Conservation* 93:265-269
- Gauthier-Clerc M, Gendner JP, Ribic CA, Fraser WR, Woehler EJ, Descamps S, Gilly C, Le Bohec C, Le Maho Y (2004) Long-term effects of flipper bands on penguins. *Proceedings of the Royal Society of London Series B-Biological Sciences* 271:S423-S426
- Gerrodette T (1987) A power analysis for detecting trends. *Ecology* 68:1364-1372
- Gibbons MJ, Thibault-Botha D (2002) The match between ocean circulation and zoogeography of epipelagic siphonophores around southern Africa. *Journal of the Marine Biological Association of the United Kingdom* 82:801-810
- Graham RT (2004) Global whale shark tourism: a "golden goose" of sustainable and lucrative income. *Shark News Newsletter of the IUCN Shark Specialist Group* 16:8-9
- Graham RT, Roberts CM (2007) Assessing the size, growth rate and structure of a seasonal population of whale sharks (*Rhincodon typus* Smith 1828) using conventional tagging and photo identification. *Fisheries Research* 84:71-80
- Graham RT, Roberts CM, Smart JCR (2006) Diving behaviour of whale sharks in relation to a predictable food pulse. *J R Soc Interface* 3:109-116
- Grant A, Benton TG (2000) Elasticity analysis for density-dependent populations in stochastic environments. *Ecology* 81:680-693
- Graves JE, McDowell JR (2003) Stock structure of the world's istiophorid billfishes: a genetic perspective. *Mar Freshw Res* 54:287-298
- Greenstreet SPR, Rogers SI (2006) Indicators of the health of the North Sea fish community: identifying reference levels for an ecosystem approach to management. *ICES Journal of Marine Science* 63:573-593
- Gruber SH, de Marignac JR, Hoenig JM (2001) Survival of juvenile lemon sharks (*Negaprion brevirostris*) at Bimini, Bahamas, estimated by mark-depletion experiments. *Transactions of the American Fisheries Society* 130:376-384
- Gudger EW (1940) Whale sharks rammed by ocean vessels. How these sluggish leviathans aid in their own destruction. *New England Naturalist* 7:1-10
- Gunn J, Polacheck T, Davis T, Sherlock M, Betlehem A (1994) The development and use of archival tags for studying the migration, behaviour and physiology of southern bluefin tuna, with an assessment of the potential for transfer of the technology to groundfish research. *ICES Proc Mini Symp on Fish Migration* 21:1-23

- Gunn JS, Patterson TA, Pepperell JG (2003) Short-term movement and behaviour of black marlin *Makaira indica* in the Coral Sea as determined through a pop-up satellite archival tagging experiment. *Marine & Freshwater Research* 54:515-525
- Gunn JS, Stevens JD, Davis TLO, Norman BM (1999) Observations on the short-term movements and behaviour of whale sharks (*Rhincodon typus*) at Ningaloo Reef, Western Australia. *Mar Biol* 135:553-559
- Hammond PS, Mizroch SA, Donovan GP (1990) Individual recognition of Cetaceans: Use of photo-identification and other techniques to Estimate Population Parameters, International Whaling Commission, Cambridge, Massachusetts
- Harpending HC (1994) Signature of ancient population-growth in a low-resolution mitochondrial-DNA mismatch distribution. *Human Biology* 66:591-600
- Hartog JD, Reijns R (2004) I³S Manual-Interactive Raggie Identification System, Version 0.2.
- Hasegawa M, Kishino H, Yano T-A (1985) Dating of the human-ape splitting by a molecular clock of mitochondrial DNA. *Journal of Molecular Evolution* 22:160-174
- Hazin FHV, Fischer AF, Broadhurst MK, Veras D, Oliveira PG, Burgess GH (2006) Notes on the reproduction of *Squalus megalops* off northeastern Brazil. *Fisheries Research* 79:251-257
- Heist EJ (1999) A review of population genetics in sharks. *American Fishery Society Symposium* 23:161-168
- Heist EJ (2004) Genetics of sharks, skates and rays. In: *Biology of sharks and their relatives*. Carrier JC, Musick JA, Heithaus MR (eds). CRC Press, Boca Raton, FL, USA, p 471-485
- Heithaus MR (2001a) The biology of tiger sharks, *Galeocerdo cuvier*, in Shark Bay, Western Australia: sex ratio, size distribution, diet, and seasonal changes in catch rates. *Environ Biol Fishes* 61:25-36
- Heithaus MR (2001b) Shark attacks on bottlenose dolphins (*Tursiops aduncus*) in Shark Bay, Western Australia: attack rate, bite scar frequencies and attack seasonality. *Marine Mammal Science* 17:526-539
- Heppell SS, Caswell H, Crowder LB (2000) Life histories and elasticity patterns: perturbation analysis for species with minimal demographic data. *Ecology* 81:654-665
- Heupel MR, Simpfendorfer CA (2002) Estimation of mortality of juvenile blacktip sharks, *Carcharhinus limbatus*, within a nursery area using telemetry data. *Can J Fish Aquat Sci* 59:624-632
- Heyman WD, Graham RT, Kjerfve B, Johannes RE (2001) Whale sharks *Rhincodon typus* aggregate to feed on fish spawn in Belize. *Marine Ecology-Progress Series* 215:275-282
- Hiby L, Lovell P (2001) An automated system for matching the callosity patterns in aerial photographs of southern right whales. *Journal of Cetacean Research and Management*
- Hillman G, Wursig B, Gailey G, Kehtarnavaz N, Drobyshevsky A, Araabi BN, Tagare HD, Weller DW (2003) Computer-assisted photo-identification of individual marine vertebrates: a multi-species system. *Journal of Aquatic Mammals* 29:117-123
- Hiruki LM, Gilmartin WG, Becker BL, Stirling I (1993) Wounding in Hawaiian monk seals (*Monachus schauinslandi*). *Canadian Journal of Zoology* 71:458-468
- Hoarau G, Holla S, Lescasse R, Stam WT, Olsen JL (2002) Heteroplasmy and evidence for recombination in the mitochondrial control region of the flatfish *Platichthys flesus*. *Molecular Biology and Evolution* 19:2261-2264

- Holloway PE (2001) A regional model of the semi-diurnal internal tide on the Australian North West Shelf. *J Geophys Res* 106:625
- Holloway PE, Nye HC (1985) Leeuwin Current and wind distributions on the Australian North West Shelf between January 1982 and July 1983. *Australian Journal of Marine and Freshwater Research* 36:123-137
- Hsu HH, Joung SJ, Liao YY, Liu KM (2007) Satellite tracking of juvenile whale sharks, *Rhincodon typus*, in the Northwestern Pacific. *Fisheries Research* 84:25-31
- Hughes GR, Luschi P, Mencacci R, Papi F (1998) The 7000-km oceanic journey of a leatherback turtle tracked by satellite. *Journal of Experimental Marine Biology and Ecology* 229:209-217
- Hunter JR (1986) *The Dynamics of Tuna Movements: An Evaluation of Past and Future Research*. Food and Agriculture Organization of the United Nations
- Inagake D, Yamada H, Segawa K, Okazaki M, Nitta A, Itoh T (2001) Migration of young bluefin tuna, *Thunnus orientalis* Temminck et Schlegel, through archival tagging experiments and its relation with oceanographic condition in the western North Pacific. *Bull Nat Res Inst Far Seas Fish* 38:53-81
- IUCN-SSC Shark Specialist Group (2002) *The Role of CITES in the Conservation and Management of Sharks*, IUCN, Gland, Switzerland
- IUCN (2005) *IUCN Red List of Threatened Species*. IUCN, Gland, Switzerland
- Iwasaki Y (1970) On the distribution and environment of the whale shark, *Rhincodon typus* in skipjack fishing groups in the western Pacific Ocean. *Journal of the College of Marine Science and Technology Tokai University* 4:37-51
- James MC, Ottensmeyer CA, Myers RA (2005) Identification of high-use habitat and threats to leatherback sea turtles in northern waters: new directions for conservation. *Ecology Letters* 8:195-201
- Jarman SN, Wilson SG (2004) DNA-based species identification of krill consumed by whale sharks. *J Fish Biol* 65:586-591
- Jellyman D, Tsukamoto K (2002) First use of archival transmitters to track migrating freshwater eels *Anguilla dieffenbachii* at sea. *Marine ecology Progress series(Halstenbek)* 233:207-215
- Jennings S, Kaiser J (1998) The effects of fishing on marine ecosystems. *Advances in Marine Biology* 34:201-352
- Jennings S, Reynolds JD, Mills SC (1998) Life history correlates of responses to fisheries exploitation. *Proceedings of the Royal Society B* 265:333-339
- Jolly GM (1965) Explicit estimates from mark-recapture data with both death and immigration-stochastic models. *Biometrika* 52:225-247
- Joung SJ, Chen CT (1995) Reproduction in the sandbar shark, *Carcharhinus plumbeus*, in the waters off northeastern Taiwan. *Copeia* 1995:659-665
- Joung SJ, Chen CT, Clark E, Uchida S, Huang WYP (1996) The whale shark, *Rhincodon typus*, is a livebearer: 300 embryos found in one 'megamamma' supreme. *Environ Biol Fishes* 46:219-223
- Joung SJ, Liao YY, Liu KM, Chen CT, Leu LC (2005) Age, growth, and reproduction of the spinner shark, *Carcharhinus brevipinna*, in the northeastern waters of Taiwan. *Zoological Studies* 44:102-110

- Kandpal RP, Kandpal G, Weissman SM (1994) Construction of libraries enriched for sequence repeats and jumping clones, and hybridization selection for region-specific markers. *Proceedings of the National Academy of Sciences of the United States of America* 91:88-92
- Karant K, Nichols JD (1998) Estimation of tiger densities in India using photographic captures and recaptures. *Ecology* 79:2852-2862
- Karlsson O, Hiby L, Lundberg T, Jussi M, Jussi I, Helander B (2005) Photo-identification, site fidelity, and movement of female gray seals (*Halichoerus grypus*) between haul-outs in the Baltic Sea. *Ambio* 34:628-634
- Keeney DB, Heist EJ (2006) Worldwide phylogeography of the blacktip shark (*Carcharhinus limbatus*) inferred from mitochondrial DNA reveals isolation of western Atlantic populations coupled with recent Pacific dispersal. *Molecular Ecology* 15:3669-3679
- Keeney DB, Heupel MR, Hueter RE, Heist EJ (2005) Microsatellite and mitochondrial DNA analyses of the genetic structure of blacktip shark (*Carcharhinus limbatus*) nurseries in the northwestern Atlantic, Gulf of Mexico, and Caribbean Sea. *Molecular Ecology* 14:1911-1923
- Kelly MJ (2001) Computer-aided photograph matching in studies using individual identification: An example from Serengeti cheetahs. *Journal of Mammalogy* 82:440-449
- Kitamura T, Takemura A, Watabe S, Taniuchi T, Shimizu M (1996) Mitochondrial DNA analysis for the cytochrome b gene and D-loop region from the bull shark *Carcharhinus leucas*. *Fisheries Science* 62:21-27
- Klimley AP (1987) The determinants of sexual segregation in the scalloped hammerhead shark, *Sphyrna lewini*. *Environ Biol Fishes* 18:27-40
- Klimley AP (1993) Highly directional swimming by scalloped hammerhead sharks, *Sphyrna lewini*, and subsurface irradiance, temperature, bathymetry, and geomagnetic field. *Mar Biol* 117:1-22
- Kohler NE, Turner PA (2001) Shark tagging: A review of conventional methods and studies. *Environ Biol Fishes* 60:191-223
- Kraus SD (1990) Rates and potential causes of mortality in North Atlantic right whales (*Eubalaena glacialis*). *Marine Mammal Science* 6:278-291
- Kukuyev IE (1996) The new finds in recently born individuals of the whale shark *Rhincodon typus* (Rhincodontidae) in the Atlantic Ocean. *Journal of Ichthyology* 36:203-205
- Laist DW, Knowlton AR, Mead JG, Collet AS, Podesta M (2001) Collisions between ships and whales. *Marine Mammal Science* 17:35-75
- Laist DW, Shaw C (2006) Preliminary evidence that boat speed restrictions reduce deaths of Florida manatees. *Marine Mammal Science* 22:472-479
- Lambertsen RH (1987) A biopsy system for large whales and its use for cytogenetics. *Journal of Mammalogy* 68:443-445
- Langtimm CA, Beck CA, Edwards HH, Fick-Child KJ, Ackerman BB, Barton SL, Hartley WC (2004) Survival estimates for Florida manatees from the photo-identification of individuals. *Marine Mammal Science* 20:438-463
- Lapolla F (2005) The Dolphin Project <http://thedolphinproject.org>.
- Last PR, Stevens JD (1994) *Sharks and Rays of Australia*. CSIRO, Hobart, Australia

- Lebreton J-D, Burnham KP, Clobert J, Anderson DR (1992) Modeling survival and testing biological hypotheses using marked animals: a unified approach with case studies. *Ecol Monog* 62:67-118
- Lee WJ, Conroy J, Howell WH, Kocher TD (1995) Structure and evolution of teleost mitochondrial control regions. *Journal of Molecular Evolution* 41:54-66
- Lenanton RC, Joll L, Penn J, Jones K (1991) The influence of the Leeuwin Current on coastal fisheries of Western Australia. *J R Soc W Aust* 74:101-114
- Link WA, Barker RJ (2006) Model weights and the foundations of multimodel inference. *Ecology* 87:2626-2635
- Liu KM, Chen CT, Liao TH, Joung SJ (1999) Age, growth, and reproduction of the pelagic thresher shark, *Alopias pelagicus* in the northwestern Pacific. *Copeia* 1999:68-74
- Loader C (1999) *Local Regression and Likelihood*. Springer
- Lohmann KJ, Lohmann CMF (1996) Detection of magnetic field intensity by sea turtles. *Nature* 380:59
- Long DJ, Jones RE (1996) White shark predation and scavenging on cetaceans in the eastern North Pacific Ocean. In: *Great white sharks - the biology of *Carcharodon carcharias** Kimley AP, Ainley DG (eds)
- Lukacs PM, Burnham KP (2005) Review of capture-recapture methods applicable to noninvasive genetic sampling. *Molecular Ecology* 14:3909-3919
- Luschi PL, Hays GC, Papi F (2003) A review of long-distance movements by marine turtles, and the possible role of ocean currents. *Oikos* 103:293-302
- MacArthur RH, Wilson EO (1967) *Island Biogeography*. Princeton University Press, New Jersey
- Maffei L, Cuellar E, Noss A (2004) One thousand jaguars (*Panthera onca*) in Bolivia's Chaco? Camera trapping in the Kaa-lyá National Park. *J Zool* 262:295-304
- Makarieva AM, Gorshkov VG, Li B-L (2005) Temperature-associated upper limits to body size in terrestrial poikilotherms. *Oikos* 111:425-436
- Martin AP, Naylor GJP, Palumbi SR (1992) Rates of Mitochondrial-DNA evolution in sharks are slow compared with mammals. *Nature* 357:153-155
- Matsumoto T, Saito H, Miyabe N (2005) Swimming behavior of adult bigeye tuna using pop-up tags in the central Atlantic Ocean. *ICCAT Coll Vol Sci Pap* 57:151-170
- Maunder MN, Sibert JR, Fonteneau A, Hampton J, Kleiber P, Harley SJ (2006) Interpreting catch per unit effort data to assess the status of individual stocks and communities. *ICES Journal of Marine Science* 63:1373-1385
- McConnell BJ, Chambers C, Fedak MA (1992) Foraging ecology of southern elephant seals in relation to the bathymetry and productivity of the Southern Ocean. *Antarctic Science* 4:393-398
- McKinnon AD, Duggan S (2001) Summer egg production rates of paracalanid copepods in subtropical waters adjacent to Australia's North West Cape. *Hydrobiologia* 453/454:121-132
- McMahon CR, Bradshaw CJA, Hays GC (2006) Branding can be justified in vital conservation research. *Nature* 439:392
- McMahon CR, Burton HR (2005) Climate change and seal survival: evidence for environmentally mediated changes in elephant seal, *Mirounga leonina*, pup survival. *P Roy Soc B-Biol Sci* 272:923-928

- Meekan MG, Bradshaw CJA, Press M, McLean C, Richards A, Quasnichka S, Taylor JG (2006) Population size and structure of whale sharks (*Rhincodon typus*) at Ningaloo Reef, Western Australia. *Mar Ecol Prog Ser* 319:275-285
- Mills LS, Doak DF, Wisdom MJ (1999) Reliability of conservation actions based on elasticity analysis of matrix models. *Conservation Biology* 13:815-829
- Mizroch SA, Beard JA, Lynde M (1990) Computer-assisted photo-identification of humpback whales. Report of the International Whaling Commission: 63-70
- Mollet HF, Cailliet GM (2002) Comparative population demography of elasmobranchs using life history tables, Leslie matrices and stage-based matrix models. *Mar Freshw Res* 53:503-516
- Mollet HF, Cailliet GM (2003a) Reply to comments by Miller *et al.* (2003) on Mollet and Cailliet (2002): confronting models with data. *Marine and Freshwater Research* 54:739-744
- Mollet HF, Cailliet GM (2003b) Reply to comments by Miller *et al.* (2003) on Mollet and Cailliet (2002): confronting models with data. *Mar Freshw Res* 54:739-744
- Mollet HF, Cliff G, Pratt HL, Stevens JD (2000) Reproductive biology of the female shortfin mako, *Isurus oxyrinchus* Rafinesque, 1810, with comments on the embryonic development of lamnoids. *Fishery Bulletin* 98:299-318
- Montgomery JC, Walker MM (2001) Orientation and navigation in elasmobranchs: which way forward? *Environ Biol Fishes* 60:109-116
- Moritz C (1994) Defining "evolutionary significant units" for conservation. *Trends in Ecology and Evolution* 9:373-375
- Morris WF, Doak DF (2002) *Quantitative Conservation Biology: Theory and Practice of Population Viability Analysis*. Sinauer Associates, Sunderland, MA
- Morrow R, Birol F (1998) Variability in the southeast Indian Ocean from altimetry - forcing mechanisms for the Leeuwin Current. *J Geophys Res Oceans* 103:18529-18544
- Musyl MK, Brill RW, Curran DS, Gunn JS, Hartog JR, Hill RD, Welch DW, Eveson JP, Boggs CH, Brainard RE (2001) Ability of archival tags to provide estimates of geographical position based on light intensity. In: *Electronic tagging and tracking in marine fisheries*. Sibert JR, Nielsen JL (eds). Kluwer, Dordrecht, p 343-367
- Myers AE, Lovell P, Hays GC (2006) Tools for studying animal behaviour: validation of dive profiles relayed via the Argos satellite system. *Animal Behaviour* 71:989-993
- Myers RA, Barrowman NJ, Hutchings JA, Rosenberg AA (1995) Population dynamics of exploited fish stocks at low population levels. *Science* 269:1106-1108
- Myers RA, Baum JK, Shepherd TD, Powers SP, Peterson CH (2007) Cascading effects of the loss of apex predatory sharks from a coastal ocean. *Science* 315:1846-1850
- Myrberg AAJ (2001) The acoustical biology of elasmobranchs. *Environ Biol Fishes* 60:31-45
- Naessig PJ, Lanyon JM (2004) Levels and probable origin of predatory scarring on humpback whales (*Megaptera novaeangliae*) in east Australian waters. *Wildlife Research* 31:163-170
- Nautical Almanac Office (1989) *Almanac For Computers 1990*, United States Naval Observatory, Washington, D.C
- Nei M (1987) *Molecular evolutionary genetics*. Columbia University Press, New York, NY, USA

- Neumann DR, Leitenberger A, Orams MB (2002) Photo-identification of short-beaked common dolphins (*Delphinus delphis*) in north-east New Zealand: a photo-catalogue of recognisable individuals. *N Z J Mar Freshw Res* 36:593-604
- Nielsen A, Bigelow KA, Musyl MK, Sibert JR (2006) Improving light-based geolocation by including sea surface temperature. *Fisheries Oceanography* 15:314-325
- Nielsen A, Sibert J (2005) KFSST: an R-package to efficiently estimate the most probable track from light-based longitude, latitude and SST
- Norman BM (1999) Aspects of the biology and ecotourism industry of the whale shark *Rhincodon typus* in north-western Australia. MPhil, Murdoch University
- Norman BM (2004) Review of the Current Conservation Concerns of the Whale Shark (*Rhincodon typus*): A Regional Perspective. Report No. Technical Report (NHT Coast & Clean Seas Project No/2127)
- O'Neill RV, Hunsaker CT, Timmins SP, Jackson BL, Jones KB, Riitters KH, Wickham JD (1996) Scale problems in reporting landscape pattern at the regional scale. *Landscape Ecology* 11:169-180
- O'Sullivan JB, Mitchell T (2000) A fatal attack on a whale shark *Rhincodon typus*, by killer whales *Orcinus orca* off Bahia de Los Angeles, Baja California. Abstract: American Elasmobranch Society Whale Shark Symposium, June 2000 La Paz, Mexico
- Ogutu JO, Piepho HP, Dublin HT, Reid RS, Bholá N (2006) Application of mark-recapture methods to lions: satisfying assumptions by using covariates to explain heterogeneity. *J Zool* 269:161-174
- Otway NM, Bradshaw CJA, Harcourt RG (2004) Estimating the rate of quasi-extinction of the Australian grey nurse shark (*Carcharias taurus*) population using deterministic age- and stage-classified models. *Biological Conservation* 119:341-350
- Pai MV, Nandakumar G, Telang KY (1983) On a Whale Shark, *Rhincodon typus* Smith landed off Karwar, Karnataka. *Indian Journal of Fisheries* 30:157-160
- Palsboll PJ (1999) Genetic tagging: contemporary molecular ecology. *Biological Journal of the Linnean Society* 68:3-22
- Palsboll PJ, Allen J, Berube M, Clapham PJ, Feddersen TP, Hammond PS, Hudson RR, Jorgensen H, Katona S, Larsen AH, Larsen F, Lien J, Mattila DK, Sigurjonsson J, Sears R, Smith T, Sponer R, Stevick P, Oien N (1997) Genetic tagging of humpback whales. *Nature* 388:767-769
- Pardini AT, Jones CS, Noble LR, Kreiser B, Malcolm H, Bruce BD, Stevens JD, Cliff G, Scholl MC, Francis M, Duffy CAJ, Martin AP (2001) Sex-biased dispersal of great white sharks - In some respects, these sharks behave more like whales and dolphins than other fish. *Nature* 412:139-140
- Parra GJ, Corkeron PJ, Marsh H (2006) Population sizes, site fidelity and residence patterns of Australian snubfin and Indo-Pacific humpback dolphins: Implications for conservation. *Biological Conservation* 129:167-180
- Parsons KM, Durban JW, Claridge DE (2003) Comparing two alternative methods for sampling small cetaceans for molecular analysis. *Marine Mammal Science* 19:224-231
- Pauly D (2002) Growth and mortality of the basking shark *Cetorhinus maximus* and their implications for whale shark *Rhincodon typus*. In: Fowler SL, Reid T, Dipper FA (eds) *Elasmobranch Biodiversity, Conservation and Management Proceedings of an*

- International Seminar and Workshop, Sabah, Malaysia. Occasional Papers of the IUCN Survival Commission No. 25, Gland, Switzerland
- Pauly D, Christensen V, Dalsgaard J, Froese R, Torres Jr. F (1998) Fishing down marine food webs. *Science* 279:860-863
- Pearce AF, Griffiths RW (1991) The mesoscale structure of the Leeuwin Current: A comparison of laboratory models and satellite imagery. *J Geophys Res* 96:16-739-716-757
- Pearce AF, Phillips BF (1988) ENSO events, the Leeuwin Current and larval recruitment of the western rock lobster. *J Cons Int Explor Mer* 45:13-21
- Peeters FJC, Acheson R, Brummer GJA, de Ruijter WPM, Schneider RR, Ganssen GM, Ufkes E, Kroon D (2004) Vigorous exchange between the Indian and Atlantic oceans at the end of the past five glacial periods. *Nature* 430:661-665
- Penven P, Lutjeharms JRE, Marchesiello P, Roy C, Weeks SJ (2001) Generation of cyclonic eddies by the Agulhas Current in the lee of the Agulhas Bank. *Geophysical Research Letters* 28:1055-1058
- Phillips RA, Silk JRD, Croxall JP, Afanasyev V, Briggs DR (2004) Accuracy of geolocation estimates for flying seabirds. *Mar Ecol Prog Ser* 266:265-272
- Polovina JJ, Balazs GH, Howell EA, Parker DM, Seki MP, Dutton PH (2004) Forage and migration habitat of loggerhead (*Caretta caretta*) and olive ridley (*Lepidochelys olivacea*) sea turtles in the central North Pacific Ocean. *Fisheries Oceanography* 13:36-51
- Polovina JJ, Kleiber P, Kobayashi DR (1999) Application of TOPEX-POSEIDON satellite altimetry to simulate transport dynamics of larvae of spiny lobster, *Panulirus marginatus*, in the Northwestern Hawaiian Islands, 1993-1996. *Fisheries Bulletin* 97:132-143
- Polovina JJ, Kobayashi DR, Ellis DM, Seki MP, Balazs GH (2000) Turtles on the edge: movement of loggerhead turtles (*Caretta caretta*) along oceanic fronts in the central North Pacific, 1997-1998. *Fisheries Oceanography* 9:71-82
- Posada D, Crandall KA (1998) MODELTEST: testing the model of DNA substitution. *Bioinformatics* 14:817-818
- Pravin P (2000) Whale shark in the Indian coast – need for conservation. *Curr Sci* 79:310-315
- R Core Development Team (2004) R: A Language and Environment for Statistical Computing. R Foundation for Statistical Computing, Vienna, Austria
- Rasmussen AS, Arnason U (1999) Phylogenetic studies of complete mitochondrial DNA molecules place cartilaginous fishes within the tree of bony fishes. *Journal of Molecular Evolution* 48:118-123
- Ratner S, Lande R (2001) Demographic and evolutionary responses to selective harvesting in populations with discrete generations. *Ecology* 82:3093-3104
- Raymond M, Rousset F (1995) An exact test for population differentiation. *Evolution* 49:1280-1283
- Reynolds JD, Dulvy NK, Goodwin NB, Hutchings JA (2005) Biology of extinction risk in marine fishes. *Proceedings of the Royal Society of London: B* 272:2337-2344
- Ricker WE (1979) Growth rates and models. *Fish Physiology* 8:677-743
- Ricker WE (1981) Change in the average size and average age of Pacific salmon. *Can J Fish Aquat Sci* 38:1636-1956

- Rio MH, Hernandez F (2004) A mean dynamic topography computed over the world ocean from altimetry, in situ measurements, and a geoid model. *J Geophys Res* 109:1-19
- Robbins WD, Hisano M, Connolly SR, Choat JH (2006) Ongoing collapse of coral-reef shark populations. *Current Biology* 16:2314-2319
- Roberts MA, Schwartz TS, Karl SA (2004) Global population genetic structure and male-mediated gene flow in the green sea turtle (*Chelonia mydas*): Analysis of microsatellite loci. *Genetics* 166:1857-1870
- Robinson PW, Tremblay Y, Crocker DE, Kappes MA, Kuhn CE, Shaffer SA, Simmons SE, Costa DP (2007) A comparison of indirect measures of feeding behaviour based on ARGOS tracking data. *Deep-Sea Res Oceanogr B* 54:356-368.
- Rocha LA, Robertson DR, Rocha CR, Van Tassell JL, Craig MT, Bowens BW (2005) Recent invasion of the tropical Atlantic by an Indo-Pacific coral reef fish. *Molecular Ecology* 14:3921-3928
- Rochford DJ (1962) Hydrology of the Indian Ocean. II. The surface waters of the south-east Indian Ocean and Arafura Sea in spring and summer. *Australian Journal of Marine and Freshwater Research* 13:226-251
- Rochford DJ (1984) Some general oceanographical features of the North West Shelf study region abstract, CSIRO Division of Fisheries Research, Cronulla, NSW
- Rogers AR, Harpending H (1992) Population-growth makes waves in the distribution of pairwise genetic-differences. *Molecular Biology and Evolution* 9:552-569
- Rokas A, Ladoukakis E, Zouros E (2003) Animal mitochondrial DNA recombination revisited. *Trends in Ecology & Evolution* 18:411-417
- Roman J, Palumbi SR (2003) Whales before whaling in the North Atlantic. *Science* 301:508-510
- Romanov EV (1998) Bycatch in the purse seine tuna fisheries in the Western Indian Ocean 7th Expert Consultation on Indian Ocean Tunas, Victoria, Seychelles, 9-14 November, 1998, Seychelles
- Rommel SA, Costidis AM, Pitchford TD, Lightsey JD, Snyder RH, Haubold EM (2007) Forensic methods for characterizing watercraft from watercraft-induced wounds on the Florida manatee (*Trichechus manatus latirostris*). *Marine Mammal Science* 23:110-132
- Rossi S, Sabates A, Latasa M, Reyes E (2006) Lipid biomarkers and trophic linkages between phytoplankton, zooplankton and anchovy (*Engraulis encrasicolus*) larvae in the NW Mediterranean. *Journal of Plankton Research* 28:551-562
- Rowat D (1997) Seychelles whale shark tagging project - pilot project report, Phelsuma, Nature Protection Trust of Seychelles
- Rowat D, Gore M (2006) Regional scale horizontal and local scale vertical movements of whale sharks in the Indian Ocean off Seychelles. *Fisheries Research* 84:32-40
- Rowat D, Meekan M, Engelhardt U, Pardigon B, Vely M (2007) Aggregations of juvenile whale sharks (*Rhincodon typus*) in the Gulf of Tadjoura, Djibouti. *Environ Biol Fishes* DOI: 10.1007/s10641-006-9148-7
- Royer F, Fromentin JM, Gaspar P (2005) A state-space model to derive bluefin tuna movement and habitat from archival tags. *Oikos* 109:473-484
- Saitou N, Nei M (1987) The neighbor-joining method: A new method for reconstructing phylogenetic trees. *Molecular Biology and Evolution* 4:406-425

- Sambrook J, Fritsch EF, Maniatis T (1989) Molecular cloning: a laboratory manual. Cold Spring Harbor Laboratory Press, New York, USA
- Satyanarayana Rao K (1986) On the capture of whale sharks off Dakshina Kannada coast, Marine Fisheries Information Service (India)
- Schaefer KM, Fuller DW (2002) Movements, behavior, and habitat selection of bigeye tuna (*Thunnus obesus*) in the eastern equatorial Pacific, ascertained through archival tags. Fish Bull 100:765-788
- Schwarz CJ, Arnason AN (1996) A general methodology for the analysis of open-population capture recapture experiments. Biometrics 52:860-873
- Schwarz CJ, Seber GAF (1999) Estimating animal abundance: Review III. Statistical Science 14:427-456
- Seber GAF (1970) Estimating time-specific survival and reporting rates for adult birds from band returns. Biometrika 57:313-318
- Seber GAF (1982) The Estimation of Animal Abundance and Related Parameters. Charles Griffin and Company, London
- Seitz AC, Norcross BL, Wilson D, Nielsen JL (2006) Evaluating light-based geolocation for estimating demersal fish movements in high latitudes. Fishery Bulletin 104:571-578
- Seitz AC, Weng KC, Boustany AM, Block BA (2002) Behaviour of a sharptail mola in the Gulf of Mexico. J Fish Biol 60:1597-1602
- Shaffer SA, Tremblay Y, Awkerman JA, Henry RW, Teo SLH, Anderson DJ, Croll DA, Block BA, Costa DP (2005) Comparison of light-and SST-based geolocation with satellite telemetry in free-ranging albatrosses. Mar Biol 147:833-843
- Shin Y-J, Rochet M-J, Jennings S, Field JG, Gislason H (2005) Using size-based indicators to evaluate the ecosystem effects of fishing. ICES Journal of Marine Science 62:384-396
- Shipping LRo (1939-2005) World Fleet Statistics. Lloyd's Register Printing Services Ltd, Burgess Hill, West Sussex, U.K
- Sibert J, Fournier D (2001) Possible models for combining tracking data with conventional tagging data. Electronic Tagging and Tracking in Marine Fisheries: Proceedings of the Symposium on Tagging and Tracking Marine Fish with Electronic Devices, February 7-11, 2000, East-West Center, University of Hawaii
- Sibert J, Hampton J, Kleiber P, Maunder M (2006) Biomass, size, and trophic status of top predators in the Pacific Ocean. Science 314:1773-1776
- Sibert JR, Musyl MK, Brill RW (2003) Horizontal movements of bigeye tuna (*Thunnus obesus*) near Hawaii determined by Kalman filter analysis of archival tagging data. Fisheries Oceanography 12:141-151
- Sibert JR, Nielsen A (2003) KTrack (Kalman Filter tracking): An Add-on Package for the Statistical Environment R to Efficiently Estimate Movement Parameters and Predict Most Probable Track from Raw Geo-locations of Archival Tagged Individuals
- Sibly RM, Barker D, Denham MC, Hone J, Pagel M (2005) On the Regulation of Populations of Mammals, Birds, Fish, and Insects. American Association for the Advancement of Science, p 607-610
- Sibly RM, Hone J (2002) Population growth and its determinants. Philosophical Transactions of the Royal Society of London Series B 357:1153-1170
- Sims DW (2003) Tractable models for testing theories about natural strategies: foraging behaviour and habitat selection of free-ranging sharks. J Fish Biol 63:53-73

- Sims DW, Nash JP, Morritt D (2001) Movements and activity of male and female dogfish in a tidal sea lough: alternative behavioural strategies and apparent sexual segregation. *Mar Biol* 139:1165-1175
- Sims DW, Quayle VA (1998) Selective foraging behaviour of basking sharks on zooplankton in a small-scale front. *Nature* 393:460-464
- Sims DW (2006) Differences in habitat selection and reproductive strategies of male and female sharks. In: *Sexual Segregation of the Vertebrates: Ecology of the Two Sexes*. Ruckstuhl KE, Neuhaus P (eds). Cambridge University Press, Cambridge, United Kingdom, p 127-147
- Slatkin M, Hudson RH (1991) Pairwise comparisons of mitochondrial DNA sequences in stable and exponentially growing populations. *Genetics* 129:555-562
- Smale MJ, Goosen AJJ (1999) Reproduction and feeding of spotted gully shark, *Triakis megalopterus*, off the Eastern Cape, South Africa. *Fishery Bulletin* 97:987-998
- Smith SE, Au DW, Show C (1998) Intrinsic rebound potential of 26 species of Pacific sharks. *Mar Freshw Res* 49:663-678
- Sokal RR, Rohlf FJ (1981) *Biometry*. Freeman, New York
- Speed CW, Meekan M, Bradshaw CJA (2007) Spot the match - wildlife photo-identification using information theory. *Frontiers in Zoology* 4:2
- Speed CW, Meekan MG, Rowat D, Pierce S, Marshall AD, Bradshaw CJA (2008) Scarring patterns and relative mortality rates of Indian Ocean whale sharks. *J Fish Biol* DOI: 10.1111/j.1095-8649.2008.01810.x
- Springer S (1967) Social organisation of shark populations. In: *Sharks, skates and rays*. Gilbert PW, Mathewson RF, Rall DP (eds). Johns Hopkins Press, Baltimore, p 149-174
- Squire JLL (1990) Distribution and apparent abundance of the basking shark, *Cetorhinus maximus*, off the central and southern California coast. *Marine Fisheries Review* 52:8-11
- Stanford A (1927) *Navigator: The Story of Nathaniel Bowditch*. William Morrow & Co, New York
- Stergiou K (2002) Overfishing, tropicalization of fish stocks, uncertainty and ecosystem management: resharpening Ockham's razor. *Fisheries Research* 55:1-9
- Stevens JD (2007) Whale shark (*Rhincodon typus*) biology and ecology: a review of the primary literature. *Fisheries Research* 84:4-9
- Stevens JD, Bonfil R, Dulvy NK, Walker PA (2000) The effects of fishing on sharks, rays, and chimaeras (chondrichthyans), and the implications for marine ecosystems. *ICES Journal of Marine Science* 57:476-494
- Stevick PT, Palsboll PJ, Smith TD, Bravington MV, Hammond PS (2001) Errors in identification using natural markings: rates, sources, and effects on capture-recapture estimates of abundance. *Can J Fish Aquat Sci* 58:1861-1870
- Stewart BS, DeLong RL (1995) Double migrations of the northern Elephant Seal, *Mirounga angustirostris*. *Journal of Mammalogy* 76:196-205
- Stewart BS, Wilson SG (2005) Threatened fishes of the world: *Rhincodon typus* (Smith 1828) (Rhincodontidae). *Environ Biol Fishes* 74:184-185
- Stokes K, Law R (2000) Fishing as an evolutionary force. *Mar Ecol Prog Ser* 208:307-309
- Strong DR (1986) Density-vague population change. *Trends in Ecology and Evolution* 1:39-42

- Sumner MD, Michael KJ, Bradshaw CJA, Hindell MA (2003) Remote sensing of Southern Ocean sea surface temperature: implications for marine biophysical models. *Remote Sensing of Environment* 84:161-173
- Swofford DL (2003) PAUP*. Phylogenetic analysis using parsimony (*and other methods). Version 4. Sinauer Associates, Sunderland, MA
- Tajima F (1989) Statistical method for testing the neutral mutation hypothesis by DNA polymorphism. *Genetics* 123:585–595
- Tamura K, Nei M (1993) Estimation of the number of nucleotide substitutions in the control region of mitochondrial-DNA in humans and chimpanzees. *Molecular Biology and Evolution* 10:512-526
- Taylor G (1994a) Whale Sharks: the giants of Ningaloo Reef. Angus and Robertson, Sydney. 176 pp.
- Taylor G, Grigg G (1991) Whale sharks of Ningaloo Reef, Canberra
- Taylor JG (1994b) Gentle giants of the deep. *Australian Geographic*
- Taylor JG (1996) Seasonal occurrence, distribution and movements of the whale shark, *Rhincodon typus*, at Ningaloo Reef, Western Australia. *Mar Freshw Res* 47:637-642
- Taylor JG, Pearce AF (1999) Ningaloo Reef currents: implications for coral spawn dispersal, zooplankton and whale shark abundance. *J R Soc W Aust* 82:57-65
- Tenhumberg B, Tyre AJ, Pople AR, Possingham HP (2004) Do harvest refuges buffer kangaroos against evolutionary responses to selective harvesting? *Ecology* 85:2003-2017
- Teo SLH, Boustany A, Blackwell S, Walli A, Weng KC, Block BA (2004) Validation of geolocation estimates based on light level and sea surface temperature from electronic tags. *Mar Ecol Prog Ser* 283:81–98
- Terborgh J, Winter B (1980) Some causes of extinction. In: *Conservation Biology: An Ecological-Evolutionary Perspective*. Soulé ME, Wilcox BA (eds). Sinauer, Sunderland, MA, p 119-134
- Theberge MM, Dearden P (2006) Detecting a decline in whale shark *Rhincodon typus* sightings in the Andaman Sea, Thailand, using ecotourist operator-collected data. *Oryx* 40:337-342
- Tremblay Y, Robinson PW, Crocker DE, Kuhn CE, Simmons S, Costa DP (2006a) Hotspots defined by Top-Predators in the Ocean: What, Where, and How. The 13th Ocean Sciences Meeting. American Geophysical Union, Honolulu, Hawaii, 20-24 February 2006
- Tremblay Y, Shaffer SA, Fowler SL, Kuhn CE, McDonald BI, Weise MJ, Bost C-A, Weimerskirch H, Crocker DE, Goebel ME, Costa DP (2006b) Interpolation of animal tracking data in a fluid environment. *J Exp Biol* 209:128-140
- Tsaousis AD, Martin DP, Ladoukakis ED, Posada D, Zouros E (2005) Widespread recombination in published animal mtDNA sequences. *Molecular Biology and Evolution* 22:925-933
- Tuck GN, Polacheck T, Croxall JP, Weimerskirch H, Prince PA, Wotherspoon S (1999) The potential of archival tags to provide long-term movement and behaviour data for seabirds: First results from Wandering Albatross *Diomedea exulans* of South Georgia and the Crozet Islands. *Emu* 99:60-68

- Turchin P (2003) Complex Population Dynamics: A Theoretical/Empirical Synthesis. Princeton University Press, Princeton, NJ, USA
- Urian K (2005) Mid-Atlantic Bottlenose Dolphin Catalog. <http://moray.ml.duke.edu/faculty/ead/mabdc.html>
- Van Dykhuizen G, Mollet HF (1992) Growth, age estimation, and feeding of captive sevengill sharks, *Notorynchus cepedianus*, at the Monterey Bay Aquarium. Australian Journal of Marine and Freshwater Research 43:297-318
- van Pijlen IA, Amos B, Burke T (1995) Patterns of genetic-variability at individual minisatellite loci in Minke Whale Balaenoptera-Acutorostrata populations from 3 different oceans. Molecular Biology and Evolution 12:459-472
- Van Tienhoven AM, Den Hartog JE, Reijns R, Peddemors VM (2007a) A computer-aided program for pattern-matching of natural marks of the spotted raggedtooth shark *Carcharias taurus*. Journal of Applied Ecology
- Van Tienhoven AM, Den Hartog JE, Reijns RA, Peddemors VM (2007b) A computer-aided program for pattern-matching of natural marks on the spotted raggedtooth shark *Carcharias taurus*. Journal of Applied Ecology 44:273-280
- Vas P (1990) The abundance of the blue shark, *Prionace glizuca*, in the western English Channel. Environ Biol Fishes 29:209-225
- Vogler AP, Desalle R (1994) Diagnosing Units of Conservation Management. Conservation Biology 8:354-363
- von Bertalanffy L (1938) A quantitative theory of organic growth. Human Biology 10:181-213
- Walker TI (1998) Can shark resources be harvested sustainably? A question revisited with a review of shark fisheries. Mar Freshw Res 49:553-572
- Walsh HE, Metzger DA, Higuchi R (1991) Chelix medium for simple extraction of DNA for PCR-based typing from forensic material. Biological Techniques 10:506-513
- Walters C (1995) Estimation of historical stock sizes and recruitment anomalies from relative abundance time-series. Can J Fish Aquat Sci 52:1523-1534
- Walters CJ, Martell SJD (2004) Fisheries Ecology and Management. Princeton University Press, Princeton, NJ
- Walther BA, Moore JL (2005) The concepts of bias, precision and accuracy, and their use in testing the performance of species richness estimators, with a literature review of estimator performance. Ecography 28:815-829
- Waples RS (1995) Evolutionary significant units and the conservation of biological diversity under the Endangered Species Act. American Fisheries Society Symposium 17:8-27
- Ward-Geiger LI, Silber GK, Baumstark RD, Pulfer TL (2005) Characterization of ship traffic in right whale critical habitat. Coastal Management 33:263-278
- Watkins WA, Daher MA, Fristrup KM, Howald TJ, Disciara GN (1993) Sperm whales tagged with transponders and tracked underwater by sonar. Marine Mammal Science 9:55-67
- Weiss RF (1970) The solubility of nitrogen, oxygen and argon in water and seawater. Deep-Sea Research II 17:721-735
- Welch DW, Eveson JP (1999) An assessment of light-based geolocation estimates from archival tags. Can J Fish Aquat Sci 56:1317-1327
- West GJ, Stevens JD (2001) Archival tagging of school shark, *Galeorhinus galeus*. Australia: initial results Environ Biol Fish 60:283-298

- White GC, Burnham KP (1999) Program MARK: survival estimation from populations of marked animals. *Bird Study* 46:120-138
- Wilkin DJ, Debure KR, Roberts ZW (1998) Query by sketch in DARWIN: digital analysis to recognize whale images on a network. In: *Storage and Retrieval for Image and Video Databases VII Proceedings of the International Society for Optical Engineering (SPIE) Vol 3656* Yeung MM, Yeo B-L, Bouman CA (eds). SPIE, Bellingham, Washington, p 41-48
- Wilson RP, McMahon CR (2006) Measuring devices on wild animals: what constitutes acceptable practice? *Frontiers in Ecology and the Environment* 4:147-154
- Wilson RP, Scolaro JA, Peters G, Laurenti S, Kierspel M, Gallelli H, Upton J (1995) Foraging areas of Magellanic penguins *Spheniscus magellanicus* breeding at San Lorenzo, Argentina, during the incubation period. *MEPS* 129:1-6
- Wilson SG, Lutcavage ME, Brill RW, Genovese MP, Cooper AB, Everly AW (2005) Movements of bluefin tuna (*Thunnus thynnus*) in the northwestern Atlantic Ocean recorded by pop-up satellite archival tags. *Mar Biol* 146:409-423
- Wilson SG, Pauly T, Meekan MG (2002) Distribution of zooplankton inferred from hydroacoustic backscatter data in coastal waters off Ningaloo Reef, Western Australia. *Mar Freshw Res* 53:1005-1015
- Wilson SG, Polovina JJ, Stewart BS, Meekan MG (2006) Movements of whale sharks (*Rhincodon typus*) tagged at Ningaloo Reef, Western Australia. *Mar Biol* 148:1157-1166
- Wilson SG, Stewart BS, Polovina JJ, Meekan MG, Stevens JD, Galuardi B (2007) Accuracy and precision of archival tag data: a multiple-tagging study conducted on a whale shark (*Rhincodon typus*) in the Indian Ocean. *Fisheries Oceanography* 16:547-554
- Wilson SG, Taylor JG, Pearce AF (2001a) The seasonal aggregation of whale sharks at Ningaloo reef, western Australia: currents, migrations and the El Niño/Southern oscillation. *Environ Biol Fishes* 61:1-11
- Wilson SG, Taylor JG, Pearce AF (2001b) The seasonal aggregation of whale sharks at Ningaloo reef, western Australia: currents, migrations and the El Niño/Southern oscillation. *Environ Biol Fishes* 61:1-11
- Wintner SP (2000) Preliminary study of vertebral growth rings in the whale shark, *Rhincodon typus*, from the east coast of South Africa. *Environ Biol Fishes* 59:441-451
- Yan B, Stamnes K, Toratani M, Li W, Stamnes JJ (2001) Evaluation of a Reflectance Model Used in the SeaWiFS Ocean Color Algorithm: Implications for Chlorophyll Concentration Retrievals. *Appl Opt* 41:6243-6259
- Yang G-J, Bradshaw CJA, Whelan PI, Brook BW (2008) Importance of endogenous feedback controlling the long-term abundance of tropical mosquito species. *Population Ecology* In press
- Zar JH (1989) *Biostatistical Analysis*. Prentice-Hall, Inc., Englewood Cliffs, NJ

APPENDIX 1

Microsatellites (pink) and primers (yellow) for whale sharks sampled at Ningaloo Reef in April-May of 2006 and 2007.

Whale Shark A101

Primer Pair # 5 Product Length: 207 Topt: 56.6 ✓
 Forward: Tm: 56.0 5'-AAA-AAT-TGA-CGA-CTC-AAC-AGT-C-'3
 Reverse: Tm: 55.3 5'-AAA-TGA-TTA-CTG-GCC-TGT-AGA-G-'3
 AAAAAAGTTNTTAAACCAAAGTTTTACAACCTGTCAGGAATATTCAGATGACAAGTTTTCTTGNTTAGTTT
 AAAAATAATGACGACTCAACAGTCAAAGATATATGCAACTACACCCCGTCTCTCTCTCTCACACACA
 CACACACACACACAAAACACACAAGGAAATATTGTATTTATAGGAGTAGCATGCTGTTTTTATCATT
 AAGATTTCAAGAATACTTTGTTGCATGTGCCTTTCTTTGGGTTGAAGA CTCTACAGGCCAGTAATCATT
 TCTTCTTGGTCTTCAATGGAAAGAGCCAGGAGTTTTAGGAACATGTATTCACTGTTTTATGTTTGCTGCA
 AGAAATCTTTGAATGGTCCACACCAATTAAGGTGCAATAGAGAAGCCCAAATGCAAAGTCCCAGTACAG
 TTCCTCAGGTAGAGAGATCAAAGTCAACCTAAGTCCCTGCCTACTGTTTTTCTCTATGGCAGGGTGCTTT
 TGCCTTACAGTTTCACATGTTTCTGATCTATATGCTCCAGTAATACAATGATTAATCTTCTGATGAGAA
 ANCTTGGTTTTGATCATGTGAN CAGANCATCTCTTCCATTATCTTCCATAATAN

Sequence : Whale Shark A102

Primer Pair # 7 Product Length: 192 Topt: 56.4 ✓
 Forward: Tm: 55.6 5'-CCT-TTA-CCA-AGT-CCC-ACT-G-'3
 Reverse: Tm: 55.1 5'-GCC-GAA-TCT-ATT-AGC-GTT-C-'3
 CTCCCTAAGGAGTTGTAATTATTACTATCATGCAATAAATCTTATTATAATCTAAGAACAGTGTCTCTAA
 GTGGTATATATTTTACTACCAGACACTAGATAGGCCAAAGACAAAGCAAGGATGAAGGCAGGTTAGTCGC
 AGCAAACAA CTTTTACCAAGTCCCCTG GTACAAGGCAAATACCAAAGATGTAAGCAATAGTCATCTGG
 GGAAGTACCACAAAACG CACACACACACACACACACACACACCTGTTGCAAGTTGTTCCAGGGCTGGGTGA
 CTACTGTAGCAATCTTCGATATTACATTTGTCACAAGTAAAAT GAACGCTAATAGATTCCGGCCAGTCCTA
 GTAGGGATTGCCGCTCCAAATTCACACAACCTACAGAATTACAGAAATAGTGAAGCTATAACAATGGGACG
 TGGTGAGAAACAATTCTTCTTTGAAT

Sequence : Whale Shark A104

Primer Pair # 6 Product Length: 310 Topt: 58.1 ✓
 Forward: Tm: 58.6 5'-CGG-AAG-GGT-TGA-TCT-AAA-GG-'3
 Reverse: Tm: 57.7 5'-TGA-TCT-GAT-CCC-AGT-TAC-ACT-G-'3
 CTGGGTTTTTGATGCCTTTCCTGTGACTTTGCTGCATGCTGTGTCTTTGCGATGGGC CGGAAGGGTTGAT
 CTAAGGGGATCTTGACATGTGCGGTGCA CACACACACACAATCACGTGCG CACACAGATACACAATAC
 CGT CACAGACACACACACA CGTGCACGATTGAGCAGACACACACATACT CACACAGACACAACACAC
 ACACACACACACACAATCATGTGCGCACACA GATACACAATACCGCTCACAGACACACACATGTGC
 ACGATTGAACAGACACACATACT CACACACACACA CC CACACACACACACACACACACAGTGCA CAGTG
 TAACTGGGATCAGATCAATCCATTTCTTTTTGGAAGGTGAAGGACAGTCTTTTTCAGTTACCCTGCTCCTG
 TCCCCTGGGGGAAGAAGGACACAGTTGAAATTTTTGCCCCCTCGGAACCCCTCCTTGCCTCTGCTCGACA
 TTTTCTTTGAAACCAAAGGAATATGAAATCTACTAAACATTAAGTTTGTCTGGAGAATGCGCATTGCT
 AGA

Sequence : Whale Shark A105

Primer Pair # 1 Product Length: 359 Topt: 56.6 ✓
 Forward: Tm: 53.0 5'-TGT-AGG-CTG-TAC-TGA-CAG-AAC-'3
 Reverse: Tm: 52.2 5'-CAC-AAT-GTG-GTA-ATG-AGT-TG-'3
 ANAATATNTTCTCTCCATACTTCTTGTGTTACTACTTGTTCAGTNTTAGATTGTTTTTTCTTCAA
 TTGACCACA TGTAGGCTGTACTGACAGAAC ATACAGAATGGTTAACACACACACATGTACAGACAGACAGAC
 AGA CACACACACACACACACA GACACACATACACACGCACATACACACAAAATATAAA CACAGACAG
 GCACACCGACACATGCACACACTTGGCGACAAA CACACACAGACATACACACATAGACATACACACACAC
 ACACACACACACACA CGCACATACAGACACATAATCATTTGA CACACACACA GATGGAGA CAGACACACAC
 ACACAGACACA GGCAGACGCGCACGCATACACACATAGACACATACAGGCACACAGTCAAAAACAGAA CA
 ACTCATTACCACATTGTG CCAAACATAAAATGGGCAAGCCAG

Sequence : Whale Shark A108

Primer Pair # 6 Product Length: 258 Topt: 57.8 ✓

Forward: Tm: 58.0 5'-CCG-AGC-CTG-AGT-TGA-CTG-'3

Reverse: Tm: 57.6 5'-GTA-ACC-CAA-TCT-TGT-GGT-CTT-C-'3

CTCTTGTGTTTTTTGGAGTCATTGAGGAGGCTGTGGTTCGTGTTAGAAGGAAACCCTCCCCAAAACACTGA
 ATCCTGTAACCATGGCAGATCCAGGCCATGTGGTGGTCAGAAAAGGAGAAGGGGTTTCAGAAGGAAGGGCAG
 ACCTTATCACTCATCGTCTTTTACCCTTCCTGACACCTGCTGCTTTGATCTGATATCGTTTACCTTTGGT
 CGAGATCCC **CCGAGCCTGAGTTGACTG**GA**CACACACACACACACACACACACACACACACACACAGACACAGACA**
CAGACACAGATG**CACAGACACAGACAGACACACACACACAC**CGTGCCTCTTGCCTGAGGCTGAGTTATTCC
 CTGTAGCAATAAGATGAGACCCTCATATGTCCCTTACCTCAGGAGCCTCCATTGGTGGATTGATAATGAA
 TCTGCCCTCTCTGAACTTGATTCTGGTGGAGGCTG**GAAGACCACAAGATTGGGTTAC**TGTCTCCAAGCTA
 GCAGCAGCCAGAACGAATGGACGTCTTTTTGTGCACGGAGTTATTTCAATCTGGTTCACACCGAGTAAAA
 GTAGAGATGGAAGCGGGATTCAATTGTAATGTTGAAAGGGAATGAGATACATTGTTAAAGAAGGGGA
 TTGCAGAAAGANGGAAGAAGTACACTAATTGGATTGCTCCTTCCAGTAGCAATGGGGTTCACAGGGACCTCT
 GGTCTGTGCCGTTTGGTTCCTGGTGAATCTGGTTAATAAACACACANGGGGTTT

Sequence : Whale Shark A109

Primer Pair # 8 Product Length: 217 Topt: 56.7 ✓

Forward: Tm: 55.7 5'-CAT-TGC-ATT-ACA-AAG-GAT-GAC-'3

Reverse: Tm: 55.5 5'-TGA-AAA-GAT-GAC-ATT-GAC-AGA-G-'3

AAAACATAGTTGTAGAATTACAAGTTAAAAATACCCACAGCACCTTGAAGTTCTGACCTTNGTGGGTCA
 TGTACTTCACCGTCATGACAAATGAAATAAGATTCACTTT**CATTGCAATACAAAGGATGAC**AAATAATTA
 AATATTATATAAAAATGTATATTTGCATTTATAAAACAACACAAACATGCCCGGTGCACG**CACACGCAC**
 GCGCGG**CACACACACACACA**CGCAGACAAA**CACACACACACACACACACATACACACACACACACACAC**
ACACACACACACACACGTACACACA**CTCTGTCAATGTCTATCTTTTCA**GTTCTAACTGCATCTCTATCAGT
 TTGTTTAGTTTTTTGGGGCGAAATATTTAATTGATCAATTGTTGATTTATATCTGAGAAGACTAGCTGG
 AGCTCACTTATTTACAACATATGGTTTGGATGAGGAGAGTAAAGGTACTGTAG

Sequence : Whale Shark A110

Primer Pair # 6 Product Length: 271 Topt: 57.2 ✓

Forward: Tm: 55.4 5'-CGG-CAG-TGG-AGT-ATG-GTA-'3

Reverse: Tm: 56.3 5'-GCG-TGA-GTG-TAT-GTG-CTT-G-'3

CTCAGNTTTTCCCTTCTGATAAGATTGCTTGCTAATCGGATCCGGGGTCCCTTCCCATTTCCANTCACGCG
 CTGTGACAGGTCCAGTAACTGTGTGAACCGTGTGCGTTAAAACCGGTAAATATACCAGTAGTAACTTCC**CG**
GCAGTGGAGTATGGTAAAACGTTTACAGAACCGACAA**CACACACACAGACACACATTTACACAAATA****CAC**
ACATACAGACACTATA**CACA**CTTACG**CATGCACA**CTTACTCATAGAC**CACACACA**ATTACACCGAAA**CAC**
CGCACACC**CACACA**AACT**CACA**GA**CACACA**AGAC**CACA**CG**CACA**CTT**CACACA**TAGACACCACCACAC
 AGACACAAAGGCGGATACATCACACATACACACTGAAACC**CAAGCACATACACTCACGC**ACATACACACA
 CGCAGACACAAATCAGACTAATCTCGTTTACAGACATAGACTCACAAACCGGACTCCGAGACTATCTGTCT
 TCTGTATTGAACAACTCGCTCTGAGTGGGATTAGTTTCTCATCGCCCTGCTCTCCACCAGCAGCCACAT
 ATTGATCACTTTTTCACTCCTTTCAGCACTTGATAATGGGGAAATATTTGGTAACTGGTTTCTCTTGGCC
 GGTCATGCTCAGCGCAGATTGGGATCATTTTCTCAATGGTCTTGGCTTTATTACTGGTTATATTATGATTC
 ACATTTTGGTTTTTA

Sequence : Whale Shark A111

Primer Pair # 8 Product Length: 287 Topt: 57.3 ✓

Forward: Tm: 56.1 5'-TGA-GGG-TAA-TCA-TCT-CGT-TG-'3

Reverse: Tm: 55.4 5'-GGT-GTG-AGG-TCT-TGC-TTA-GA-'3

AAAGTTTTGGCAGTTGTTTGAAGGCAAGAAATGGAGGCGTAGGGAAGATCGTGG**TGAGGGTAATCATCTC**
GTTGACGATGTGTTGAAGGGTGCAGAAGCATGGCATAGTTTCTCTGCTCCGGGGAAGTACTGGATGATG
 AAGGGTACCCTATTGGTTGTATCTCATGTCTGTCTTCT**CACA**CTCTCTCAAACACAAA**CACACACACACA**
CACACACACACACACACAAAATTGTTTTCATCCAAGATGTTTGTGTAGTTGCAGATACATTCTGTTTTGC
 TCCAGAAAAAACCTGACCCAGTTTAAAACATAGACAGAT**TCTAAGCAAGACCTCACACCT**AAAAATGCA
 TTGTCTGACCTGAGAAGTCACTCTTGTATACATTGATAAAAACCTCTAATTATCTCAGGATAATGACTTG
 AGAGGAATCTGGATTTTGCATTTTAAATCAGTAGTCTCCTTCCCTAAGTATTAAAGATTAAAATCACAGGT
 TATAGACACGAGATTATAGTTCAACAGGTTTATTTGAAGACACAAG

Sequence : Whale Shark A114

Primer Pair # 2 Product Length: 135 Topt: 54.8 ✓
 Forward: Tm: 55.3 5'-CTC-CTC-CAA-TCC-CTC-ATC-'3
 Reverse: Tm: 53.3 5'-CGT-GAG-AGT-GTA-TGT-CTA-TGT-G-'3
 CTCAGAAATCTTCCCTCCACCCTCTCCTTTTCATTCGGCCCTCCACCCCTCCA**CTCCTCCAATCCCTCAT**
CTTTCCATCCCTCCACTCTCCATACCTCCACACCCCCATGCATCCATCCACCCCGC**CACACTCACGCTCA**
CACACACACACTCACTCATGCACACA**CACATAGACATACTCTCAG**TACTCACACAGTATTACACACA
 CACACACAAACACACAGACACAGACACGCACATACGTCACTCAGACACACACACACATACAGTACAC
 ACACACACACACAGTACACAGACACACACATAGTTACACAGACACACACACACACAGTACACACACAC
 AGACTCAGACACAGACATACAGTACACAGACACACACATACTCTCTCTCTCTCTCTCTCACACACAC
 ACACACACACACACACACCCAGGCCTGGGGTTAACAGTTTATGCTGTTTACCCCTGACACTGCCTATG
 TGTTAGATTTTGGGTTTTTCCACCAATGAGATGACAGGAATAAGAACAGCCATTATCCACANCTTGGG
 CCCACCNAACCCAACTCAGAGGGAAAGAGTGGGGACAGAAATTCGAAGGGAGGGCTTTGGGGGCTTGGG
 ATTGAANAAAGCNTTGGCATTGGCCCTGGCAGGGGTGCAACTTCTTANAAAGGGGATCCCCGGGGGGTA
 ACCCGNAGNCNTCCGAAANTTTCCACCTNGGGCCCGGTTTCGNTTTTTTANANAAAACGGTTCGGTTGNAA
 CNNGGGGGGAAAAAAAACCCCTTGGGGGGGTTTTTAACCCCAA

Sequence : Whale Shark A114a

Primer Pair # 7 Product Length: 325 Topt: 57.7 ✓
 Forward: Tm: 56.1 5'-ACT-CAT-GCA-CAC-ACA-CAT-AGA-C-'3
 Reverse: Tm: 56.0 5'-AGG-GGT-AAA-CAG-CAT-AAA-CTG-'3
 CTCAGAAATCTTCCCTCCACCCTCTCCTTTTCATTCGGCCCTCCACCCCTCCACTCCTCCAATCCCTCAT
 CTTTCCATCCCTCCACTCTCCATACCTCCACACCCCCATGCATCCATCCACCCCGCCACACTCACGCTCA
 CACACACACTC**ACTCATGCACACACACATAGAC**ATACACTCTCACGTA**CACACAGTATTACACACA**
CACACACAAACACACAGACACAGACACGCACATACGTCACTCAGACACACACACATACAGTACAC
 ACACACACACACAGTACACAGACACACACATAGTTACACAGACACACACACACAGTACACACACAC
 AGACTCAGACACAGACATACAGTACACAGACACACACATACTCTCTCTCTCTCTCTCTCACACACAC
ACACACACACACACACCCCAGGCCTGGGGTTAAC**CAGTTTATGCTGTTTACCCCT**GACACTGCCTATG
 TGTTAGATTTTGGGTTTTTCCACCAATGAGATGACAGGAATAAGAACAGCCATTATCCACANCTTGGG
 CCCACCNAACCCAACTCAGAGGGAAAGAGTGGGGACAGAAATTCGAAGGGAGGGCTTTGGGGGCTTGGG
 ATTGAANAAAGCNTTGGCATTGGCCCTGGCAGGGGTGCAACTTCTTANAAAGGGGATCCCCGGGGGGTA
 ACCCGNAGNCNTCCGAAANTTTCCACCTNGGGCCCGGTTTCGNTTTTTTANANAAAACGGTTCGGTTGNAA
 CNNGGGGGGAAAAAAAACCCCTTGGGGGGGTTTTTAACCCCAA

Sequence : Whale Shark A118

Primer Pair # 8 Product Length: 194 Topt: 56.4 ✓
 Forward: Tm: 55.1 5'-TCT-GGA-TGT-CCT-GGT-GTA-TAG-'3
 Reverse: Tm: 55.4 5'-TGT-GTT-TTA-ACC-TGG-AGT-CAG-'3
 CACCGCCAGGAAGTTCGCAGAATCCCAATGCCGTATCTTTAAAGTTCAGCTGTGTTATCCAAGNTCAAAA
 CTGCCCTACACAGTTCCTGTCACTTACTTACAGACATATGGGCACAGCAAATGGCACTCTGCTTTGCC
 ATGGGGA**TCTGGATGCTCCTGGTATAG**GGGATGAATGCATTCAGTCCCACTTCTCTCTCTCTCTCT**CACACTCAC**
ACACACACACACACACACACACACACACACACACCTATGGGATGAATTATCTCATCCAATATGTTTGTGT
 ATTTGCAGATACATTTCTATTTTGTCAAAAAAACCCAAAC**CTGACTCCAGGTTAAAACACA**GTGATTC
 TAAACACACCTGAAATGCATTGTCTGACCTAGATGTCACCTCTTNGCATTACACTGGATTAAAACCTTTA
 ATTATCTTGGGGTAATGACTTGAAGAAGTTCCTGGGATTTGCNTTTT

Sequence : Whale Shark A119

Primer Pair # 2 Product Length: 279 Topt: 57.7 ✓
 Forward: Tm: 56.9 5'-TCA-TCC-GTA-AAC-TTG-CTA-ACC-'3
 Reverse: Tm: 57.1 5'-TGC-CTT-CTC-ACC-GTA-ACC-'3
 AAAGGTATCTGGATGGGTATANGAAGTGAAGGGTTCAGAGGAATANAGGCCAAACACAGGGCAAATGGA
 CTAGATTAATTTCCGGTACCTGGTACAGATGGACATATTTGGGCCAAAGGATTTGTTCCCATACTGTATAT
 CTTTATGATTCATTCATCCAATTTGATCAAGATCTCTTTGTAATCTTGGATAACCTTCCCTGTCTACGGTT
 CAAATAATCTCAGTG**TATCCGTAACCTTGCTAAC**ACTGCCTTCTATAATTTTCATCTGAATCATTTCTT
 AAATGAAAAAGAAACGTAAATCCAGCACTGATCCCTGTGGATCACCCTAGT**CACAGGCTCCAGTCTGA**
 AGGACAATCCTCCATGACCACCTGTCTCCTGCCATTAAGCAGAAATA**CACACACACACACACACACACA**
CACACACACACACAGCCGTGTCTTTAAGACAGAGATAGATACGTTTGGATTAATAAGCAGATCAAG**GGTT**
ACGGTGAGAAGGCAAGAGAATTTGTTTTGAGAAACATGTCAAGCATAATCGAACAGCAGCACAGACTTGAT
 GGGNCAAATGGCTAATTTCTGCTCCAATTTCTTATGCTGGCCTGGGTCTGGAAGGTATCNNGAATTATTTT
 CCCCAGAANAAGCCAGTGGATGGGCTGGANGGTTGGATTAAATTACTTTTACTGGAACNAGAAGTTCGA
 ATCCGGGAATGGGTTGGAAGTTAAGGTTTTTGAAGGGAAATGAAATGGNCCTNACATTCTNGCTNCCT

TATTTTGGGTGGTGGCTNCCTTTAAAAGAAGGANGGTAACCTTGGCCTGGTGGANGGTTNAAGCCTTTGCA
 ATTGNCCCTGCAGGGTCAACTCCTTAAAANGGANTCCCCGGGGTTACCGAAGCTCGAAATTCCACTGGC
 CCGGCC

Sequence : Whale Shark A120

Primer Pair # 1 Product Length: 279 Topt: 57.3 ✓
 Forward: Tm: 56.3 5'-CCA-GGC-TGC-CAA-AGT-TAT-'3
 Reverse: Tm: 55.8 5'-ACC-ACT-GGT-CCT-GTG-TAG-G-'3
 AAATATCAGAGGAAAAGTAAAATAGGAAGAAGCTGGGATTCACTAACAAAAATTTCTTACTAATAATTTAG
 TAACTTGTGTGTTTATGTATCAAGGCAAAGCAGGCAAGTTAAAACTCTTGCCTCCAATTGCATCTTCT
 ACCTCATGTTTCTCAGTTTCTACAATAGTAATTCCTGAATTCCTGTATACTGTTGTACTTAGTATGTATTG
 TCATGATCATGTACTAAAATTTGATCCTAAACCTGAAATTGCAAATTCACCAGGTGCCAAAACAATATC
 AAAGAATAATTTAGGCCATTAATAACAGTAACAATGATAGTCTCATTCCATTTCACTTCATTAATAACT
 CTAATATGGAGTAACTACCTTGTGAACCTGATTCCAGGCTGCCAAAGTTATGTTAAGATCTAATAAGG
 ACTAATCATTACTTAAGTGAGAAATCCAGAACTTTATTAAGAGAATAAAGCTGTGAGATTAAGATTTTG
 AACAAACAATAAATTTCACTTAACTAAAGCAGTAAAATAGTCTCATACACACACACACACACACACAC
 AC
 ACCCAATACTTACTGGTTTTATGACTCTCAAGACTT
 ATTCCTTAGCCTCACTACACAGGACCAGTGGTTTCAGTTATCTTTCTCAGCAGCCACTTTATCCTGGCG
 TGGGAGTTTTATTCCTCTACTCTCACCCTCGTACTATCAGAATTCAAAAGTTAACTAANTTAG

Sequence : Whale Shark A121

Primer Pair # 8 Product Length: 185 Topt: 57.3 ✓
 Forward: Tm: 58.6 5'-CAA-TTT-ACC-TGA-CGT-TCA-GAC-C-'3
 Reverse: Tm: 58.7 5'-GCC-TAT-ACG-TGA-CTC-CAG-ACC-'3
 AAAGGGTACACACTGGTGCCC CAATTTACCTGACGTTTCAGACCAGNGNTTGATAGAAAGTCCCTTCTTCT
 TTANTA CAC
 CACA CGCCCCCAGAGGGCAGTTAAGTGTCAAT CACA TTGCTGTG GGTCTGGAGTCACGTATAGGC CAGA
 CCAGGTAAGGATGGCGTTTTCTTTCCATAAGGGTATTAATAAACACACACAAGTTTTTTCAACAATCAACA
 ATGATTCATAGTCAATTATCAGACTCCTAATTCAGATGTTTTATTGAATACAAATTCACAATCTCCATA
 GCAGGGTTCAAACCAGGGTCCCATCAGAACATTACCAGGGTCTCTGGATTACTAGTCTAGCAATAATAC
 CACTAGGCCATCACCTCCCAATATATGGATGAACTCCAG

Sequence : Whale Shark A122

Primer Pair # 1 Product Length: 280 Topt: 58.5 ✓
 Forward: Tm: 59.6 5'-CAC-CCT-GTC-TCC-TGC-CAT-A-'3
 Reverse: Tm: 59.5 5'-GCC-ATC-ACT-GCT-CTC-TTG-G-'3
 AAATGACAAACAAAAGTAAAGTCCAGCACCGATCCCTGNTGGATCACTGCTAATCACAGGCCTTCCNAGNT
 TGAGAACAAATCCTCCATGAC CACCCTGTCTCCTGCCATAAAGCAAAAATA CACACACACACACACACACA
 CAC
 GCCATGTC TTTAAGACAGAGATAGATATGTCTTGATTAATAAGCAGATCAAG
 GGTTACGGTGAGAAGGCAAGAGAATGTTTTGAGAAACATGTCAAGCATAATCGAACAGCAGAGCAGACT
 TGATGGGCCAAATGGATAACTCTGCTCAACTTCTCATGTCTGCTGGTCTGAAGGTATCAGGATATTTTT
 CCAAGAGAGCAGTGATGGCTGAGATTTCATAAATCTGAACGAGAGTTCGGAATGTGGAGTAG
 GTTTGAGGGAATGAATGGCCTACATCTGCTCCTATTTGTTGTGCTCCTTAAAGAGGAGGTAACCTGCTGT
 GAGGTTAACACACTTCAANGGAGTTCTCTCAATAAACNTTGGAGAATAAGAATGGTTTTCTTCCCCCTTT
 AAAAATGGNGCCGGCCGGTATGGTCCCCATNCCCCAGGGACC

Sequence : Whale Shark A123

Primer Pair # 8 Product Length: 224 Topt: 58.0 ✓
 Forward: Tm: 59.3 5'-CTT-CCG-TTT-TGC-ATT-CAG-TG-'3
 Reverse: Tm: 59.3 5'-AGG-TGC-TTC-AAG-GGC-ATA-AG-'3
 CTGCTCACACTGNNTTGTCTCCTTTCTCTGNTTCTTT CTTCCGTTTTGCATTGAGTGGCCTGNTTAC
 GAGA CA
 CATACCTACCTACCTACCGCTTTTTGGGCAAACCTCGTTTCTTTACTTTGCCCATTTCCGAGCTCCTTTG
 CCTTTGCATCATGAAACCTCTGTGTTTCATCT CTTATGCCCTTGAAGCACCTTCAACAGACCTTTTCCC
 TCTTGATCTGTGACCGTCACTCCCCACCCGTTCACTCAAATCTATTACATCTGCTTTTTCTG
 AGTTCTGATGAAGAACATTACCCAAGTCAATGTCTCCTCTTATTATCTCTCCCCACTGCTGCCTGAG
 TAATCCGAGCATATTTCTGCTTTTATTTTCAGATTTCCGGCACCTGCGGTGTTTTGCTTCTGGTTTCTGATC
 CTAATTGCAATCAATATCACTATCATTTGCAGACCGAAGATGAGGAGACATCCATTACTTTTTATGAATCCA
 GGAAGATTGACCAATGGTCTTCAATTTGACTGGCCTCTTGCTGAGCGTCTTCTGGTTAAAGTCAGAGCA
 GTTAAGTCAAGCCTACAGCACTAAACATACCAACCGGTAAAANCATGGG

Sequence : Whale Shark E125

Primer Pair # 3 Product Length: 133 Topt: 56.7 ✓

Forward: Tm: 59.8 5'-GGA-CTG-TTC-CTG-TGC-TGT-ACT-G-'3

Reverse: Tm: 59.7 5'-CCA-CTC-TTT-CCC-CAT-TAC-ATT-C-'3

ACGCCTCGGGTCAGTGACCTCCCTCAGAATGGAAGCAGATGGGATTAGTTTGTAGAAATGGGTTATAAATTA
 GCACAGACATGTGGGCCGACA **GGACTGTTCCCTGTGCTGTACTG**TTCTGTGTTCTATGAAGCAGAGAGAGA
GATTGGGACA **GAGAGAGAGAGAGA** **GGCAGAGAGA** **AAAGAGAGAGAGAGA**GTGTGAGTCAAAGA **GAATGTAA**
TGGGGAAAGAGTGGGAGAGACAGGGAAAGTGAAGCCGACGTTGGGAAGCAGAGAAAACAGAAAACACAGAGA
 GAGAGAGAGAGATGCACAAAAGAAAGAGAGAGACAGAGAGAAACTATGTGCCAGACGGAGACAGTGTGAGC
 GTGAGCCAGAGAGACTCTGGGTCTGACAGTGTGAGAAGATGAGAGAGACAGGAAAGATTTGTATGCAGGG
 AGGGGTGACAATTGAGAGTTGGAGTGAATGAGCAGTTTTTAATCGAAGATCCGGAAGAGAACAGAGTGTCTG
 GTGTCCAGTTACACATCCAGGCCTAATACATTTGTTCCCTGATGTTTGCAGAG

Sequence : Whale Shark E128

Primer Pair # 3 Product Length: 153 Topt: 56.4 ✓

Forward: Tm: 57.3 5'-GGT-CTG-TTT-CCT-TGC-TGT-ATG-'3

Reverse: Tm: 57.9 5'-TCT-GTT-TGT-CTC-TCC-ATC-TGT-G-'3

AGACATCTGCATGGGTACATGAATAGGAAGGGTTTATAGGGATATGGGCCAAATGCTGGGCCAAATGAGA
 CTAGATTAATTTAGGATATCTGGTCAGCATGGATGAGTTAGACCAGAG **GGTCTGTTTCCTTGCTGTATGA**
 CTCCATGACTCTAGAACCCTCTCCCTTTCTCCCTTTAAAAACACTTGTGAAAACGCTCCGAACTTCACTT
TGAGAGAGA **CAGAGAGA** **CAGAGAGT** **GAGAGA** **CAGAAAGA** **CACAGATGGAGAGACAAAACAGAGAGAGGCAG**
 AGACAGAAAGAGACAGAGAGAGAGAGACAGAGAGGGAGACAGAGAAAAGACAGAGAGACAGAAAGATAG
 AGAGACAGATGGAGAGAGAAAAACAGAGAAAGGTAGAGAGCAAGAGACAAGGAGGAGAGTGGGAGAGAGA
 GGGAGAGAAAGAGAAGGAGAGAGAANCAGAGAAAAGAGACNGAGAGAGAGATNGAGAGATAGATAGAGAGA
 GGGAGAGAGAGACAGGNCCCCNAGAGAGTGANACAGAGAGACACNGNCCCAGAGAGTGTGATCGNCCGA
 NNGACGAGAAANCTTTGNNTTGCCTGCAGGGTCGACT

APPENDIX 2

Summary of satellite tag deployments at Ningaloo Reef, WA from 2004-2007.

PTT#	Tag Type	Deployment Latitude (East)	Deployment Longitude (South)	Deployment Date	Deployment Time	Shark Sex	Shark Length (m)
-	PSAT	22°38.2'	113°36.7'	03/05/2004	10:42	Male	4.5
-	PSAT	22°40.1'	113°37.3'	03/05/2004	12:50	Female	8.5
-	PSAT	22°38.2'	113°36.7'	03/05/2004	13:30	Female	7.5
-	PSAT	22°38.2'	113°38.7'	04/05/2004	10:20	Female	4.7
-	PSAT	22°30.0'	113°40.3'	04/05/2004	10:47	Female	4.5
-	PSAT	22°30.0'	113°40.3'	04/05/2004	10:58	Female	11
-	PSAT	22°37.6'	113°36.3'	04/05/2004	12:30	Female	7.3
-	PSAT	22°37.5'	113°41.8'	05/05/2004	11:09	Unknown	4.7
-	PSAT	22°38.7'	113°38.5'	05/05/2004	13:52	Female	7.6
-	PSAT	22°31.8'	113°38.9'	07/05/2004	13:29	Female	5.6
-	PSAT	22°41.7'	113°38.2'	07/05/2004	14:50	Female	7.6
-	PSAT	22°29.7'	113°39.5'	08/05/2004	12:47	Female	6.2
-	PSAT	22°25.9'	113°47.7'	08/05/2004	13:15	Male	7
-	PSAT	22°24.7'	113°43.1'	08/05/2004	13:35	Female	7
-	PSAT	22°40.5'	113°37.6'	09/05/2004	10:45	Female	5.3
4220	PSAT	22°39.432'	113°34.206'	28/04/2005	10:55	Female	4-5
57012	PSAT	22°39.176'	113°34.437'	28/04/2005	12:25	Female	4-5
11616	PSAT	22°39.766'	113°35.593'	05/05/2005	11:05	Male	4-4.5
57014	PSAT	22°39.044'	113°35.90'	05/05/2005	10:30	Male	4-4.5
57210	SPLASH	22°39.044'	113°35.90'	05/05/2005	10:45	Male	4-4.5
57013	PSAT	22°44.559'	113°34.20'	05/05/2005	12:10	Unknown	7-8
57214	SPLASH	22°44.559'	113°34.20'	05/05/2005	12:10	Unknown	7-8
57015	PSAT	22°44.439'	113°36.740'	05/05/2005	13:55	Male	~8
57016	PSAT	22°43.165'	113°36.730'	06/05/2005	12:25	Female	4-4.5
57209	SPLASH	22°43.165'	113°36.730'	06/05/2005	12:25	Female	4-4.5
11617	PSAT	22°42.175'	113°34.617'	07/05/2005	10:35	Female	6-7
11618	PSAT	22°41.764'	113°35.032'	07/05/2005	10:45	Unknown	5-6
57211	SPLASH	22°42.015'	113°35.578'	01/05/2005	13:45	Unknown	3-4
57212	SPLASH	22°42.569'	113°37.182'	05/05/2005	13:45	Unknown	4-5
57213	SPLASH	22°35.667'	113°37.449'	06/05/2005	10:45	Female	~4
11619	PSAT	22°38.133'	113°35.370'	28/04/2006	11:25	Male	6-7
9156	PSAT	22°37.810'	113°35.595'	28/04/2006	11:56	Unknown	3-5
65811	SPLASH	22°38.295'	113°36.243'	29/04/2006	10:45	Female	4.5
9157	PSAT	22°44.193'	113°38.013'	29/04/2006	12:32	Female	3-4
65813	SPLASH	22°42.831'	113°38.382'	29/04/2006	12:47	Unknown	4

Population monitoring protocols for whale shark

PTT#	Tag Type	Deployment Latitude (East)	Deployment Longitude (South)	Deployment Date	Deployment Time	Shark Sex	Shark Length (m)
66000	PSAT	22° 35.375'	113° 35.822'	02/05/2006	14:15	Male	5-6
65810	SPLASH	22° 35.213'	113° 35.465'	02/05/2006	14:55	Unknown	7
66001	PSAT	22° 35.430'	113° 35.322'	02/05/2006	15:05	Unknown	4
65809	SPLASH	22° 36.558'	113° 37.267'	03/05/2006	10:50	Female	5-6
65812	SPLASH	22° 36.160'	113° 37.357'	03/05/2006	11:13	Unknown	5-6
65816	SPOT	22° 40.816'	113° 37.402'	03/05/2006	13:25	Unknown	5-6
-	SPOT	22° 41.387'	113° 37.766'	03/05/2006	13:55	Male	6.5
65818	SPOT	22° 37.346'	113° 37.002'	04/05/2006	10:35	Male	5.5
65813	SPLASH	22° 49.622'	113° 40.806'	02/05/2007	15:50	Unknown	3.5
75378	SPLASH	22° 44.403'	113° 36.650'	29/05/2007	12:29	Unknown	5
65817	SPOT	22° 44.987'	113° 36.972'	29/05/2007	13:00	Unknown	6.5
75376	SPLASH	22° 49.351'	113° 40.372'	30/05/2007	13:00	Male	4.5
75377	SPLASH	22° 49.234'	113° 40.680'	30/05/2007	15:15	Unknown	3
75379	SPOT	22° 47.005'	113° 40.545'	31/05/2007	10:30	Unknown	4

APPENDIX 3

List of publications that are included in this report and/or supplied as supplementary information on CD.

1. Castro ALF, Stewart BS, Wilson SG, Hueter RE, Meekan MG, Motta PJ, Bowen BW, Karl SA (2007) Population genetic structure of Earth's largest fish, the whale shark (*Rhincodon typus*). *Molecular Ecology* 16: 5183-5192.
2. Bradshaw CJA, Mollet HF, Meekan MG (2007) Inferring population trends for the world's largest fish from mark-recapture estimates of survival. *Journal of Animal Ecology* 76: 480-489.
3. Fitzpatrick B, Meekan M, Richards A (2006) Shark attacks on a whale shark (*Rhincodon typus*) at Ningaloo Reef, western Australia. *Bulletin of Marine Science* 78: 397-402.
4. Meekan MG, Bradshaw CJA, Press M, McLean C, Richards A, Quasnichka S, Taylor JG (2006) Population size and structure of whale sharks (*Rhincodon typus*) at Ningaloo Reef, Western Australia. *Marine Ecology Progress Series* 319: 275-285.
5. Rowat D, Meekan M, Engelhardt U, Pardigon B, Vely M (2007) Aggregations of juvenile whale sharks (*Rhincodon typus*) in the Gulf of Tadjoura, Djibouti. *Environmental Biology of Fishes* 80:465-472.
6. Sleeman JC, Meekan MG, Wilson SG, Jenner CKS, Jenner MN, Boggs GS, Steinberg CC, Bradshaw CJA (2007) Biophysical correlates of relative abundances of marine megafauna at Ningaloo Reef, Western Australia. *Marine and Freshwater Research* 58: 608-623.
7. Speed CW, Meekan M, Bradshaw CJA (2007) Spot the match - wildlife photo-identification using information theory. *Frontiers in Zoology* 4:2.
8. Speed CW, Meekan MG, Rowat D, Pierce S, Marshall AD, Bradshaw CJA (2008) Scarring patterns and relative mortality rates of Indian Ocean whale sharks. *Journal of Fish Biology* DOI: 10.1111/j.1095-8649.2008.01810.x
9. Speed CW, Meekan MG, Russell BC, Bradshaw CJA (2008) Recent whale shark (*Rhincodon typus*) beach strandings in Australia. *Journal of the Marine Biological Association of the UK*. Biodiversity Records. Published online.
10. Wilson SG, Polovina JJ, Stewart BS, Meekan MG (2006) Movements of whale sharks (*Rhincodon typus*) tagged at Ningaloo Reef, Western Australia. *Marine Biology* 148: 1157-1166.
11. Wilson SG, Stewart BS, Polovina JJ, Meekan MG, Stevens JD, Galuardi B (2007) Accuracy and precision of archival tag data: a multiple-tagging study conducted on a whale shark (*Rhincodon typus*) in the Indian Ocean. *Fisheries Oceanography* 16:547-554.